MECHANISMS OF PLANT-ALUMINUM INTERACTIONS IN ACIDIC SOILS

EDITED BY: Jian Li Yang, Wei Fan and Peter Ryan

PUBLISHED IN: Frontiers in Plant Science

frontiers Research Topics

frontiers

ISSN 1664-8714
ISBN 978-2-88945-909-4
DOI 10.3389/978-2-88945-909-4

About Frontiers

Frontiers is more than just an open-access publisher of scholarly articles: it is a pioneering approach to the world of academia, radically improving the way scholarly research is managed. The grand vision of Frontiers is a world where all people have an equal opportunity to seek, share and generate knowledge. Frontiers provides immediate and permanent online open access to all its publications, but this alone is not enough to realize our grand goals.

Frontiers Journal Series

The Frontiers Journal Series is a multi-tier and interdisciplinary set of open-access, online journals, promising a paradigm shift from the current review, selection and dissemination processes in academic publishing. All Frontiers journals are driven by researchers for researchers; therefore, they constitute a service to the scholarly community. At the same time, the Frontiers Journal Series operates on a revolutionary invention, the tiered publishing system, initially addressing specific communities of scholars, and gradually climbing up to broader public understanding, thus serving the interests of the lay society, too.

Dedication to Quality

Each Frontiers article is a landmark of the highest quality, thanks to genuinely collaborative interactions between authors and review editors, who include some of the world's best academicians. Research must be certified by peers before entering a stream of knowledge that may eventually reach the public - and shape society; therefore, Frontiers only applies the most rigorous and unbiased reviews.
Frontiers revolutionizes research publishing by freely delivering the most outstanding research, evaluated with no bias from both the academic and social point of view. By applying the most advanced information technologies, Frontiers is catapulting scholarly publishing into a new generation.

What are Frontiers Research Topics?

Frontiers Research Topics are very popular trademarks of the Frontiers Journals Series: they are collections of at least ten articles, all centered on a particular subject. With their unique mix of varied contributions from Original Research to Review Articles, Frontiers Research Topics unify the most influential researchers, the latest key findings and historical advances in a hot research area! Find out more on how to host your own Frontiers Research Topic or contribute to one as an author by contacting the Frontiers Editorial Office: researchtopics@frontiersin.org

MECHANISMS OF PLANT-ALUMINUM INTERACTIONS IN ACIDIC SOILS

Topic Editors:
Jian Li Yang, Zhejiang University, China
Wei Fan, Yunnan Agricultural University, China
Peter Ryan, Commonwealth Scientific and Industrial Research Organisation (CSIRO), Australia

Citation: Yang, J. L., Fan, W., Ryan, P., eds. (2019). Mechanisms of Plant-Aluminum Interactions in Acidic Soils. Lausanne: Frontiers Media.
doi: 10.3389/978-2-88945-909-4

Table of Contents

frontiers in Plant Science

ORIGINAL RESEARCH
published: 18 December 2018
doi: 10.3389/fpls.2018.01838

Mining Beneficial Genes for Aluminum Tolerance Within a Core Collection of Rice Landraces Through Genome-Wide Association Mapping With High Density SNPs From Specific-Locus Amplified Fragment Sequencing

Minghui Zhao[1†], *Jiayu Song*[1†], *Aiting Wu*[1], *Tao Hu*[1] and *Jinquan Li*[2,3*]

[1] Rice Research Institute, Shenyang Agriculture University, Shenyang, China, [2] State Key Laboratory for Conservation and Utilization of Subtropical Agro-Bioresources, South China Agricultural University, Guangzhou, China, [3] Department of Plant Breeding and Genetics, Max Planck Institute for Plant Breeding Research, Cologne, Germany

Trivalent Aluminum (Al^{3+}) in acidic soils is harmful to root growth and significantly reduce crop yields. Therefore, mining beneficial genes for Al tolerance is valuable for rice production. The objective of this research is to identify some beneficial genes for Al tolerance from rice landraces with high density SNP set from SLAF-seq (Specific-Locus Amplified Fragment sequencing). A total of 67,511 SNPs were obtained from SLAF-seq and used for genome-wide association study (GWAS) for Al tolerance with the 150 accessions of rice landraces in the Ting's rice core collection. The results showed that rice landraces in the Ting's rice core collection possessed a wide-range of variation for Al tolerance, measured by relative root elongation (RRE). With the mixed linear models, GWAS identified a total of 25 associations between SNPs and Al tolerant trait with $p < 0.001$ and false discovery rate (FDR) <10%. The explained percentage by quantitative trait locus (QTL) to phenotypic variation was from 7.27 to 13.31%. Five of twenty five QTLs identified in this study were co-localized with the previously cloned genes or previously identified QTLs related to Al tolerance or root growth/development. These results indicated that landraces are important sources for Al tolerance in rice and the mapping results could provide important information to breed Al tolerant rice cultivars through marker-assisted selection.

Keywords: Aluminum tolerance, genome-wide association mapping, relative root elongation, rice landraces, Al tolerant QTL, SLAF-seq

OPEN ACCESS

Edited by:
Peter Ryan,
Commonwealth Scientific and Industrial Research Organisation (CSIRO), Australia

Reviewed by:
Harsh Raman,
New South Wales Department of Primary Industries, Australia
Wricha Tyagi,
Central Agricultural University, India
Saul Justin Newman,
Australian National University, Australia

***Correspondence:**
Jinquan Li
lijinquan@scau.edu.cn

[†]These authors have contributed equally to this work

Specialty section:
This article was submitted to Plant Abiotic Stress, a section of the journal Frontiers in Plant Science

Received: *09 March 2018*
Accepted: *27 November 2018*
Published: *18 December 2018*

Citation:
Zhao M, Song J, Wu A, Hu T and Li J (2018) Mining Beneficial Genes for Aluminum Tolerance Within a Core Collection of Rice Landraces Through Genome-Wide Association Mapping With High Density SNPs From Specific-Locus Amplified Fragment Sequencing. Front. Plant Sci. 9:1838. doi: 10.3389/fpls.2018.01838

INTRODUCTION

Rice (*Oryza sativa* L.) is an important crop in the world. There is about 13% of global rice field on acidic soils (Vonuexkull and Mutert, 1995). Trivalent aluminum (Al^{3+}) in acidic soils is harmful to root growth and reduces significantly rice yield (Liu et al., 2012). It is a major toxin for plants on acid soils (Delhaize et al., 2012). Therefore, exploring the genetic mechanism of Al tolerance in rice is of importance to understand why Al^{3+} is toxic to the plants and to breed Al tolerant varieties for rice production.

Serval researches on the genetic mechanism of Al tolerance in rice have been reported (e.g., Famoso et al., 2010, 2011; Cai et al., 2011). Previous researchers have identified a number of quantitative trait loci (QTLs) for Al tolerance in rice (Nguyen et al., 2002; Ma and Furukawa, 2003; Mao et al., 2004; Xue et al., 2007; Famoso et al., 2011), and found a few genes linked to Al tolerance (e.g., Yokosho et al., 2011; Chen et al., 2012; Huang et al., 2012; Xia et al., 2013; Li et al., 2014). In the context of QTL mapping for Al tolerance, most of these previous researches were conducted with bi-parent segregation populations and linkage mapping. Genome-wide association study (GWAS) make it possible to exploit natural genetic diversity and mine beneficial genes in the genome (Zhu et al., 2008). It is important to apply GWAS with modern genotyping technology for QTL mapping for Al tolerance.

In recent years, many QTLs for multiple traits have been identified using GWAS. For example, Huang et al. (2010) conducted GWAS for 14 agronomic traits with high density SNP set and 517 *indica* landraces of rice. Using GWAS with a diverse rice set of 383 accessions, Famoso et al. (2011) found 48 QTLs for Al tolerance, four of which co-localized with previously identified candidate genes for Al tolerance and two of which co-localized with previously identified Al-tolerant QTLs. Using 274 SSR markers and the same populations as this study, Zhang et al. (2016) performed an association study and found a total of 23 QTLs for Al tolerance. However, to our knowledge, no GWAS for rice Al tolerance has been performed using high-density SNPs with a core collection of rice landraces.

Recently, the whole genome sequencing technology is being increasingly used to accurately and rapidly detect numerous variants across the entire genome at the molecular level. The recently developed next-generation sequencing-based genotyping approach, i.e., specific-locus amplified fragment sequencing (SLAF-seq) method is a simplified genome sequencing technology that has shown to be highly accurate and cost-effective (Sun et al., 2013). SLAF-seq has been applied in genetic map construction, QTL mapping, and molecular breeding. However, to our knowledge, no high-density SNPs obtained from SLAF-seq technology has been applied for GWAS in a core collection of rice landraces.

Abundant germplasm resources for Al tolerance are available in the Asian cultivated rice, especially in rice landraces. As early as in 1920–1964, a total of 7,128 accessions of rice landraces had been collected by Prof. Ying Ting, which was named as Ting's rice collection (Li et al., 2011). They were from all over China as well as from some main rice cultivation countries. Based on 48 phenotypic data, Li et al. (2011) has constructed a rice core collection consisting of 150 accessions. The analysis of population structure indicated that there existed two subgroups mainly corresponding to *indica* and *japonica* subspecies and the LD decays to the threshold, i.e., the 95% quantile of r^2 between unlinked loci pairs, at 1.03 cM in the entire collection, which was about 200–500 kb in physical distance (Zhang et al., 2011; Li and Zhang, 2012). The large variation within the core collection provides an important gene pool of genetic diversity and beneficial genes for rice breeding. Therefore, it is worth to perform GWAS with such a core collection for Al tolerance in rice.

The objectives of the study were to (1) perform GWAS for rice Al tolerance to reveal the genetic basis for this complex trait; (2) identify novel functional candidate genes underlying the mapped regions; and (3) to mine the beneficial genes within the Ting's core collection of rice landraces with the newly developed high-density SNP set from SLAF-seq approach.

MATERIALS AND METHODS

Plant Material

The Ting's rice core collection, i.e., a total of 150 accessions of rice landraces were used to screen their Al tolerance (**Table S1**). The core collection was constructed from 2,262 accessions of 7,128 based on a strategy of stepwise clustering and preferred sampling on adjusted Euclidean distances and weighted pair-group average method using integrated qualitative and quantitative traits (Li et al., 2011). It represents the diversity in the Ting's rice collection. Furthermore, Nipponbare and Xiangnuo 1 (Yang et al., 2007) were chosen as tolerant control and Nante (Fu et al., 2010), Xiangzhongxian 2 (Xu et al., 2004), and IR64 (Khatiwada et al., 1996) for Al sensitive control. These varieties were used to identify an appropriate concentration for Al toxicity.

Phenotyping for Al Tolerance

The Al tolerance for the 150 accessions of rice landraces were examined according to our previous research (Zhang et al., 2016). To choose an optimal Al^{3+} concentration to screen Al tolerance, the seedlings for two Al tolerant and three Al sensitive rice varieties were exposed to 0.5 mM $CaCl_2$ (pH = 4.0) containing 50, 100, 150, 200, 250, 300, 350, 400, 450, and 500 μM $AlCl_3$ (no other nutrient solution was applied), respectively. The Al^{3+} concentration under which the largest difference of relative root elongation length (RRE) between the sensitive and tolerant varieties was chosen as an optimal Al^{3+} concentration for screening of Al tolerance in the following experiment. In this case, the largest difference in RRE was observed at 100 μM between the two tolerant and three sensitive varieties. Therefore, the 100 μM $AlCl_3$ was used for screening of Al tolerance.

The 150 accessions of rice landraces cultivated at the farm of South China Agricultural University, Guangzhou (23°16N, 113°8E), during late season (July-November) in 2008 and 2009. The seeds were harvested each year. Uniform seeds in each year were surface sterilized in 1% H_2O_2 for 30 min and rinsed

with deionized water. Then the seeds were put into deionized water at 30°C for 2 days in darkness for germination. The uniform seedlings were transferred to a net floating on a 0.5 mM $CaCl_2$ (pH = 4.0) solution in a 1.5 L plastic container. A randomized complete block design (RCBD) with three replicates was applied. Seedlings were grown at 28°C for 48 h before being used for Al toxicity treatment. Then, the seedlings were exposed to 0.5 mM $CaCl_2$ (pH = 4.0) containing $AlCl_3$ for 24 h, and the root elongation length was measured for each sample. Then RRE was used to evaluate the degrees of Al tolerance of all landraces. RRE was calculated as follows: (root elongation length with Al treatment)/(root elongation length without Al treatment). Root length of 10 seedlings in each treatment was measured before and after treatments. The RRE for each genotype across the three replicates for 2008 and 2009 were calculated, respectively. The mean of RRE for 2 years was also calculated for each genotype. These phenotypic data were used for GWAS.

Genotyping of SNP Markers

The SLAF sequencing were conducted based on the standard protocol from Beijing Biomarker Technologies Corporation (http://www.biomarker.com.cn) and the introduction by Sun et al. (2013) and Song et al. (2018). To simplify, the first step was to perform a SLAF pre-design experiment with 8 accessions of landraces and different enzymes combinations. This step was used to evaluate the appropriate enzymes and sizes of restriction fragments. The SLAFs obtained by this step should be evenly distributed ascross the genome. The second step was to construct the SLAF library in accordance to the pre-design scheme. In this step, genomic DNA was digested by enzymes designed for individuals. Double barcodes were added to two rounds of PCR reactions to discriminate each individual and to facilitate the pooling of samples. In the third step, the purified DNA tags with indices and adaptors (SLAFs) of 300–400 bp were used and diluted for pair-end sequencing on an Illumina High-seq 2500 sequencing platform according to the Illumina sample preparation guide (Illumina, Inc.; San Diego, CA, US) at Beijing Biomarker Technologies Corporation. All polymorphic SLAF loci were genotyped according to the SNP loci at the reference genome. The SNPs with missing data > 20% across all genotypes as well as the SNPs with a minor allele frequency (MAF) (<5%) were excluded for the following statistical analysis. After filtration, 150 accessions of rice landraces with a total of 40,708 polymorphic SNPs were used for GWAS. The data of the SLAF sequencing have been uploaded to the BioSample database (BioSample accession SAMN10448484).

Statistical Analyses

The statistical model used for GWAS analysis was the PK mixed:$M_{ip} = \mu + a_p + \sum_{u=1}^{z} D_{iu}\upsilon_u + g_i{}^* + e_{ip}$, where M_{ip} was the phenotypic value of the ith entry carrying allele p, a_p the effect of allele p, e_{ip} the residual, υ_u the effect of the uth column of the population structure matrix D, and g_i^* was the residual genetic effect of the ith entry (Yu et al., 2006; Stich et al., 2008).

Principal coordinate analysis (PCoA) was performed based on all SNPs after filtration. The first and second principal component was used as a D matrix of the above-mentioned association approach.

The kinship coefficient K_{ij} between inbreds i and j were calculated on the basis of all SNP markers according to:$K_{Tij} = \frac{S_{ij}-1}{1+T} + 1$, where S_{ij} was the proportion of marker loci with shared variants between inbreds i and j and T the average probability that a variant from one parent of inbred i and a variant from one parent of inbred j are alike in state, given that they are not identical by descent (Bernardo, 1993). For the series of T-values 0, 0.025, …, 0.975 **K** matrix between all inbreds was calculated. Negative kinship values between inbreds were set to 0. The optimum T-value was calculated according to Stich et al. (2008).

The R package EMMA Kang et al. (2008) was used to perform GWAS. The significance threshold of 0.001 and a false discovery rate (FDR) <10% were applied to test for significant associations between the traits and the SNP markers. The Bonferroni correction was used to adjust false positive rate in the multiple tests (Pocock et al., 1987). The FDR was calculated according to Benjamini and Hochberg (1995). For genome-wide studies with high density SNPs, one must consider the non-independence of SNPs because of linkage disequilibrium (LD) when interpreting statistical significance (Li et al., 2012). To achieve this, we followed Duggal et al. (2008) to randomly select 1 SNP per LD block in addition to all the SNPs outside of blocks. The p-values for these SNPs were used for calculation of the FDR. The significantly associated SNPs with Al tolerance within the LD decay distance (i.e., 500 kb from our previous study) was grouped as one QTL. The percentage of genotypic variation explained by the significant SNPs was calculated by $R^2_{LR} = 1 - \exp(-\frac{2}{n}(\log L_M - \log L_0))$, where exp is an exponential function, $\log L_M$ is the maximum log-likelihood of the model of interest, $\log L_0$ is the maximum log-likelihood of the intercept-only model, n is the number of observations (Sun et al., 2010).

Searching Candidate Genes

To validate our mapping results and find a robust set of candidate genes, we searched the flanking regions ± 500 kb (the maximum LD decay distance in the core collection) of the significant associated SNP loci with Al tolerance to find previously mapped QTLs from the Rice QTL Map database (http://qtaro.abr.affrc.go.jp/qtab/table). Similarly, we searched the flanking regions of the significant associated loci (±500 kb) with Al tolerance to find previously cloned/identified candidate genes related to Al tolerance from the QTARO database (http://qtaro.abr.affrc.go.jp/ogro/table). Because our measurement for Al tolerance was the relative root length with/without Al treatment, i.e., RRE, we think that the genes related to root development are corresponding to Al tolerance. Therefore, we mainly searched the candidate genes related to root development and Al tolerance within the searching regions. Aluminum tolerance genes identified by reverse genetics were found in the OryGenesDB (http://orygenesdb.cirad.fr/cgi-bin/searching.pl).

RESULTS

The landraces in the Ting's core collection have RRE values ranged from 0.22 to 0.95, indicating a large variation for Al tolerance. The phenotypic distribution of RRE showed a normal distribution, indicating that aluminum tolerance is a quantitively inherited trait. The broad-sense heritability was 88.73% for Al tolerance.

With SLAF sequencing approach, a total of 116,643 high-quality SLAFs were detected, with 24,889 polymorphic SLAF tags and a polymorphism rate of 21.34%. Each SLAF tag had an average coverage depth of 5.2×. The inner region of the polymorphic SLAF tags were further sequenced and a total of 67,511 SNPs were detected. After filtering the SNPs with missing data ≧20% across all genotypes and MAF ≦0.05, a total of 40,708 polymorphic SNPs were used for GWAS.

PCoA indicated that there were two clusters for the entire population (**Figure 1**), which was corresponding to their classification as *indica* and *japonica* types. Most of the kinship coefficients for any pair of landraces were zero (**Figures S1**, **S2**), indicating that these landraces are unrelated, which is due to that they were collected from a world-wide area and were from a core collection. There were also a few pairs of landraces showing high kinship coefficients.

A mixed linear model, i.e., PK model (Yu et al., 2006; Stich et al., 2008), which accounts for population structure and kinship, was used for GWAS for Al tolerance. To balance the false positive and negative rate, $p < 0.001$ and FDR <10% were used as the significant threshold to indicate whether a SNP was significantly associated with Al tolerance. The QQ plot indicated that the PK model effectively control the false positive (**Figure 2**). A total of 25 SNP regions were shown significantly associated with Al tolerance (**Table 1**, **Figure 3**, **Figures S3**, **S4**), but none of them reached the Bonferroni threshold (with a raw $p < 2.46 \times 10^{-8}$). They were located on chromosomes 1-4, 6-7, 9 and 11. The QTLs explained individually from 7.27 to 13.31% of the phenotypic variance. The fixed effect was ranged from 0.092 to 0.256. There were different number of QTLs on each chromosome ranged from 1 to 7. The number of significantly associated SNPs for each QTL ranged from 1 to 17. Among them, *qALT3.3* and *qALT7.2* were detected in both years data as well as the mean of both years. Most QTLs were detected with the mean of both years data. The beneficial alleles for each significant QTL and their genotype background were further examined (**Tables S2**, **S3**).

To validate the mapping results, two databases, i.e., QTARO database and OryGenesDB, were used to screen the previously cloned genes and mapped QTLs around the flanking regions ±500 kb of the significant associated SNP loci with Al tolerance. A total of three QTLs mapped in this study were mapped to the same regions as the previously mapped QTLs for Al tolerance (**Table 1**). The closest distance for the previously mapped QTLs to the QTLs in this study ranged from 60.15 to 446.02 kb.

A total of three QTLs in this study were co-localized with the previously clone/identified genes (**Table 1**), including the well-known Al tolerance gene *STAR1*. The candidate genes functions include Al tolerance, root growth, root development (e.g., root length, elongation, crown root). The closest distance for the candidate genes to QTLs in this study ranged from 3.85 to 449.75 kb.

Furthermore, one Al tolerance genes identified by mutation analysis from previous research, i.e., *Os02g49790.1*, was co-localized with the QTLs in this study (**Table 1**). The distance for the gene to the QTLs in this study is 264.06 kb. The gene has the

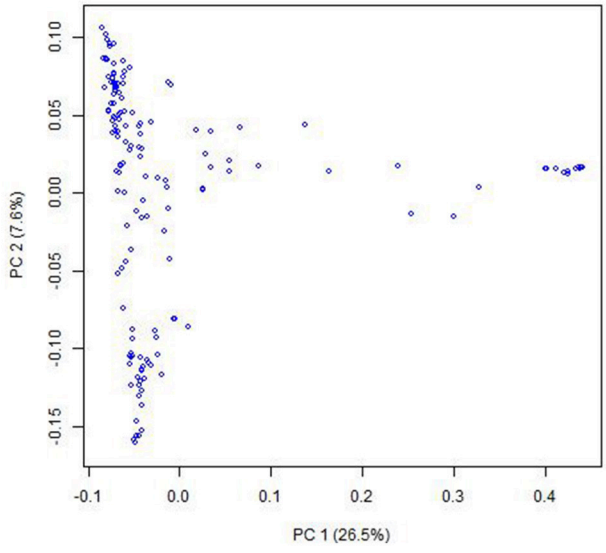

FIGURE 1 | Population structure of the Ting's core collection of rice landraces detected by Principal coordinate analysis. The principal coordinate analysis was based on the entire SNP set for the core collection. PC 1 and PC 2 refer to the first and second principal components, respectively. The number in the brackets indicated the percentage of genotypic variance explained by the principal components.

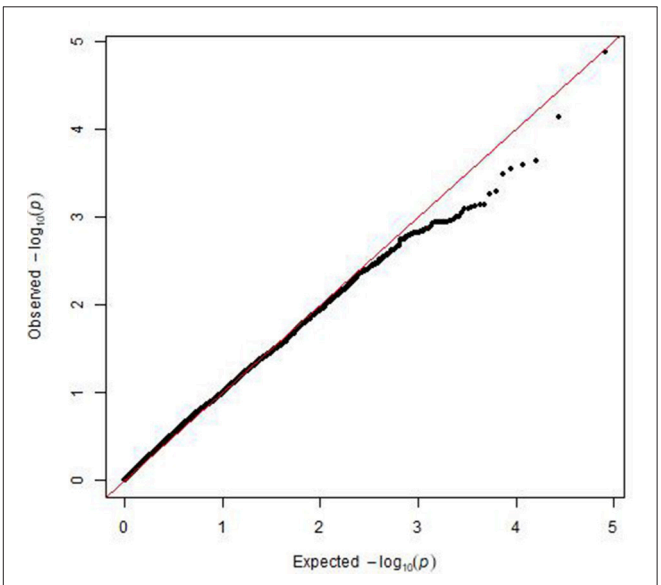

FIGURE 2 | Plot of observed vs. expected *P*-values by using MLM (PK) model for the genome-wide association mapping for aluminum tolerance.

TABLE 1 | Genome-wide association study (GWAS) results for aluminum tolerance and related candidate genes/previously mapped QTLs, where *PV%* is the explained percentage by quantitative trait locus (QTL) to phenotypic variation, FDR is the false discovery rate, and the information on the previously mapped QTLs were from the Rice QTL Map (http://qtaro.abr.affrc.go.jp/ogro/table), the information on the previously clone/identified genes were from the QTARO database (http://qtaro.abr.affrc.go.jp/ogro/table), alumium-activated malate transporter genes were from the OryGenesDB database (http://orygenesdb.cirad.fr/cgi-bin/searching.pl).

QTLs	Chr.	Position (bp)	*P*-value	*PV*%	Fixed effect	No. Significant SNPs	Previously mapped/clone genes	Closest distance to QTLs in this study (kb)	Previously mapped QTLs	Closest distance to QTLs in this study (kb)	FDR(%)
qALT1.1	1	5,170,120	0.000255	9.64%	0.128	10					8.51%
qALT1.2	1	11,375,341	0.000346	10.03%	0.153	6					9.33%
qALT1.3	1	13,652,501	7.38E-05	11.64%	−0.143	2					7.02%
qALT1.4	1	22,591,416	0.00016	10.81%	−0.146	3					6.54%
qALT1.5	1	24,383,999	0.000298	10.04%	0.119	2					6.54%
qALT1.6	1	41,150,101	9.27E-06	13.26%	−0.243	17	*OsFRDL4*	433.58	(Wu et al., 1999, 2000; Mao et al., 2004)	108.94	8.51%
qALT2.1	2	9,045,415	0.000952	7.89%	−0.165	1					9.40%
qALT2.2	2	29,749,048	0.000558	8.78%	0.231	5	*Os02g49790.1*	264.06			8.51%
qALT2.3	2	35,731,595	0.000735	8.56%	0.207	2					6.54%
qALT3.1	3	9,890,146	0.000986	7.76%	−0.128	1	*OsApx1*	3.85	(Zhang et al., 2016)	60.15	8.51%
qALT3.2	3	18,562,071	1.33E-05	13.31%	−0.150	6					6.54%
qALT3.3	3	19,197,531	7.22E-05	11.28%	0.256	11					6.54%
qALT3.4	3	20,589,044	0.000249	9.16%	−0.092	10					6.54%
qALT3.5	3	21,188,740	0.000129	11.44%	0.178	14					6.54%
qALT3.6	3	28,065,043	0.000574	8.29%	−0.142	2					9.33%
qALT3.7	3	36,959,662	0.000354	9.18%	0.164	2					6.54%
qALT4.1	4	1,751,622	0.000655	8.99%	−0.155	1					2.22%
qALT4.2	4	31,480,910	0.000235	9.85%	−0.172	2					2.22%
qALT6.1	6	27,430,269	0.000298	9.62%	0.171	3					9.40%
qALT6.2	6	30,477,271	0.000257	10.32%	−0.173	13	*STAR1*	449.75			2.15%
qALT7.1	7	8,865,818	0.000665	8.69%	0.172	2					9.40%
qALT7.2	7	25,216,755	0.000148	10.25%	−0.111	6					8.51%
qALT9.1	9	23,500,139	0.000229	9.60%	0.105	2					3.20%
qALT11.1	11	4,955,718	0.001512	7.27%	0.126	9			(Xue et al., 2007)	446.02	9.40%
qALT11.2	11	17,203,545	0.000448	9.48%	−0.135	1					9.40%

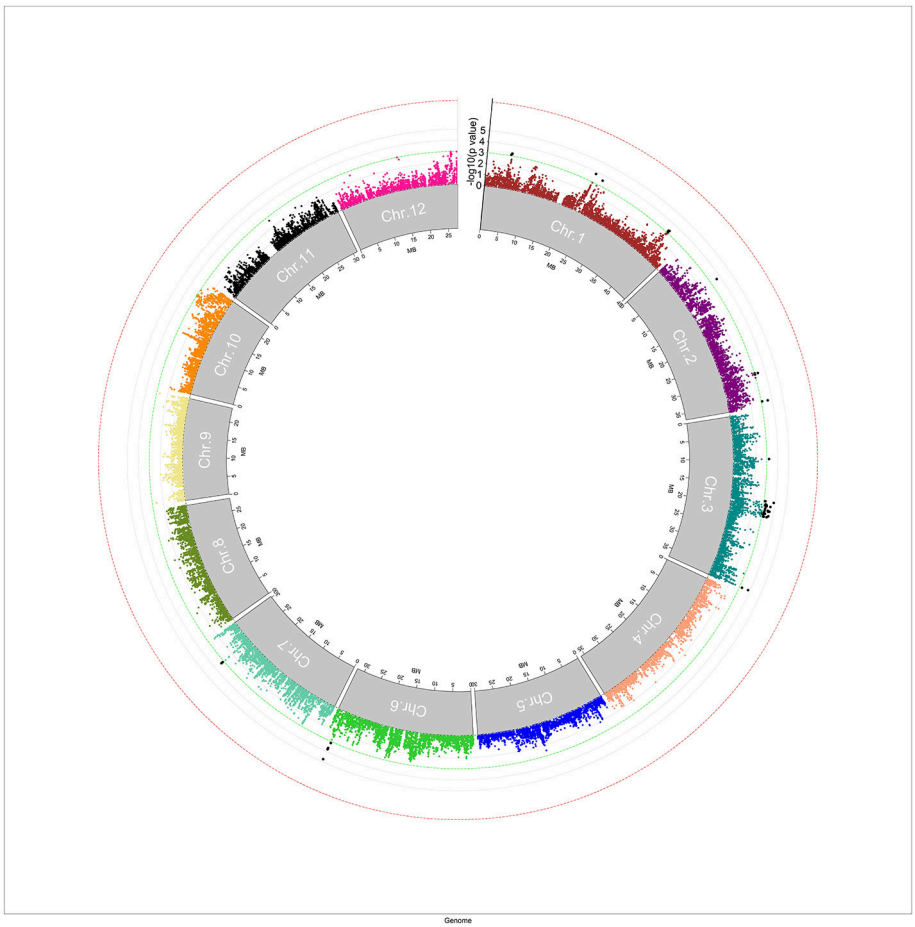

FIGURE 3 | Manhattan plot for genome-wide association study (GWAS) for aluminum tolerance measured by means of relative root elongation length (RRE). The green line indicated the significant threshold at $p < 0.001$, and the red line indicated the Bonferroni significant threshold at $p < 0.001$ (with a raw $p < 2.46 \times 10^{-8}$).

function as aluminum-activated malate transporter or aluminum resistance protein.

In total, five of 25 QTLs identified in this study were co-localized with the previously cloned genes or previously identified QTLs related to Al tolerance and root traits.

DISCUSSIONS

Asian cultivated rice (*Oryza sativa*) was domesticated from its wild relative *O. rufipogon* (Kovach et al., 2007; Sang and Ge, 2007). Because of domestication and artificial selection of rice, genetic diversity has been remarkably reduced in many cases, and favorable alleles or genes might have been lost in the modern cultivars. Rice landraces are the intermediate form between modern cultivars and their ancestral species. Because of the less impact by artificial selection, landraces contain abundant genetic diversity and useful beneficial genes for modern cultivars. Moreover, transfer of beneficial genes from the intermediate forms to modern cultivars is considerably easier than from the ancestral wild species. Therefore, the identification and utilization of valuable genetic resources in landraces can be highly valuable for the genetic improvement of modern rice cultivars, for example, breeding varieties for Al tolerance.

The Ting's core collection of rice landraces is one of the earliest rice collection in China. Our previous studies indicated that two subgroups were presented in Ting's core collection, corresponding to *indica* and *japonica* subspecies (Zhang et al., 2011). Association studies were performed with 274 SSR markers for important agronomic trait and Al tolerance (Zhang et al., 2014, 2016), which confirmed that the core collection is a good population to map natural variations existing in the rice landraces. Compared to this study, a total of three QTLs, i.e., *qALT1.1, qALT3.1*, and *qALT3.2*, were identified in both our results and the previous research of Zhang et al. (2016). The closest distance for the QTL of Zhang et al. (2016) to the QTLs in this study ranged from 60.15 to 623.69 kb. In addition, there were three QTLs in the research of Zhang et al. (2016) having a distance between 1.7 and 2 Mb (about 8 cM) to the QTLs in this study. However, the mapping results were limited by the numbers of markers used in the previous studies. Because of its high-throughput and cost-effective nature, SLAF-seq is an

ideal method for genotyping by sequencing and hence has been applied in this study. This method allowed us to obtain a total of 67,511 high-quality SNPs, which provide good foundation for our GWAS in this study.

In this study, we detected a total of 25 QTLs for Al tolerance (**Table 1**). The significant associations were distributed 8 of 12 chromosomes in rice, which was in accordance with the research of Famoso et al. (2011). The QTLs explained individually from 7.27 to 13.31% of the phenotypic variance in this study, which was smaller than those in research of Nguyen et al. (2003) and Famoso et al. (2011), while it was larger than that in research of Xue et al. (2007). This might be explained by different mapping populations used in the aforementioned studies and the total phenotypic variation were different. A total of 5 from 25 QTLs in this study were co-localized with the previously cloned genes or previously identified QTLs related to Al tolerance and root traits (**Table 1**), which was similar with the research of Famoso et al. (2011).

Huang C. F. et al. (2009) and Huang X. H. et al. (2009) found two genes, i.e., *STAR1* and *STAR2*, responsible for Al tolerance in rice. The QTL *qALT6.2* was co-localized with *STAR1* with a minimum distance of 449.75 kb. Moreover, *qALT6.2* was also co-localized with other two candidate genes *OsHMA2* and *OsPTR9* with a minimum distance of 61 and 237.92 kb, respectively, which have the function of Zn and Cd translocation, and lateral root formation.

Furthermore, the *qALT1.1* in this study located at 938.62 kp away from the Al tolerance gene *OsCDT3*, which was identified by knockdown method (Xia et al., 2013). This QTLs was at 623.69 kb away from a previous mapped Al tolerance QTL (Zhang et al., 2016). The *qALT1.6* in this study was co-localized with a candidate gene, i.e., *OsFRDL4* with a distance of 433.58 kb (**Table 1**). *OsFRDL4* is an Al tolerance gene identified by mutant method (Yokosho et al., 2011). Moreover, this QTL was co-localized with QTLs for Al tolerance identified by some previous researches (Wu et al., 1999, 2000; Mao et al., 2004) (**Table 1**) with a minimum distance of 108.94 kb.

The QTL *qALT2.2* was co-localized with an aluminum-activated malate transporter gene (*Os02g49790.1*) with a minimum distance of 264.06 kb (**Table 1**). A previous mapped QTL associated with arsenic accumulation was located 228.11 kb away (Zhang et al., 2008), which implied that the mechanism of tolerance to metal ion (for example, Fe, As, Zn, Cd, etc) might have a similar metabolism way. The explanation could be supported by the observation that several candidate genes co-localized with the QTLs in this study have the functions on Fe and Cadmium uptake, Zn and Cd translocation, etc. The QTL *qALT3.1* was co-localized with an Al tolerant QTL (Zhang et al., 2016).

It is interesting that the regions between 18,562,071 and 21,188,740 on chromosome 3 showed several peaks (the number of significant SNPs ranged from 6 to 14), corresponding to *qALT3.2, qALT3.3, qALT3.4*, and *qALT3.5*, significantly associated with Al tolerance in this study. However, only six candidate genes were identified within this region from the *QTARO* database and only one candidate gene was related to Cadmium and Iron uptake. No candidate genes were identified to associate with Al or other metal ion tolerance. As the mapping results in this study were highly significant, this region as well as other QTLs (*qALT1.2, qALT1.5, qALT2.3, qALT3.6, qALT3.7, qALT4.1, qALT6.1*, and *qALT9.1*) in this study where no candidate genes/previous mapped QTLs were found, could be new loci for Al tolerance and required further research.

AUTHOR CONTRIBUTIONS

JL and MZ designed the study. MZ, JS, AW, and TH performed SLAF-seq experiment and data analyses. JL performed GWAS and statistical analyses. MZ, JL, and JS performed searching candidate genes/QTLs. JL wrote the paper. All authors read and approved the final manuscript.

FUNDING

This work was supported by Fund of the National Natural Science Foundation of China grant 30700494, 31430062, National Natural Science Foundation of Liaoning province (201602670) and the National Key Research and Development Program of China (2016YFD0200707).

ACKNOWLEDGMENTS

We are grateful to Dr. Peng Zhang from South China Agricultural University (SCAU) for providing aluminum tolerance measurement data, to Dr. Xiaoling Li, Dr. Xuelin Fu, and Prof. Xiangdong Liu for their assistance in the experiment, to Academician Prof. Yonggen Lu from SCAU and Academician Prof. Wenfu Chen from Shenyang agricultural university (SYAU) for their useful instructions.

SUPPLEMENTARY MATERIAL

The Supplementary Material for this article can be found online at: https://www.frontiersin.org/articles/10.3389/fpls.2018.01838/full#supplementary-material

Figure S1 | Kinship distribution for the landraces in the Ting's core collection.

Figure S2 | Kinship distribution for the landraces in the Ting's core collection, where the kinship coefficient equal to zero were excluded.

Figure S3 | Manhattan plot for genome-wide association study (GWAS) for aluminum tolerance measured by relative root elongation length (RRE) in 2008. The green line indicated the significant threshold at $p < 0.001$, and the red line indicated the Bonferroni significant threshold at $p < 0.001$ (with a raw $p < 2.46 \times 10^{8}$).

Figure S4 | Manhattan plot for genome-wide association study (GWAS) for aluminum tolerance measured by relative root elongation length (RRE) in 2009. The green line indicated the significant threshold at $p < 0.001$, and the red line indicated the Bonferroni significant threshold at $p < 0.001$ (with a raw $p < 2.46 \times 10^{-8}$).

Table S1 | Variety names, origin, and classification of *indica-japonica* for the 150 accessions of rice landraces in the Ting's core collection, where TI, IC, TJ, JC represent typical *indica*, *indica*-clined, typical *japonica*, *japonica*-clined rice, respectively.

Table S2 | SNP data for significant QTLs for each genotype with their relative root elongation length (RRE) values.

Table S3 | Allelic effect for the significant QTLs.

REFERENCES

Benjamini, Y., and Hochberg, Y. (1995). Controlling the false discovery rate: a practical and powerful approach to multiple testing. *J. Royal Stat. Soc. Ser. B* 57, 289–300.

Bernardo, R. (1993). Estimation of coefficient of coancestry using molecular markers in maize. *Theor. Appl. Genet*. 85, 1055–1062. doi: 10.1007/BF00215047

Cai, M., Zhang, S., Xing, C., Wang, F., Ning, W., and Lei, Z. (2011). Developmental characteristics and aluminum resistance of root border cells in rice seedlings. *Plant Sci.* 180, 702–708. doi: 10.1016/j.plantsci.2011.01.017

Chen, Z. C., Yamaji, N., Motoyama, R., Nagamura, Y., and Ma, J. F. (2012). Up-regulation of a magnesium transporter gene OsMGT1 is required for conferring aluminum tolerance in rice. *Plant Physiol.* 159, 1624–1633. doi: 10.1104/pp.112.199778

Delhaize, E., Ma, J. F., and Ryan, P. R. (2012). Transcriptional regulation of aluminum tolerance genes. *Trends Plant Sci.* 17, 341–348. doi: 10.1016/j.tplants.2012.02.008

Duggal, P., Gillanders, E. M., Holmes, T. N., and Bailey-Wilson, J. E. (2008). Establishing an adjusted *p*-value threshold to control the family wide type 1 error in genome wide association studies. *BMC Genomics* 9:516. doi: 10.1186/1471-2164-9-516

Famoso, A. N., Clark, R. T., Shaff, J. E., Craft, E., McCouch, S. R., and Kochian, L. V. (2010). Development of a novel aluminum tolerance phenotyping platform used for comparisons of cereal aluminum tolerance and investigations into rice aluminum tolerance mechanisms. *Plant Physiol.* 153, 1678–1691. doi: 10.1104/pp.110.156794

Famoso, A. N., Zhao, K., Clark, R. T., Tung, C. W., Wright, M. H., Bustamante, C., et al. (2011). Genetic architecture of aluminum tolerance in rice (*Oryza sativa*) determined through genome-wide association analysis and QTL mapping. *PLoS Genet.* 7:e1002221. doi: 10.1371/journal.pgen.1002221

Fu, X., Chen, W., Pan, C., Feng, J., Liu, X., and Lu, Y. (2010). A comparative study on aluminum tolerance between *Oryza sativa* and *O.rufipogon* in Gaozhou. *Sci. Agric. Sin.* 4, 661–669.

Huang, C. F., Yamaji, N., Chen, Z., and Ma, J. F. (2012). A tonoplast-localized half-size ABC transporter is required for internal detoxification of aluminum in rice. *Plant J.* 69, 857–867. doi: 10.1111/j.1365-313X.2011.04837.x

Huang, C. F., Yamaji, N., Mitani, N., Yano, M., Nagamura, Y., and Ma, J. F. (2009). A bacterial-type ABC transporter is involved in aluminum tolerance in rice. *Plant Cell* 21, 655–667. doi: 10.1105/tpc.108.064543

Huang, X., Feng, Q., Qian, Q., Zhao, Q., Wang, L., Wang, A. et al. (2009). High-throughput genotyping by whole-genome resequencing. *Genome Res.* 19:1068. doi: 10.1101/gr.089516.108

Huang, X., Wei, X., Sang, T., Zhao, Q., Feng, Q., et al. (2010). Genome-wide association studies of 14 agronomic traits in rice landraces. *Nat. Genet.* 42, 961–967. doi: 10.1038/ng.695

Kang, H. M., Zaitlen, N. A., Wade, C. M., Kirby, A., Heckerman, D., Daly, M. J., et al.,(2008). Efficient control of population structure in model organism association mapping. *Genetics* 178, 1709–1723. doi: 10.1534/genetics.107.080101

Khatiwada, S. P., Senadhira, D., Carpena, A. L., Zeigler, R. S., and Fernandez, P. G. (1996). Variability and genetics of tolerance for aluminum toxicity in rice (Oryza sativa L.). *Theor. Appl. Genet.* 93, 738–744. doi: 10.1007/BF00224070

Kovach, M. J., Sweeney, M. T., and Mccouch, S. R. (2007). New insights into the history of rice domestication. *Trends Genet.* 23, 578–587. doi: 10.1016/j.tig.2007.08.012

Li, J., and Zhang, P. (2012). "Assessment and utilization of the genetic diversity in rice," in *Genetic Diversity in Plants*, ed M. Caliskan (London: InTech-Open Access Publisher), 87–102. doi: 10.5772/2640

Li, J. Y., Liu, J., Dong, D., Jia, X., McCouch, S. R., and Kochian, L. V. (2014). Natural variation underlies alterations in Nramp aluminum transporter (NRAT1) expression and function that play a key role in rice aluminum tolerance. *Proc. Natl. Acad. Sci. U. S. A.* 111, 6503–6508. doi: 10.1073/pnas.1318975111

Li, M. X., Yeung, J. M. Y., Cherny, S. S., and Sham, P. C. (2012). Evaluating the effective numbers of independent tests and significant *p*-value thresholds in commercial genotyping arrays and public imputation reference dataset. *Hum. Genet.* 131, 747–756. doi: 10.1007/s00439-011-1118-2

Li, X., Lu, Y., Li, J., Xu, H., and Shahid, M. (2011). Strategies on sample size determination and qualitative and quantitative traits integration to construct core collection of rice (*Oryza sativa*). *Rice Sci.* 18, 46–55. doi: 10.1016/S1672-6308(11)60007-3

Liu, J., Luo, X., Shaff, J., Liang, C., Jia, X., Li, Z., et al. (2012). A promoter-swap strategy between the AtALMT and AtMATE genes increased *Arabidopsis* aluminum resistance and improved carbon-use efficiency for aluminum resistance. *Plant J.* 71, 327–337. doi: 10.1111/j.1365-313X.2012.04994.x

Ma, J. F., and Furukawa, J. (2003). Recent progress in the research of external Al detoxification in higher plants: a mini review. *J. Inorg. Biochem.* 97, 46–51. doi: 10.1016/S0162-0134(03)00245-9

Mao, C., Yi, K., Yang, L., Zheng, B., Wu, Y., Liu, F., et al. (2004). Identification of aluminum-regulated genes by cDNA-AFLP in rice (*Oryza sativa* L.): aluminum-regulated genes for the metabolism of cell wall components. *J. Exp. Bot.* 55, 137–143. doi: 10.1093/jxb/erh030

Nguyen, B. D., Brar, D. S., Bui, B. C., Nguyen, T. V., Pham, L. N., and Nguyen, H. T. (2003). Identification and mapping of the QTL for aluminum tolerance introgressed from the new source, *Oryza Rufipogon* Griff., into *indica* rice (*Oryza sativa* L.). *Theor. Appl. Genet.* 106, 583–593. doi: 10.1007/s00122-002-1072-4

Nguyen, V. T., Nguyen, B. D., Sarkarung, S., Martinez, C., Paterson, A. H., and Nguyen, H. T. (2002). Mapping of genes controlling aluminum tolerance in rice: comparison of different genetic backgrounds. *Mol. Genet. Genomics* 267, 772–780. doi: 10.1007/s00438-002-0686-1

Pocock, S. J., Geller, N. L., and Tsiatis, A. A. (1987). The analysis of multiple endpoints in clinical traits. *Biometric* 43, 487–498. doi: 10.2307/2531989

Sang, T., and Ge, S. (2007). Genetics and phylogenetics of rice domestication. *Curr. Opin. Genet. Dev.* 17, 533–538. doi: 10.1016/j.gde.2007.09.005

Song, J., Li, J., Sun, J., Hu, T., Liu, S., Wang, W., et al. (2018). Genome-wide association mapping for cold tolerance in a core collection of rice (*Oryza sativa* L.) landraces by using high-density single nucleotide polymorphism markers from specific-locus amplified fragment sequencing. *Front Plant Sci.* 9:875. doi: 10.3389/fpls.2018.00875

Stich, B., Möhring, J., Piepho, H., Heckenberger, M., Buckler, E. S., and Melchinger, A. E. (2008). Comparison of mixed-model approaches for association mapping. *Genetics* 178, 1745–1754. doi: 10.1534/genetics.107.079707

Sun, G., Zhu, C., Kramer, M. H., Yang, S. S., Song, W., Piepho, H. P., and Yu, J. (2010). Variation explained in mixed-model association mapping. *Heredity* 105, 33–340. doi: 10.1038/hdy.2010.11

Sun, X., Liu, D., Zhang, X., Li, W., Liu, H., Hong, W., et al. (2013). SLAF-seq: an efficient method of large-scale *de novo* SNP discovery and genotyping using high-throughput sequencing. *PLoS ONE* 8:e58700. doi: 10.1371/journal.pone.0058700

Vonuexkull, H. R., and Mutert, E. (1995). Global extent, development and economic-impact of acid soils. *Plant Soil* 171, 1–15. doi: 10.1007/BF00009558

Wu, P., Liao, C. Y., Hu, B., Yi, K. K., Jin, W. Z., Ni, J. J., et al. (2000). QTLs and epistasis for aluminum tolerance in rice (*Oryza sativa* L.) at different seedling stages. *Theor. Appl. Genet.* 100, 1295–1303. doi: 10.1007/s001220051438

Wu, P., Liao, C. Y., Hu, B., Yi, K. K., Wei, J., Ni, J. J., et al. (1999). Genetic analysis for aluminum tolerance in rice (*Oryza sativa* L.) via molecular markers. *Rice Genet. Newslett.* 16, 48–51.

Xia, J., Yamaji, N., and Ma, J. F. (2013). A plasma membrane-localized small peptide is involved in rice aluminum tolerance. *Plant J.* 76, 345–355. doi: 10.1111/tpj.12296

Xu, H. S., Gu, W. L., Dong, D. F., and Peng, X. X. (2004). Differential resistance of two subtropical rice cultivars to aluminum toxicity. *J. Plant Nutr.* 27, 1601–1609. doi: 10.1081/PLN-200026003

Xue, Y., Jiang, L., Su, N., Wang, J. K., Deng, P., Ma, J. F., et al. (2007). The genetic basic and fine-mapping of a stable quantitative-trait loci for aluminum tolerance in rice. *Planta* 227, 255–262. doi: 10.1007/s00425-007-0613-0

Yang, Q., Wang, Y., Zhang, J., Shi, W., Qian, C., and Peng, X. (2007). Identification of aluminum-responsive proteins in rice roots by a proteomic approach: cysteine synthase as a key player in Al response. *Proteomics* 7, 737–749. doi: 10.1002/pmic.200600703

Yokosho, K., Yamaji, N., and Ma, J. F. (2011). An Al-inducible MATE gene is involved in external detoxification of Al in rice. *Plant J.* 68, 1061–1069. doi: 10.1111/j.1365-313X.2011.04757.x

Yu, J., Pressoir, G., Briggs, W. H., Bi, I. V., Yamasaki, M., et al. (2006). A unified mixed-model method for association mapping that accounts for multiple levels of relatedness. *Nat. Genet.* 38, 203–208. doi: 10.1038/ng1702

Zhang, J., Zhu, Y. G., Zeng, D. L., Cheng, W. D., Qian, Q., and Duan, G. L. (2008). Mapping quantitative trait loci associated with arsenic accumulation in rice (*Oryza sativa*). *New Phytol.* 177, 350–355. doi: 10.1111/j.1469-8137.2007.02267.x

Zhang, P., Li, J., Li, X., Liu, X., Zhao, X., and Lu, Y. (2011). Population structure and genetic diversity in a rice core collection (*Oryza sativa* L.) investigated with SSR markers. *PLoS ONE* 6:e27565. doi: 10.1371/journal.pone.0027565

Zhang, P., Liu, X., Tong, H., Lu, Y., and Li, J. (2014). Association mapping for important agronomic traits in core collection of rice (*Oryza sativa* L.) with SSR markers. *PLoS ONE* 9:e111508. doi: 10.1371/journal.pone.0111508

Zhang, P., Zhong, K., Tong, H., Shahid, M., and Li, J. (2016). Association mapping for aluminum tolerance in a core collection of rice landraces. *Front. Plant Sci.* 7:1415. doi: 10.3389/fpls.2016.01415

Zhu, C. S., Gore, M., Buckler, E. S., and Yu, J. M. (2008). Status and prospects of association mapping in plants. *Plant Genome* 1, 5–20. doi: 10.3835/plantgenome2008.02.0089

Conflict of Interest Statement: The authors declare that the research was conducted in the absence of any commercial or financial relationships that could be construed as a potential conflict of interest.

frontiers in Plant Science

ORIGINAL RESEARCH
published: 15 October 2018
doi: 10.3389/fpls.2018.01334

Assessing How the Aluminum-Resistance Traits in Wheat and Rye Transfer to Hexaploid and Octoploid Triticale

Peter R. Ryan[1], Dengfeng Dong[1,2], Felix Teuber[1], Neele Wendler[1,3], Karl H. Mühling[3], Jie Liu[1,4], Muyun Xu[1], Naike Salvador Moreno[1,5†], Jiangfeng You[6], Hans-Peter Maurer[7], Walter J. Horst[8] and Emmanuel Delhaize[1]*

[1] CSIRO Agriculture and Food, Canberra, ACT, Australia, [2] College of Agriculture, Guangxi University, Nanning, China, [3] Institute of Plant Nutrition and Soil Science, Kiel University, Kiel, Germany, [4] College of Agronomy, Sichuan Agricultural University, Chengdu, China, [5] Department of Genetics, Faculty of Biology, Universidad Complutense, Madrid, Spain, [6] Laboratory of Soil and Plant Molecular Genetics, College of Plant Science, Jilin University, Changchun, China, [7] State Plant Breeding Institute, Universitaet Hohenheim, Stuttgart, Germany, [8] Institute for Plant Nutrition, Leibniz University Hanover, Hanover, Germany

OPEN ACCESS

Edited by:
Meixue Zhou,
University of Tasmania, Australia

Reviewed by:
Atanas Ivanov Atanassov,
Joint Genomic Center, Bulgaria
Gaofeng Zhou,
Murdoch University, Australia

***Correspondence:**
Peter R. Ryan
peter.ryan@csiro.au

†Present Address:
Naike Salvador Moreno,
Department of Cancer Biology and Comprehensive Cancer Center, Wake Forest University School of Medicine, Winston-Salem, NC, United States

Specialty section:
This article was submitted to Plant Abiotic Stress, a section of the journal Frontiers in Plant Science

Received: *30 April 2018*
Accepted: *24 August 2018*
Published: *15 October 2018*

Citation:
Ryan PR, Dong D, Teuber F, Wendler N, Mühling KH, Liu J, Xu M, Salvador Moreno N, You J, Maurer H-P, Horst WJ and Delhaize E (2018) Assessing How the Aluminum-Resistance Traits in Wheat and Rye Transfer to Hexaploid and Octoploid Triticale. Front. Plant Sci. 9:1334. doi: 10.3389/fpls.2018.01334

The mechanisms of aluminum (Al) resistance in wheat and rye involve the release of citrate and malate anions from the root apices. Many of the genes controlling these processes have been identified and their responses to Al treatment described in detail. This study investigated how the major Al resistance traits of wheat and rye are transferred to triticale (x *Tritosecale* Wittmack) which is a hybrid between wheat and rye. We generated octoploid and hexaploid triticale lines and compared them with the parental lines for their relative resistance to Al, organic anion efflux and expression of some of the genes encoding the transporters involved. We report that the strong Al resistance of rye was incompletely transferred to octoploid and hexaploid triticale. The wheat and rye parents contributed to the Al-resistance of octoploid triticale but the phenotypes were not additive. The Al resistance genes of hexaploid wheat, *TaALMT1*, and *TaMATE1B*, were more successfully expressed in octoploid triticale than the Al resistance genes in rye tested, *ScALMT1* and *ScFRDL2*. This study demonstrates that an important stress-tolerance trait derived from hexaploid wheat was expressed in octoploid triticale. Since most commercial triticale lines are largely hexaploid types it would be beneficial to develop techniques to generate genetically-stable octoploid triticale material. This would enable other useful traits that are present in hexaploid but not tetraploid wheat, to be transferred to triticale.

Keywords: roots, acid soil, malate, citrate, *Secale cereale*, *Triticum aestivum*

INTRODUCTION

Many important crop species are stable allopolyploids resulting from hybridisations between two separate but related species. Triticale (× Triticosecale Wittmack) is an allopolyploid because it is a hybrid between rye (*Secale cereale* L.) and wheat (*Triticum aestivum* L.). Triticale is a valuable grain crop that combines useful traits from wheat and rye. Wheat has greater yield and superior grain quality while rye is a forage crop with outstanding resistance to many biotic and abiotic stresses

including pathogens, low nutrient availability, soil pH and low temperatures. Wheat is typically used as the female parent and rye as the male parent because crosses are more stable if female plants have the larger ploidy of the two parents. The grain from this hybridisation are often sterile so the zygote from this cross is treated with colchicine to induce polyploidy and improve fertility (Mergoum and Gómez-Macpherson, 2004). When rye (diploid with genome RR) is hybridized with a hexaploid or bread wheat (hexaploid with genome AABBDD) the result is an "octoploid" triticale (AABBDDRR). When rye is hybridized with a tetraploid wheat (AABB) the result is a "hexaploid" triticale (AABBRR). Therefore triticale is amphidiploid meaning that it is diploid for the two parental genomes. Commercial triticale lines are mostly second generation hexaploid types because they often show better stability and performance than the octoploid types (Mergoum and Gómez-Macpherson, 2004).

Aluminum (Al) toxicity is a major limitation to crop production on acid soils because the concentration of soluble trivalent cations (Al^{3+}) increases when soil pH falls below ∼4.5. Many species show a significant genotypic variation in resistance to Al stress and this is also the case for rye and bread wheat but not for durum wheat which is very sensitive of Al. Rye is among the most Al-resistant cereal species along with rice (*Oryza sativa* L.). Aniol and Gustafson (1984) investigated the Al resistance of triticale, wheat and rye and concluded that Al resistance of the wheat parent was an important determinant of the Al resistance of triticale. They also found that the strong resistance of rye was partially suppressed in the hybrid. When that report was published little information was available on the mechanisms of Al resistance in any plant species. It was later revealed that the major mechanisms for Al resistance in wheat and rye involve the release or efflux of malate and citrate anions from the root apices (Li et al., 2000; Ma et al., 2000; Delhaize et al., 2007; Stass et al., 2008; Ryan et al., 2011). Stass et al. (2008) compared contrasting genotypes of wheat and rye with the triticale hybrids and concluded that the Al resistance of triticale was mostly determined by citrate efflux, a trait that was largely controlled by the wheat genome.

Differences in malate efflux account for most of the genotypic variation in Al resistance in bread wheat but citrate efflux is important when malate efflux is absent (Ryan et al., 2009). Malate efflux is facilitated by an anion channel encoded by the *aluminum-activated malate transporter*, *TaALMT1*, gene on chromosome 4DL (Sasaki et al., 2004; Raman et al., 2005). Al-resistant genotypes show a greater constitutive expression of *TaALMT1* in the root apices than sensitive genotypes which is not affected by Al treatment. However, the TaALMT1 protein requires Al^{3+} cations to trigger the malate release which means Al rapidly activates malate release (Sasaki et al., 2004). This rapid activation has been described as a Type I response which is consistent with the channel proteins being constitutively expressed and activated by Al (Ma et al., 2001). Citrate release from bread wheat is controlled by TaMATE1B, a transporter from the *multidrug and toxic compound exudation* (MATE) family (Ryan et al., 2009; Tovkach et al., 2013). TaMATE1B is encoded by a gene on chromosome 4BL. The greater citrate efflux is caused by a transposable element-like insertion near the transcription start site of *TaMATE1B* which results in a greater level of constitutive expression (Tovkach et al., 2013).

Members of these two gene families also control the release of malate and citrate from rye. Fontecha et al. (2007) identified a rye homolog of the wheat *TaALMT1* gene on chromosome 7RS and showed that its expression was induced by Al to a greater degree in the resistant cultivar *Ailés* than the sensitive cultivar *Riodeva*. Quantitative trait loci (QTL) for Al resistance were subsequently linked to this same region in two separate rye populations (Benito et al., 2005; Matos et al., 2005; Collins et al., 2008; Silva-Navas et al., 2012). In one of these populations, generated from the *M39A-1-6* (resistant) and *M77A-1* (sensitive) haplotypes, a cluster of *ScALMT* genes and one *ScMATE* gene was located on the 7RS locus (Collins et al., 2008). The resistant parent had five copies of the *ScALMT* gene and expression of two of these (*ScALMT1-M39.1* and *ScALMT1-M39.2*) was induced by Al in the root apices. By contrast, the sensitive parent had two copies of the *ScALMT* gene but only one (*ScALMT1-M77.1*) was induced by Al (Collins et al., 2008). Collins et al. (2008) was able to segregate the *MATE* gene from the resistance locus indicating that it was not contributing to the variation in Al resistance of that population. Those authors concluded that the *ScALMT* genes on 7RS controlled the Al-dependent efflux of malate from rye.

The first *MATE* gene in rye associated with citrate efflux from roots was the *ferric reductase-like 2* gene (*ScFRDL2*) (Yokosho et al., 2010). The expression of *ScFRDL2* in the roots was induced 15-fold by 50 μM Al and closely coincided with the Al-dependent changes in citrate efflux. Another *MATE* gene identified in the same study, *ScFRDL1*, was considered unlikely to be involved in Al resistance because it was induced by iron deficiency and not by Al treatment (Yokosho et al., 2010). Silva-Navas et al. (2012) later examined the population generated from *Ailés* and *Riodeva* and mapped a *MATE* gene which they named *aluminum-activated citrate transporter 1* (*ScAACT1*) in the Al-resistance QTL on chromosome 7RS. The authors proposed that *ScAACT1*, *ScFRDL1*, and *ScMATE* are all the same gene but this conclusion remains uncertain. For example, unlike *ScAACT1*, expression of *ScFRDL1* was not induced by Al treatment according to Yokosho et al. (2010) and the Al resistance QTL excluded the *MATE* gene in the population described by Collins et al. (2008). Silva-Navas et al. (2012) argued that these inconsistencies could be explained partly by differences in the parental lines and partly by differences in the length of treatments and Al concentrations used. Whereas Yokosho et al. (2010) used 50 μM Al treatments over 12 h, Silva-Navas et al. (2012) used 300 μM Al treatment over 24 h. The relatedness of these *MATE* genes requires further clarification.

The aim of the present study was to examine how well the Al-resistance traits in the wheat and rye parental lines were transferred to the allopolyploid triticale. Two sets of diverse lines were used for this purpose. One set included octoploid triticale lines generated from an Al-resistant rye and hexaploid wheat. The second set included hexaploid triticale lines generated by crossing a durum line with rye. Measurements were made of relative Al resistance, anion efflux and expression of selected Al-resistance genes in the parental material and triticale lines.

MATERIALS AND METHODS

Genetic Material

Two sets of germplasm were used in the experiments (**Table 1**). The first set included two wheat cultivars, *Carazhino* and *Egret*, an Al-resistant rye line, ***L185***, and two second generation octoploid triticale lines generated from these wheat and rye parents. The triticale lines are depicted as *Carazinho*x***L185*** and *Egret*x***L185***. *Carazinho* is a highly Al-resistant wheat cultivar from Brazil that shows the Al-activated malate efflux controlled by *TaALMT1* and the constitutive release of citrate controlled by *TaMATE1B*. *Egret* is Al-sensitive and shows little or no organic anion efflux with or without Al treatment. The second set of germplasm included a tetraploid (durum) wheat named *5020-30,* an Al-resistant rye, ***390***, and a closely-related but Al-sensitive rye, ***389***, and the two primary hexaploid triticale lines derived from crossing these parents designated as *5020-30*x***390*** and *5020-30*x***389***. The triticale lines were generated at the University of Hohenheim, Germany.

Aluminum Resistance

Seeds were germinated for 2 days on moist filter paper and then planted over 20 L of aerated nutrient solution on laboratory benches. To estimate relative root length (RRL) the length of the longest root was measured before and after 4 days growth in the same nutrient solution with different Al concentrations. Therefore RRL was calculated as (net root growth in Al treatment net root growth in control solution) $\times$ 100.

Measurement of Citrate and Malate Efflux

The measurement of organic anion efflux from intact seedlings followed the procedures described previously (Delhaize et al., 1993; Ryan et al., 1995; Wang et al., 2007). Briefly, seeds were surface sterilized with bleach and thoroughly rinsed in sterile water. In preliminary experiments the seedlings were grown in aerated 20 L tubs with nutrient solution (pH 4.4) or in sterile conical flasks with 20 mL of 0.2 mM $CaCl_2$ (pH 4.3) on a rotary shaker and exudates collected from excised roots. The large volume of the tubs maintained the root relatively free of microbial contamination and so both growth methods gave similar exudate results. Only results from the tubs are presented here. The excised root segments (eight to twelve per replicate) were washed in small vials with 1 mL of control solution (0.2 mM $CaCl_2$, pH 4.3) for 1 h on a platform shaker (60 rpm). The solutions were rinsed and replaced by 1 mL of treatment solution (control solution with or without 40 μM $AlCl_3$) and returned to the shaker for 2 h. After 2 h collection the malate and citrate concentrations in each solution were estimated enzymatically as described by Ryan et al. (1995). Malate assays used 0.1 mL of each sample and citrate assay used the remaining 0.9 mL. For the citrate assays the solutions were dried on a rotary vacuum drier and resuspended in 80 μL of assay solution as described by Ryan et al. (2009). All chemicals were obtained from Sigma-Aldrich Pty. Ltd. (Castle Hill, Australia). The concentrations were corrected to obtain the original malate and citrate contents in each sample and efflux was standardized for the number of apices and time of collection. In other experiments half of the seedlings were pretreated with 30 μM $AlCl_3$ for at least 24 h prior to measurements as described in the figure legends.

Measurements of Gene Expression

RNA was extracted from the root apices with the RNeasy PlantMini Kit (Qiagen) after grinding tissues in liquid nitrogen. cDNA was synthesized with the SuperScript III First-Strand Synthesis System (Invitrogen) as recommended using 1 μg RNA of each extraction. Gene expression was determined by qRT-PCR using the SYBR Green Supermix (Bio-Rad) kit on a Bio-Rad CFX96 Real Time System. Data were analyzed with the Bio-Rad CFX Manager software. The primers selected for measuring the expression of the Al-resistance genes in wheat and rye were specific for those genes and did not hybridize with sequences in the other species. Primers for *TaALMT1* expression in bread wheat were (5′-3′) CGTGAAAGCAGCGGA AAGCC (fwd) and CCCTCGACTCACGGTACTAACA (rev). Primers for *TaMATE1B* expression in bread wheat were AGG GTGGTAGCAGTGACTTC (fwd) and GCGGCAATCACCTTC TTGTG (rev). Annealing temperatures during cycling were 67°C for *TaMATE1B* and 61.5°C for *TaALMT1*. The primers for measuring *ScALMT1* expression in rye were GCAAACAAT ACCGTGGTTGTG (fwd) and ATCCCTCGAGTTAAGGCACC (rev). These primers could amplify products from the expressed copies of *ScALMT1* in the resistant and sensitive haplotypes of rye (*ScALMT1-M39.1*, *ScALMT1-M39.2*, *ScALMT1-M77.1*) described by Collins et al. (2008). We measured expression of *ScFRDL2* which is one of the candidate Al-resistance genes in rye because its Al-induced expression in the root apices by 50 μM Al is closely correlated with the release of citrate from roots (Yokosho et al., 2010). Primers used for measuring *ScFRDL2* expression were GGCTGCATTCCAGATTTGCTTG (fwd) and AGAAGCCCCAAGATCAATCCG (rev). Annealing temperatures were 68°C for *ScFRDL2* and *ScALMT1*.

The reference genes are important in the expression analyses because of the genetic differences between wheat and rye. Therefore the two reference genes chosen have previously been shown to be relatively stable across members of the triticaeae (Paolacci et al., 2009; Giménez et al., 2011). These gene are glyceraldehyde-3-phosphate dehydrogenase (*GAPDH*; Ta30768, Genbank EF592180) with primers GTTGAGGGTTTG ATGACCAC (fwd) TCAGACTCCTCCTTGATAGC (rev) and the cell division control protein (AAA-superfamily of ATPases) (*CDC*; Ta54227) with primers GCCTGGTAGTCGCAGGAGAT (fwd) and ATGTCTGGCCTGTTGGTAGC (rev). In preliminary tests reliable amplicons were generated from wheat, rye and triticale with both sets of reference primers. Relative expression levels of the Al resistance genes were generally similar with both references genes and the results using *CDC* are presented.

Statistical Analysis

Al resistance was estimated by calculating relative root length (RRL) since this accounts for inherent differences in growth between different species (see above). Since RRL is a ratio of means (net root growth in different treatments) each of which has an error, then the result requires a new accumulated error. The formula for calculating this accumulated error and the procedure

TABLE 1 | Summary of germplasm used in this study.

Genotypes	Description	Al resistance mechanisms[†]	Al-resistance genes[††]	References
GERMPLASM SET 1				
Carazinho	Wheat (hexaploid, Al-res)	Malate efflux Citrate efflux	*TaALMT1* *TaMATE1B*	Sasaki et al., 2004; Tovkach et al., 2013
Egret	Wheat (hexaploid, Al-sens)			
Carazinho x ***L185***	Triticale (octoploid)			
Egret x ***L185***	Triticale (octoploid)			
L185	Rye (diploid, Al-res)	Malate efflux Citrate efflux	*ScALMT1* *ScFRDL1 ScFRDL2 ScMATE* *ScAACT1*	Fontecha et al., 2007; Collins et al., 2008; Yokosho et al., 2010; Silva-Navas et al., 2012
GERMPLASM SET 2				
5020–30	Wheat (tetraploid, Al-sens)			
5020–30 x ***389***	Triticale (hexaploid)			
5020–30 x ***390***	Triticale (hexaploid)			
389	Rye (diploid, Al-sens)			
390	Rye (diploid, Al-res)	Malate efflux Citrate efflux		As above

[†] *Likely mechanism from previous work but not previously investigated in these rye and triticale lines.*
[††] *These include known Al-resistance genes and candidate resistance genes. Note that some of the genes listed for citrate efflux might represent the same gene.*

used for determining whether two RRL values are statistically different from one another is described previously by Zhou et al. (2013). The assumptions for this test are that the data are normally distributed and the variances are not different.

Other statistical analysis used the statistical software in SigmaPlot™ ver 14.0. Anion efflux results were analyzed with a one way ANOVA. In cases where the data failed an initial normality test the data were first transformed with the natural log function (*ln*). Analyses were then determined by applying the Student-Newman-Keuls method for multiple pairwise comparisons. Analysis of gene expression was similar and used three biological replicates except as stated. Note that rye was not included in the analysis of the expression of wheat genes, and conversely, wheat lines were not included in the analysis of the expression of rye genes.

RESULTS

Two sets of germplasm were compared for Al resistance, organic anion efflux and expression of selected Al-resistance genes. The first set was comprised of two bread wheat cultivars (*Carazinho* and *Egret*), a rye cultivar (***L185***) and the two octoploid triticale lines generated from crossing the rye to each of the wheat cultivars (*Carazinho*x***L185*** and *Egret*x***L185***). *Egret* is an Al-sensitive cultivar that shows little or no malate or citrate release. *Carazinho* is an Al-resistant wheat that has the Al-resistant alleles for *TaALMT1* and *TaMATE1B*. *Carazinho* has greater expression of these two genes than *Egret* and displays an Al-activated efflux of malate and a constitutive release of citrate from the root apices (Ryan et al., 2009). The second set of germplasm included a tetraploid (durum) wheat line (*5020-30*), two closely-related lines of rye with contrasting resistance to Al (***390*** resistant and ***389*** sensitive) and the two hexaploid triticale lines generated by crossing the durum wheat with each rye line (*5020-30*x***390*** and *5020-30*x***389***). The mechanisms of Al resistance in the ***390*** have not previously been investigated in detail.

Octoploid Triticale

Al resistance of the wheat, rye and octoploid triticale lines was compared by estimating relative root length after 4 d growth in a range of Al concentrations (**Figure 1**). Egret wheat was sensitive of all Al treatments while the Carazinho wheat and triticale lines were more resistant. At the highest Al treatment L185 rye was most resistant with 62% RRL while the wheat and triticale lines were similar at 25%. These results indicate that rye could contribute to the Al resistance of triticale because EgretxL185 triticale was significantly more resistant than Egret wheat. However, the Al resistance of rye and wheat was not additive in triticale because the resistance of CarazinhoxL185 was no greater than either the wheat or rye parent. It would be instructive to confirm the Al resistance measured in hydroponics reflects the measurements in field trials with acidic soil.

Malate and citrate release are known mechanisms for Al resistance in rye and wheat and fluxes of these organic anions were measured from each genotype. The results showed some variation between replicated experiments, especially in the triticale lines and rye material so the experiments were repeated several times. In the first series of experiments seedlings were grown in control nutrient solution and then malate and citrate efflux were measured in the presence or absence of Al. This means that the root tips were only exposed to Al for 2 h as exudates were collected. In the absence of Al, malate efflux from all genotypes was less than 0.05 nmol apex^{-1} h^{-1} (**Figure 2**). When 40 μM Al was included in the treatment solution, malate efflux increased significantly in all genotypes except for *Egret* wheat. The largest malate release was from *Carazinho* and *Carazinho*x***L185***. This

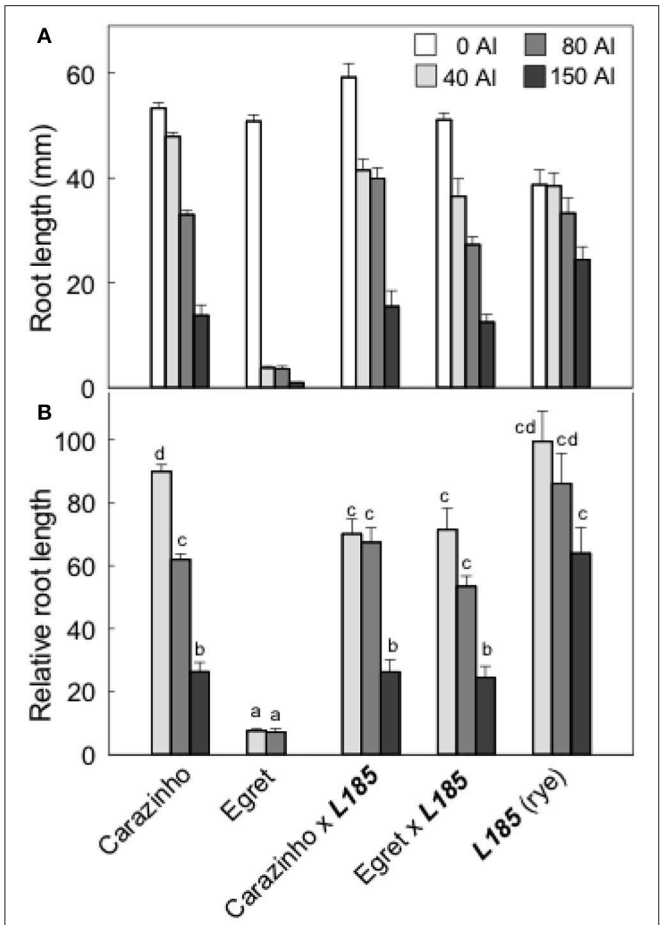

FIGURE 1 | Al resistance of the wheat and rye parents and the resulting triticale lines. Root length after 4 days growth in a range of Al concentrations **(A)** and relative root length **(B)** was measured in two hexaploid wheats, *Carazinho* (Al-resistant) and *Egret* (Al-sensitve), a rye genotype ***L185***, and the triticales generated by crossing the rye with each wheat parent. Data show means, SE ($n = 6$–10). Data with different letters in **(B)** are significantly different from one another ($p < 0.05$).

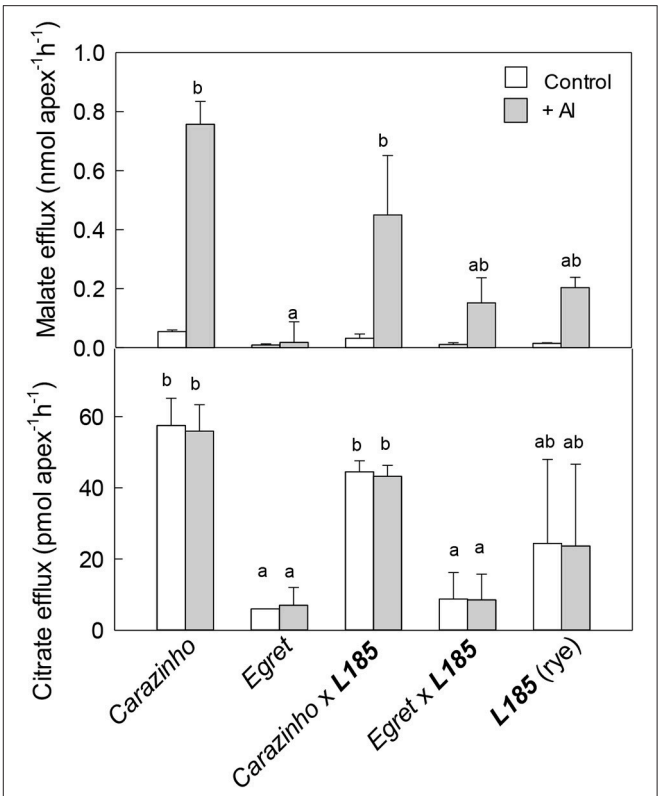

FIGURE 2 | Malate and citrate efflux from genotypes in the presence and absence of Al. Malate and citrate efflux were measured from excised root apices over 2 h with and without 40 μM Al in the collection solution. Data show the mean and SE ($n = 3$ or 4). Data with different letters are significantly different from one another ($p < 0.05$). Note the statistical analysis in **(A)** included the +Al treatment only whereas in **(B)** both treatments were included.

result is consistent with the Al-activation of malate efflux from wheat reported previously (Delhaize et al., 1993; Ryan et al., 1995) and indicates that the malate efflux trait from *Carazinho* wheat was fully expressed in the *Carazinho*x***L185*** triticale. Citrate efflux from *Carazinho* and *Carazinho*x***L185*** was large in the presence and absence of Al and indicates that citrate efflux was constitutive in these genotypes (**Figure 2**). Citrate efflux from *Egret* and *Egret*x***L185*** was smaller regardless of Al, while efflux from rye was very variable. These results support previous observations in *Carazinho* and *Egret* and indicate that the large constitutive efflux of citrate from *Carazinho* was also transferred to the triticale.

Organic anion efflux in some plant species is induced by Al treatment over many hours or longer (Pellet et al., 1995; Li et al., 2000; Ma et al., 2001; Magalhaes et al., 2007; Delhaize et al., 2012). Anion release was therefore measured after pretreating the seedlings in Al. In these experiments, half the seedlings were pretreated in 30 μM $AlCl_3$ for at least 24 h prior to the measurements and the other seedlings were only exposed to Al during the 2 h collection period. The results in **Figure 3A** show that the pretreatment in Al did not affect malate efflux from any genotype. Efflux from *Carazinho* wheat and *Carazinho*x***L185*** triticale remained greater than from *Egret*, ***L185*** rye and *Egret*x***L185*** triticale. Citrate efflux from *Carazinho* and ***L185***x*Carazinho* was large and unaffected by pretreatment in Al (**Figure 3B**). Citrate efflux from ***L185*** rye increased significantly after Al pretreatment while efflux from ***L185***x*Egret* showed a small but significant increase following pretreatment. These results demonstrated the following: (i) the Al-activated efflux of malate and the constitutive efflux of citrate was fully transferred from *Carazinho* wheat to the *Carazinho*x***L185*** triticale; (ii) Al pretreatment enhanced the efflux of citrate but not of malate from ***L185*** rye; (iii) the citrate efflux phenotype in rye was not fully transferred to triticale.

We next measured the expression of the *ALMT* genes, *TaALMT1* and *ScALMT1*, that control malate release from wheat and rye roots. Note that the primers used for *ScALMT1* recognize several copies of the *ScALMT1* genes located in the *Alt4* locus in rye as reported by Collins et al. (2008). Expression of the wheat gene *TaALMT1* was greater in *Carazinho* and *Carazinho*x***L185*** than the other genotypes and unaffected by pretreatment with Al (**Figure 4A**). *TaALMT1* expression was low in *Egret* and

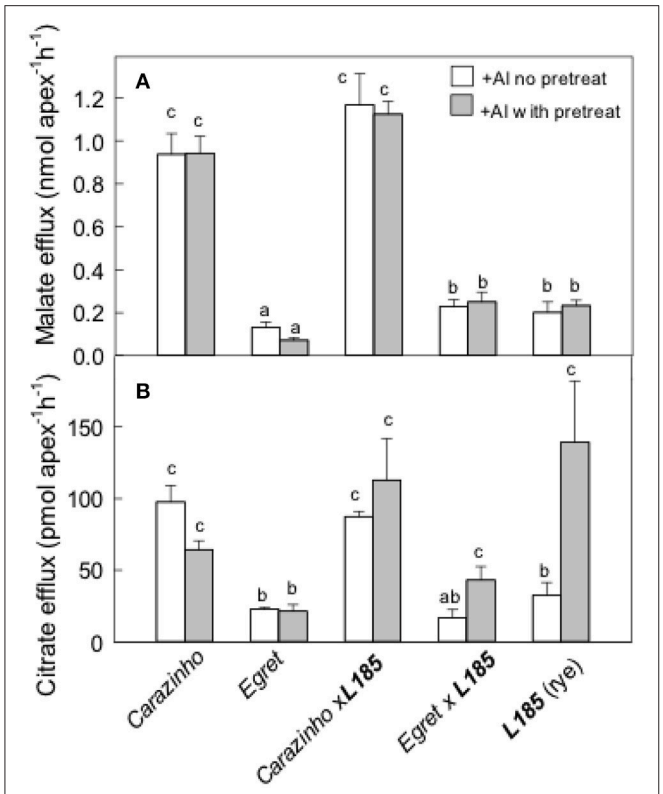

FIGURE 3 | Malate and citrate efflux from genotypes with and without pre-treatment in Al. Malate **(A)** and citrate **(B)** efflux were measured from apices over 2 h in 40 μM Al with and without a pretreatment in 30 μM Al for at least 24 h. Mean ±SE ($n = 3$ or 4). Data with different letters indicate significant differences after a one factor ANOVA ($p < 0.05$) using the Student-Newman-Keuls method for multiple pairwise comparisons. The data in **(B)** were first transformed with natural logarithm to satisfy normality.

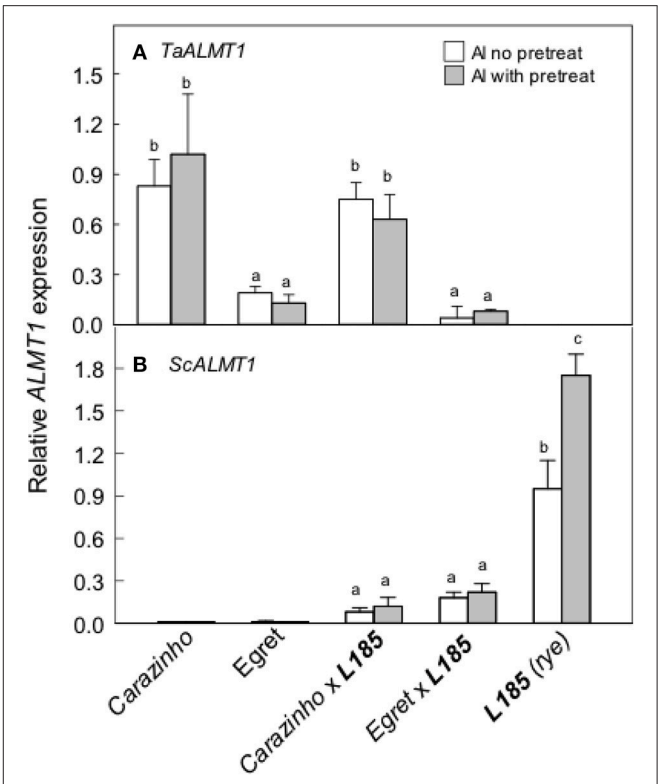

FIGURE 4 | Expression of the *ALMT1*-type genes in wheat, rye and triticale lines. Relative expression of the *TaALMT1* **(A)** and the *ScALMT1* **(B)** genes was measured with or without a pretreatment in 30 μM $AlCl_3$ for at least 24 h. Data show means and SE ($n = 3$ biological replicates). Data with different letters indicate significant differences at $p < 0.05$ using a one factor ANOVA.

*Egret*x***L185*** as expected. *ScALMT1* expression was significantly greater in ***L185*** rye than the two triticale lines (**Figure 4B**). Pretreatment tended to induce expression but the difference in this experiment was not significant. These results indicate that expression of the rye *ScALMT1* gene was suppressed in octoploid triticale.

The *TaMATE1B* and *ScFRDL2* genes encode transporters that likely facilitate citrate efflux from wheat and rye respectively. *TaMATE1B* expression levels were high in *Carazinho* and *Carazinho*x***L185*** and unaffected by pretreatment with Al (**Figure 5A**). Little or no expression was detected in *Egret* and *Egret*x***L185***. These data indicate that *TaMATE1B* was expressed similarly in wheat and triticale. *ScFRDL2* expression was detected in ***L185***, *Egret*x***L185*** but it was suppressed in *Carazinho*x***L185*** (**Figure 5B**). These data indicate that the rye *ScFRDL2* gene was expressed in triticale but the level of expression varied with the different wheat parents.

Hexaploid Triticale

The second set of experiments examined the rye lines ***390*** and ***389***, a tetraploid (durum) wheat line (*5020-30*) and the two hexaploid triticale lines generated from crossing each rye line to the durum wheat (*5020-30*x***390*** and *5020-30*x***389***). The ***390*** rye is resistant to Al and ***389*** is closely related but more sensitive to Al. The Al resistance of these lines was compared by estimating relative root length after 4 d growth in 0, 15, and 60 μM Al (**Figure 6**). Rye ***390*** showed no inhibition of root growth at 60 μM Al which is consistent with it being the most resistant genotype. RRL for most other genotypes was 20% or less for all treatments. The exception was *5020-30*x***390*** triticale where RRL was ∼50% in 15 μM Al (**Figure 6B**). These data indicate that the Al resistance of the ***390*** rye was incompletely transferred to hexaploid triticale.

Malate and citrate efflux from these genotypes was measured with or without a pretreatment in 30 μM Al (**Figure 7**). Malate efflux from the Al-resistant rye ***390*** was induced by Al pretreatment and was five-fold greater than the other genotypes (**Figure 7A**). Citrate efflux from the resistant ***390*** rye showed a large induction by Al pretreatment while efflux from the *5020-30*x***390*** triticale showed a smaller induction reaching only ∼30% of the rye (**Figure 7B**). Efflux from the other genotypes remained small. These results show that malate and citrate efflux likely contribute to the Al resistance of the ***390*** rye. They also indicate that the malate efflux detected in the ***390*** rye was not transferred to the hexaploid triticale *5020-30*x***390*** while citrate efflux was only partially transferred to triticale.

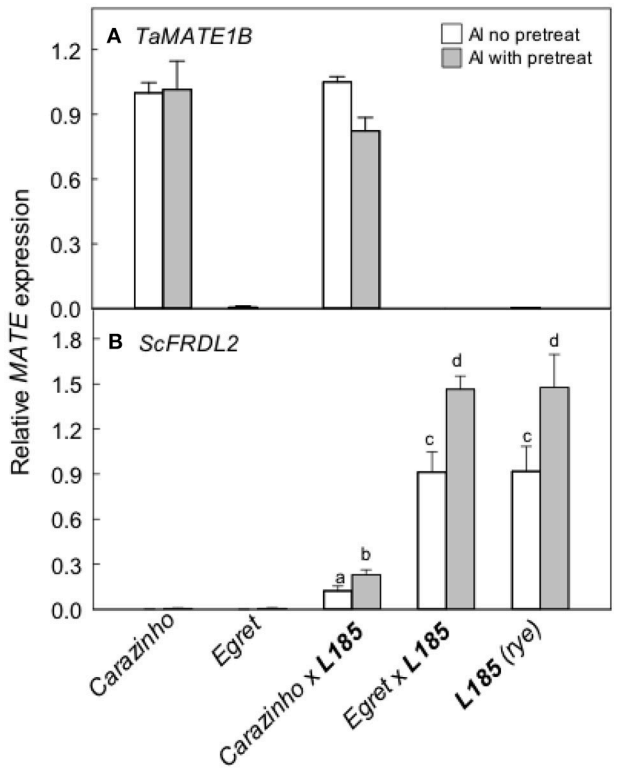

FIGURE 5 | Expression of specific *MATE*-type genes in wheat, rye and the triticale lines. Relative expression of the *TaMATE1B* **(A)** and the *ScFRDL2* **(B)** genes was measured with and without a pretreatment in 30 μM $AlCl_3$ for 24 h. Means, SE ($n = 3$ biological replicates for *TaMATE1B* and $n = 3$–4 for *ScFRDL2*). Data with different letters indicate significant differences after a one way ANOVA ($p < 0.05$) using the Student-Newman-Keuls method for multiple pairwise comparisons. The data in **(B)** were first transformed with natural logarithm to satisfy normality.

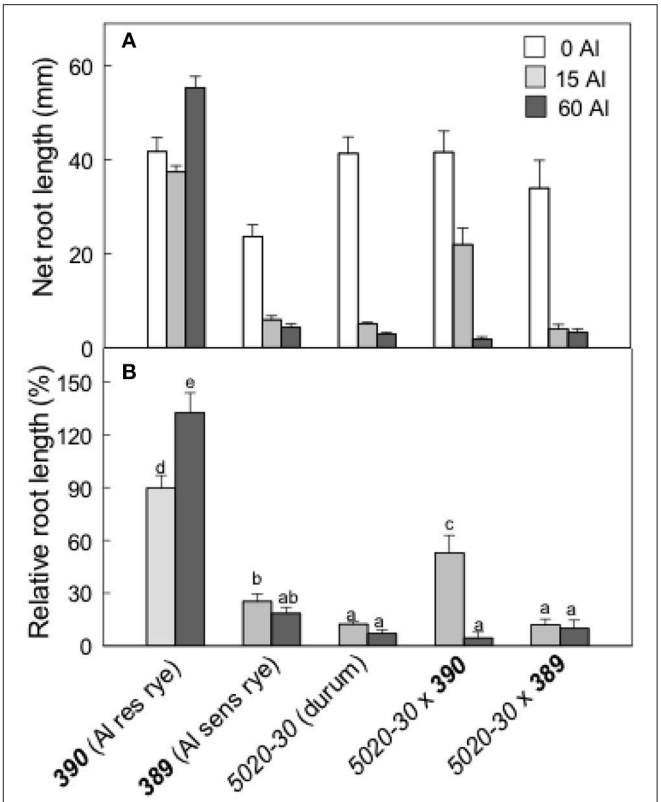

FIGURE 6 | Al resistance of the wheat, rye and triticale lines. Net root length in a range of Al concentrations **(A)** after 4 days and relative root length **(B)** in Al-resistant (***390***) and sensitive (***389***) rye lines, a durum wheat (tetraploid) and the triticale lines. Data show means with SE ($n = 6$–10). Data with the different letters in **(B)** are significantly different at $p < 0.05$.

Expression of the rye genes contributing to malate and citrate, *ScALMT1* and *ScFRDL2* respectively, were then measured with and without pretreatment in Al (**Figure 8A**). Without a pretreatment, *ScALMT1* expression was low in all lines. After a pretreatment in Al, *ScALMT1* expression in ***390*** rye increased 10-fold but was not induced in any of the other lines. These responses are consistent with the measured efflux of malate. The expression of *ScFRDL2* was significantly increased by Al pretreatment in ***390*** rye and *5020-30*x***390*** triticale but remained lower in the other lines (**Figure 8B**). These results indicate that the *ScFRDL2* gene was induced by Al in the Al-resistant ***390*** rye and the *5020-30*x***390*** triticale but that expression of *ScALMT1* was suppressed in the *5020-30*x***390*** triticale.

DISCUSSION

Al-resistance in hexaploid wheat and rye relies on the efflux of malate and citrate anions from the root apices. These phenotypes are controlled in part by the *TaALMT1* and *TaMATE1B* genes in hexaploid wheat and by the *ScALMT* and *ScFRDL2* genes in rye. This study investigated the transfer of these resistance mechanisms from wheat and rye lines to triticale. The first set of germplasm examined included Al-sensitive (*Egret*) and resistant (*Carazinho*) hexaploid wheat cultivars, an Al-resistant rye (***L185***) and the two octoploid triticale lines generated by crossing each wheat with the rye. All of these lines except for the *Egret* wheat showed strong resistance to Al toxicity (**Figure 1**). The following conclusions can be made from these first set of lines: (1) The wheat and rye parents both contributed to the Al-resistance of octoploid triticale. Support for this conclusion comes from the finding that *Egret*x***L185*** triticale was significantly more Al-resistant than *Egret* (**Figure 1**) which indicates that ***L185*** contributed to the phenotype. Further, the malate and citrate efflux in *Carazinho*x***L185*** resembled the responses in *Carazinho* wheat but not that of rye (**Figures 2**, **3**) indicating that wheat contributed to those traits. These responses generally reflected the relative expression of the genes involved. (2) Al resistance of the parental lines was not additive in triticale. This supported by the finding that neither triticale line was more resistant than the rye or Al-resistant wheat parents. (3) Function of the Al resistance genes in hexaploid wheat were more completely transferred to triticale than the rye genes. This is shown by the expression levels of the two wheat genes *TaALMT1* and *TaMATE1B* which were similar in *Carazinho* and *Carazinho*x***L185*** whereas expression of the rye genes, *ScALMT* and *ScFRDL2*, in triticale was inconsistent (**Figures 4**, **5**). In a

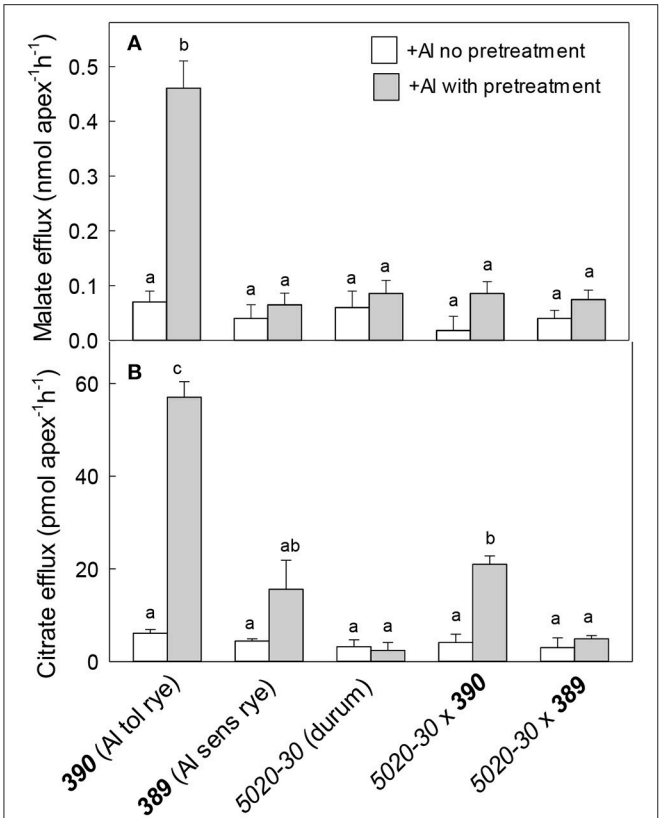

FIGURE 7 | Malate and citrate efflux from wheat, rye and triticale with and without a pre-treatment in Al. Malate **(A)** and citrate **(B)** efflux were measured in the presence of 40 μM Al with and without a pre-treatment in 30 μM Al for at least 24 h. Data show mean and SE ($n = 3$ or 4). Data with different letters are significantly different at ($p < 0.05$) after a one factor ANOVA.

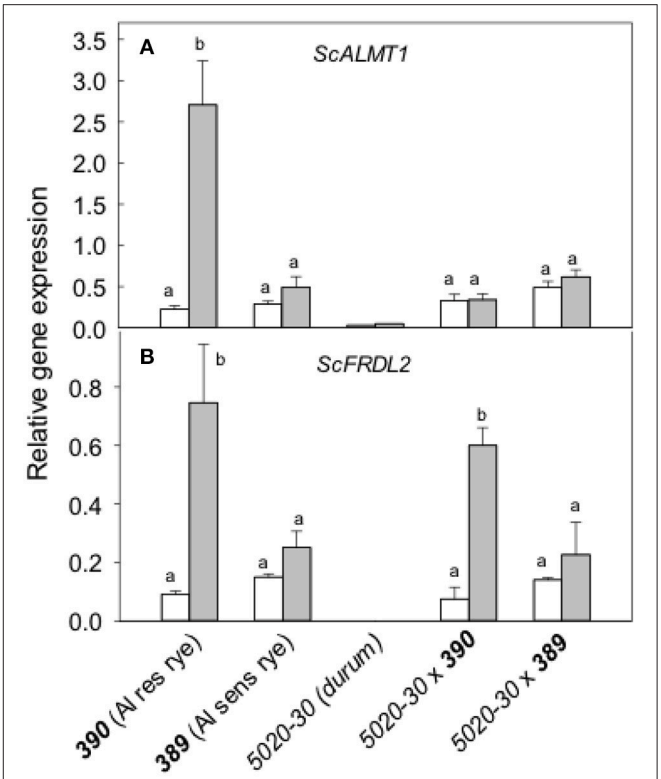

FIGURE 8 | Relative expression of the rye *ScALMT* and *ScFRDL2* genes in different genotypes. Relative expression of *ScALMT* **(A)** and *ScFRDL2* **(B)** was measured without (white) and with (gray) a pre-treatment in 30 μM Al for at least 24 h. Data show mean and SE ($n = 3$ biological replicates). Data with different letters are significantly different at ($p < 0.05$) after a one factor ANOVA.

previous study, Stass et al. (2008) concluded that the Al resistance of triticale was determined by citrate efflux which was largely controlled by the wheat parent. The present results indicate that malate efflux from hexaploid wheat can also contribute to the resistance of triticale. (4) The expression of the rye *ScFRDL2* gene in triticale depended on the genotype of the wheat parent. This is supported by the observations that relative expression of *ScFRDL2* was significantly greater in *Egret*x***L185*** than *Carazinho*x***L185*** (**Figure 5**). It is interesting to speculate whether this finding is related to the different expression levels of the wheat gene *TaMATE1B* in *Carazinho* and *Egret*.

The second set of germplasm included a durum wheat (*5020-30*), a pair of closely-related rye lines (***389*** and ***390***) that differed in Al resistance and the two hexaploid triticale lines generated by crossing each rye with the durum. The main conclusions drawn from those results include the following: (1) Malate and citrate efflux contribute to the Al resistance of ***390*** rye and these fluxes were correlated with increases in *ScALMT1* and *ScFRDL2* expression in ***390*** rye. (2) The Al resistance of 390 rye was not fully transferred to the 5020-30 x 390 triticale (**Figure 6**). This was consistent with the reduced efflux of organic anions from 5020-30 x 390 compared to the resistant rye (**Figure 8**). The Al resistance of these lines appeared to be most closely correlated with citrate efflux and expression of ScFRDL2.

The important observation from both sets of lines was that the Al resistance of rye was incompletely transferred to triticale—whether to a hexaploid or a octoploid triticale. Similar observations have been made previously for other rye genes in triticale (Neves et al., 1995; Kalinka and Achrem, 2018). By contrast, the Al resistance traits from hexaploid wheat did transfer more successfully to octoploid triticale.

The incomplete transfer of the Al-resistance traits of rye to triticale may be explained by the modifications that commonly occur to the genome of *de novo* allopolyploids mentioned above. When related species such as wheat and rye hybridize to form a stable allopolyploid many genes become duplicated and genetic changes that occur can affect gene expression. Furthermore, homeolog copies of all genes in allopolyploids are not expressed equally. Sequences can be lost and mutations generated due to chromosomal rearrangements or transposon activity (Ma and Gustafson, 2008), and gene transcription can be affected by epigenetic modifications and microRNAs (Cheng and Murata, 2002; Kashkush et al., 2002, 2003; Kraitshstein et al., 2010; Li et al., 2014, 2015; Kalinka and Achrem, 2018). Cytosine residues in DNA are prone to methylation when they occur as CpG, CpHpG, and CpHpH sites (where H represents any nucleotide except guanine) and methylation of gene promoter regions can interfere with transcription. In *de novo* allopolyploids, such as the primary triticale lines used here, DNA methylation appears to be

a more important factor decreasing gene expression than genetic instability with some estimates suggesting 1 to 12% of genes are silenced this way (Kashkush et al., 2002; He et al., 2003; Mochida et al., 2004; Bottley et al., 2006). The homeologous genes from one parent genome in *de novo* allopolyploids can be silenced more than the other parent and this can even vary between different organs (Bottley et al., 2006; Zhao et al., 2011).

We propose that the rye traits are incompletely transferred to triticale because its genome is naive to the polyploid environment and therefore more prone to epigenetic modification. Hexaploid wheat, by contrast, has emerged from two major hybridization events. The first hybridization occurred about 0.5 million years ago between a diploid species (likely *Triticum uratu*, *AA* genome) and another unknown parent with the *BB* genome which generated an ancestral tetraploid wheat. The second event occurred only 10,000 years ago between a tetraploid species such as *Triticum turgidum* (*BBAA*) and the diploid grass *Aegilops tauschii* (*DD*) and generated hexaploid wheat. Since wheat has been subject to epigenetic silencing pressure for a long period, its genome is likely to be more resistant to further silencing processes than the rye genome in a wheat-rye hybrid. This idea is consistent with the outcome of previous studies that compared the expression of genes in tetraploid and diploid lines with their expression in *de novo* hexaploid wheat lines. For example, microarray analysis and RNA-seq techniques demonstrated that more genes from the diploid parent had reduced expression levels in the hexaploid line than the tetraploid parent. This indicates an "expression bias" toward the tetraploid genome parent compared to the diploid genome (Akhunova et al., 2010; Li et al., 2014). Future work will test this hypothesis by investigating how methylation states of specific Al-resistance genes in the wheat and rye parents change in the primary triticale lines.

Significant variation was detected between certain repeated experiments and in some instances anion fluxes did not correlate well with gene expression. For example, the relative expression of *ScALMT1* in ***L185*** and *Egret*x***L185*** did not reflect the measured fluxes of malate. This variation could be related, in part, to the variable delay in gene induction by Al and the possible involvement of other Al resistance genes not targeted in this study. More than one *ALMT* and *MATE* gene could contribute to anion efflux (see Introduction). The variation may also be related to the instability of the primary triticale lines which can continue in subsequent generations (Ma and Gustafson, 2008; Kalinka and Achrem, 2018). The grain used in these experiments were bulked on two occasions so some variation was not unexpected. However each experiment was performed several times and the results presented here reflect the same general trends. Future studies could, nevertheless, quantify the stability of the triticale lines by determining the chromosome number of individual plants within each line and in different generations. The expression levels of target genes could also be measured and Al-resistance assessed in field trials on acidic and limed soils over several sites and seasons. These experiments would provide further insight into the genetic stability of the primary triticale material.

Triticale was developed to combine the favorable attributes of rye and wheat and to generate diversity. The triticale material used in this study were primary triticale lines generated by crossing rye pollen to female wheat plants. The reverse cross (rye as the female parent) is possible but less successful. Nevertheless, since the mitochondrial and plastid genomes are maternally inherited some traits are under cytoplasmic control (Thiede, 1998; Battich et al., 2015). Additional diversity might be generated if improved technologies enabled the reverse crosses to occur more efficiently so that the origins of the mitochondrial and plastid genomes in triticale would be rye instead of wheat.

Most triticale grown around the world are hexaploid types because they tend to show better vigor and stability (Mergoum et al., 2009). The present study found that the strong Al-resistance of rye was not fully expressed in either the hexaploid or octoploid triticale whereas the Al-resistance traits derived from Carazinho hexaploid wheat did transfer to octoploid triticale more successfully. If this pattern is indicative of other phenotypes then hexaploid triticale is potentially missing other valuable traits that may occur in some hexaploid wheat but not tetraploid wheat. Consideration should be given to developing cytological techniques that improve the genetic stability of octoploid triticale so that beneficial traits of hexaploid wheat (e.g., flour quality, nutrient content) can be captured in the hybrid. Such an approach could further improve the value of triticale production.

AUTHOR CONTRIBUTIONS

WH and PR conceived the project and coordinated with the breeder to access the germplasm. Experimental word was performed by DD, NW, JL, MX, NSM, JY, ED and PR. Supervision of experimental work was provided by PR, ED and KM. The manuscript was drafted by PR with help from all authors.

ACKNOWLEDGMENTS

The authors are grateful to the critical contribution from H-PM for generating and supplying the germplasm. We acknowledge FT for providing technical assistance and Anthony Condon for critically reading the manuscript.

REFERENCES

Akhunova, A. R., Matniyazov, R. T., Liang, H., and Akhunov, E. D. (2010). Homoeolog-specific transcriptional bias in allopolyploid wheat. *BMC Genomics* 11:505. doi: 10.1186/1471-2164-11-505

Aniol, A., and Gustafson, J. P. (1984). Chromosome location of genes controlling aluminium tolerance in wheat, rye and triticale. *Can. J. Genet. Cytol.* 26, 701–705. doi: 10.1139/g84-111

Battich, N., Stoeger, T., and Pelkmans, L. (2015). Control of transcript variability in single mammalian cells. *Cell* 163, 1596–1610. doi: 10.1016/j.cell.2015.11.018

Benito, C., Fontecha, G., Silva-Navas, J., Herna'ndez-Riquer, V., Eguren, M., Escribano, R. M., et al. (2005). Chromosomal location of molecular markers linked to aluminum tolerance genes in rye. *Czech J. Genet. Plant Breed.* 41:288. doi: 10.17221/6193-CJGPB

Bottley, A., Xia, G. M., and Koebner, R. M. D. (2006). Homeologous gene silencing in hexaploidy wheat. *Plant J.* 47, 897–906. doi: 10.1111/j.1365-313X.2006.02841.x

Cheng, Z. J., and Murata, M. (2002). Loss of chromosomes 2R and 5RS in octoploid triticale selected for agronomic traits. *Genes Genet. Syst.* 77, 23–29. doi: 10.1266/ggs.77.23

Collins, N. C., Shirley, N. J., Saeed, M., Pallotta, M., and Gustafson, J. P. (2008). An ALMT1 gene cluster controlling aluminum tolerance at the Alt4 locus of rye (*Secale cereale* L.). *Genetics* 179, 669–692. doi: 10.1534/genetics.107.083451

Delhaize, E., Gruber, B. D., and Ryan, P. R. (2007). The roles of organic anion permeases in aluminium resistance and mineral nutrition. *FEBS Lett.* 581, 2255–2262. doi: 10.1016/j.febslet.2007.03.057

Delhaize, E., Ma, J. F., and Ryan, P. R. (2012). Transcriptional regulation of Al^{3+}-tolerance genes. *Trends Plant Sci.* 17, 341–348. doi: 10.1016/j.tplants.2012.02.008

Delhaize, E., Ryan, P. R., and Randall, P. J. (1993). Aluminum tolerance in wheat (*Triticum aestivum* L.) II Aluminum stimulated excretion of malic acid from root apices. *Plant Physiol.* 103, 695–702. doi: 10.1104/pp.103.3.695

Fontecha, G., Silva-Navas, J., Benito, C., Mestres, M. A., Espino, F. J., Hrnandezriquer, V., et al. (2007). Candidate gene identification of an aluminum-activated organic acid transporter gene at the *Alt4* locus for aluminum tolerance in rye (*Secale cereale* L.). *Theor. Appl. Genet.* 114, 249–260. doi: 10.1007/s00122-006-0427-7

Giménez, M. J., Pistón, F., and Atienza, S. G. (2011). Identification of suitable reference genes for normalization of qPCR data in comparative transcriptomics analyses in the Triticeae. *Planta* 233, 163–173. doi: 10.1007/s00425-010-1290-y

He, P., Friebe, B. R., Gill, B. S., and Zhou, J. M. (2003). Allopolyploidy alters gene expression in the highly stable hexaploid wheat. *Plant Mol. Biol.* 52, 401–414. doi: 10.1023/A:1023965400532

Kalinka, A., and Achrem, M. (2018). Reorganization of wheat and rye genomes in octoploid triticale (× Triticosecale). *Planta* 247,807–829. doi: 10.1007/s00425-017-2827-0

Kashkush, K., Feldman, M., and Levy, A. (2002). Gene loss, silencing and activation in a newly synthesised hexaploid wheat. *Genetics* 160, 1651–1659.

Kashkush, K., Feldman, M., and Levy, A. (2003). Transcriptional activation of retrotransposons alters the expression of adjacent genes in wheat. *Nat. Genet.* 33, 102–106. doi: 10.1038/ng1063

Kraitshstein, Z., Yaakov, B., Khasdan, V., and Kashkush, K. (2010). Genetics and epigenetic dynamics of a retrotransposon after allopolyploidization of wheat. *Genetics* 186, 801–812. doi: 10.1534/genetics.110.120790

Li, A., Geng, S., Zhang, L., Liu, D., and Mao, L. (2015). Making the bread: Insights from newly synthesized allohexaploid wheat. *Mol. Plant* 8, 847–859. doi: 10.1016/j.molp.2015.02.016

Li, A., Liu, D., Wu, J., Zhao, X., Hao, M., Geng, S., et al. (2014). mRNA and small RNA transcriptomes reveal insights into dynamic homoeolog regulation of allopolyploid heterosis in nascent hexaploid wheat. *Plant Cell* 26, 1878–1900. doi: 10.1105/tpc.114.124388

Li, X. F., Ma, J. F., and Matsumoto, H. (2000). Pattern of aluminum-induced secretion of organic acids differs between rye and wheat. *Plant Physiol.* 123,1537–1154. doi: 10.1104/pp.123.4.1537

Ma, J. F., Ryan, P. R., and Delhaize, E. (2001). Aluminium tolerance in plants and the complexing role of organic acids. *Trends Plant Sci.* 6, 273–278. doi: 10.1016/S1360-1385(01)01961-6

Ma, J. F., Taketa, S., and Yang, Z. M. (2000). Aluminum tolerance genes on the short arm of chromosome 3R are linked to organic acid release in triticale. *Plant Physiol.* 122, 687–694. doi: 10.1104/pp.122.3.687

Ma, X.-F., and Gustafson, J. P. (2008). Allolpollyploidization-accommodated genomic sequence changes in triticale. *Ann. Bot.* 101, 825–832. doi: 10.1093/aob/mcm331

Magalhaes, J. V., Liu, J., Guimaraes, C. T., Lana, U. G. P., Alves, V. M. C., Wang, Y. H., et al. (2007). A gene in the multidrug and toxic compound extrusion (MATE) family confers aluminum tolerance in sorghum. *Nat. Genet.* 39, 1156–1161. doi: 10.1038/ng2074

Matos, M., Camacho, M. V., Pérez-Flores, V., Pernaute, B., Pinto-Carnide, O., and Benito, C. (2005). A new aluminum tolerance gene located on rye chromosome arm 7RS. *Theor. Appl. Genet.* 111, 360–369. doi: 10.1007/s00122-005-2029-1

Mergoum, M., and Gómez-Macpherson, H. (eds.). (2004). "Triticale improvement and production," in *Food Production and Protection Paper 179* (Food and Agriculture Organization of the United Nations).

Mergoum, M., Singh, P. K., Peña, R. J., Lozano-del Río, A. J., Cooper, K. V., Salmon, D. F., et al. (2009). "Triticale: a "new" crop with old challenges," in *Cereals,* ed M. J. Carena (New York, NY: Springer), 267–286.

Mochida, K., Yamazaki, Y., and Ogihara, Y. (2004). Discrimination of homeologous gene expression in hexaploidy wheat by SNP analysis of contigs from a large number of expressed sequence tags. *Mol. Genet. Genom.* 270, 371–377. doi: 10.1007/s00438-003-0939-7

Neves, N., Heslop-Harrison, J. S., and Viegas, W. (1995). rRNA gene activity and control of expression mediated by methylation and imprinting during embryo development in wheat x rye hybrids. *Theor. Appl. Genet.* 91, 529–533. doi: 10.1007/BF00222984

Paolacci, A. R., Oronzo, A. T., Porceddu, E., and Ciaffi, M. (2009). Identification and validation of reference genes for quantitative RT-PCR normalization in wheat. *BMC Mol. Biol.* 10:11. doi: 10.1186/1471-2199-10-11

Pellet, D. M., Grunes, D. L., and Kochian, L. V. (1995). Organic acid exudation as an aluminum-tolerance mechanism in maize (*Zea mays* L.). *Planta* 196,788–795. doi: 10.1007/BF01106775

Raman, H., Zhang, K., Cakir, M., Appels, R., Moroni, J. S., Maron, L. G., et al. (2005). Molecular characterization and mapping of *ALMT1*, the aluminium-tolerance gene of bread wheat (*Triticum aestivum* L.). *Genome* 48, 781–791. doi: 10.1139/g05-054

Ryan, P. R., Delhaize, E., and Randall, P. J. (1995). Characterisation of Al-stimulated efflux of malate from the apices of Al-tolerant wheat roots. *Planta* 196, 103–111. doi: 10.1007/BF00193223

Ryan, P. R., Raman, H., Gupta, S., Horst, W. J., Delhaize, E. (2009). A second mechanism for aluminum resistance in wheat maps to chromosome 4BL and relies on constitutive efflux of citrate from roots. *Plant Physiol.* 149, 340–351. doi: 10.1104/pp.108.129155

Ryan, P. R., Tyerman, S. D., Sasaki, T., Yamamoto, Y., Zhang, W. H., and Delhaize, E. (2011). Identification of aluminium-resistance genes in plants provides an opportunity for enhancing the acid-soil tolerance of crop species. *J. Exp. Bot.* 62, 9–20. doi: 10.1093/jxb/erq272

Sasaki, T., Yamamoto, Y., Ezaki, B. B., Katsuhara, M., Ahn, S. J., Ryan, P. R., et al. (2004). A wheat gene encoding an aluminum-activated malate transporter. *Plant J.* 37, 645–653. doi: 10.1111/j.1365-313X.2003.01991

Silva-Navas, J., Benito, C., Te'llez-Robledo, B., Abd El-Moneim, D., and Gallego, F. J. (2012). The *ScAACT1* gene at the *Qalt5* locus as a candidate for increased aluminum tolerance in rye (*Secale cereale* L.) *Mol. Breed.* 30, 845–856. doi: 10.1007/s11032-011-9668-5

Stass, A., Smit, I., Eticha, D., Oettler, G., and Horst, W. J. (2008). The significance of organic anion exudation for the aluminum resistance of primary triticale derived from wheat and rye parents differing in aluminum resistance. *J. Plant Nutr. Soil Sci.* 171, 634–642. doi: 10.1002/jpln.200700331

Thiede, D. A. (1998). Maternal inheritance and its effect on adaptive evolution: a quantitative genetic analysis of maternal effects in a natural plant population. *Evolution* 52, 998–1015. doi: 10.1111/j.1558-5646.1998.tb01829.x

Tovkach, A., Ryan, P. R., Richardson, A. E., Lewis, D., Rathjen, T. M., Ramesh, S., et al. (2013). Transposon-mediated alteration of *TaMATE1B* expression in wheat roots confers constitutive citrate efflux from root apices. *Plant Physiol.* 161, 880–892. doi: 10.1104/pp.112.207142

Wang, J., Raman, H., Zhou, M., Ryan, P. R., Delhaize, E., Hebb, D. M., et al. (2007). High-resolution mapping of Alp, the aluminium tolerance locus in barley (*Hordeum vulgare* L.), identifies a candidate gene controlling tolerance. *Theor. Appl. Genet.* 115, 265–276. doi: 10.1007/s00122-007-0562-9

Yokosho, K., Yamaji, N., and Ma, J. F. (2010). Isolation and characterisation of two *MATE* genes in rye. *Funct. Plant Biol.* 37, 296–303. doi: 10.1071/FP09265

Zhao, N., Zhu, B., Li, M., Wang, L., Xu, L., Zhang, H., et al. (2011). Extensive and heritable epigenetic remodelling and genetic stability accompany allohexaploidization of wheat. *Genetics* 188, 499–509. doi: 10.1534/genetics.111.127688

Zhou, G., Delhaize, E., Zhou, M., and Ryan, P. R. (2013). The barley *MATE* gene, *HvAACT1*, increases citrate efflux and Al^{3+}-tolerance when expressed in wheat and barley. *Ann. Bot.*112, 603–612. doi: 10.1093/aob/mct135

Conflict of Interest Statement: The authors declare that the research was conducted in the absence of any commercial or financial relationships that could be construed as a potential conflict of interest.

frontiers in Plant Science

REVIEW
published: 26 September 2018
doi: 10.3389/fpls.2018.01420

Emerging Pleiotropic Mechanisms Underlying Aluminum Resistance and Phosphorus Acquisition on Acidic Soils

Jurandir V. Magalhaes[1,2], Miguel A. Piñeros[3]*, Laiane S. Maciel[1,2] and Leon V. Kochian[4]*

[1] Embrapa Maize and Sorghum, Sete Lagoas, Brazil, [2] Departamento de Biologia Geral, Universidade Federal de Minas Gerais, Belo Horizonte, Brazil, [3] Robert W. Holley Center for Agriculture and Health, USDA-ARS, Cornell University, Ithaca, NY, United States, [4] Global Institute for Food Security, University of Saskatchewan, Saskatoon, SK, Canada

Aluminum (Al) toxicity on acidic soils significantly damages plant roots and inhibits root growth. Hence, crops intoxicated by Al become more sensitive to drought stress and mineral nutrient deficiencies, particularly phosphorus (P) deficiency, which is highly unavailable on tropical soils. Advances in our understanding of the physiological and genetic mechanisms that govern plant Al resistance have led to the identification of Al resistance genes, both in model systems and in crop species. It has long been known that Al resistance has a beneficial effect on crop adaptation to acidic soils. This positive effect happens because the root systems of Al resistant plants show better development in the presence of soil ionic Al^{3+} and are, consequently, more efficient in absorbing sub-soil water and mineral nutrients. This effect of Al resistance on crop production, by itself, warrants intensified efforts to develop and implement, on a breeding scale, modern selection strategies to profit from the knowledge of the molecular determinants of plant Al resistance. Recent studies now suggest that Al resistance can exert pleiotropic effects on P acquisition, potentially expanding the role of Al resistance on crop adaptation to acidic soils. This appears to occur *via* both organic acid (OA)- and non-OA transporters governing a joint, iron-dependent interplay between Al resistance and enhanced P uptake, *via* changes in root system architecture. Current research suggests this interplay to be part of a P stress response, suggesting that this mechanism could have evolved in crop species to improve adaptation to acidic soils. Should this pleiotropism prove functional in crop species grown on acidic soils, molecular breeding based on Al resistance genes may have a much broader impact on crop performance than previously anticipated. To explore this possibility, here we review the components of this putative effect of Al resistance genes on P stress responses and P nutrition to provide the foundation necessary to discuss the recent evidence suggesting pleiotropy as a genetic linkage between Al resistance and P efficiency. We conclude by exploring what may be needed to enhance the utilization of Al resistance genes to improve crop production on acidic soils.

Keywords: abiotic stress resistance, transporters, plant breeding, pleiotropy, aluminum tolerance, phosphorus acquisition, phosphorus efficiency

OPEN ACCESS

Edited by:
Peter Ryan,
Commonwealth Scientific and Industrial Research Organisation (CSIRO), Australia

Reviewed by:
Takayuki Sasaki,
Okayama University, Japan
Manny Delhaize,
Plant Industry (CSIRO), Australia

****Correspondence:***
Jurandir V. Magalhaes
jurandir.magalhaes@embrapa.br
Miguel A. Piñeros
map25@cornell.edu

Specialty section:
This article was submitted to Plant Abiotic Stress, a section of the journal Frontiers in Plant Science

Received: *01 March 2018*
Accepted: *06 September 2018*
Published: *26 September 2018*

Citation:
Magalhaes JV, Piñeros MA, Maciel LS and Kochian LV (2018) Emerging Pleiotropic Mechanisms Underlying Aluminum Resistance and Phosphorus Acquisition on Acidic Soils. Front. Plant Sci. 9:1420. doi: 10.3389/fpls.2018.01420

INTRODUCTION

Acidic soils are globally widespread, extending to more than half of the world arable lands (von Uexküll and Mutert, 1995). These low-pH soils, which are commonly found in tropical and subtropical regions, include areas where food production needs to be increased to cope with a continuously growing population (Godfray et al., 2010). For example, there have been a number of studies in the literature addressing the extent of Al-toxic acidic soils in Africa, with approximately 25% of the soils being highly acidic (FAO and ITPS, 2015; Tully et al., 2015). Two of the major constraints for crop production on acidic soils, including those in Sub-Saharan Africa (Doumbia et al., 1993, 1998), are aluminum (Al) toxicity and low phosphorus (P) availability.

Aluminum and iron (Fe) oxides, which are enriched in the clay fraction of acidic soils upon intensive weathering of primary minerals (Shaw, 2001), drive both types of abiotic stresses, causing a general coincidental occurrence of Al toxicity and low P availability on tropical soils (Sanches and Salinas, 1981). Phosphorus forms strong, covalent bounds with these oxides, becoming highly unavailable for uptake by the plants (Marschner, 1995; Lynch, 2011), due to restricted P diffusive fluxes from the soil toward the root surface. In addition, P diffusion on highly weathered soils is highly dependent on the soil water content (Novais and Smith, 1999), which varies during the crop season, making P supply to the plant and, consequently, P uptake, highly discontinuous. Under low pH, Al present in aluminosilicates and oxides is released as the rhizotoxic Al^{3+} ion into the soil solution, damaging the root system and inhibiting root growth (Delhaize and Ryan, 1995).

Aluminum resistance has long been associated with overall crop adaptation to acidic soils by indirectly enhancing mineral nutrient uptake and drought resistance (Foy et al., 1993). Accordingly, undamaged, "Al resistant" root systems are more effective in absorbing sub-soil water, and nutrients, particularly those that are highly unavailable on acidic soils, such as P. It is important to note that Al toxicity typically extends to sub-soil layers, where liming is highly ineffective in increasing soil pH, enhancing the deleterious effects of drought stress in reducing crop yields.

The widespread nature of Al toxicity and its global impact has spurred extensive research on the physiological, genetic, and molecular mechanisms that enable crops to withstand Al toxicity on acidic soils. Clearly, impressive progress has been made in the last two decades on the molecular underpinnings of crop Al resistance (reviewed by Kochian et al., 2015). These discoveries led to the isolation of a number of the previously anonymous molecular determinants of Al resistance in loci that had been identified previously *via* genetic mapping in crops such as wheat, barley, rye, sorghum, and maize, as well as in model systems such as in *Arabidopsis thaliana*.

It is reasonable to expect that the identification of the molecular drivers of plant Al resistance can be instrumental in the development of novel strategies for improving crop performance on acidic soils in a more efficient way. Marker-assisted backcross to improve Al resistance based on single major loci has been a feasible approach long before major Al resistance genes were cloned. Beyond that, these genes now offer opportunities for large scale germplasm screening approaches based on functional markers, which can streamline the utilization of large germplasm banks in favor of plant breeding (Tanksley and McCouch, 1997; Hufnagel et al., 2018). Most importantly, it is possible that the value of Al resistance for crop production in the context of the multiple stress scenario on acidic soil regions (Bahia Filho et al., 1997) has been somewhat underappreciated. Some possible reasons for that are the lack of systematic efforts to map Al saturation both in the surface and below ground soils and a rather incomplete quantification of the grain yield effect of known Al resistance genes *in soil*, which is to some extent understandable due to the highly complex chemical nature of acidic soils.

There is now an interesting body of emerging evidence suggesting that Al resistance genes may have an additional, pleiotropic effect on acidic soils, which involves enhancement of P acquisition. In conjunction with the known effect of Al resistance in enhancing water and mineral uptake, by promoting better root growth on acidic soils, this would further justify deliberate efforts to design novel, gene-based molecular breeding strategies aimed at developing cultivars adapted to acidic soil regions. These strategies can help in realizing the great potential there is in expanding the world's agricultural frontier, by exploring the vast areas under acidic soils in the tropics and subtropics, which show in general a favorable topography for agriculture (Sanches and Salinas, 1981).

Here, our objective is not to review the current available information on plant Al resistance or P efficiency, which is defined here as improved performance in soils with low P availability. For that, readers are directed to many available comprehensive reviews (Delhaize and Ryan, 1995; Kochian, 1995; Ma et al., 2001; Kochian et al., 2004; Delhaize et al., 2007, 2012; López-Arredondo et al., 2014; Eekhout et al., 2017). Our goal here is to explore the emerging connections between Al resistance genes and P deficiency responses that help maintain favorable P nutrition, which happens possibly *via* alterations in root system architecture. We recognize these studies are just emerging and are still found largely in the realm of model species, in this case, Arabidopsis. This makes some of the crop-related implications drawn in this paper somewhat speculative in nature. However, due to the efficacy and breeding potential of common mechanisms underlying two important abiotic stress factors on acidic soils, taking advantage of the convergence of Al resistance and P efficiency *via* pleiotropic genes could have a significant impact in enhancing global food security. In the next section, we will briefly review the components comprising mechanisms that might jointly control Al resistance and P nutrition. We will then explore the emerging, underlying basis for such pleiotropy and will close with a brief discussion of the future directions to further explore Al resistance genes as tools to improve P acquisition and crop performance on acidic soils.

OVERVIEW OF POSSIBLE PLEIOTROPIC MECHANISMS CONTROLLING BOTH Al RESISTANCE AND ROOT TRAITS THAT MAY LEAD TO ENHANCED PHOSPHORUS ACQUISITION UNDER LOW P CONDITIONS

Physiological Basis

The ability of a plant to tolerate low P availability in the soil may be achieved both by internal mechanisms, acting to optimize the way plants internally utilize phosphorus, and by mechanisms to improve phosphorus acquisition from the soil. Mendes et al. (2014) genetically assessed the contribution of those mechanisms in maize grown on a tropical soil with low P availability and found that 80% of the QTLs mapped for P acquisition efficiency co-localized with those for P use efficiency (i.e., the ratio between grain yield and the amount of P supplied to the crop), indicating that the efficiency in acquiring P is the main determinant of P use efficiency in tropical maize. Since P acquisition efficiency achieved *via* changes in root morphology is the physiological basis of possible pleiotropy between Al resistance and better P nutrition, here we will briefly discuss this mechanism. For a broader view of mechanisms possibly contributing to enhanced crop performance under low P, which may involve modulation of P transporters, root system architecture modifications in response to low P, exudation of organic acids (OAs) and phosphatases, and mycorrhizal associations, in addition to internal mechanisms of P efficiency, readers are directed to recent reviews in this area (e.g., López-Arredondo et al., 2014).

Since P is in general highly unavailable on acidic soils, results such as those reported by Mendes et al. (2014) are expected, as enhanced capacity to acquire P is the logical first limiting step for P efficiency. However, other mechanisms have also been shown to exert beneficial effects on crop performance under low P in the field (López-Arredondo et al., 2014). The work by Gamuyao et al. (2012) provided a molecular foundation for the importance of root system architecture on the efficiency with which plants acquire P on soils with low P availability. The rice serine/threonine receptor-like kinase, OsPSTOL1, which is a member of the LRK10L-2 subfamily, was shown to enhance early root growth and grain yield on a P-deficient soil *via* increased P uptake, regulating crown root development (Gamuyao et al., 2012). Subsequently, a low but positive correlation between root surface area assessed in younger plants and grain yield under low P was instrumental in the identification of sorghum homologs of *OsPSTOL1*, designated *SbPSTOL1* genes, that also act to enhance root growth, thereby leading to enhanced P acquisition and grain yield in a sorghum association panel (Hufnagel et al., 2014). Mechanistically, plant P deficiency leads to inhibition of primary root growth due to a shift from an indeterminate to a determinate developmental program, which is caused by reduced cell elongation followed by the loss of meristematic cells in the root apical meristem (RAM) (Sánchez-Calderón et al., 2005). Hence, this release of apical dominance leads to enhanced proliferation of lateral roots, and increased lateral root branching increasing P uptake as observed in maize (Zhu and Lynch, 2004; Postma et al., 2014).

From the physicochemical standpoint, the supply of a nutrient like P from the soil solution toward the root surface *via* a diffusive flow can be modeled by the Fick′s law (Nobel, 1991), which depends on the P concentration gradient generated by the interplay between root P absorption and P in the soil solution. This concentration gradient can thus be thought as the "force" driving diffusion fluxes; as the root system grows into new soil regions still rich in P, the distance through which diffusion occurs is reduced, thus enhancing the diffusive flow (Novais and Smith, 1999), which is also maintained by the uptake process. Finally, we point out that changes in the three-dimensional configuration of the root system, such as proliferation of shallow roots, can also enhance P uptake [for more details on such mechanisms, please see Li et al. (2016) and Lynch (2011)].

Molecular Basis

Malate and Citrate Transporters

Organic acid transport and homeostasis is emerging as a central hub in a network of acidic soil stress responses. The first OA transporters involved in Al resistance were the wheat TaALMT1 and Arabidopsis AtALMT1, both shown to encode plasma membrane anion channel proteins that mediate root tip malate efflux (Sasaki et al., 2004; Hoekenga et al., 2006; Piñeros et al., 2008; Zhang et al., 2008). Although being the founding members of a novel class of plant anion transporters, it is now well established that, as a family, ALMT functions extend well beyond Al resistance, and participate in a variety of other physiological processes, including guard cell regulation, fruit quality, anion homeostasis, seed development, and plant–microbe interactions (Sharma et al., 2016). However, electrophysiological analysis of TaALMT1 and AtALMT1 (i.e., those transporters associated with Al-dependent responses) in heterologous systems has shown a distinct functional feature of these two transporters in that although they have transport activity in the absence of extracellular Al^{3+}, this activity is enhanced by extracellular Al^{3+} (Hoekenga et al., 2006; Piñeros et al., 2008). This so-called "Al activation" is analogous to processes occurring in ligand-gated channels, with the agonistic binding of Al^{3+} to the ALMT protein triggering a conformational change that favors its open state, consequently increasing its transport activity and facilitating anion (i.e., malate) flux. Although the molecular determinants involved in the binding of Al^{3+} to the ALMT protein remain unknown, a combination of functional analysis of structurally modified TaALMT1 and AtALMT proteins and phylogenetic studies on ALMTs indicate that several different domains in these two proteins are likely to act together in the Al-mediated enhancement of transport activity (Sasaki et al., 2004; Furuichi et al., 2010; Ligaba et al., 2013). Overall, the Al-dependent enhancement of the transport activity of an anion channel mediating the selective efflux of malate represents an elegant regulatory component of root malate exudation associated with Al exclusion processes.

More recently, a second novel transport substrate and new regulatory mechanisms have been described for the TaALMT1 transporter (Ramesh et al., 2015, 2018). It has generally been assumed that malate efflux is the primary transport function associated with TaALMT1. Recently, it was shown that TaALMT1 also has a high permeability to the non-protein amino acid, gamma-aminobutyric acid (GABA), a zwitterion molecule associated with signaling cascades in plants. GABA is not only transported by TaALMT1 but also modulates the activity of the transporter protein. Similarly, the apoplastic pH and anion composition also appear to regulate TaALMT1 transport activity, such that increased anion concentrations and/or more alkaline apoplastic conditions stimulate transport activity (Ramesh et al., 2015). These functional characteristics provide additional regulatory layers to Al^{3+}-mediated regulation of TaALMT1 activity. Consequently, in alkaline environments, enhancement of TaALMT1 activity resulting in both malate and GABA efflux has been suggested by Ramesh et al. (2015) to promote extracellular acidification *via* H^+ efflux coupled to the efflux of the malate anion, thereby potentially ameliorating and providing tolerance to high pH soils. Verification of such a tolerance mechanism operating in response to alkaline environments, and validation of the tantalizing functional plasticity of TaALMT1 in tolerance to abiotic stresses, awaits further investigation. It should be noted that the initial studies on this topic have not found increased tolerance or malate efflux in plants grown on alkaline soils and hydroponic media simulating alkaline field conditions (Silva et al., 2018).

The second type of Al resistance OA transporters belong to a subgroup of plasma membrane-localized MATE transporters identified from the map-based cloning of the major Al resistance loci in sorghum (*SbMATE*) (Magalhaes et al., 2004, 2007) and barley (*HvAACT1*) (Furukawa et al., 2007; Wang et al., 2007). Functional characterization of SbMATE, HvAACT1, and subsequently identified homologs in Arabidopsis (AtMATE1) (Liu et al., 2009), maize (ZmMATE1) (Maron et al., 2009), wheat (Ryan et al., 2009; Tovkach et al., 2013), rice bean (VuMATE1/2) (Yang et al., 2011; Liu et al., 2018), and rice (OsFRD2/4) (Yokosho et al., 2011, 2016) indicates that this subgroup of MATE transporters mediate citrate transport, and therefore as with ALMTs, these transporters underlie Al-exclusion *via* root tip OA root release. However, it is worthwhile to comment about the common assumption that ALMTs and MATEs are functionally very similar, as this is not the case. The functional analysis of several of the MATE transporters involved in Al resistance has established that, when expressed in heterologous systems, this subgroup of MATE transporters mediates constitutive pH-dependent citrate transport that is not activated by Al^{3+} in *Xenopus oocytes* (Magalhaes et al., 2007; Maron et al., 2009; Yang et al., 2011; Melo et al., 2013; Doshi et al., 2017; Liu et al., 2018), although some exceptions have been also reported both in X. oocytes (Furukawa et al., 2007; Yokosho et al., 2011) and tobacco suspension cells (Yokosho et al., 2016). Electrophysiological analysis indicates that, in the absence of exogenous intracellular citrate, these MATE transporters mediate an electrogenic transport that appears to be due to a large cation influx (H^+, Na^+, and/or K^+). Differences in the OA transport mechanism between ALMTs and MATEs raises interesting questions. Because of the large inwardly directed voltage gradient or membrane potential across the root cell plasma membrane, the efflux of the malate and citrate anions is a thermodynamically passive process. This is consistent with the ALMT transporters functioning as anion channels mediating the passive movement of the malate anion out of the root cell.

On the other hand, the MATE transporters use a thermodynamically active (H^+-driven) antiport mechanism associated with the passive efflux of $citrate^{2-}$ anions down its outwardly directed electrochemical gradient. One interesting and quite speculative explanation for this is that an alternative substrate, rather than the free $citrate^{2-}$ anion, is the substrate being transported out of the root cells. In the recent publication by Doshi et al. (2017), electrophysiological, radiolabeled, and fluorescence-based transport assays in two heterologous expression systems (oocytes and yeast) demonstrated that SbMATE has a fairly broad substrate recognition, mediating proton and/or sodium-driven efflux of the ^{14}C-citrate anion, as well as efflux of the organic monovalent cation, ethidium, but not its divalent analog, propidium.

Consistent with those findings, MATE proteins were found to transport a wide range of organic substrates (Omote et al., 2006), both anionic and cationic (Tanihara et al., 2007), and including ethidium in the case of the first characterized MATE family protein, the bacterial MATE, NorM (Morita et al., 2000). Nevertheless, it was somewhat surprising to the field of MATE researchers when it was discovered that the plant MATEs involved in Al resistance mediate the efflux of the anion, citrate. Thus, the findings in the recent Doshi et al. publication showing that at least SbMATE has a more broad transport substrate recognition allows us to very speculatively propose that SbMATE (and its orthologs) mediate the efflux of a complexed rather than free anionic form of citrate. This alternative could help explain the antiporter nature of these MATE transporters, as Al–citrate complexes, for instance, could actively be removed from the symplasm in a process energized by passive H^+ influx. Under this scenario, this group of MATE transporters would still mediate an Al resistance response by actively removing and detoxifying Al from the symplasm of root cells (i.e., mediating resistance), rather than mediating a process where Al is prevented from entering the root cell.

Malate and Citrate Transporters as Part of a Common Stress-Responsive Hub

Transcription factors including the Cys_2His_2-type zinc finger transcription factors OsART1 in rice (Yamaji et al., 2009) and AtSTOP1 and 2 (Sawaki et al., 2009), AtWRKY46 (Ding et al., 2013) in Arabidopsis, and the rice ASR (abscisic acidic, stress, and ripening) 1 and 5 (Arenhart et al., 2013, 2016; Lima et al., 2011), are involved with the regulation of membrane transporter genes. OsART1, an AtSTOP1 ortholog, modulates the expression of a number of membrane transporters involved in rice Al resistance, OsNrat1, OsMGT1, and OsFRDL4 (Xia et al., 2010; Yokosho et al., 2011; Chen et al., 2013). Similarly, AtSTOP1 modulates the expression of membrane transporters associated with Al resistance including *AtALMT1*, *AtMATE1*,

and *AtALS3* (Liu et al., 2009; Sawaki et al., 2009), in response to both Al and H^+ rhizotoxicity. Recently, as discussed in the next sections, changes in *AtSTOP1* regulation of *AtALMT1* have been shown to constitute a major component of P sensing pathways (Balzergue et al., 2017; Mora-Macías et al., 2017). Likewise, expression of *AtALMT1* is also regulated by other signaling pathways involving reactive oxygen species (ROS) and phytohormones (Daspute et al., 2017). Biotic stresses, such as that caused by infection of shoots by pathogenic *Pseudomonas syringae*, also triggered upregulation of *AtALMT1* expression and increased root malate exudation, which attracts the beneficial rhizobacterium, *Bacillus subtilis*, into the root microbiome and stimulates Arabidopsis immune responses (Rudrappa et al., 2008). Overall, these more recent observations indicate that the regulatory role of *AtSTOP1* on *AtALMT1* expression and associated physiological stress responses extend well beyond the original signaling roles associated with Al and H^+ stress.

Al Resistance Transporters That Do Not Transport Organic Acids: Aluminum-Sensitive 3 (ALS3)

Screening for Arabidopsis mutants with altered responses to Al toxicity led to the identification of mutants with increased sensitivity to Al, within which the recessive Al sensitive mutant, *als3*, showed 80% root growth inhibition by Al compared to 24–38% inhibition in the wild type (Larsen et al., 1996). This Al sensitive response was unrelated to enhanced Al uptake by *als3* plants (Larsen et al., 1997). Subsequently, map-based cloning identified ALS3 as an ABC transporter-like protein that is localized to leaf hydathodes and the phloem, in addition to the root cortex (Larsen et al., 2005). Based on its likely plasma membrane localization, it was suggested that ALS3 functions in an Al-specific manner to move Al away from sensitive tissues, thus providing Al resistance. ABC transporters contain both a nucleotide (ATP)-binding domain and a transmembrane (TM) domain (Rea, 2007). Larsen and colleagues noted that both ALS3 and the homologous putative bacterial metal resistance protein, ybbM, do not possess the ATP binding domain, which is normally needed for ABC transporters to function.

The ABC transporter, *sensitive to Al rhizotoxicity* (AtSTAR1), which possesses only the ATP-binding domain and not the TM domain, was implicated in Al resistance in Arabidopsis (Huang et al., 2010). AtSTAR1 is a homolog of rice OsSTAR1. Huang et al. (2009) showed that OsSTAR1 (which contains the nucleotide-binding domain) forms an ABC complex with OsSTAR2 (which contains the TM domain), which results in an active ABC transporter involved in Al resistance possibly by mediating UDP glucose efflux into the rice root cell wall. The actual mechanism whereby this activated form of glucose may provide Al tolerance still remains to be elucidated. However, Huang and collaborators hypothesize that UDP glucose may be transported by membrane-localized STAR1–STAR2 from the cytosol into vesicles, from which either UDP-glucose or derived glycoside would be released into the apoplast *via* exocytosis across the plasma membrane, and used to mask the sites for Al binding in the cell wall, thus providing Al resistance. In Arabidopsis, Huang et al. (2010) presented findings suggesting that AtSTAR1 may form a complex with ALS3, with ALS3 providing the TM domain enabling the formation of a functional AtSTAR1/ALS3 complex, which may mediate Al efflux from the outer cell layers of the root tip. These findings indicate that Arabidopsis Al resistance is complex, and also include AtALMT1 (Hoekenga et al., 2006) and AtMATE (Liu et al., 2009) providing root Al exclusion *via* root malate and citrate efflux. In addition to ALS3, a number of other putative Al transporters have been identified that could mediate Al resistance. These include OsNrat1, a rice root plasma membrane uptake transporter that ultimately results in Al storage in the root vacuole (Xia et al., 2010), AtNIP1, a root tip plasma membrane aquaporin protein that mediates root Al uptake (as an Al–malate complex) and sequestration (Wang et al., 2017), and another Arabidopsis ABC transporter, ALS1 (Larsen et al., 2007; Nezames et al., 2012).

Research based on suppressor screens have focused on the identification of molecular factors in the form of mutations that could complement the Al-sensitive phenotype of *als3* (Gabrielson et al., 2006). These studies implicated DNA damage as a biochemical target of Al (Rounds and Larsen, 2008; Nezames et al., 2012; Sjogren et al., 2015; Sjogren and Larsen, 2017), which is viewed as a possible venue to enhance crop Al resistance (Eekhout et al., 2017). One component is the cell cycle checkpoint factor, *ALUMINUM TOLERANT2* (*ALT2*), which may recruit members of the machinery involved with the detection and repair of DNA damage elicited by Al toxicity (Nezames et al., 2012). Accordingly, it was proposed that ALT2, and also ataxia telangiectasia-mutated and Rad3-related (ATR), impair the cell cycle and drive quiescent center differentiation in response to DNA damage caused by Al, leading to root growth arrest elicited by Al. It will be very interesting to assess the effect of the molecular factors involved with the biochemical targets of Al toxicity, such as DNA damage, in enhancing crop performance on acidic soils. Genetic manipulation of the underlying factors for Al toxicity is thought to hold potential for increasing global food security on acidic soils (Rounds and Larsen, 2008). Within the realm of natural variation for Al resistance in crop plants, the allelic effects of such factors may prove to be milder compared to that of major Al resistance genes encoding plasma membrane transporters. Nevertheless, exploiting such distinct biochemical pathways in concert, in the context of plant breeding, may offer potential for identifying transgressive segregants that could enhance even further crop perform on acidic soils.

POSSIBLE PLEIOTROPIC EFFECTS UNDERLYING Al RESISTANCE AND P ACQUISITION EFFICIENCY

SbMATE and TaALMT1 Increase Grain Yield on Al-Toxic and P-Deficient Soils

Overexpression of the wheat Al resistance gene, *TaALMT1*, in transgenic barley under the control of the ubiquitin promoter has been shown to enhance both P uptake and grain production on an acidic, high P-fixing soil (Delhaize et al., 2009). This effect was attributed in large part to the role of TaALMT1 in maintaining root growth under soil acidity, which likely results

from Al resistance. However, the observed greater P uptake per unit length in *TaALMT1*-expressing barley lines might also have resulted to some extent from P mobilization from the soil clays by the malate released into the rhizosphere, thus favoring P uptake (Delhaize et al., 2009). When the soil was limed, which substantially reduced Al saturation, grain yield of the transgenic and non-transgenic lines were similar, suggesting that enhanced P uptake under soil acidity was indeed largely achieved as an indirect effect of *TaALMT1* enhancing Al resistance. It should be noted that clay acidic soils generally have a strong buffering capacity and, although liming can be used to reduce Al^{3+} in the topsoil, neutralization of subsoil Al^{3+} is often difficult to achieve. In the absence of liming, Al resistance can have an important indirect effect on crop performance *via* both enhanced root proliferation in the topsoil, where P is primarily located on acidic soils (Lynch and Brown, 2001), and improved water acquisition by better root development in the subsoil. With liming, Al tolerance may most strongly benefit crop yields by enhanced water acquisition from deeper, acidic soils layers.

Allelic variation at the sorghum chromosome 3 Al resistance locus, Alt_{SB} (Magalhaes et al., 2004), where the citrate transporter, *SbMATE*, resides (Magalhaes et al., 2007), explains a large portion of the sorghum Al resistance phenotype. Recently, a sorghum recombinant inbred line (RIL) population was assessed for Al resistance both in lab-based hydroponics (relative root growth) and in the field (grain yield) under +/−Al exposure, in a phenotyping site located at the Embrapa Maize and Sorghum station in Brazil (Carvalho et al., 2016). In that study, sorghum hybrids were also constructed that were either homozygous for the Al-sensitive or -resistant *SbMATE* allele, or heterozygous for *SbMATE*. These hybrids were isogenic, so that Alt_{SB} alleles from different donors could be compared within a homogeneous genetic background, thus isolating the effect of *SbMATE* from genetic background effects.

The resulting isogenic hybrids were assessed for grain yield in the field on control (absence of Al toxicity in the soil) or in an Al toxic soil with 56% Al saturation in the top soil (0–20 cm) and ∼70% Al saturation in the sub-soil (20–40 cm). A major QTL underlying both Al resistance assessed in hydroponics and grain yield under Al toxicity in the field was co-located with *SbMATE* on sorghum chromosome 3, and explained a large portion of the genetic variance in the Al toxic but not in the non Al-toxic soil. The allele associated with increased Al resistance was donated by the Al tolerant parent, SC283, and the Al resistance allele did not decrease grain yield in the absence of Al toxicity, indicating that no yield penalty arises from Al-induced citrate release elicited by SbMATE. This genetic approach allowed the authors to estimate a consistent effect of a single Al resistance allele of *SbMATE* as a grain yield increase of ∼0.6 ton ha^{-1}, both in the RILs and in hybrid combinations. The rather additive gene action of *SbMATE* in grain yield production indicates that, when in homozygosity, *SbMATE* increases grain yield by more than 1.0–ha^{-1}, or more than 50% over the population mean. The Al saturation level in the Al toxic site, 56%, is well above the 20% critical level beyond which sorghum yields are reduced (Gourley, 1987). Therefore, most of the yield advantage of *SbMATE* is likely caused by its effect on Al resistance itself. However, the typical acidic soil in question also has high P fixation capacity and P diffusion is known to be highly depend on the soil water content (Novais and Smith, 1999). Therefore, as Al stress and low P availability in general co-exist on acidic soils, a smaller portion of the yield advantage caused by *SbMATE* may have originated from citrate-based enhanced P mobilization (Drouillon and Merckx, 2003) from the soil clays into the root surface, which is expected to favor P uptake.

A more compelling evidence for a pleiotropic effect of SbMATE on P acquisition comes from a genome-wide association mapping study conducted in West Africa (Leiser et al., 2014), which included gene-specific markers developed for *SbMATE* (Caniato et al., 2014). This study revealed that *SbMATE* SNPs were highly associated with grain yield and the associations were found especially under low P conditions for sorghum cultivated in soils at 29 different sites in West Africa, explaining up to 16% of the genotypic variance (Leiser et al., 2014). The average Al saturation was only 10% in the 16 field trials that were analyzed for Al saturation in the Leiser et al. (2014) study, and only one site had Al saturation reasonable above (27.5%) the critical level of Al saturation determined for sorghum (20%, Gourley, 1987). This suggests a direct pleiotropic effect of Al-activated citrated release promoted by SbMATE in enhancing P uptake and sorghum yields under low P availability in West Africa. It should be noted, however, that Al toxicity varies according to the chemical and mineral nature of the soils, which ultimately controls free Al^{3+} activity in the soil solution. Therefore, in sandy soils, such as those commonly found in West Africa, we cannot rule out that higher Al^{3+} activity in some of the sites may have led SbMATE activity to improve sorghum grain yield *via* Al resistance.

Evidence for a Pleiotropic Role of the STOP1/ALMT1 Module and ALS3 on P Acquisition *via* Changes in Root Morphology in Response to P Deficiency

Recent research findings exposed a possible direct link between AtALMT1 function and both Al resistance and changes in root growth triggered by response to low P (Balzergue et al., 2017; Mora-Macías et al., 2017). Previously, an antagonistic connection was established between phosphate and Fe availability, leading to adjustments in root growth (Müller et al., 2015). It was found that the *LPR1* (ferroxidase)/*PDR2* (P5-type ATPase) module enhances cell-specific Fe and callose deposition in the meristem and elongation zones under low P conditions. Under low Pi, accumulated ROS, possibly resulting from Fe toxicity triggered by Fe^{3+} accumulation in the apoplast *via* LPR1-dependent Fe oxidation, may lead to callose deposition. In turn, according to the proposed model, callose deposition in the RAM under low P impairs cell-to-cell movement of the SHORT-ROOT (SHR) transcription factor, which is important for stem cell maintenance, hence providing a checkpoint for primary root growth control in response to low P.

A mutation screen in Arabidopsis indicated that both ALMT1 and its transcriptional regulator, STOP1, repress primary root growth under −P conditions (Mora-Macías et al., 2017).

Furthermore, P deficiency was also shown to upregulate *ALMT1* expression in Arabidopsis, and experiments where exogenous malate was applied to the RAM restored the short root phenotype in *almt1* and *stop1* mutants in a concentration-dependent manner. Fe accumulation in the RAM was found to be required to activate the inhibition of primary root growth under −P conditions (Müller et al., 2015). Hence, the primary root growth inhibition by malate was suggested to occur *via* malate chelating and solubilizing Fe in the rhizosphere, which would promote Fe accumulation in the RAM apoplast (Mora-Macías et al., 2017). Accordingly, the resulting RAM exhaustion process leading to inhibition of the primary root growth under low P (Sánchez-Calderón et al., 2005) happens in the presence of Fe in the growth medium. Callose deposition, which is stimulated by ROS, may be involved in the root elongation inhibition following the model proposed by Müller et al. (2015). Hence, impaired cell-to-cell movement of the SHR transcription factor, which is important for stem cell maintenance, was suggested to lead to meristem exhaustion, inhibiting primary root growth (Müller et al., 2015; Mora-Macías et al., 2017). Because the enhanced proliferation of lateral roots coincides with the inhibition of the primary root (release of root apical dominance) under low P conditions (Sánchez-Calderón et al., 2005), ALMT1 may ultimately increase P uptake on acidic soils *via* increases in total root surface area, thereby favoring P diffusion toward the root surface.

A strikingly similar mechanism for an Al resistance gene leading to changes in root growth as a response to P deficiency has been proposed for ALS3 (Larsen et al., 1996, 2005) and AtSTAR1 (Huang et al., 2010; Belal et al., 2015; Dong et al., 2017). Together, STAR1 and STAR2 (a rice homolog of *als3*) form an ABC transporter implicated in Al resistance likely *via* the transport of UDP glucose into the root apoplast, which is believed to modify the cell wall leading to Al resistance (Huang et al., 2009) as previously discussed in Section "Al Resistance Transporters That do not Transport Organic Acids: Aluminum-Sensitive 3 (ALS3)." The commonality between the putative pleiotropic pathways mediated by *ALMT1* and *ALS3*/*AtSTAR1* is striking, particularly taking into consideration that those genes underlie distinctly different Al resistance mechanisms. Both pathways involve cross-talk between low P responses and Fe homeostasis, with involvement of LOW PHOSPHATE ROOT (LPR) oxidases; mutations in *LPR* leads to reduced Fe^{3+} accumulation in roots and thereby root growth insensitivity to low Pi (Müller et al., 2015; Dong et al., 2017; Mora-Macías et al., 2017). However, the ALS3 pathway involves UDP glucose, which reverses Fe^{3+} overaccumulation and rescues the short root phenotype in *als3* subjected to −P conditions (Dong et al., 2017). However, unlike the T-DNA mutants for *AtALMT1* and *STOP1*, *als3* shows enhanced inhibition of primary root growth under P deficiency (Dong et al., 2017), suggesting possible antagonism between Al resistance conferred by ALS3 and P acquisition.

These studies offer a radically different stance on root OA release enhancing resistance to low P solely *via* increased P availability in the rhizosphere, as root developmental changes caused by ALMT1/STOP1 and ALS3 appear to be a low P-specific response that is focused on root development. A common physiological basis centered on Fe homeostasis underlying the effect of distinctly different Al resistance pathways encoded by ALMT1/STOP1 and ALS3 on root remodeling under low P seems likely. Should those responses prove to persist for crops cultivated on acidic soils, it will be tempting to speculate that the close soil chemistry associations between Al toxicity and low P availability, which is centered on the presence of Fe and Al oxides, may have resulted in co-selective pressure for pleiotropic mechanisms enabling plants both to tolerate Al^{3+} and to acquire P more efficiently. Nevertheless, there is a strong need for strategies to validate whether the direction of this hypothetical pleiotropic effect is consistent with a positive net benefit on acidic soil performance.

Are Wall-Associated Kinases Associated With a Joint Effect on Al Resistance and P Acquisition?

Wall-associated kinases (WAKs), which are receptor-like kinase proteins (Kohorn and Kohorn, 2012) that span the plasma membrane and extend out into the cell wall (He et al., 1999), have been shown to play roles in cell expansion, development, morphogenesis, and defense responses to environmental stimuli (Sivaguru et al., 2003; Brutus et al., 2010; Kohorn and Kohorn, 2012; Gramegna et al., 2016; Mangeon et al., 2016). Sivaguru et al. (2003) reported that *AtWAK1* expression was rapidly induced by Al and disappeared after 9 h of Al exposure and that transgenic plants overexpressing *AtWAK1* showed enhanced Al resistance. Recently, a T-DNA knockout of the glycine-rich protein, AtGRP3, which interacts with AtWAK1 (Park et al., 2001), has also been shown to enhance Al resistance in Arabidopsis, similar to *AtWAK1* (Mangeon et al., 2016). However, *AtGRP3* expression was not modulated by Al and *grp3* had a long root phenotype in the absence of Al exposure. Therefore, it remains to be verified whether the lower root growth inhibition in *grp3* exposed to Al compared to the wt is in fact due to a mechanism enhancing Al resistance or is influenced to some extent by a leaky *grp* mutation, based on the role for *AtGRP3* in repressing root growth.

Wall-associated kinases form a subfamily within the receptor kinase (RLKs)/Pelle superfamily, which includes other subfamilies such as WAK-like kinase (WAKL) and Leaf rust 10 disease-resistance locus receptor-like protein kinase (LRK10), that share similar protein architectures with the WAK proteins (Shiu and Bleecker, 2003; Hou et al., 2005; Lim et al., 2014). The general WAK protein architecture features an extracellular moiety containing a cysteine-rich (Cys-rich) galacturonan-binding domain (Gub_Wak), epidermal growth factor (EGF) repeats, and a TM domain, in addition to a cytoplasmic serine/threonine kinase domain (Anderson et al., 2001; Decreux and Messiaen, 2005; Decreux et al., 2006).

Using association mapping, Hufnagel et al. (2014) showed that sorghum homologs of the rice serine/threonine receptor kinase, OsPSTOL1 (Gamuyao et al., 2012), are involved in increases in root surface area leading to enhanced P acquisition

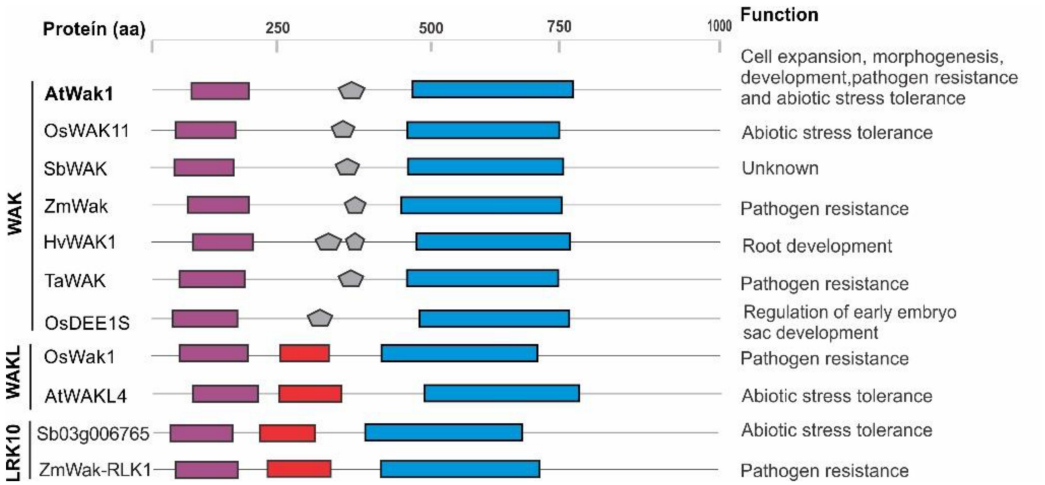

FIGURE 1 | Structure and possible function of WAK, WAKL, and LRK10 members of the RLKs/Pelle superfamily. Protein domains are represented with the following colors: purple (Gub_Wak), red (Wak association), and blue (Kinase). Amino acidic sequences were obtained from the National Center for Biotechnology Information (NCBI; http://www.ncbi.nlm.nih.gov) and Phytozome (www.phytozome.org) databases. The SbWAK protein sequence is available at Phytozome under accession Sobic.004G008100.1. The amino acidic alignment was performed with ClustalW (www.ebi.ac.uk/Tools/msa/clustalw2), and protein domain prediction was carried out using the Pfam (http://pfam.xfam.org/) and Smart (http://smart.embl-heidelberg.de/) tools. Inferences on functions for AtWak1(Anderson et al., 2001; Sivaguru et al., 2003; Brutus et al., 2010; Gramegna et al., 2016), OsWAK11(Hu et al., 2014), ZmWAK (Zuo et al., 2015), HvWAK1 (Kaur et al., 2013), TaWAK (Yang et al., 2014), OsDEE1S (Wang et al., 2012), OsWak1(Li et al., 2009), AtWAKL4 (Hou et al., 2005), Sb03g006765 (Hufnagel et al., 2014), and ZmWak-RLK1 (Hurni et al., 2015) are shown.

and grain yield under low P availability in the soil. In sorghum, these SbPSTOL1 proteins are predicted to have a signal peptide consistent with the targeting to a secretory pathway, as well as a TM domain and cell wall association domains. For example, the Sb03g006765 protein associated with P efficiency and increased root surface area is predicted to have a Cys-rich GUB_Wak domain and a wall-associated receptor kinase domain (WAK_association) located C-terminal to the GUB_Wak domain. Similarities between SbPSTOL1 and WAK proteins such as AtWAK1, which appears to be involved in Al resistance (Sivaguru et al., 2003), arise primarily from the presence of the GUB_Wak and TM domains, similar intron–exon organization, and a genomic localization in tight physical clusters (Hufnagel et al., 2014). Recent studies have suggested that amino acids in the Gub_Wak domain bind covalently to native pectins and oligogalacturonides in the cell wall (Verica and He, 2002; Decreux and Messiaen, 2005; Decreux et al., 2006; Kohorn and Kohorn, 2012; Kohorn et al., 2016). This leads us to speculate that SbPSTOL1 proteins may function as WAKs, functioning as receptors for the activation of signaling cascades in response to extracellular stimuli (in this case, P deficiency). However, in place of the EGF repeats, which is a hallmark of WAK proteins (Kanneganti and Gupta, 2008), WAKL and LRK10 members, including Sb03g006765, possess a WAK_association domain.

The GUB_Wak domain is present in certain plant proteins suggested to be involved in responses to abiotic and biotic stresses that belong to three subfamilies in the RLK superfamily, the WAKL, WAK, and LRK10 subfamilies (with Sb03g006765 within the LRK10 subfamily). These proteins are depicted in **Figure 1**. Sequence alignment of the GUB_Wak amino acidic sequences in these proteins does not show a high degree of conservation. However, this domain has conserved clusters of hydrophobicity that are essential for the association of these proteins *via* the extracellular residues, including a Cys-rich region and a conserved YPF motif. Therefore, it remains to be seen whether the SbPSTOL1 proteins functionally work as WAKs such as AtWAK1. If so, given the predicted role for SbPSTOL1 in enhancing root growth and P uptake in sorghum, this class of proteins could jointly control Al resistance and P uptake.

CONCLUSION

We are at a stage in research on crop plant adaptation to acidic soils where a number of different Al resistance genes have been identified. These genes have been discovered using a variety of both forward and reverse genetic strategies, ranging from candidate genes validated primarily *via* ectopic overexpression in transgenic plants or identified *via* mutant screens to map-based cloning of Al resistance genes underlying loci previously known to play a role in the genetic variation of Al resistance. In most cases, very little work has been done to translate the findings from the basic research used to identify and characterize the genes to practical applications to generate crop varieties in breeding programs. The research that connects with genetic variation present within crop species to identify Al resistance genes is certainly the most amenable to providing molecular tools for the breeding of crops with improved production on acidic soils. In the cases where genetic determinants of Al resistance have been found by other

approaches, efforts to assess whether those determinants are also active in crop plants in field conditions are sorely needed if the ultimate goal is indeed to generate crops more adapted to cultivation on acidic soils. While the effect of Al resistance on crop performance on acidic soils is known, pleiotropic effects of such genes on P uptake efficiency needs to be explored in crop species grown in the field. In both cases, detailed quantification is needed to gage the true potential of Al resistance genes in coping with agriculture in stress-prone areas. Particularly in a scenario where global climate change is resulting in greater drought stress, the potential of those genes to ensure food security worldwide may be far greater than initially believed.

AUTHOR CONTRIBUTIONS

JM and MP delineated and wrote this review. LM and LK wrote this review. LK also edited the manuscript.

FUNDING

JM and LM acknowledge support from the Fundação de Amparo a Pesquisa do Estado de Minas Gerais (FAPEMIG) and the National Council for Scientific and Technological Development (CNPq).

REFERENCES

Anderson, C. M., Wagner, T. A., Perret, M., He, Z. H., He, D., and Kohorn, B. D. (2001). WAKs: cell wall-associated kinases linking the cytoplasm to the extracellular matrix. *Plant Mol. Biol.* 47, 197–206. doi: 10.1023/A:1010691701578

Arenhart, R. A., De Lima, J. C., Pedron, M., Carvalho, F. E. L., Da Silveira, J. A. G., Rosa, S. B., et al. (2013). Involvement of ASR genes in aluminium tolerance mechanisms in rice. *Plant Cell Environ.* 36, 52–67. doi: 10.1111/j.1365-3040.2012.02553.x

Arenhart, R. A., Schunemann, M., Neto, L. B., Margis, R., Wang, Z. Y., and Margis-Pinheiro, M. (2016). Rice ASR1 and ASR5 are complementary transcription factors regulating aluminium responsive genes. *Plant Cell Environ.* 39, 645–651. doi: 10.1111/pce.12655

Bahia Filho, A. F. C., Magnavaca, R., Schaffert, R. E., and Alves, V. M. C. (1997). "Identification, utilization, and economic impact of maize germplasm tolerant to low levels of phosphorus and toxic levels of exchangeable aluminum in Brazilian soils," in *Plant-Soil Interactions at Low pH: Sustainable Agriculture and Forestry Production*, eds A. C. Moniz, A. M. C. Furlani, R. E. Schaffert, N. K. Fageria, C. A. Rosolem, and H. Cantarella (Campinas/Viçosa: Brazilian Soil Science Society), 59–70.

Balzergue, C., Dartevelle, T., Godon, C., Laugier, E., Meisrimler, C., Teulon, J. M., et al. (2017). Low phosphate activates STOP1-ALMT1 to rapidly inhibit root cell elongation. *Nat. Commun.* 8:15300. doi: 10.1038/ncomms15300

Belal, R., Tang, R., Li, Y., Mabrouk, Y., Badr, E., and Luan, S. (2015). An ABC transporter complex encoded by aluminum sensitive 3 and NAP3 is required for phosphate deficiency responses in *Arabidopsis*. *Biochem. Biophys. Res. Commun.* 463, 18–23. doi: 10.1016/j.bbrc.2015.05.009

Brutus, A., Sicilia, F., Macone, A., Cervone, F., and De Lorenzo, G. (2010). A domain swap approach reveals a role of the plant wall-associated kinase 1 (WAK1) as a receptor of oligogalacturonides. *Proc. Natl. Acad. Sci. U.S.A.* 107, 9452–9457. doi: 10.1073/pnas.1000675107

Caniato, F. F., Hamblin, M. T., Guimaraes, C. T., Zhang, Z., Schaffert, R. E., Kochian, L. V., et al. (2014). Association mapping provides insights into the origin and the fine structure of the sorghum aluminum tolerance locus, AltSB. *PLoS One* 9:e87438. doi: 10.1371/journal.pone.0087438

Carvalho, G Jr, Schaffert, R. E., Malosetti, M., Viana, J. H., Menezes, C. B., Silva, L. A., et al. (2016). Back to acid soil fields: the citrate transporter SbMATE is a major asset for sustainable grain yield for sorghum cultivated on acid soils. *G3* 6, 475–484. doi: 10.1534/g3.115.025791

Chen, Z. C., Yokosho, K., Kashino, M., Zhao, F. J., Yamaji, N., and Ma, J. F. (2013). Adaptation to acidic soil is achieved by increased numbers of cis-acting elements regulating ALMT1 expression in *Holcus lanatus*. *Plant J.* 76, 10–23. doi: 10.1111/tpj.12266

Daspute, A. A., Sadhukhan, A., Tokizawa, M., Kobayashi, Y., Panda, S. K., and Koyama, H. (2017). Transcriptional regulation of aluminum-tolerance genes in higher plants: clarifying the underlying molecular mechanisms. *Front. Plant Sci.* 8:1358. doi: 10.3389/fpls.2017.01358

Decreux, A., and Messiaen, J. (2005). Wall-associated kinase WAK1 interacts with cell wall pectins in a calcium-induced conformation. *Plant Cell Physiol.* 46, 268–278. doi: 10.1093/pcp/pci026

Decreux, A., Thomas, A., Spies, B., Brasseur, R., Cutsem, P., Van, et al. (2006). In vitro characterization of the homogalacturonan-binding domain of the wall-associated kinase WAK1 using site-directed mutagenesis. *Phytochemistry* 67, 1068–1079. doi: 10.1016/j.phytochem.2006.03.009

Delhaize, E., Gruber, B. D., and Ryan, P. R. (2007). The roles of organic anion permeases in aluminium resistance and mineral nutrition. *FEBS Lett.* 581, 2255–2262. doi: 10.1016/j.febslet.2007.03.057

Delhaize, E., Ma, J. F., and Ryan, P. R. (2012). Transcriptional regulation of aluminium tolerance genes. *Trends Plant Sci.* 17, 341–348. doi: 10.1016/j.tplants.2012.02.008

Delhaize, E., and Ryan, P. R. (1995). Aluminum toxicity and tolerance in plants. *Plant Physiol.* 107, 315–321. doi: 10.1104/pp.107.2.315

Delhaize, E., Taylor, P., Hocking, P. J., Simpson, R. J., Ryan, P. R., and Richardson, A. E. (2009). Transgenic barley (*Hordeum vulgare* L.) expressing the wheat aluminium resistance gene (TaALMT1) shows enhanced phosphorus nutrition and grain production when grown on an acid soil. *Plant Biotechnol. J.* 7, 391–400. doi: 10.1111/j.1467-7652.2009.00403.x

Ding, Z. J., Yan, J. Y., Xu, X. Y., Li, G. X., and Zheng, S. J. (2013). WRKY46 functions as a transcriptional repressor of ALMT1, regulating aluminum-induced malate secretion in *Arabidopsis*. *Plant J.* 76, 825–835. doi: 10.1111/tpj.12337

Dong, J., Piñeros, M. A., Li, X., Yang, H., Liu, Y., Murphy, A. S., et al. (2017). An *Arabidopsis* ABC transporter mediates phosphate deficiency-induced remodeling of root architecture by modulating iron homeostasis in roots. *Mol. Plant* 10, 244–259. doi: 10.1016/j.molp.2016.11.001

Doshi, R., McGrath, A. P., Piñeros, M., Szewczyk, P., Garza, D. M., Kochian, L. V., et al. (2017). Functional characterization and discovery of modulators of SbMATE, the agronomically important aluminium tolerance transporter from *Sorghum bicolor*. *Sci. Rep.* 7:17996. doi: 10.1038/s41598-017-18146-8

Doumbia, M. D., Hossner, L. R., and Onken, A. B. (1993). Variable sorghum growth in acid soils of subhumid West Africa. *Arid Soil Res. Rehabil.* 7, 335–346. doi: 10.1080/15324989309381366

Doumbia, M. D., Hossner, L. R., and Onken, A. B. (1998). Sorghum growth in acid soils of West Africa: variations in soil chemical properties. *Arid Land Res. Manage.* 12, 179–190. doi: 10.1080/15324989809381507

Drouillon, M., and Merckx, R. (2003). The role of citric acid as a phosphorus mobilization mechanism in highly P-fixing soils. *Gayana. Bot.* 60, 55–62. doi: 10.4067/S0717-66432003000100009

Eekhout, T., Larsen, P., and De Veylder, L. (2017). Modification of DNA checkpoints to confer aluminum tolerance. *Trends Plant Sci.* 22, 102–105. doi: 10.1016/j.tplants.2016.12.003

FAO and ITPS (2015). *Status of the World's Soil Resources (Main Report)*. Rome: FAO.

Foy, C. D., Duncan, R. R., Waskom, R. M., and Miller, D. R. (1993). Tolerance of sorghum genotypes to an acid, aluminum toxic *Tatum subsoil*. *J. Plant Nutr.* 16, 97–127. doi: 10.1080/01904169309364517

Furuichi, T., Sasaki, T., Tsuchiya, Y., Ryan, P. R., Delhaize, E., and Yamamoto, Y. (2010). An extracellular hydrophilic carboxy-terminal domain regulates the activity of TaALMT1, the aluminum-activated malate transport protein of wheat. *Plant J.* 64, 47–55. doi: 10.1111/j.1365-313X.2010.04309.x

Furukawa, J., Yamaji, N., Wang, H., Mitani, N., Murata, Y., Sato, K., et al. (2007). An aluminum-activated citrate transporter in barley. *Plant Cell Physiol.* 48, 1081–1091. doi: 10.1093/pcp/pcm091

Gabrielson, K. M., Cancel, J. D., Morua, L. F., and Larsen, P. B. (2006). Identification of dominant mutations that confer increased aluminium tolerance through mutagenesis of the Al-sensitive *Arabidopsis* mutant, als3-1. *J. Exp. Bot.* 57, 943–951. doi: 10.1093/jxb/erj080

Gamuyao, R., Chin, J. H., Pariasca-tanaka, J., Pesaresi, P., Catausan, S., Dalid, C., et al. (2012). The protein kinase Pstol1 from traditional rice confers tolerance of phosphorus deficiency. *Nature* 488, 535–539. doi: 10.1038/nature11346

Godfray, H. C. J., Beddington, J. R., Crute, I. R., Haddad, L., Lawrence, D., Muir, J. F., et al. (2010). Food security: the challenge of feeding 9 billion people. *Science* 327, 812–818. doi: 10.1126/science.1185383

Gourley, J. M. (1987). "Finding and utilizing exotic Al-tolerant sorghum germplasm," in *Sorghum for Acid Soils: Proceedings of a Workshop on Evaluating Sorghum for Tolerance to Al-toxic Tropical Soils in Latin America*, eds L. M. Gourley and J. G. Salinas (Palmira: CIAT), 293–309.

Gramegna, G., Modesti, V., Savatin, D. V., Sicilia, F., Cervone, F., and De Lorenzo, G. (2016). GRP-3 and KAPP, encoding interactors of WAK1, negatively affect defense responses induced by oligogalacturonides and local response to wounding. *J. Exp. Bot.* 67, 1715–1729. doi: 10.1093/jxb/erv563

He, Z. H., Cheeseman, I., He, D., and Kohorn, B. D. (1999). A cluster of five cell wall-associated receptor kinase genes, wak1-5, are expressed in specific organs of *Arabidopsis*. *Plant Mol. Biol.* 39, 1189–1196. doi: 10.1023/A:1006197318246

Hoekenga, O. A., Maron, L. G., Piñeros, M. A., Cançado, G. M. A., Shaff, J., Kobayashi, Y., et al. (2006). AtALMT1, which encodes a malate transporter, is identified as one of several genes critical for aluminum tolerance in *Arabidopsis*. *Proc. Natl. Acad. Sci. U.S.A.* 103, 9738–9743. doi: 10.1073/pnas.0602868103

Hou, X., Tong, H., Selby, J., Dewitt, J., Peng, X., and He, Z. H. (2005). Involvement of a cell wall-associated kinase, WAKL4, in *Arabidopsis* mineral responses. *Plant Physiol.* 139, 1704–1716. doi: 10.1104/pp.105.066910

Hu, W., Lv, Y., Lei, W., Li, X., Chen, Y., Zheng, L., et al. (2014). Cloning and characterization of the *Oryza sativa* wall-associated kinase gene OsWAK11 and its transcriptional response to abiotic stresses. *Plant Soil* 384, 335–346. doi: 10.1007/s11104-014-2204-8

Huang, C.-F., Yamaji, N., and Ma, J. F. (2010). Knockout of a bacterial-type ATP-binding cassette transporter gene, AtSTAR1, results in increased aluminum sensitivity in *Arabidopsis*. *Plant Physiol.* 153, 1669–1677. doi: 10.1104/pp.110.155028

Huang, C. F., Yamaji, N., Mitani, N., Yano, M., Nagamura, Y., and Ma, J. F. (2009). A bacterial-type ABC transporter is involved in aluminum tolerance in rice. *Plant Cell* 21, 655–667. doi: 10.1105/tpc.108.064543

Hufnagel, B., de Sousa, S. M., Assis, L., Guimaraes, C. T., Leiser, W., Azevedo, G. C., et al. (2014). Duplicate and conquer: multiple homologs of PHOSPHORUS-STARVATION TOLERANCE1 enhance phosphorus acquisition and sorghum performance on low-phosphorus soils. *Plant Physiol.* 166, 659–677. doi: 10.1104/pp.114.243949

Hufnagel, B., Guimaraes, C. T., Craft, E. J., Shaff, J. E., Schaffert, R. E., Kochian, L. V., et al. (2018). Exploiting sorghum genetic diversity for enhanced aluminum tolerance: allele mining based on the *AltSB* locus. *Sci. Rep.* 8:10094. doi: 10.1038/s41598-018-27817-z

Hurni, S., Scheuermann, D., Krattinger, S. G., Kessel, B., Wicker, T., Herren, G., et al. (2015). The maize disease resistance gene Htn1 against northern corn leaf blight encodes a wall-associated receptor-like kinase. *Proc. Natl. Acad. Sci. U.S.A.* 112, 8780–8785. doi: 10.1073/pnas.1502522112

Kanneganti, V., and Gupta, A. K. (2008). Wall associated kinases from plants – An overview. *Physiol. Mol. Biol. Plants* 14, 109–118. doi: 10.1007/s12298-008-0010-6

Kaur, R., Singh, K., and Singh, J. (2013). A root-specific wall-associated kinase gene, HvWAK1, regulates root growth and is highly divergent in barley and other cereals. *Funct. Integr. Genomics* 13, 167–177. doi: 10.1007/s10142-013-0310-y

Kochian, L. V. (1995). Cellular mechanisms of aluminum toxicity and resistance in plants. *Annu. Rev. Plant Physiol. Plant Mol. Biol.* 46, 237–260. doi: 10.1146/annurev.pp.46.060195.001321

Kochian, L. V., Hoekenga, O. A., and Piñeros, M. A. (2004). How do crop plants tolerate acid soils? Mechanisms of aluminum tolerance and phosphorous efficiency. *Annu. Rev. Plant Biol.* 55, 459–493. doi: 10.1146/annurev.arplant.55.031903.141655

Kochian, L. V., Piñeros, M. A., Liu, J., and Magalhaes, J. V. (2015). Plant adaptation to acid soils: the molecular basis for crop aluminum resistance. *Annu. Rev. Plant Biol.* 66, 571–598. doi: 10.1146/annurev-arplant-043014-114822

Kohorn, B. D., Hoon, D., Minkoff, B. B., Sussman, M. R., and Kohorn, S. L. (2016). Rapid oligo-galacturonide induced changes in protein phosphorylation in *Arabidopsis*. *Mol. Cell. Proteom.* 15, 1351–1359. doi: 10.1074/mcp.M115.055368

Kohorn, B. D., and Kohorn, S. L. (2012). The cell wall-associated kinases, WAKs, as pectin receptors. *Front. Plant Sci.* 3:88. doi: 10.3389/fpls.2012.00088

Larsen, P. B., Cancel, J., Rounds, M., and Ochoa, V. (2007). Arabidopsis ALS1 encodes a root tip and stele localized half type ABC transporter required for root growth in an aluminum toxic environment. *Planta* 225, 1447–1458. doi: 10.1007/s00425-006-0452-4

Larsen, P. B., Geisler, M. J. B., Jones, C. A., Williams, K. M., and Cancel, J. D. (2005). ALS3 encodes a phloem-localized ABC transporter-like protein that is required for aluminum tolerance. *Plant J.* 41, 353–363. doi: 10.1111/j.1365-313X.2004.02306.x

Larsen, P. B., Kochian, L. V., and Howell, S. H. (1997). Al inhibits both shoot development and root growth in als3, an Al-sensitive *Arabidopsis* mutant. *Plant Physiol.* 114, 1207–1214. doi: 10.1104/pp.114.4.1207

Larsen, P. B., Tai, C. Y., Kochian, L. V., and Howell, S. H. (1996). *Arabidopsis* mutants with increased sensitivity to aluminum. *Plant Physiol.* 110, 743–751. doi: 10.1104/pp.110.3.743

Leiser, W. L., Rattunde, H. F. W., Weltzien, E., Cisse, N., Abdou, M., Diallo, A., et al. (2014). Two in one sweep: aluminum tolerance and grain yield in P-limited soils are associated to the same genomic region in West African Sorghum. *BMC Plant Biol.* 14:206. doi: 10.1186/s12870-014-0206-6

Li, H., Zhou, S. Y., Zhao, W. S., Su, S. C., and Peng, Y. L. (2009). A novel wall-associated receptor-like protein kinase gene, OsWAK1, plays important roles in rice blast disease resistance. *Plant Mol. Biol.* 69, 337–346. doi: 10.1007/s11103-008-9430-5

Li, X., Zeng, R., and Liao, H. (2016). Improving crop nutrient efficiency through root architecture modifications. *J. Integr. Plant Biol.* 58, 193–202. doi: 10.1111/jipb.12434

Ligaba, A., Dreyer, I., Margaryan, A., Schneider, D. J., Kochian, L., and Piñeros, M. (2013). Functional, structural and phylogenetic analysis of domains underlying the Al sensitivity of the aluminum-activated malate/anion transporter, TaALMT1. *Plant J.* 76, 766–780. doi: 10.1111/tpj.12332

Lim, C. W., Yang, S. H., Shin, K. H., Lee, S. C., and Kim, S. H. (2014). The AtLRK10L1.2, *Arabidopsis* ortholog of wheat LRK10, is involved in ABA-mediated signaling and drought resistance. *Plant Cell Rep.* 34, 447–455. doi: 10.1007/s00299-014-1724-2

Lima, J. C., Arenhart, R. A., Margis-Pinheiro, M., and Margis, R. (2011). Aluminum triggers broad changes in microRNA expression in rice roots. *Genet. Mol. Res.* 10, 2817–2832. doi: 10.4238/2011.November.10.4

Liu, J., Magalhaes, J. V., Shaff, J., and Kochian, L. V. (2009). Aluminum-activated citrate and malate transporters from the MATE and ALMT families function independently to confer *Arabidopsis aluminum* tolerance. *Plant J.* 57, 389–399. doi: 10.1111/j.1365-313X.2008.03696.x

Liu, M. Y., Lou, H. Q., Chen, W. W., Piñeros, M. A., Xu, J. M., Fan, W., et al. (2018). Two citrate transporters coordinately regulate citrate secretion from rice bean root tip under aluminum stress. *Plant. Cell Environ.* 41, 809–822. doi: 10.1111/pce.13150

López-Arredondo, D. L., Leyva-González, M. A., González-Morales, S. I., López-Bucio, J., and Herrera-Estrella, L. (2014). Phosphate nutrition: improving low-phosphate tolerance in crops. *Annu. Rev. Plant Biol.* 65, 95–123. doi: 10.1146/annurev-arplant-050213-035949

Lynch, J. P. (2011). Root phenes for enhanced soil exploration and phosphorus acquisition: tools for future crops. *Plant Physiol.* 156, 1041–1049. doi: 10.1104/pp.111.175414

Lynch, J. P., and Brown, K. M. (2001). Topsoil foraging – An architectural adaptation of plants to low phosphorus availability. *Plant Soil* 237, 225–237. doi: 10.1023/A:1013324727040

Ma, J. F., Ryan, P. R., and Delhaize, E. (2001). Aluminium tolerance in plants and the complexing role of organic acids. *Trends Plant Sci.* 6, 273–278. doi: 10.1016/S1360-1385(01)01961-6

Magalhaes, J. V., Garvin, D. F., Wang, Y., Sorrells, M. E., Klein, P. E., Schaffert, R. E., et al. (2004). Comparative mapping of a major aluminum tolerance gene in sorghum and other species in the Poaceae. *Genetics* 167, 1905–1914. doi: 10.1534/genetics.103.023580

Magalhaes, J. V., Liu, J., Guimarães, C. T., Lana, U. G. P., Alves, V. M. C., Wang, Y.-H., et al. (2007). A gene in the multidrug and toxic compound extrusion (MATE) family confers aluminum tolerance in sorghum. *Nat. Genet.* 39, 1156–1161. doi: 10.1038/ng2074

Mangeon, A., Pardal, R., Menezes-Salgueiro, A. D., Duarte, G. L., de Seixas, R., Cruz, F. P., et al. (2016). AtGRP3 is implicated in root size and aluminum response pathways in *Arabidopsis*. *PLoS One* 11:e0150583. doi: 10.1371/journal.pone.0150583

Maron, L. G., Piñeros, M. A., Guimarães, C. T., Magalhaes, J. V., Pleiman, J. K., Mao, C., et al. (2009). Two functionally distinct members of the MATE (multidrug and toxic compound extrusion) family of transporters potentially underlie two major aluminum tolerance QTLs in maize. *Plant J.* 61, 728–740. doi: 10.1111/j.1365-313X.2009.04103.x

Marschner, H. (ed.). (1995). "Adaptation of plants to adverse chemical soil conditions," in *Mineral Nutrition of Higher Plants* (London: Academic Press), 596–657. doi: 10.1016/B978-012473542-2/50018-3

Melo, J. O., Lana, U. G. P., Piñeros, M. A., Alves, V. M. C., Guimarães, C. T., Liu, J., et al. (2013). Incomplete transfer of accessory loci influencing SbMATE expression underlies genetic background effects for aluminum tolerance in sorghum. *Plant J.* 73, 276–288. doi: 10.1111/tpj.12029

Mendes, F. F., Guimarães, L. J. M., Souza, J. C., Guimarães, P. E. O., Magalhaes, J. V., Garcia, A. A. F., et al. (2014). Genetic architecture of phosphorus use efficiency in tropical maize cultivated in a low-P soil. *Crop Sci.* 54, 1530–1538. doi: 10.2135/cropsci2013.11.0755

Mora-Macías, J., Ojeda-Rivera, J. O., Gutiérrez-Alanís, D., Yong-Villalobos, L., Oropeza-Aburto, A., Raya-González, J., et al. (2017). Malate-dependent Fe accumulation is a critical checkpoint in the root developmental response to low phosphate. *Proc. Natl. Acad. Sci. U.S.A.* 114, E3563–E3572. doi: 10.1073/pnas.1701952114

Morita, Y., Kataoka, A., Shiota, S., Mizushima, T., and Tsuchiya, T. (2000). NorM of *Vibrio parahaemolyticus* is an Na+ −driven multidrug efflux pump. *J. Bacteriol.* 182, 6694–6697. doi: 10.1128/JB.182.23.6694-6697.2000

Müller, J., Toev, T., Heisters, M., Teller, J., Moore, K. L., Hause, G., et al. (2015). Iron-dependent callose deposition adjusts root meristem maintenance to phosphate availability. *Dev. Cell* 33, 216–230. doi: 10.1016/j.devcel.2015.02.007

Nezames, C. D., Sjogren, C. A., Barajas, J. F., and Larsen, P. B. (2012). The *Arabidopsis* cell cycle checkpoint regulators TANMEI/ALT2 and ATR mediate the active process of aluminum-dependent root growth inhibition. *Plant Cell Online* 24, 608–621. doi: 10.1105/tpc.112.095596

Nobel, P. S. (1991). *Physicochemical and Environmental Plant Physiology*. London: Academic Press.

Novais, R. F., and Smith, T. F. (1999). "Difusão," in *Fósforo em Solo e Planta em Condições Tropicais*, eds R. F. Novais and T. F. Smith (San Francisco, CA: Scribd), 213–234.

Omote, H., Hiasa, M., Matsumoto, T., Otsuka, M., and Moriyama, Y. (2006). The MATE proteins as fundamental transporters of metabolic and xenobiotic organic cations. *Trends Pharmacol. Sci.* 27, 587–593. doi: 10.1016/j.tips.2006.09.001

Park, A. R., Cho, S. K., Yun, U. J., Jin, M. Y., Lee, S. H., Sachetto-Martins, G., et al. (2001). Interaction of the *Arabidopsis* receptor protein kinase Wak1 with a glycine-rich protein, AtGRP-3. *J. Biol. Chem.* 276, 26688–26693. doi: 10.1074/jbc.M101283200

Piñeros, M. A., Cancado, G. M. A., and Kochian, L. V. (2008). Novel properties of the wheat aluminum tolerance organic acid transporter (TaALMT1) revealed by electrophysiological characterization in *Xenopus oocytes*: functional and structural implications. *Plant Physiol.* 147, 2131–2146. doi: 10.1104/pp.108.119636

Postma, J. A., Dathe, A., and Lynch, J. P. (2014). The optimal lateral root branching density for maize depends on nitrogen and phosphorus availability. *Plant Physiol.* 166, 590–602. doi: 10.1104/pp.113.233916

Ramesh, S. A., Kamran, M., Sullivan, W., Chirkova, L., Okamoto, M., Degryse, F., et al. (2018). Aluminum-activated malate transporters can facilitate GABA transport. *Plant Cell* 30, 1147–1164. doi: 10.1105/tpc.17.00864

Ramesh, S. A., Tyerman, S. D., Xu, B., Bose, J., Kaur, S., Conn, V., et al. (2015). GABA signalling modulates plant growth by directly regulating the activity of plant-specific anion transporters. *Nat. Commun.* 6:7879. doi: 10.1038/ncomms8879

Rea, P. A. (2007). Plant ATP-binding Cassette transporters. *Annu. Rev. Plant Biol.* 58, 347–375. doi: 10.1146/annurev.arplant.57.032905.105406

Rounds, M. A., and Larsen, P. B. (2008). Aluminum-dependent root-growth inhibition in *Arabidopsis* results from AtATR-regulated cell-cycle arrest. *Curr. Biol.* 18, 1495–1500. doi: 10.1016/j.cub.2008.08.050

Rudrappa, T., Czymmek, K. J., Paré, P. W., and Bais, H. P. (2008). Root-secreted malic acid recruits beneficial soil bacteria. *Plant Physiol.* 148, 1547–1556. doi: 10.1104/pp.108.127613

Ryan, P. R., Raman, H., Gupta, S., Horst, W. J., and Delhaize, E. (2009). A second mechanism for aluminum resistance in wheat relies on the constitutive efflux of citrate from roots. *Plant Physiol.* 149, 340–351. doi: 10.1104/pp.108.129155

Sanches, P. A., and Salinas, J. G. (1981). Low input technology for managing oxisol and utisols in tropical America. *Adv. Agron.* 34, 229–406.

Sánchez-Calderón, L., López-Bucio, J., Chacón-López, A., Cruz-Ramírez, A., Nieto-Jacobo, F., Dubrovsky, J. G., et al. (2005). Phosphate starvation induces a determinate developmental program in the roots of *Arabidopsis thaliana*. *Plant Cell Physiol.* 46, 174–184. doi: 10.1093/pcp/pci011

Sasaki, T., Yamamoto, Y., Ezaki, B., Katsuhara, M., Ahn, S. J., Ryan, P. R., et al. (2004). A wheat gene encoding an aluminum-activated malate transporter. *Plant J.* 37, 645–653. doi: 10.1111/j.1365-313X.2003.01991.x

Sawaki, Y., Iuchi, S., Kobayashi, Y. Y. Y., Kobayashi, Y. Y. Y., Ikka, T., Sakurai, N., et al. (2009). STOP1 regulates multiple genes that protect *Arabidopsis* from proton and aluminum toxicities. *Plant Physiol.* 150, 281–294. doi: 10.1104/pp.108.134700

Sharma, T., Dreyer, I., Kochian, L., and Piñeros, M. A. (2016). The ALMT family of organic acid transporters in plants and their involvement in detoxification and nutrient security. *Front. Plant Sci.* 7:1488. doi: 10.3389/fpls.2016.01488

Shaw, J. N. (2001). Iron and aluminum oxide characterization for highly-weathered Alabama ultisols. *Commun. Soil Sci. Plant Anal.* 32, 49–64. doi: 10.1081/CSS-100102992

Shiu, S., and Bleecker, A. B. (2003). Expansion of the receptor-like kinase/Pelle gene family and receptor-like proteins in *Arabidopsis*. *Plant Physiol.* 132, 530–543. doi: 10.1104/pp.103.021964.tochaud

Silva, C. M. S., Zhang, C., Habermann, G., Delhaize, E., and Ryan, P. R. (2018). Does the major aluminium-resistance gene in wheat, TaALMT1, also confer tolerance to alkaline soils? *Plant Soil* 424, 451–462. doi: 10.1007/s11104-017-3549-6

Sivaguru, M., Ezaki, B., He, Z. H., Tong, H., Osawa, H., Baluska, F., et al. (2003). Aluminum-induced gene expression and protein localization of a cell wall-associated receptor kinase in *Arabidopsis*. *Plant Physiol.* 132, 2256–2266. doi: 10.1104/pp.103.022129.plasma

Sjogren, C. A., Bolaris, S. C., and Larsen, P. B. (2015). Aluminum-dependent terminal differentiation of the *Arabidopsis* root tip is mediated through an ATR-, ALT2-, and SOG1-regulated transcriptional response. *Plant Cell* 27, 2501–2515. doi: 10.1105/tpc.15.00172

Sjogren, C. A., and Larsen, P. B. (2017). SUV2, which encodes an ATR-related cell cycle checkpoint and putative plant ATRIP, is required for aluminium-dependent root growth inhibition in Arabidopsis. *Plant Cell Environ.* 40, 1849–1860. doi: 10.1111/pce.12992

Tanihara, Y., Masuda, S., Sato, T., Katsura, T., Ogawa, O., and Inui, K. (2007). Substrate specificity of MATE1 and MATE2-K, human multidrug and toxin extrusions/H+ -organic cation antiporters. *Biochem. Pharmacol.* 74, 359–371. doi: 10.1016/j.bcp.2007.04.010

Tanksley, S. D., and McCouch, S. R. (1997). Seed banks and molecular maps: unlocking genetic potential from the wild. *Science* 277, 1063–1066. doi: 10.1126/science.277.5329.1063

Tovkach, A., Ryan, P. R., Richardson, A. E., Lewis, D. C., Rathjen, T. M., Ramesh, S., et al. (2013). Transposon-mediated alteration of TaMATE1B expression in wheat confers constitutive citrate efflux from root apices. *Plant Physiol.* 161, 880–892. doi: 10.1104/pp.112.207142

Tully, K., Sullivan, C., Weil, R., and Sanchez, P. (2015). The state of soil degradation in sub-Saharan Africa: baselines, trajectories, and solutions. *Sustain* 7, 6523–6552. doi: 10.3390/su7066523

Verica, J., and He, Z. (2002). The cell wall-associated kinase (WAK) and WAK-like kinase gene family. *Plant Physiol.* 129, 455–459. doi: 10.1104/pp.011028.1

von Uexküll, H. R., and Mutert, E. (1995). Global extent, development and economic impact of acid soils. *Plant Soil* 171, 1–15. doi: 10.1007/BF00009558

Wang, J., Raman, H., Zhou, M., Ryan, P. R., Delhaize, E., Hebb, D. M., et al. (2007). High-resolution mapping of the Alp locus and identification of a candidate

gene HvMATE controlling aluminium tolerance in barley (*Hordeum vulgare* L.). *Theor. Appl. Genet.* 115, 265–276. doi: 10.1007/s00122-007-0562-9

Wang, N., Huang, H.-J., Ren, S.-T., Li, J.-J., Sun, Y., Sun, D.-Y., et al. (2012). The rice wall-associated receptor-like kinase gene OsDEES1 plays a role in female gametophyte development. *Plant Physiol.* 160, 696–707. doi: 10.1104/pp.112.203943

Wang, Y., Li, R., Li, D., Jia, X., Zhou, D., Li, J., et al. (2017). NIP1;2 is a plasma membrane-localized transporter mediating aluminum uptake, translocation, and tolerance in *Arabidopsis*. *Proc. Natl. Acad. Sci. U.S.A.* 114, 5047–5052. doi: 10.1073/pnas.1618557114

Xia, J., Yamaji, N., Kasai, T., and Ma, J. F. (2010). Plasma membrane-localized transporter for aluminum in rice. *Proc. Natl. Acad. Sci. U.S.A.* 107, 18381–18385. doi: 10.1073/pnas.1004949107

Yamaji, N., Huang, C. F., Nagao, S., Yano, M., Sato, Y., Nagamura, Y., et al. (2009). A zinc finger transcription factor ART1 regulates multiple genes implicated in aluminum tolerance in rice. *Plant Cell* 21, 3339–3349. doi: 10.1105/tpc.109.070771

Yang, K., Qi, L., and Zhang, Z. (2014). Isolation and characterization of a novel wall-associated kinase gene TaWAK5 in wheat (*Triticum aestivum*). *Crop J.* 2, 255–266. doi: 10.1016/j.cj.2014.04.010

Yang, X. Y., Yang, J. L., Zhou, Y., Piñeros, M. A., Kochian, L. V., Li, G. X., et al. (2011). A de novo synthesis citrate transporter, *Vigna umbellata* multidrug and toxic compound extrusion, implicates in Al-activated citrate efflux in rice bean (*Vigna umbellata*) root apex. *Plant Cell Environ.* 34, 2138–2148. doi: 10.1111/j.1365-3040.2011.02410.x

Yokosho, K., Yamaji, N., Fujii-Kashino, M., and Ma, J. F. (2016). Functional analysis of a MATE gene OsFRDL2 revealed its involvement in Al-induced secretion of citrate, but a lower contribution to Al tolerance in rice. *Plant Cell Physiol.* 57, 976–985. doi: 10.1093/pcp/pcw026

Yokosho, K., Yamaji, N., and Ma, J. F. (2011). An Al-inducible MATE gene is involved in external detoxification of Al in rice. *Plant J.* 68, 1061–1069. doi: 10.1111/j.1365-313X.2011.04757.x

Zhang, W.-H., Ryan, P. R., Sasaki, T., Yamamoto, Y., Sullivan, W., and Tyerman, S. D. (2008). Characterization of the TaALMT1 protein as an Al3+-activated anion channel in transformed tobacco (*Nicotiana tabacum* L.) cells. *Plant Cell Physiol.* 49, 1316–1330. doi: 10.1093/pcp/pcn107

Zhu, J., and Lynch, J. P. (2004). The contribution of lateral rooting to phosphorus acquisition efficiency in maize (*Zea mays*) seedlings. *Funct. Plant Biol.* 31:949. doi: 10.1071/FP04046

Zuo, W., Chao, Q., Zhang, N., Ye, J., Tan, G., Li, B., et al. (2015). A maize wall-associated kinase confers quantitative resistance to head smut. *Nat. Genet.* 47, 151–157. doi: 10.1038/ng.3170

Conflict of Interest Statement: The authors declare that the research was conducted in the absence of any commercial or financial relationships that could be construed as a potential conflict of interest.

The reviewer MD and handling Editor declared their shared affiliation.

frontiers in Plant Science

REVIEW
published: 18 June 2018
doi: 10.3389/fpls.2018.00807

Aluminum–Nitrogen Interactions in the Soil–Plant System

Xue Q. Zhao[1] *and Ren F. Shen*[1,2]*

[1] State Key Laboratory of Soil and Sustainable Agriculture, Institute of Soil Science, Chinese Academy of Sciences, Nanjing, China, [2] University of Chinese Academy of Sciences, Beijing, China

Aluminum (Al) is the most abundant metal in the Earth's crust and is not an essential element for plant growth. In contrast, nitrogen (N) is the most important mineral element for plant growth, but this non-metal is often present at low levels in soils, and plants are often N deficient. Aluminum toxicity is dominant in acid soils, and so plants growing in acid soils have to overcome both Al toxicity and N limitation. Because of low N-use efficiency, large amounts of N fertilizers are applied to crop fields to achieve high yields, leading to soil acidification and potential Al toxicity. Aluminum lowers plant N uptake and N-use efficiency because Al inhibits root growth. Although numerous studies have investigated the interactions between Al and N, a complete review of these studies was lacking. This review describes: (1) the link between plant Al tolerance and ammonium/nitrate (NH_4^+/NO_3^-) preference; (2) the effects of NH_4^+/NO_3^- and pH on Al toxicity; (3) the effects of Al on soil N transformations; and (4) the effects of Al on NH_4^+/NO_3^- uptake and assimilation by plants. Acid soils are characterized chemically by a relatively high ratio of NH_4^+ to NO_3^- and high concentrations of toxic Al. Aluminum-tolerant plants generally prefer NH_4^+ as an N source, while Al-sensitive plants prefer NO_3^-. Compared with NO_3^-, NH_4^+ increases the solubilization of toxic Al into soil solutions, but NH_4^+ generally alleviates Al phytotoxicity under solution culture because the protons from NH_4^+ compete with Al^{3+} for adsorption sites on the root surface. Plant NO_3^- uptake and nitrate reductase activity are both inhibited by Al, while plant NH_4^+ uptake is inhibited to a smaller degree than NO_3^-. Together, the results of numerous studies indicate that there is a synergistic interaction between plant Al tolerance and NH_4^+ nutrition. This has important implications for the adaptation of plants to acid soils that are dominated chemically by toxic Al as well as NH_4^+. Finally, we discuss how this knowledge can be used to increase plant Al tolerance and N-use efficiency in acid soils.

Keywords: aluminum, nitrogen, ammonium, nitrate, interaction, plant, acid soil

OPEN ACCESS

Edited by:
Peter Ryan, Commonwealth Scientific and Industrial Research Organisation (CSIRO), Australia

Reviewed by:
Brent N. Kaiser, University of Sydney, Australia
Francesco Di Gioia, University of Florida, United States

***Correspondence:**
Ren F. Shen
rfshen@issas.ac.cn

Specialty section:
This article was submitted to Plant Abiotic Stress, a section of the journal Frontiers in Plant Science

Received: *06 February 2018*
Accepted: *25 May 2018*
Published: *18 June 2018*

Citation:
Zhao XQ and Shen RF (2018) Aluminum–Nitrogen Interactions in the Soil–Plant System. Front. Plant Sci. 9:807. doi: 10.3389/fpls.2018.00807

INTRODUCTION

Acid soils cover approximately 30% of the ice-free land and up to 70% of potentially arable soils worldwide (von Uexküll and Mutert, 1995). Acid soils occur mainly in humid tropical and temperate areas (von Uexküll and Mutert, 1995), where water and heat are generally abundant for plant growth, implying that acid soils have huge productive potential. However, plant productivity

in acid soils is limited primarily by aluminum (Al) toxicity accompanied by deficiencies of some nutrients (Zhao et al., 2014). The improvement of crop productivity in acid soils depends on the dual enhancement of plant Al tolerance and nutrient-use efficiency.

Nitrogen (N) is the most abundant mineral nutrient required by plants. Soil N availability greatly affects the growth and development of crops worldwide (Gutiérrez, 2012). Nitrogen deficiency is a widespread problem for plants grown in terrestrial ecosystems (Vitousek and Howarth, 1991), and it is also a major factor limiting plant growth in acid soils (Fageria and Baligar, 2001). Large amounts of N fertilizers are used in agriculture to grow crops that feed an increasing global population every year. Erisman et al. (2008) estimated that N fertilizer has supported around 4 billion people born since 1908, accounting for approximately 27% of the world's population over the past century. At the same time, excess N fertilization is causing environmental problems such as water eutrophication, greenhouse gas emissions, nitrate (NO_3^-) loss, acid rain, and soil acidification due to low N-use efficiency (Ju et al., 2009). High yields and high nutrient-use efficiency are essential for contemporary agriculture. Therefore, there is an urgent need to increase plant N-use efficiency by understanding the responses to N (Kant et al., 2011).

Aluminum is the most abundant metal in the Earth's crust. It is not an essential element for plants, and excess Al is toxic to most plants. The primary symptom of Al phytotoxicity is the inhibition of root elongation, which can occur after exposure to Al^{3+} at concentrations as low as μM levels within 1 h (Matsumoto, 2000; Kochian et al., 2005; Ma, 2007). This inhibition can be caused by reductions in cell elongation and cell division, which are attributed to Al interference with the cell wall, plasma membrane, the cytoskeleton, oxidative stress, signal transduction pathways, cytoplasm calcium homeostasis, magnesium uptake, and auxin polar transport (Ma, 2007). Plants have two strategies to detoxify Al (Ma, 2007). One is to exclude Al from the root tips (exclusion mechanism) and the other is to tolerate Al that enters the plant body (internal tolerance mechanism). Roots are the main organ for plants to take up nutrients from the growth medium, so Al toxicity inevitably affects the ability of plants to acquire nutrients from acid soils. On one hand, the inhibitory effects of Al on root growth can reduce the amounts of nutrients taken up by plants because of the small root volume. On the other hand, Al may directly affect the transport and metabolism of nutrients within plants. Interactions between Al and many nutrients often occur within soils and plants (Zhao et al., 2014). Most reports have focused on the effects of various externally added nutrients on Al phytotoxicity (Zhao et al., 2014), but the effects of Al on the uptake of these nutrients by plants and their corresponding mechanisms have received relatively little attention.

Aluminum is beneficial and even potentially essential for some plant species (Bojórquez-Quintal et al., 2017), because of the Al-induced stimulation of nutrient uptake (Watanabe and Osaki, 2002). Aluminum supply was shown to stimulate N uptake by several plant species adapted to acid soils (Osaki et al., 1997), and Al treatments increased shoot N contents in wheat and rye (Dinev and Stancheva, 1993). In contrast, Al reduced root N uptake and its upward translocation to shoots in sorghum and corn (Gomes et al., 1985; Pintro et al., 1996). Aluminum promoted the growth of plants supplied with ammonium (NH_4^+) but inhibited that of plants supplied with NO_3^- (Zhao et al., 2014). Nitrogen is a metabolic element involved in the synthesis of amino acids and proteins within plants. Knowledge about Al–N interactions may supply new information to explain instances where Al benefits plant growth.

Several reviews have focused on the interactions between Al and phosphorus (Chen et al., 2012), calcium (Rengel and Zhang, 2003; Meriño-Gergichevich et al., 2010), magnesium (Bose et al., 2011; Chen and Ma, 2013), boron, and silicon (Hodson and Evans, 1995; Horst et al., 2010). Aluminum is a metal and a toxic element to many plants, while N is a non-metal and is an essential element for all plants. More than 100 papers have reported on Al–N interactions so far, highlighting the importance of this topic. Despite the large amount of literature on Al–N interactions, there has been no systematic review of this topic so far. Here, we provide a detailed description and analysis of studies on the interactions between Al and N, including the link between plant Al tolerance and NH_4^+/NO_3^- preference, the effects of NH_4^+/NO_3^- and pH on Al toxicity, the effects of Al on soil N transformations, and the effects of Al on NH_4^+/NO_3^- uptake and assimilation. We also propose a strategy for improving plant Al tolerance and N-use efficiency in acid soils.

LINK BETWEEN PLANT Al TOLERANCE AND INORGANIC N PREFERENCE

Acid soils are characterized by poor nitrification and high levels of soluble Al, while neutral to calcareous soils show high nitrification and lower levels of Al toxicity (Zhao et al., 2014; Che et al., 2015). The two main inorganic N sources available for plant growth are NH_4^+ and NO_3^-. Therefore, on the basis of the environment driving evolution, plants originating from acid soils are Al tolerant and prefer NH_4^+ to NO_3^-, while those originating from neutral to calcareous soils are Al sensitive and prefer NO_3^- to NH_4^+ (Gigon and Rorison, 1972; Foy and Fleming, 1978; Rorison, 1985; Falkengren-Grerup, 1995; Marschner, 1995; Maathuis, 2009; Zhao et al., 2013b) (**Table 1**). For instance, the growth of lowbush blueberry, which is adapted to strongly acid soils, was shown to be greatly promoted by NH_4^+ but strongly inhibited by NO_3^- (Townsend, 1966; Townsend and Blatt, 1966). Wheat and barley are Al-sensitive and prefer NO_3^- (Malhi et al., 1988; Cramer and Lewis, 1993; Famoso et al., 2010), while tea and rice are Al-tolerant and prefer NH_4^+ (Ruan et al., 2007; Famoso et al., 2010; Zhao et al., 2013b). The activity of NO_3^- reductase could not be detected in some calcifuge species, suggesting that they have a restricted ability to utilize NO_3^- (Havill et al., 1974). Rice (*Oryza sativa*) has two subspecies, *indica* and *japonica*. *Indica* rice cultivars generally prefer NO_3^-, while *japonica* cultivars prefer NH_4^+ (Zhao et al., 2013b; Hu et al., 2015). Correspondingly, *indica* rice cultivars are generally Al sensitive, while *japonica* cultivars are Al tolerant (Zhao et al., 2013b). Among different rice cultivars, Al tolerance is closely related to NH_4^+ and NO_3^- preference (Zhao et al., 2013b).

TABLE 1 | Aluminum tolerance and NH_4^+/NO_3^- preference of plant species.

Taxon	Al tolerance	NH_4^+/NO_3^- preference	Reference
Vaccinium angustifolium	Tolerant	NH_4^+	Townsend, 1966; Townsend and Blatt, 1966
Deschampsia flexuosa	Tolerant	NH_4^+	Rorison, 1985
Oxalis acetosella, Carex pilulifera, Festuca gigantea, Poa nemoralis, Deschampsia flexuosa, Stellaria holostea, Rumex acetosella	Tolerant	NH_4^+	Falkengren-Grerup, 1995
Camellia sinensis	Tolerant	NH_4^+	Ruan et al., 2007
Oryza sativa subsp. *japonica*	Tolerant	NH_4^+	Zhao et al., 2013b
Holcus lanatus, Bromus erectus	Sensitive	NO_3^-	Rorison, 1985
Hordeum vulgare	Sensitive	NO_3^-	Malhi et al., 1988
Triticum aestivum	Sensitive	NO_3^-	Cramer and Lewis, 1993; Famoso et al., 2010
Urtica dioica, Ficaria verna, Melandrium rubrum, Aegopodium podagraria, Geum urbanum, Bromus benekenii, Sanguisorba minor, Melica ciliata, Silene rupestris, Viscaria vulgaris, Plantago lanceolata	Sensitive	NO_3^-	Falkengren-Grerup, 1995
Oryza sativa subsp. *indica*	Sensitive	NO_3^-	Zhao et al., 2013b

The above analyses collectively suggest that Al-tolerant plant species and genotypes utilize NH_4^+ more efficiently than NO_3^- (**Table 1**). This knowledge is helpful for the selection of crop genotypes with both high Al tolerance and N-use efficiency via breeding or genetic modification. The selection of such genotypes should reduce the amount of N fertilizer required and improve plant growth in acid soils. However, the molecular mechanism underlying the link between plant Al tolerance and inorganic N preference is unclear. The two characteristics of grain protein content and acidity tolerance were found to be positively correlated among different wheat lines (Mesdag et al., 1970). In addition, a quantitative trait locus genetic analysis revealed that loci associated with Al tolerance and NH_4^+ utilization were located in similar regions of rice genome (Ogawa et al., 2014). An important goal for future research is to uncover the mechanism of the link between plant Al tolerance and inorganic N preference at the molecular and genetic levels.

EFFECTS OF NH_4^+, NO_3^-, AND pH ON Al TOLERANCE

In recent decades, various anthropogenic activities have greatly accelerated soil acidification in Chinese crop fields (Guo et al., 2010; Liang et al., 2013). Among these activities is the excess use of NH_4^+ fertilizer (Barak et al., 1997; Fang et al., 2014). Atmospheric NH_4^+ deposition is also an important factor resulting in soil acidification (van Breemen et al., 1982). Nitrification is the mechanism by which NH_4^+ acidifies soils. During the nitrification of NH_4^+ to NO_3^-, H^+ are released into soils, which increase the concentration of soluble Al (van Breemen et al., 1982; Mulder et al., 1989; Mulder and Stein, 1994; Che et al., 2015) (**Figure 1**). Thus, NH_4^+ facilitates the occurrence of Al toxicity much more than NO_3^- does. However, increased soluble Al content in soils caused by low pH does not always increase Al phytotoxicity, because lower pH can result in the desorption of Al from plant roots into the rhizosphere solution (**Figure 1**).

Early studies showed that changes in root zone pH due to ion uptake imbalances were related to Al tolerance in triticale, wheat, and rye under certain solution and soil conditions (Mugwira and Patel, 1977). The plant growth medium can be acidified due to NH_4^+ uptake by plant roots and the nitrification of NH_4^+ to NO_3^-. Alternatively, the growth medium can be alkalinized due to the uptake of NO_3^- by plant roots. Because Al toxicity occurs in acid soils, one could speculate that the preferential utilization of NO_3^- relative to NH_4^+ can enhance plant Al tolerance through increasing the pH of the growth medium via NO_3^- uptake. The Al tolerance of some wheat varieties was attributable to their abilities to preferentially utilize NO_3^- relative to NH_4^+ through rhizosphere alkalization (Foy et al., 1965, 1967; Foy and Fleming, 1978, 1982; Fleming, 1983; Taylor and Foy, 1985a,b,c). The results of subsequent studies, however, indicated that genotypic differences in wheat Al tolerance were not caused by differences in rhizosphere pH induced by the differential uptake of NH_4^+ and NO_3^- (Taylor, 1988a,b; Miyasaka et al., 1989). Instead, the differences in the uptake of NH_4^+ and NO_3^- among different wheat genotypes were suggested to be the result of, rather than the cause of, differences in A1 tolerance among genotypes (Taylor, 1988a,b; Miyasaka et al., 1989). Another research demonstrated that the decrease in the growth medium pH under Al stress was greater for an Al-tolerant wheat genotype than an Al-sensitive one (Ikeda and Yamanishi, 1999). Therefore, genotypic differences in the relative Al tolerance of wheat could not be explained by root-induced pH changes due to the uptake of NH_4^+ and NO_3^-.

Three reports on rice plants drew different conclusions. In two studies, an Al-tolerant rice genotype had a stronger ability than an Al-sensitive genotype to increase nutrient solution pH through efficient NO_3^- uptake and metabolism (Ganesan et al., 1993; Justino et al., 2006). However, another study (van Hai et al., 1989)

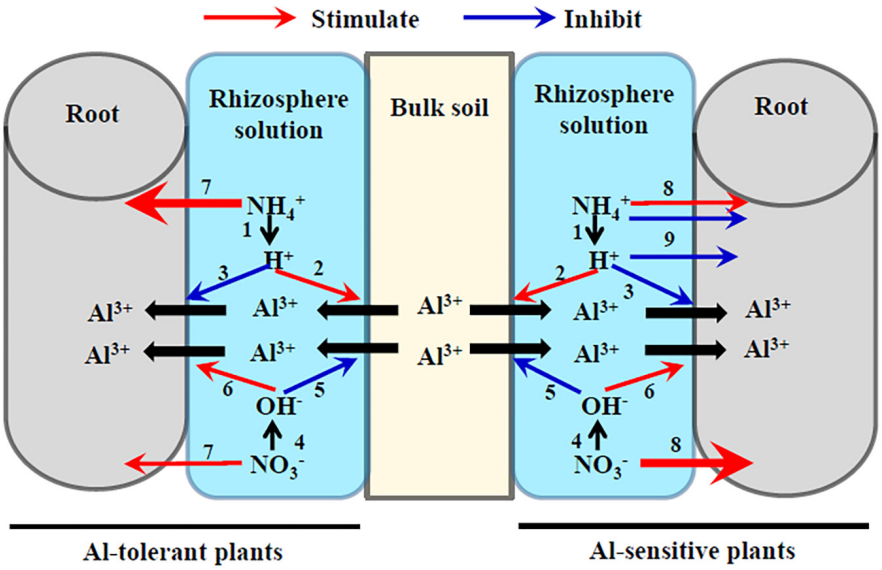

FIGURE 1 | Schematic diagram of possible effects of NH_4^+ and NO_3^- on the adsorption and desorption of Al on the root–soil interface. NH_4^+ acidifies rhizosphere solution (1), which stimulates the desorption of Al from bulk soils into rhizosphere solution (2) but inhibits the adsorption of Al from rhizosphere solutions to plant roots (3) both because of the competition between Al^{3+} and H^+. In contrast, NO_3^- alkalizes rhizosphere solution (4), which inhibits the desorption of Al from soils into rhizosphere solution (5) but stimulates the adsorption of Al from rhizosphere solutions to plant roots (6) because NO_3^--increased negative electrical charge of root surface. Al-tolerant plant species prefer NH_4^+ to NO_3^- (7), while Al-sensitive plant species prefer NO_3^- to NH_4^+ (8). Excess NH_4^+ and H^+ are both toxic to the growth of Al-sensitive plant species (9). Consequently, NH_4^+ alleviates Al toxicity to Al-tolerant plant species while aggravates Al toxicity to Al-sensitive plant species compared with NO_3^-.

obtained the opposite result, in that an Al-resistant genotype took up more NH_4^+ and acidified the nutrient solution to a greater degree than did an Al-sensitive one. In barley, Al tolerance of different cultivars was not related to the root-induced pH change by the uptake of inorganic N sources from the growth medium (Wagatsuma and Yamasaku, 1985). Similarly, differences in pH changes in the growth medium were not related to differences in A1 tolerance between two sorghum genotypes (Galvez and Clark, 1991). In fact, the NO_3^- uptake rate was found to be higher in an Al-sensitive sorghum genotype than in an Al-tolerant one (Cambraia et al., 1989). Genotypic differences in the Al tolerance of soybean plants were not associated with the difference in NH_4^+ uptake vs. NO_3^- uptake and root-induced pH changes (Klotz and Horst, 1988b). Changes in the medium pH were also not related to Al tolerance in triticale (Antunes and Antonieta Nunes, 1997). These analyses further demonstrated that genotypic differences in the Al tolerance of diverse plant species cannot be explained only by root-induced pH changes due to NH_4^+ and NO_3^- uptake.

Since low pH increases the concentrations of soluble Al in soils, the alkalization of the rhizosphere was proposed to be an important mechanism of plant Al tolerance (Matsumoto, 2000; Kochian et al., 2004; Ma, 2007). However, several studies demonstrated that H^+ could alleviate Al toxicity because H^+ competed with Al^{3+} for adsorption to the root surface (Kinraide et al., 1992; Godbold et al., 1995; Zhao et al., 2009; Zhao et al., 2014). A supply of H^+ also alleviated Al toxicity in bacteria (Kinraide and Sweeney, 2003) and yeast (Zhao et al., 2017). These results implied that Al toxicity is much lower at low pH than at high pH under a certain acid pH range (pH < 5.0) because of the H^+ alleviation of Al phytotoxicity. The uptake of NH_4^+ and NO_3^- decreases and increases the pH of the medium, respectively. Many reports have indicated that NH_4^+ supply can enhance plant Al tolerance, while NO_3^- supply aggravates Al toxicity (**Table 2**). In some studies, Al was found to stimulate the growth of some grasses (Rorison, 1985), tropical trees (Watanabe et al., 1998), *Lespedeza bicolor* (Chen et al., 2010), and rice (Zhao et al., 2013b) when supplied with NH_4^+, but not when supplied with NO_3^-. The stimulatory effects of Al on plant growth may be related to the effects of Al to alleviate H^+ toxicity (Kinraide et al., 1992). Thus, NH_4^+ alleviates Al toxicity, and Al enhances NH_4^+ utilization.

It is now accepted that the NH_4^+-induced rhizosphere acidification is the primary mechanism underlying the NH_4^+ enhancement of Al tolerance in plants (Zhao et al., 2009; Wang et al., 2015) (**Figure 1**). Relative to NO_3^-, NH_4^+ uptake by rice roots reduces the pH of the nutrient solution. Lower pH further decreases the number of Al-binding functional groups and enhances the positive electrical potential of the root surface (Wang et al., 2015; Liu et al., 2016). Consequently, NH_4^+-fed roots adsorb less Al than do NO_3^--fed roots, thereby alleviating Al toxicity. The ability of NH_4^+ to alleviate Al toxicity was also observed under constant pH conditions (Rorison, 1985; Klotz and Horst, 1988a,b; Grauer and Horst, 1990), indicating that factors other than pH may be involved. It is possible that intermediate products of N metabolism such as nitric oxide (NO) play a role in the alleviation of Al toxicity by NH_4^+ (Zhao and Shen, 2013).

TABLE 2 | Summary of NH_4^+ effects on plant Al tolerance relative to NO_3^-: (+) enhancement, (–) decrease, and (0) no change.

Taxon	Effects	Reference
Holcus lanatus	+	McCain and Davies, 1983
Deschampsia flexuosa, Holcus lanatus, *Bromus erectus*	+	Rorison, 1985
Spruce and beech	+	Van Praag et al., 1985[a]
Glycine max	+	Klotz and Horst, 1988a,b
Secale cereal, *Lupinus luteus*	+	Grauer and Horst, 1990
Pinus rigida	+	Cumming, 1990[a]; Cumming and Weinstein, 1990[a]; Schier and McQuattie, 1999[a]
Triticosecale	+	Antunes and Antonieta Nunes, 1997; Domingues, 2010
Melastoma malabathricum, Acacia mangium, *Melaleuca cajuputi*	+	Watanabe et al., 1998
Oryza sativa	+	Zhao et al., 2009, 2013b; Wang et al., 2015
Lespedeza bicolor	+	Chen et al., 2010
Sorghum bicolor	+ or –[b]	Tan et al., 1992
Sorghum bicolor	0	Keltjens, 1987
Picea abies	0	Godbold et al., 1988
Mucuna pruriens	0	Hairiah et al., 1994
Triticum aestivum	–	Fleming, 1983; Taylor and Foy, 1985a,b,c

[a] *Study was conducted using sand culture irrigated with nutrient solutions. Studies not marked by superscript letter were conducted using hydroponic systems.*
[b] *Effect was dependent on plant genotypes.*

Several studies found that NH_4^+ aggravated Al toxicity, relative to NO_3^- (**Table 2**), which may reflect differences in plants' sensitivity to NH_4^+. Some studies on the aggravating effects of NH_4^+ on Al toxicity used wheat as the experimental material (Fleming, 1983; Taylor and Foy, 1985a,b,c). Wheat plants prefer NO_3^- to NH_4^+ and are sensitive to both Al and NH_4^+ (**Table 1**). If wheat plants are supplied only with NH_4^+, then NH_4^+ toxicity may occur and may be more serious than Al toxicity. Thus, NH_4^+ may aggravate rather than alleviate Al toxicity in wheat plants. Some sorghum genotypes showed lower Al toxicity and some showed higher Al toxicity with NH_4^+ relative to NO_3^- N (Tan et al., 1992). Because an Al-sensitive sorghum genotype was more NH_4^+-sensitive than an Al-tolerant one, NH_4^+ toxicity probably masked Al toxicity in sorghum (Keltjens, 1987). Consequently, it is difficult to observe the NH_4^+ alleviation of Al toxicity in NH_4^+-sensitive plant species (Keltjens, 1987). Thus, plants grown in acid soils may suffer from Al toxicity accompanied by NH_4^+ toxicity due to poor soil nitrification.

Most studies on the effects of NH_4^+ and NO_3^- on Al tolerance have been conducted using hydroponic experiments (**Table 2**), which might not reflect the real effects of NH_4^+ and NO_3^- on Al tolerance. In soils, lower root rhizosphere pH will result in greater solubilization of Al ions from the soil into the rhizosphere solution, potentially increasing Al toxicity to plants. However, under nutrient solution culture, lower rhizosphere pH will only affect Al speciation (Keltjens and van Loenen, 1989). Lower pH due to NH_4^+ uptake by plants increases the solubilization of Al^{3+} from bulk soils into the rhizosphere solution (**Figure 1**). Nevertheless, for plant roots, more H^+ in the rhizosphere solution can decrease Al^{3+} adsorption by roots through cation competition and increasing the positive electrical potential of the root surface. Thus, whether Al toxicity is exacerbated or alleviated by NH_4^+ or NO_3^- may depend on the relative dominance of the effects of pH on Al desorption from soils into the rhizosphere solution and Al adsorption from the rhizosphere solution into the roots. Further studies on this topic should be conducted on soil-grown plants.

EFFECTS OF Al ON N TRANSFORMATIONS IN SOILS

Although the effects of nitrification on soil pH and Al solubility are well known, less is known about the effects of Al on soil N transformations such as nitrification and ammonification. The nitrification rate is lower in acid soils than in neutral to calcareous soils (Che et al., 2015), although the reasons for this are still unclear. It is generally considered that low pH inhibits the activity of nitrifying microbes. Higher levels of soluble Al are often concomitant with lower soil pH. Soil N transformations are controlled by microbes. Most microbes are very sensitive to Al (Piña and Cervantes, 1996), while fungi are relatively more tolerant than bacteria to Al and acids (Zhao et al., 2013a, 2017). Low pH does not always result in high concentrations of active Al in soils, because Al ions can form complexes with various organic and inorganic ligands. Future research should explore the role of Al in regulating soil N transformations and in N cycle as a whole.

In a paper published almost 100 years ago (Denison, 1922), Al salts stimulated ammonifying microbes but adversely affected nitrifying bacteria. However, more recent reports showed that Al did not affect the nitrification potential and abundance of ammonia-oxidizing *amoA* gene of archaea and bacteria (Kasuga et al., 2010; Lin et al., 2017). Bacterial growth was shown to gradually decrease as the pH decreased from 6.5 to 4.0 (Rousk et al., 2010), while soil exchangeable Al linearly increased as the pH decreased from 5.4 to 3.7 (Aciego Pietri and Brookes, 2008). In addition, the OTU richness and Shannon's diversity index of both ammonia-oxidizing archaea and bacteria showed significantly negative correlation with soil pH ranging from 3.77 to 8.46 (Hu et al., 2013). Therefore, microbial growth was found to be limited at soil pHs lower than 5.4 when Al became soluble, but was limited by low pH rather than Al toxicity at pHs ranging from 6.5 to 5.4. These analyses suggested that the inhibition of soil nitrification that transformed NH_4^+ to NO_3^- was due to acid stress rather than Al toxicity, when soil pH decreased from 6.5 to 5.4. There are several soil N transformation processes such as nitrification, denitrification, and ammonification, and different types of microbes control the different pathways of transformations. To clarify the effects of Al on soil N transformation, further studies should evaluate N transformation-related microbial populations and Al

solubility under controlled conditions with variable soil pH and NH_4^+/NO_3^- supply.

EFFECTS OF Al ON NO_3^- UPTAKE BY PLANT ROOTS

Approximately 30 published studies have focused on the effects of Al toxicity on NO_3^- uptake, and most of them found that Al inhibited NO_3^- uptake (**Table 3**). Jerzykiewicz (2001) observed that an extremely high concentration of Al (5 mM) even resulted in NO_3^- efflux from cucumber roots. The mechanism by which Al inhibits NO_3^- uptake is still unclear, but some possible mechanisms have been proposed. In one study, a high Al concentration resulted in large amounts of Al entering the symplast of soybean roots, leading to symplastic Al concentrations that were high enough to inhibit NO_3^- transport across the membrane (Lazof et al., 1994). Thus, one proposed mechanism by which Al inhibits NO_3^- uptake is that intracellular Al may bind to NO_3^- transporters, NO_3^- metabolic enzymes, and other components of systems related to NO_3^- uptake. Plant NO_3^- transport involves at least three systems; the constitutive high-affinity transport system (cHATS), the inducible high-affinity transport system (iHATS), and the constitutive low-affinity transport system (cLATS) (Crawford and Glass, 1998; Miller et al., 2007). The constitutive systems function without NO_3^- pretreatment, but the inducible system is stimulated by external NO_3^-. The cHATS has low values of both K_m (6–20 μM) and V_{max} (0.3–0.82 μmol g^{-1} h^{-1}), while the iHATS is characterized by higher K_m (20–100 μM) and V_{max} (3–8 μmol g^{-1} h^{-1}) values and is induced by exposure to NO_3^- for hours to days. The cLATS functions at NO_3^- concentrations above 250 μM and does not become saturated even when NO_3^- concentrations are as high as 50 mM. Durieux et al. (1993) reported that Al exerted stronger effects on the inducible system than on the constitutive systems. Their results also suggested that high concentrations of Al inhibited the activity of NO_3^- transporters in the inducible system rather than affected the number of NO_3^- transporters (Durieux et al., 1993). Pretreatment with Al had little effect on NO_3^- uptake by plants (Jarvis and Hatch, 1986; Durieux et al., 1993), and NO_3^- transport quickly recovered when Al was removed from the external growth medium (Durieux et al., 1993). These results suggested that Al directly interacts with NO_3^- transporters but that this interaction is reversible, leading to the inhibition of NO_3^- uptake by Al.

The inhibition of root elongation is the main symptom of Al phytotoxicity. Root elongation was inhibited much more than NO_3^- uptake in the presence of high Al concentrations in soybean (Rufty et al., 1995). The Al-inhibition of NO_3^- uptake was found to be similar across different Al-tolerant soybean genotypes and different root regions (Lazof et al., 1994). The

TABLE 3 | Summary of effects of aluminum on NO_3^- uptake: (–) inhibition, (+) stimulation, and (0) no change.

Taxon	Al (μM)	NO_3^- (mM)	Al duration	Effects	Reference
Triticum aestivum	111	3.5	29 days	–	Fleming, 1983
Trifolium repens	25–100	0.7	21 days	–	Jarvis and Hatch, 1986
Sorghum bicolor	55–370	0.1–14	15 h–36 days	–	Keltjens, 1987, 1988; Keltjens and van Ulden, 1987; Cambraia et al., 1989; Galvez and Clark, 1991
Pinus rigida	200	2–4	42 days	–	Cumming, 1990[a]
Picea abies	37–1483	1	14 days	–	Peuke and Tischner, 1991
Zea mays	5–166	0.2–0.6	1.5 h–7 days	–	Durieux et al., 1993, 1995; Calba and Jaillard, 1997; Purcino et al., 2003
Glycine max	80	0.3	30 m–2 h	–	Lazof et al., 1994
Triticosecale	185, 370	1.6–12	4–7 days	–	Antunes and Antonieta Nunes, 1997; Domingues, 2010
Musa spp.	78.5	1.8	40 days	–	Rufyikiri et al., 2001
Lotus japonicus	10^2–10^4	0.15	24 h	–	Pal'ove-Balang and Mistrík, 2007
Lotus corniculatus	10^3	0.15	72 h	–	Pal'ove-Balang and Zelinova, 2013
Oryza sativa	50	2.86	24–96 h	–	Zhou et al., 2016
Broadleaf trees	600	3.5	3 h	–	Burnham et al., 2017[b]
Camellia sinensis	400	3.6	24 h	0	Morita et al., 1998
Glycine max	56	1.4	14 h	+	Klotz and Horst, 1988b
Oryza sativa	0–1111	0.36	65 days	+ (<185 μM Al) or – (>185 μM Al)	van Hai et al., 1989
Hordeum vulgare	10^2	0.37	5 min	+	Nichol et al., 1993
Glycine max	0–45	0.3	72 h	+ (<10 μM Al) or – (>10 μM Al)	Rufty et al., 1995
Cucumis sativus	500, 10^3, 5×10^3	1	1–6 h	+ (0.5 mM Al exposure for 3 h) or – (1 mM or 5 mM Al exposure for 6 h)	Jerzykiewicz, 2001
Quercus serrata	10^3	2.8	3–14 days	+	Tomioka et al., 2007

[a]*Study was conducted using sand culture irrigated with nutrient solutions.* [b]*Study was conducted using soil culture. Studies not marked by superscript letters were conducted using hydroponic systems.*

root apex is the primary target of Al toxicity to plants (Ryan et al., 1993). However, NO_3^- uptake rates by corn root tips only accounted for a low percentage of NO_3^- taken up by the total root system, and N in root tips was mainly derived from N adsorbed through other root regions (Lazof et al., 1992). The mechanism by which Al inhibits root elongation was suggested to differ from the mechanism of Al inhibition of NO_3^- uptake in maize (Durieux et al., 1995). The results of these studies indicated that the mechanism of Al inhibition of NO_3^- uptake might differ from the mechanism(s) of plant Al sensitivity and Al-inhibited root elongation, at least in maize and soybean. This should be further tested using more plant species.

The effects of Al on NO_3^- uptake may depend on Al concentrations, Al exposure time, plant species, and plant genotype. Aluminum does not always affect NO_3^- uptake, for example, in Al-tolerant tea trees (Morita et al., 1998) (**Table 3**). A stimulatory effect of Al on root NO_3^- uptake has been observed in studies where Al was supplied at low concentrations (van Hai et al., 1989; Rufty et al., 1995; Jerzykiewicz, 2001), or for a short-term (Nichol et al., 1993; Jerzykiewicz, 2001), and/or in studies on wild plant species that prefer Al (Tomioka et al., 2007) (**Table 3**). Similar to the observed stimulatory effects of Al on NO_3^- uptake, N uptake and partitioning were found to be enhanced by lower Al concentrations (20–200 μM Al) but inhibited by high Al concentrations (1000 μM Al) in defoliated grasses (Thornton, 1998). In wheat, N uptake by root tips was inhibited by Al in an Al-sensitive genotype, but stimulated in an Al-tolerant genotype (Ikeda and Yamanishi, 1999). These results suggested that low Al accumulation in plants could stimulate NO_3^- uptake.

Several possible mechanisms were suggested to be responsible for the stimulation of NO_3^- uptake by low concentrations of Al (Rufty et al., 1995; Jerzykiewicz, 2001) (**Figure 2**). First, the increase in the positive electrical potential of the cell surface by Al^{3+} could facilitate the access of negatively charged NO_3^- to the root cell surface. Second, Al-induced H^+ extrusion under acid stress could increase NO_3^- transport across the membrane via H^+/NO_3^- co-transport. Finally, NO_3^- efflux from cells could be diminished by the binding of extracellular Al to the cell membrane if Al impairs the structural integrity of plasma membranes and alters their permeability (Cakmak and Horst, 1991). However, direct and specific evidence for each of these mechanisms is still lacking.

Rufty et al. (1995) compared experimental conditions including the Al concentration, medium pH, and calcium concentration among several papers reporting different effects of Al on NO_3^- uptake. This comparative analysis suggested that pH and calcium levels, rather than Al concentrations, explained the differences in results among studies (Rufty et al., 1995). Under acid stress and low calcium levels, Al ameliorated acid

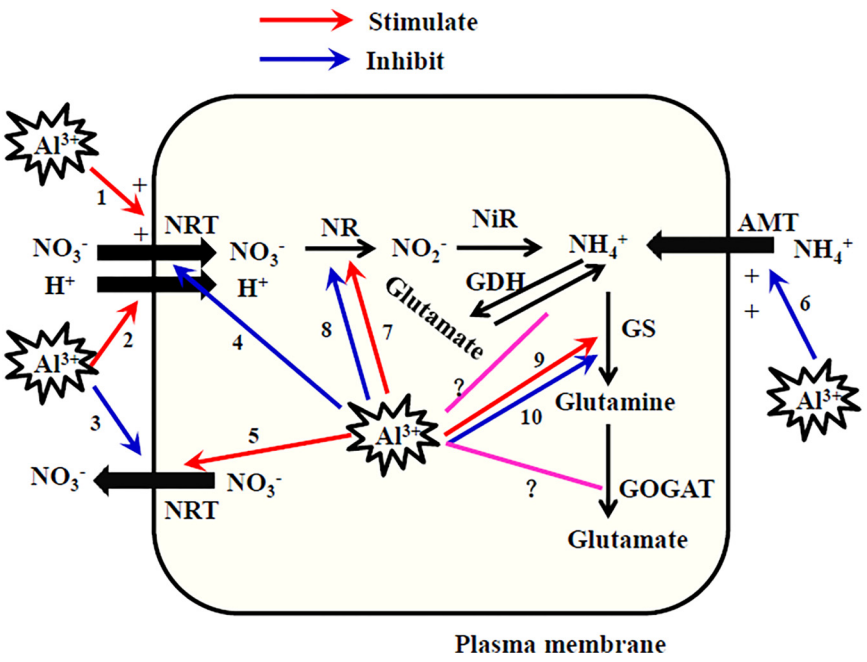

FIGURE 2 | Schematic diagram of possible effects of Al on uptake and assimilation of NH_4^+ and NO_3^- by plants. NRT, nitrate transporter; AMT, ammonium transporter; NR, nitrate reductase; NiR, nitrite reductase; GS, glutamine synthetase; GOGAT, glutamate synthase; GDH, Glutamate dehydrogenase. When plant roots accumulate low concentrations of Al in the apoplastic space, root NO_3^- uptake is stimulated by apoplastic Al because of Al^{3+}-increased positive electrical charge of cell surface (1), enhanced H^+-NO_3^- cotransport (2), and diminished NO_3^- efflux (3). When plant roots accumulate large amounts of Al that enters the symplasm of roots, intracellular Al inhibits NO_3^- uptake as Al binds to NO_3^- transporter (4) and induces enhanced efflux of NO_3^- (5). Al^{3+}-increased positive electrical charge of cell surface results in the Al inhibition of NH_4^+ uptake (6). Low concentrations of Al stimulates NRA (7) because of Al-stimulated NO_3^- uptake by the three ways (1, 2, and 3), while high concentrations of Al inhibits NRA (8) because of Al-inhibited NO_3^- uptake by the two ways (4 and 5). Al stimulates GS activity (9) due to the binding of Al with GS while inhibits that (10) due to the inhibition of NH_4^+ uptake (6). The effects of Al on GOGAT and GDH are still uncertain (?).

stress to roots, thereby enhancing NO_3^- influx into cells (Rufty et al., 1995). Further studies using carefully designed experiments should explore how pH and calcium affect the ability of Al to alter NO_3^- uptake.

Based on the analyses summarized above, we present a schematic diagram to explain the mechanisms of the effects of Al on NO_3^- uptake (**Figure 2**). When plant roots accumulate low concentrations of Al in the apoplastic space of roots, extracellular Al may stimulate NO_3^- uptake because of an Al^{3+}-induced increase in the positive electrical charge of the cell surface, enhanced H^+-NO_3^- cotransport, and diminished NO_3^- efflux. When large amounts of Al enter the symplasm of roots, root NO_3^- uptake is inhibited by Al because Al binds to the NO_3^- transporter and enhances NO_3^- efflux. We emphasize that this schematic diagram is based only on the published reports. There is still no direct evidence for these proposed mechanisms. Just as the molecular basis for N uptake has been discovered in recent years, the molecular basis of both the Al-stimulation and Al-inhibition of NO_3^- transport can be explored in molecular studies on plant mutants defective in NO_3^- transport.

EFFECTS OF Al ON NH_4^+ UPTAKE BY PLANT ROOTS

Various studies have reported that root NH_4^+ uptake was either inhibited, stimulated, or unaffected by Al (**Table 4**). However, most studies have reported inhibitory effects of Al on NH_4^+ uptake by plants. Nichol et al. (1993) indicated that Al treatment for 5 min suppressed the movement of cations (NH_4^+, Ca^{2+}, and K^+) across the plasma membrane but facilitated the movement of anions (NO_3^- and phosphate). Aluminum ions may bind to the cell surface and form a positively charged layer, thereby inhibiting the adsorption of positively charged cations to the cell surface but stimulating the adsorption of negatively charged anions. Thus, similar to the mechanisms responsible for the Al stimulation of NO_3^- uptake described above, the Al^{3+}-induced increase in the positive electrical charge of the cell surface is responsible for the inhibition of NH_4^+ uptake by Al (**Figure 2**).

In general, Al exerts a smaller negative effect on NH_4^+ uptake than on NO_3^- uptake. In maize roots, Al reduced the uptake of both NH_4^+ and NO_3^- but increased the uptake ratio NH_4^+/NO_3^-, indicating that NH_4^+ uptake was inhibited much less than NO_3^- uptake by Al (Purcino et al., 2003). An Al treatment reduced NO_3^- uptake but not NH_4^+ uptake in maize and triticale (Durieux et al., 1993; Calba and Jaillard, 1997; Domingues, 2010), while Al inhibited NO_3^- uptake but stimulated NH_4^+ uptake in sorghum and triticale (Keltjens and van Ulden, 1987; Antunes and Antonieta Nunes, 1997). Leaf N content was increased by A1 when NH_4^+ was supplied but reduced by Al when NO_3^- was supplied (Van Praag et al., 1985). An Al treatment reduced the NO_3^- concentration but increased the free NH_4^+ concentration in the leaves of corn plants (Souza et al., 2016).

The studies reporting that Al stimulated root NH_4^+ uptake generally used N sources comprising a mixture of NH_4^+ and NO_3^- (Keltjens, 1987, 1988; Keltjens and van Ulden, 1987; Antunes and Antonieta Nunes, 1997). Since Al inhibited NO_3^- uptake in those studies, we may infer that N deficiency caused by the inhibition of NO_3^- uptake might explain the stimulation of NH_4^+ uptake by Al. When NO_3^- cannot meet the N demands of plants under Al stress, plants may take up more NH_4^+ in place of NO_3^- to alleviate N deficiency.

EFFECTS OF Al ON NO_3^- REDUCTION

Nitrate reductase (NR) represents the first enzymatic and rate-limiting step of NO_3^- assimilation in plants. It catalyzes the reduction of nitrate to nitrite and is a substrate-inducible enzyme (Tischner, 2000). A large body of research has indicated that Al inhibits NR activity (NRA) in roots, shoots, or both (**Table 5**). Several studies reported that Al toxicity reduced NRA much more in Al-sensitive plant genotypes than in Al-tolerant ones (Foy

TABLE 4 | Summary of effects of aluminum on NH_4^+ uptake: (–) inhibition, (+) stimulation, and (0) no change.

Taxon	Al (μM)	NH_4^+ (mM)	Al duration	Effects	Reference
Oryza sativa	0–1111	0.36	65 days	–	van Hai et al., 1989
Sorghum bicolor	300	0.36–3.6	2–18 days	–	Galvez and Clark, 1991
Hordeum vulgare	100	0.03	5 min	–	Nichol et al., 1993
Triticum aestivum	10, 100	2	2–3 days	–	Ikeda and Yamanishi, 1999
Musa spp.	78.5	0.2	40 days	–	Rufyikiri et al., 2001
Lotus japonicus	10^2–10^4	0.2	24 h	–	Pal'ove-Balang and Mistrík, 2007
Lotus corniculatus	10^3	0.2	72 h	–	Pal'ove-Balang and Zelinova, 2013
Zea mays	166	0.2	7 days	–	Purcino et al., 2003
Zea mays	5–100	0.2–0.24	0.5 h–3 days	0	Durieux et al., 1993; Calba and Jaillard, 1997
Camellia sinensis	400	3.6	24 h	0	Morita et al., 1998
Triticosecale	370	0.2–1.6	4 days	0	Domingues, 2010
Triticosecale	185	0.8, 1.4	5–7 days	+ or 0	Antunes and Antonieta Nunes, 1997
Sorghum bicolor	55–370	2–4	96 h–36 days	+	Keltjens, 1987, 1988; Keltjens and van Ulden, 1987
Glycine max	56	1.4	14 h	+	Klotz and Horst, 1988b

All studies used hydroponic systems.

and Fleming, 1982; Keltjens and van Ulden, 1987; Justino et al., 2006). In wheat and sorghum, Al significantly inhibited NRA in shoots rather than roots (Foy and Fleming, 1982; Keltjens and van Ulden, 1987). In contrast, Al inhibited NRA in roots rather than shoots in red spruce (Cumming and Brown, 1994). The inhibitory effect of Al on NRA may result from Al-inhibition of NO_3^- uptake, as the decreased level of the substrate, NO_3^-, would lead to decreased NRA (Gomes et al., 1985; Keltjens and van Ulden, 1987; Keltjens, 1988; Justino et al., 2006; Pal'ove-Balang and Mistrík, 2007; Souza et al., 2016). The Al-induced decrease in NO_3^- content in plants was proposed to be the main mechanism by which Al inhibits NRA, so the interaction between Al and NR may be indirect. Roots generally accumulate more Al than do shoots. However, Al significantly inhibited NRA in the shoots but not in roots of wheat and sorghum (Foy and Fleming, 1982; Keltjens and van Ulden, 1987), suggesting that a direct interaction between NR and Al is unlikely. The ratio of absorbed $^{15}NO_3^-$ to reduced ammonia-containing N remained constant with increasing Al, also suggesting an indirect effect of Al on NR (Rufty et al., 1995). However, in another study, Al inhibited the shoot NRA of sorghum, and this could not be reversed by increased NO_3^- concentrations (Cambraia et al., 1989). Aluminum decreased NO_3^- accumulation in cucumber roots and maize leaves but enhanced their NRA (Lidon et al., 1998; Jerzykiewicz, 2001).

In some studies, Al was found to increase NRA (**Table 5**). At low concentrations, Al stimulated NRA in spruce (<37 μM Al; Peuke and Tischner, 1991) and rice (80 μM Al; Sharma and Dubey, 2005). Aluminum stimulated NRA in the Al-preferring species *Quercus serrata* (Tomioka et al., 2007, 2012) and tea

TABLE 5 | Summary of effects of aluminum on nitrate reductase activity: (–) inhibition, (+) stimulation, (0) no change and (N) not studied.

Taxon	Al (μM)	Al duration	Effects		Reference
			Root	Shoot	
Sorghum bicolor	50–185	5–30 days	–	–	Cambraia et al., 1989; Cruz et al., 2011[a]
Sorghum bicolor	55–370	48 h–24 days	0	–	Keltjens and van Ulden, 1987; Keltjens, 1988
Oryza sativa	160–500	5–21 days	–	–	Ganesan et al., 1993; Justino et al., 2006; Mishra and Dubey, 2011[a]
Picea rubens	37–370	2–42 days	–	N	Yandow and Klein, 1986
Picea rubens	200	10 weeks	–	0	Cumming and Brown, 1994[a]
Pinus rigida	200	6 weeks	–	N	Cumming, 1990[a]
Lotus japonicus	10^2–10^4	24 h	–	N	Pal'ove-Balang and Mistrík, 2007
Zea mays	5×10^4–2×10^5	15 days	N	–	Souza et al., 2016[a]
Helianthus annuus	100	15 days	N	–	Ruiz et al., 2007
Hordeum vulgare	2×10^3–6×10^3	6 days	N	–	Shahnawaz et al., 2017
Triticum aestivum	19–111	20	0	– (Al-sensitive genotype) or 0 (Al-tolerant genotype)	Foy and Fleming, 1982
Mucuna pruriens	110	4 weeks	N	0	Hairiah et al., 1994
Oryza sativa	80, 160	15 days	+ (80 μM Al) or – (160 μM Al)	+ (80 μM Al) or – (160 μM Al)	Sharma and Dubey, 2005[a]
Zea mays	100	15 days	– or + (dependent on genotypes and N source)	N	Mihailovic et al., 2015
Glycine max	56	6 h–4 days	+ or – (dependent on genotype and root distance)	N	Klotz and Horst, 1988b
Zea mays	10^3	20 days	N	+	Lidon et al., 1998[b]
Triticum aestivum	30	3 h	+	N	Sun et al., 2014
Glycine max	50, 100	24 h	+	N	Wang et al., 2017
Phaseolus vulgaris	50	6–24 h	+	N	Wang et al., 2010
Quercus serrata	10^3–2.5×10^3	1 h–14 days	+	N	Tomioka et al., 2007, 2012
Cucumis sativus	500, 10^3, 5×10^3	24 h	+	N	Jerzykiewicz, 2001
Triticum aestivum, Triticale hexaploidae, and *Secale cereale*	37–370	20 days	N	+ (*Triticum aestivum*, and *Triticale hexaploidae*); – (*Secale cereale*)	Dinev and Stancheva, 1993
Camellia sinensis	300	14 days	+	+	Hajiboland et al., 2014
Picea abies	37–741	2–3 months	+ (<37 μM Al) or – (>37 μM Al)	+	Peuke and Tischner, 1991

[a]*study was conducted using sand culture irrigated with nutrient solutions.* [b]*Study was conducted using vermiculite culture irrigated with nutrient solutions. Other studies not marked with superscript letters were conducted using hydroponic systems.*

(Hajiboland et al., 2014). The production of NO mediated by NR alleviated Al toxicity in red kidney bean, wheat, and soybean by alleviating oxidative stress, where Al significantly enhanced NRA in root tips (Wang et al., 2010, 2017; Sun et al., 2014). In another study, Al more strongly promoted NRA in Al-tolerant wheat than in Al-sensitive wheat (Sun et al., 2014).

The interaction between Al and NR appears to be complex, and can be positive or negative, direct or indirect. Many environmental factors are known to modulate NRA (Tischner, 2000). In various studies, the effects of A1 on NRA depended on the plant genotype (Foy and Fleming, 1982; Keltjens and van Ulden, 1987; Justino et al., 2006; Sun et al., 2014; Mihailovic et al., 2015), plant species (Dinev and Stancheva, 1993), plant part (Foy and Fleming, 1982; Keltjens and van Ulden, 1987), medium pH (Yandow and Klein, 1986), Al levels (Peuke and Tischner, 1991; Sharma and Dubey, 2005), N source and levels (Cumming, 1990; Mihailovic et al., 2015; Gupta et al., 2016), and inoculation treatments (Cumming, 1990). Although the Al–NR interaction is complex, we can conclude that NRA is generally inhibited by high Al concentrations, and stimulated by low Al concentrations (**Figure 2**). This overall trend is similar to the effects of Al on NO_3^- uptake, because NO_3^- is the primary factor regulating NRA.

Further research with detailed and well-designed experiments using different plant materials is necessary to clarify the details of the interaction between NR and Al. Recently, several genes encoding NR in maize (*Zea mays*) were found to be differently modulated at the transcriptional level by Al toxicity (Cantú et al., 2016). Molecular biology techniques could be helpful to clarify the detailed mechanisms of the interaction between Al and NR as well as NO_3^- uptake.

EFFECTS OF Al ON NH_4^+ ASSIMILATION

In plants, NH_4^+ is mainly assimilated by the GS/GOGAT (glutamine synthetase/glutamate synthase) cycle, where GS catalyzes the reaction between NH_4^+ and glutamate to form glutamine. Glutamine subsequently combines with 2-oxoglutarate in a reaction catalyzed by GOGAT to form two molecules of glutamate (Masclaux-Daubresse et al., 2010). Glutamate dehydrogenase (GDH) is considered to be an alternative pathway to incorporate NH_4^+ into glutamate when plants are exposed to high NH_4^+ concentrations under stress. However, there is more evidence that GDH functions mainly in glutamate deamination (Masclaux-Daubresse et al., 2010). The presence of Al was shown to decrease the concentrations of NO_3^--N and asparagine but increase the concentrations of amino acid-N and glutamine in the xylem sap of sorghum plants, potentially indicating that Al interferes with the synthesis and/or interconversion of N in plants (Gomes et al., 1985).

Pécsváradi's research group reported the activating effect of the Al(III)-tartrate 1:3 complex and the Al(III)–nitrilotriacetic acid complex on the activity of GS extracted from roots and leaves of wheat (Kertész et al., 2002; Pécsváradi et al., 2009). This activating effect was attributable to the specific binding of Al to the protein chain of GS, similar to the role of Mg in activating GS activity (Pécsváradi et al., 2009). Except for those two reports (Kertész et al., 2002; Pécsváradi et al., 2009), all of the other studies summarized here reported Al inhibition of GS activity in both roots and shoots (**Table 6**). However, Al either activated, suppressed, or did not affect the activities of GOGAT and GDH (**Table 6**). The effects of Al on the activities of N-assimilating enzymes were found to vary between Al-tolerant and Al-sensitive maize varieties and depend on the N form supplied. In maize, NH_4^+ facilitated the Al stimulation of N assimilation in the roots of an Al-tolerant maize genotype (Mihailovic et al., 2015). Here, we suggest that Al might stimulate GS activity by binding to it, or inhibit it by limiting NH_4^+ uptake (**Figure 2**). However, it is difficult to draw clear conclusions about the interaction between Al and NH_4^+ assimilation on the basis of studies published to date. Therefore, more research is required to explore the effects of Al on these enzymes involved in NH_4^+ assimilation.

CONCLUDING REMARKS

A complex interaction between Al and N occurs in the soil–plant system. Relative to NO_3^-, NH_4^+ uptake by roots generally alleviates Al phytotoxicity under solution culture conditions,

TABLE 6 | Summary of effects of aluminum on the activities of glutamine synthetase (GS), glutamate synthase (GOGAT), and glutamate dehydrogenase (GDH): (–) inhibition, (+) stimulation, (0) no change, and (N) not studied.

Taxon	Al (μM)	Al duration	Effects		Reference
			Root	Shoot	
Triticum aestivum	10–100	5 days	GS: +	GS: +	Kertész et al., 2002; Pécsváradi et al., 2009
Zea mays	166	3–9 days	GS: –; NADH-GDH: +; GOGAT: 0	GS: 0; NADH-GDH: –; GOGAT: 0	Purcino et al., 2003
Zea mays	100	15 days	GS, NADH-GDH: (dependent on genotypes and N source)	N	Mihailovic et al., 2015
Lotus japonicus	10^2–10^4	24 h, 72 h	GS and GOGAT: –	N	Pal'ove-Balang and Mistrík, 2007, 2011
Helianthus annuus	100	15 days	N	GS and GOGAT: –	Ruiz et al., 2007
Oryza sativa	160–320	5–20	GS: –; NADH-GDH: +	GS: –; NADH-GDH: +	Mishra and Dubey, 2011[a]

[a]*study was conducted using sand culture irrigated with nutrient solutions. Other studies were conducted using hydroponic systems.*

while NH_4^+ aggravates the solubilization of toxic Al from soils into rhizosphere solutions. Both the alleviation and aggravation effects mainly result from NH_4^+-induced H^+ excretion due to NH_4^+ uptake by plant roots and/or soil nitrification.

Compared with the effects of N on Al, the effects of Al on N are much more complicated because N is involved in multiple physiological processes within plants. Many reports have demonstrated that Al toxicity inhibits NO_3^- uptake by plant roots because Al binds to the NO_3^- transporter and stimulates NO_3^- efflux. In some cases, such as low Al concentrations, short-term Al exposure, and Al-preferring plants, the Al stimulation of NO_3^- uptake is probably because of an increase in the positive electrical charge at the root-surface, enhanced H^+-NO_3^- cotransport, and diminished NO_3^- efflux. The inhibitory effect of Al is generally smaller for root NH_4^+ uptake than for NO_3^- uptake. Similar to the Al inhibition of NO_3^- uptake, the activity of NR can be inhibited by Al treatment because of decreased internal NO_3^- accumulation. Low concentrations of Al can stimulate NR activity as a result of stimulating NO_3^- uptake. The effects of Al on the activities of GS, GOGAT, and GDH are still uncertain.

Despite the diverse interactions between Al and N in many studies as described above, it is clear that Al-tolerant plants generally prefer NH_4^+, while Al-sensitive plants prefer NO_3^-. This relationship between plant Al tolerance and NH_4^+/NO_3^- preference may be the result of ecological evolution and natural selection because acid soils are characterized by a relatively higher ratio of NH_4^+ to NO_3^- and higher concentrations of toxic Al than are neutral to calcareous soils.

Together, the results of numerous studies have suggested that the synergistic interaction between plant Al tolerance and NH_4^+-N nutrition may be an important strategy of plants to thrive in acid soils dominated by both toxic Al and NH_4^+. In addition, the Al stimulation of N uptake and assimilation can help to explain why Al stimulates plant growth in some cases.

Many studies have focused on the interactions between Al and N in plants, but the exact mechanisms underlying these interactions are still unclear. The Al–N interactions have been studied mainly at the physiological level rather than the molecular level. Physiological effects are indirectly affected by many factors and are not specific. Many genes that function in N uptake, N assimilation, and Al tolerance/toxicity have been identified (Masclaux-Daubresse et al., 2010; Ryan et al., 2011; Schroeder et al., 2013; Ma et al., 2014). The use of mutants with knocked-out or knocked-down expression of these genes could be helpful to explore the detailed mechanisms of Al–N interactions. In addition, we emphasize the importance of soil experiments for researching Al–N interactions, because the ultimate goal of understanding Al–N interactions is to improve the growth of plants in soils. Unfortunately, most studies on Al–N interactions have been conducted under solution culture conditions. As discussed above, the Al–N interactions in solutions may differ from those in soils.

How can the existing knowledge of Al–N interactions be used to improve the productivity of plants grown in acid soils? Plants need to overcome the dual limitation of Al toxicity and N deficiency in acid soils. Due to poor nitrification, acid soils have a higher NH_4^+ to NO_3^- ratio than do neutral to calcareous soils. Large-area forest decline has been linked to both NH_4^+ toxicity and soil acidification, and NH_4^+ toxicity has become an important issue in global agriculture and ecology (Britto and Kronzucker, 2002). Symptoms of NH_4^+ toxicity, such as leaf chlorosis, growth suppression, and even death generally appear when the external NH_4^+ concentrations exceed 0.1 to 0.5 mM, depending on the plant (Britto and Kronzucker, 2002). Thus, any enhancements in plant Al tolerance in acid soils should be accompanied by improvements in plant NH_4^+ utilization or reduced plant NH_4^+ sensitivity. Although NH_4^+ supply generally enhances plant Al tolerance, it also increases the concentrations of toxic Al in soils and leads to potentially toxic NH_4^+ concentrations. How can we solve this contradiction? Which type of N fertilizer should be applied in acid soils, NH_4^+ or NO_3^-? The NO_3^- fertilizers are much more expensive than NH_4^+ fertilizers. In addition, NO_3^- is lost to water more readily than is NH_4^+ because NO_3^- binds weakly to soil particles, which are generally negatively charged. Therefore, applying NO_3^- fertilizers to acid soils appears to be impractical at the moment.

Fortunately, plants originating from acid soils are generally both Al-tolerant and NH_4^+-preferring. Thus, one way to increase productivity from acid soils is to breed and develop genotypes that are both Al-tolerant and NH_4^+-preferring. This strategy may synergistically enhance plant Al tolerance and N-use efficiency, and reduce NH_4^+ sensitivity and NO_3^- loss. The improvement of N-use efficiency could reduce the amounts of N fertilizers applied to soils, thereby alleviating soil acidification and Al toxicity. Recently, an *in situ* ^{15}N-labeling experiment showed that soluble soil Al inhibited the relative uptake of NO_3^- by six tree species, potentially increasing NO_3^- loss from acid soils into the surrounding water environment (Burnham et al., 2017). Thus, knowledge about Al–N interactions is important for agriculture, ecology, and the environment.

AUTHOR CONTRIBUTIONS

XZ wrote the manuscript. RS checked and revised the manuscript.

FUNDING

This work was supported financially by the National Natural Science Foundation of China (No. 31672229), the Strategic Priority Research Program of the Chinese Academy of Sciences (Nos. XDB15030202 and XDB15030302), and the National Key Basic Research Program of China (No. 2014CB441000).

ACKNOWLEDGMENTS

We are grateful to the National Natural Science Foundation of China, the Chinese Academy of Sciences, and the Ministry of Science and Technology of the People's Republic of China.

We thank the Editor and two reviewers for their nice and detailed comments. We also thank Jennifer Smith, Ph.D., from Liwen Bianji, Edanz Group China (www.liwenbianji.cn/ac), for editing the English text of a draft of this manuscript.

REFERENCES

Aciego Pietri, J. C., and Brookes, P. C. (2008). Relationships between soil pH and microbial properties in a UK arable soil. *Soil Biol. Biochem.* 40, 1856–1861. doi: 10.1016/j.soilbio.2008.03.020

Antunes, A. M. G., and Antonieta Nunes, M. (1997). Effects of aluminum on nutrient solution pH and nitrate/ammonium uptake by triticale. *J. Plant Nutr.* 20, 1391–1401. doi: 10.1080/01904169709365342

Barak, P., Jobe, B. O., Krueger, A. R., Peterson, L. A., and Laird, D. A. (1997). Effects of long-term soil acidification due to nitrogen fertilizer inputs in Wisconsin. *Plant Soil* 197, 61–69. doi: 10.1023/A:1004297607070

Bojórquez-Quintal, E., Escalante-Magaña, C., Echevarría-Machado, I., and Martínez-Estévez, M. (2017). Aluminum, a friend or foe of higher plants in acid soils. *Front. Plant Sci.* 8:1767. doi: 10.3389/fpls.2017.01767

Bose, J., Babourina, O., and Rengel, Z. (2011). Role of magnesium in alleviation of aluminium toxicity in plants. *J. Exp. Bot.* 62, 2251–2264. doi: 10.1093/jxb/erq456

Britto, D. T., and Kronzucker, H. J. (2002). NH_4^+ toxicity in higher plants: a critical review. *J. Plant Physiol.* 159, 567–584. doi: 10.1078/0176-1617-0774

Burnham, M. B., Cumming, J. R., Adams, M. B., and Peterjohn, W. T. (2017). Soluble soil aluminum alters the relative uptake of mineral nitrogen forms by six mature temperate broadleaf tree species: possible implications for watershed nitrate retention. *Oecologia* 185, 327–337. doi: 10.1007/s00442-017-3955-8

Cakmak, I., and Horst, W. J. (1991). Effect of aluminum on net efflux of nitrate and potassium from root tips of soybean (*Glycine max* L.). *J. Plant Physiol.* 138, 400–403. doi: 10.1016/S0176-1617(11)80513-4

Calba, H., and Jaillard, B. (1997). Effect of aluminium on ion uptake and H^+ release by maize. *New Phytol.* 137, 607–616. doi: 10.1046/j.1469-8137.1997.00858.x

Cambraia, J., Pimenta, J. A., Estevão, M. M., and Sant'Anna, R. (1989). Aluminum effects on nitrate uptake and reduction in sorghum. *J. Plant Nutr.* 12, 1435–1445. doi: 10.1080/01904168909364048

Cantú, T., Vieira, C. E., Piffer, R. D., Luiz, G. C., and de Souza, S. G. H. (2016). Transcriptional modulation of genes encoding nitrate reductase in maize (*Zea mays*) grown under aluminum toxicity. *Afr. J. Biotechnol.* 15, 2465–2473. doi: 10.5897/AJB2016.15585

Che, J., Zhao, X. Q., Zhou, X., Jia, Z. J., and Shen, R. F. (2015). High pH-enhanced soil nitrification was associated with ammonia-oxidizing bacteria rather than archaea in acidic soils. *Appl. Soil Ecol.* 85, 21–29. doi: 10.1016/j.apsoil.2014.09.003

Chen, R. F., Zhang, F. L., Zhang, Q. M., Sun, Q. B., Dong, X. Y., and Shen, R. F. (2012). Aluminium–phosphorus interactions in plants growing on acid soils: does phosphorus always alleviate aluminium toxicity? *J. Sci. Food Agric.* 92, 995–1000. doi: 10.1002/jsfa.4566

Chen, Z. C., and Ma, J. F. (2013). Magnesium transporters and their role in Al tolerance in plants. *Plant Soil* 368, 51–56. doi: 10.1007/s11104-012-1433-y

Chen, Z. C., Zhao, X. Q., and Shen, R. F. (2010). The alleviating effect of ammonium on aluminum toxicity in *Lespedeza bicolor* results in decreased aluminum-induced malate secretion from roots compared with nitrate. *Plant Soil* 337, 389–398. doi: 10.1007/s11104-010-0535-7

Cramer, M. D., and Lewis, O. A. M. (1993). The influence of nitrate and ammonium nutrition on the growth of wheat (*Triticum aestivum*) and maize (*Zea mays*) Plants. *Ann. Bot.* 72, 359–365. doi: 10.1006/anbo.1993.1119

Crawford, N. M., and Glass, A. D. M. (1998). Molecular and physiological aspects of nitrate uptake in plants. *Trends Plant Sci.* 3, 389–395. doi: 10.1016/S1360-1385(98)01311-9

Cruz, F. J. R., Lobato, A. K. S., Costa, R. C. L., Lopes, M. J. S., Neves, H. K. B., Neto, C. F. O., et al. (2011). Aluminum negative impact on nitrate reductase activity, nitrogen compounds and morphological parameters in sorghum plants. *Aust. J. Crop Sci.* 5, 641–645.

Cumming, J. R. (1990). Nitrogen source effects on Al toxicity in nonmycorrhizal and mycorrhizal pitch pine (*Pinus rigida*) seedlings. II. Nitrate reduction and NO_3^- uptake. *Can. J. Bot.* 68, 2653–2659. doi: 10.1139/b90-335

Cumming, J. R., and Brown, S. M. (1994). Effects of elevated nitrate and aluminum on the growth and nutrition of red spruce (*Picea rubens*) seedlings. *Tree Physiol.* 14, 589–599. doi: 10.1093/treephys/14.6.589

Cumming, J. R., and Weinstein, L. H. (1990). Nitrogen source effects Al toxicity in nonmycorrhizal and mycorrhizal pitch pine (*Pinus rigida*) seedlings. I. Growth and nutrition. *Can. J. Bot.* 68, 2644–2652. doi: 10.1139/b90-334

Denison, I. A. (1922). The nature of certain aluminum salts in the soil and their influence on ammonification and nitrification. *Soil Sci.* 13, 81–106.

Dinev, N., and Stancheva, I. (1993). Changes in nitrate reductase activity, plastid pigment content, and plant mineral composition of wheat, rye, and triticale grown in the presence of aluminum. *J. Plant Nutr.* 16, 2397–2409. doi: 10.1080/01904169309364696

Domingues, A. M. (2010). Nitrogen nutrition of young triticale plants grown under aluminium stress. *Rev. Ciênc. Agrár.* 33, 40–52.

Durieux, R. P., Bartlett, R. J., and Magdoff, F. R. (1995). Separate mechanisms of aluminum toxicity for nitrate uptake and root elongation. *Plant Soil* 172, 229–234. doi: 10.1007/BF00011325

Durieux, R. P., Jackson, W. A., Kamprath, E. J., and Moll, R. H. (1993). Inhibition of nitrate uptake by aluminum in maize. *Plant Soil* 151, 97–104. doi: 10.1007/BF00010790

Erisman, J. W., Sutton, M. A., Galloway, J., Klimont, Z., and Winiwarter, W. (2008). How a century of ammonia synthesis changed the world. *Nat. Geosci.* 1, 636–639. doi: 10.1038/ngeo325

Fageria, N. K., and Baligar, V. C. (2001). Improving nutrient use efficiency of annual crops in Brazilian acid soils for sustainable crop production. *Commun. Soil Sci. Plant Anal.* 32, 1303–1319. doi: 10.1081/CSS-100104114

Falkengren-Grerup, U. (1995). Interspecies differences in the preference of ammonium and nitrate in vascular plants. *Oecologia* 102, 305–311. doi: 10.1007/BF00329797

Famoso, A. N., Clark, R. T., Shaff, J. E., Craft, E., McCouch, S. R., and Kochian, L. V. (2010). Development of a novel aluminum tolerance phenotyping platform used for comparisons of cereal aluminum tolerance and investigations into rice aluminum tolerance mechanisms. *Plant Physiol.* 153, 1678–1691. doi: 10.1104/pp.110.156794

Fang, X. M., Chen, F. S., Hu, X. F., Yuan, P. C., Li, J., and Chen, X. (2014). Aluminum and nutrient interplay across an age-chronosequence of tea plantations within a hilly red soil farm of subtropical China. *Soil Sci. Plant Nutr.* 60, 448–459. doi: 10.1080/00380768.2014.912950

Fleming, A. L. (1983). Ammonium uptake by wheat varieties differing in Al tolerance. *Agron. J.* 75, 726–730. doi: 10.2134/agronj1983.00021962007500050003x

Foy, C. D., Burns, G. R., Brown, J. C., and Fleming, A. L. (1965). Differential aluminum tolerance of two wheat varieties associated with plant induced pH changes around their roots. *Soil Sci. Soc. Am. Proc.* 29, 64–67. doi: 10.2136/sssaj1965.03615995002900010019x

Foy, C. D., and Fleming, A. L. (1978). "The physiology of plant tolerance to excess available aluminum and manganese in acid soils," in *Crop Tolerance to Suboptimal Land Conditions*, ed. G. A. Jung (Madison, WI: American Society of Agronomy special publication), 301–328.

Foy, C. D., and Fleming, A. L. (1982). Aluminum tolerances of two wheat genotypes related to nitrate reductase activities. *J. Plant Nutr.* 5, 1313–1333. doi: 10.1080/01904168209363064

Foy, C. D., Fleming, A. L., Burns, G. R., and Armiger, W. H. (1967). Characterization of differential aluminum tolerance among varieties of wheat and barley. *Soil Sci. Soc. Am. Proc.* 31, 513–521. doi: 10.2136/sssaj1967.03615995003100040027x

Galvez, L., and Clark, R. B. (1991). Nitrate and ammonium uptake and solution pH changes for Al-tolerant and Al-sensitive sorghum (*Sorghum bicolor*) genotypes grown with and without aluminium. *Plant Soil* 134, 179–188. doi: 10.1007/BF00010730

Ganesan, K., Sankaranarayanan, C., and Balakumar, T. (1993). Physiological basis of differential aluminum tolerance in rice genotypes. *Commun. Soil Sci. Plant Anal.* 24, 2179–2191. doi: 10.1080/00103629309368947

Gigon, A., and Rorison, I. H. (1972). The response of some ecologically distinct plant species to nitrate- and to ammonium-nitrogen. *J. Ecol.* 60, 93–102. doi: 10.2307/2258043

Godbold, D. L., Dictus, K., and Hüttermann, A. (1988). Influence of aluminium and nitrate on root growth and mineral nutrition of Norway spruce (*Picea abies*) seedlings. *Can. J. For. Res.* 18, 1167–1171. doi: 10.1139/x88-179

Godbold, D. L., Jentschke, G., and Marschner, P. (1995). Solution pH modifies the response of Norway spruce seedlings to aluminium. *Plant Soil* 171, 175–178. doi: 10.1007/BF00009583

Gomes, M. M. S., Cambraia, J., Sant'anna, R., and Estevão, M. M. (1985). Aluminum effects on uptake and translocation of nitrogen in sorghum (*Sorghum bicolor*, L. Moench). *J. Plant Nutr.* 8, 457–465. doi: 10.1080/01904168509363360

Grauer, U. E., and Horst, W. J. (1990). Effect of pH and nitrogen source on aluminium tolerance of rye (*Secale cereale* L.) and yellow lupin (*Lupinus luteus* L.). *Plant Soil* 127, 13–21. doi: 10.1007/BF00010832

Guo, J. H., Liu, X. J., Zhang, Y., Shen, J. L., Han, W. X., Zhang, W. F., et al. (2010). Significant acidification in major Chinese croplands. *Science* 327, 1008–1010. doi: 10.1126/science.1182570

Gupta, P., Sarengthem, J., Dhamgaye, S., and Gadre, R. (2016). Differential effect of aluminium on enzymes of nitrogen assimilation in excised bean leaf segments. *Adv. Biol. Chem.* 6, 106–113. doi: 10.4236/abc.2016.63009

Gutiérrez, R. A. (2012). Systems biology for enhanced plant nitrogen nutrition. *Science* 336, 1673–1675. doi: 10.1126/science.1217620

Hairiah, K., Stulen, I., Noordwijk, M., and Kuiper, P. J. C. (1994). Al avoidance and Al tolerance of *Mucuna pruriens* var. *utilis*: effects of a heterogeneous root environment and the nitrogen form in the root environment. *Plant Soil* 167, 67–72. doi: 10.1007/BF01587600

Hajiboland, R., Bahrami-Rad, S., and Bastani, S. (2014). Aluminum alleviates boron-deficiency induced growth impairment in tea plants. *Biol. Plant.* 58, 717–724. doi: 10.1007/s10535-014-0425-6

Havill, D. C., Lee, J. A., and Stewart, G. R. (1974). Nitrate utilisation by species from acidic and calcareous soils. *New Phytol.* 73, 1221–1231. doi: 10.1111/j.1469-8137.1974.tb02151.x

Hodson, M. J., and Evans, D. E. (1995). Aluminium/silicon interactions in higher plants. *J. Exp. Bot.* 46, 161–171. doi: 10.1093/jxb/46.2.161

Horst, W. J., Wang, Y., and Eticha, D. (2010). The role of the root apoplast in aluminium-induced inhibition of root elongation and in aluminium resistance of plants: a review. *Ann. Bot.* 106, 185–197. doi: 10.1093/aob/mcq053

Hu, B., Wang, W., Ou, S., Tang, J., Li, H., Che, R., et al. (2015). Variation in *NRT1.1B* contributes to nitrate-use divergence between rice subspecies. *Nat. Genet.* 47, 834–838. doi: 10.1038/ng.3337

Hu, H. W., Zhang, L. M., Dai, Y., Di, H. J., and He, J. Z. (2013). pH-dependent distribution of soil ammonia oxidizers across a large geographical scale as revealed by high-throughput pyrosequencing. *J. Soil Sediment* 13, 1439–1449. doi: 10.1007/s11368-013-0726-y

Ikeda, M., and Yamanishi, T. (1999). Accumulation of nitrogen supplied as ammonium in the root tips of aluminum-stressed wheat cultivars differing in aluminum sensitivity. *J. Fac. Agric. Kyushu Univ.* 44, 33–38.

Jarvis, S. C., and Hatch, D. J. (1986). The effects of low concentrations of aluminium on the growth and uptake of nitrate-N by white clover. *Plant Soil* 95, 43–55. doi: 10.1007/BF02378851

Jerzykiewicz, J. (2001). Aluminium effect on nitrate assimilation in cucumber (*Cucumis sativus* L.) roots. *Acta Physiol. Plant.* 23, 213–219. doi: 10.1007/s11738-001-0011-3

Ju, X. T., Xing, G. X., Chen, X. P., Zhang, S. L., Zhang, L. J., Liu, X. J., et al. (2009). Reducing environmental risk by improving N management in intensive Chinese agricultural systems. *Proc. Natl. Acad. Sci. U.S.A.* 106, 3041–3046. doi: 10.1073/pnas.0813417106

Justino, G. C., Cambraia, J., Oliva, M. A., and Oliveira, J. A. (2006). Uptake and reduction of nitrate in two rice cultivars in the presence of aluminum. *Pesqui. Agropec. Bras.* 41, 1285–1290. doi: 10.1590/S0100-204X2006000800011

Kant, S., Bi, Y. M., and Rothstein, S. J. (2011). Understanding plant response to nitrogen limitation for the improvement of crop nitrogen use efficiency. *J. Exp. Bot.* 62, 1499–1509. doi: 10.1093/jxb/erq297

Kasuga, I., Nakagaki, H., Kurisu, F., and Furumai, H. (2010). Abundance and diversity of ammonia-oxidizing archaea and bacteria on biological activated carbon in a pilot-scale drinking water treatment plant with different treatment processes. *Water Sci. Technol.* 61, 3070–3077. doi: 10.2166/wst.2010.204

Keltjens, W. G. (1987). Nitrogen source and aluminum toxicity of two sorghum genotypes differing in aluminum susceptibility. *J. Plant Nutr.* 10, 841–856. doi: 10.1080/01904168709363614

Keltjens, W. G. (1988). Short-term effects of Al on nutrient uptake, H^+ efflux, root respiration and nitrate reductase activity of two sorghum genotypes differing in Al-susceptibility. *Commun. Soil Sci. Plant Anal.* 19, 1155–1163. doi: 10.1080/00103628809368002

Keltjens, W. G., and van Loenen, E. (1989). Effects of aluminium and mineral nutrition on growth and chemical composition of hydroponically grown seedlings of five different forest tree species. *Plant Soil* 119, 39–50. doi: 10.1007/BF02370267

Keltjens, W. G., and van Ulden, P. S. R. (1987). Effects of Al on nitrogen (NH_4^+ and NO_3^-) uptake, nitrate reductase activity and proton release in two sorghum cultivars differing in Al tolerance. *Plant Soil* 104, 227–234. doi: 10.1007/BF02372536

Kertész, S., Fábián, A., Zsoldos, F., Vashegyi, Á., Labádi, I., Bona, L., et al. (2002). Changes in glutamate synthetase activity in presence of aluminium complexes. *Acta Biol. Szeged.* 45, 103–104.

Kinraide, T. B., Ryan, P. R., and Kochian, L. V. (1992). Interactive effects of Al^{3+}, H^+, and other cations on root elongation considered in terms of cell-surface electrical potential. *Plant Physiol.* 99, 1461–1468. doi: 10.1104/pp.99.4.1461

Kinraide, T. B., and Sweeney, B. K. (2003). Proton alleviation of growth inhibition by toxic metals (Al, La, Cu) in rhizobia. *Soil Biol. Biochem.* 35, 199–205. doi: 10.1016/S0038-0717(02)00246-8

Klotz, F., and Horst, W. J. (1988a). Effect of ammonium- and nitrate-nitrogen nutrition on aluminium tolerance of soybean (*Glycine max* L.). *Plant Soil* 111, 59–65. doi: 10.1007/BF02182037

Klotz, F., and Horst, W. J. (1988b). Genotypic differences in aluminium tolerance of soybean (*Glycine max* L.) as affected by ammonium and nitrate-nitrogen nutrition. *J. Plant Physiol.* 132, 702–707. doi: 10.1016/S0176-1617(88)80232-3

Kochian, L. V., Hoekenga, O. A., and Piñeros, M. A. (2004). How do crop plants tolerate acid soils? Mechanisms of aluminum tolerance and phosphorous efficiency. *Annu. Rev. Plant Biol.* 55, 459–493. doi: 10.1146/annurev.arplant.55.031903.141655

Kochian, L. V., Piñeros, M. A., and Hoekenga, O. A. (2005). The physiology, genetics and molecular biology of plant aluminum resistance and toxicity. *Plant Soil* 274, 175–195. doi: 10.1007/s11104-004-1158-7

Lazof, D. B., Rincon, M., Rufty, T. W., MacKown, C. T., and Carter, T. E. (1994). Aluminum accumulation and associated effects on $^{15}NO_3^-$ influx in roots of two soybean genotypes differing in A1 tolerance. *Plant Soil* 164, 291–297. doi: 10.1007/BF00010081

Lazof, D. B., Rufty, T. W., and Redinbaugh, M. G. (1992). Localization of nitrate absorption and translocation within morphological regions of the corn root. *Plant Physiol.* 100, 1251–1258. doi: 10.1104/pp.100.3.1251

Liang, L. Z., Zhao, X. Q., Yi, X. Y., Chen, Z. C., Dong, X. Y., Chen, R. F., et al. (2013). Excessive application of nitrogen and phosphorus fertilizers induces soil acidification and phosphorus enrichment during vegetable production in Yangtze River Delta, China. *Soil Use Manage.* 29, 161–168. doi: 10.1111/sum.12035

Lidon, F. C., Ramalho, J. C., and Barreiro, M. G. (1998). Aluminium toxicity modulates nitrate to ammonia reduction. *Photosynthetica* 35, 213–222. doi: 10.1023/A:1006906722469

Lin, J., Zhong, Y., Fan, H., Song, C., Yu, C., Gao, Y., et al. (2017). Chemical treatment of contaminated sediment for phosphorus control and subsequent effects on ammonia-oxidizing and ammonia-denitrifying microorganisms and on submerged macrophyte revegetation. *Environ. Sci. Pollut. Res.* 24, 1007–1018. doi: 10.1007/s11356-016-7828-1

Liu, Z., Wang, H., and Xu, R. (2016). The effects of root surface charge and nitrogen forms on the adsorption of aluminum ions by the roots of rice with different aluminum tolerances. *Plant Soil* 408, 43–53. doi: 10.1007/s11104-016-2909-y

Ma, J. F. (2007). Syndrome of aluminum toxicity and diversity of aluminum resistance in higher plants. *Int. Rev. Cytol.* 264, 225–252. doi: 10.1016/S0074-7696(07)64005-4

Ma, J. F., Chen, Z. C., and Shen, R. F. (2014). Molecular mechanisms of Al tolerance in gramineous plants. *Plant Soil* 381, 1–12. doi: 10.1007/s11104-014-2073-1

Maathuis, F. J. M. (2009). Physiological functions of mineral macronutrients. *Curr. Opin. Plant Biol.* 12, 250–258. doi: 10.1016/j.pbi.2009.04.003

Malhi, S. S., Nyborg, M., Caldwell, C. D., Hoyt, P. B., and Leitch, R. H. (1988). Effect of ammonium and nitrate on growth and yield of barley on acid soils. *Commun. Soil Sci. Plant Anal.* 19, 1049–1063. doi: 10.1080/00103628809367994

Marschner, H. (1995). *Mineral Nutrition of Higher Plants*. London: Academic Press.

Masclaux-Daubresse, C., Daniel-Vedele, F., Dechorgnat, J., Chardon, F., Gaufichon, L., and Suzuki, A. (2010). Nitrogen uptake, assimilation and remobilisation in plants: challenges for sustainable and productive agriculture. *Ann. Bot.* 105, 1141–1157. doi: 10.1093/aob/mcq028

Matsumoto, H. (2000). Cell biology of aluminum toxicity and tolerance in higher plants. *Int. Rev. Cytol.* 200, 1–46. doi: 10.1016/S0074-7696(00)00001-2

McCain, S., and Davies, M. S. (1983). The influence of background solution on root responses to aluminium in *Holcus lanatus* L. *Plant Soil* 73, 425–430. doi: 10.1007/BF0218432

Meriño-Gergichevich, C., Alberdi, M., Ivanov, A. G., and Reyes-Díaz, M. (2010). Al^{3+}-Ca^{2+} interaction in plants growing in acid soils: Al-phytotoxicity response to calcareous amendments. *J. Soil Sci. Plant Nutr.* 10, 217–243.

Mesdag, J., Slootmaker, L. A. J., and Post, J. (1970). Linkage between tolerance to high soil acidity and genetically high protein content in the kernel of wheat, *Triticum aestivum* L. and its possible use in breeding. *Euphytica* 19, 163–174. doi: 10.1007/BF01902940

Mihailovic, N., Vucinic, Z., and Sukalovic, V. H. (2015). Ammonium enables aluminum-induced stimulation of nitrogen assimilation in roots of Al-tolerant maize genotypes. *J. Plant Nutr.* 38, 371–383. doi: 10.1080/01904167.2014.934471

Miller, A. J., Fan, X., Orsel, M., Smith, S. J., and Wells, D. M. (2007). Nitrate transport and signalling. *J. Exp. Bot.* 58, 2297–2306. doi: 10.1093/jxb/erm066

Mishra, P., and Dubey, R. S. (2011). Nickel and Al-excess inhibit nitrate reductase but upregulate activities of aminating glutamate dehydrogenase and aminotransferases in growing rice seedlings. *Plant Growth Regul.* 64, 251–261. doi: 10.1007/s10725-011-9566-1

Miyasaka, S. C., Kochian, L. V., Shaff, J. E., and Foy, C. D. (1989). Mechanisms of aluminum tolerance in wheat. An investigation of genotypic differences in rhizosphere pH, K^+, and H^+ transport and root cell membrane potentials. *Plant Physiol.* 91, 1188–1196. doi: 10.1104/pp.91.3.1188

Morita, A., Ohta, M., and Yoneyama, T. (1998). Uptake, transport and assimilation of ^{15}N-nitrate and ^{15}N-ammonium in tea (*Camellia sinensis* L.) plants. *Soil Sci. Plant Nutr.* 44, 647–654. doi: 10.1080/00380768.1998.10414488

Mugwira, L. M., and Patel, S. U. (1977). Root zone pH changes and ion uptake imbalances by triticale, wheat and rye. *Agron. J.* 69, 719–722. doi: 10.2134/agronj1977.00021962006900040047x

Mulder, J., and Stein, A. (1994). The solubility of aluminum in acidic forest soils: long-term changes due to acid deposition. *Geochim. Cosmochim. Acta* 58, 85–94. doi: 10.1016/0016-7037(94)90448-0

Mulder, J., van Breemen, N., and Eijck, H. C. (1989). Depletion of soil aluminium by acid deposition and implications for acid neutralization. *Nature* 337, 247–249. doi: 10.1038/337247a0

Nichol, B. E., Oliveira, L. A., Glass, A. D. M., and Siddiqi, M. Y. (1993). The effects of aluminum on the influx of calcium, potassium, ammonium, nitrate, and phosphate in an aluminum-sensitive cultivar of barley (*Hordeum vulgare* L.). *Plant Physiol.* 101, 1263–1266. doi: 10.1104/pp.101.4.1263

Ogawa, S., Selvaraj, M. G., Fernando, A. J., Lorieux, M., Ishitani, M., McCouch, S., et al. (2014). N- and P-mediated seminal root elongation response in rice seedlings. *Plant Soil* 375, 303–315. doi: 10.1007/s11104-013-1955-y

Osaki, M., Watanabe, T., and Tadano, T. (1997). Beneficial effect of aluminum on growth of plants adapted to low pH soils. *Soil Sci. Plant Nutr.* 43, 551–563. doi: 10.1080/00380768.1997.10414782

Pal'ove-Balang, P., and Mistrík, I. (2007). Impact of low pH and aluminium on nitrogen uptake and metabolism in roots of *Lotus japonicus*. *Biologia* 62, 715–719. doi: 10.2478/s11756-007-0133-1

Pal'ove-Balang, P., and Mistrík, I. (2011). Effect of aluminium on nitrogen assimilation in roots of *Lotus japonicus*. *Plant Biosyst.* 145, 527–531. doi: 10.1080/11263504.2011.575608

Pal'ove-Balang, P., and Zelinova, A. M. V. (2013). Nitrogen uptake and free amino-acid accumulation in roots of *Lotus corniculatus* cultivars under Al-stress. *Agric. Trop. Subtrop.* 46, 5–9. doi: 10.2478/ats-2013-0001

Pécsváradi, A., Nagy, Z., Varga, A., Vashegyi, Á., Labádi, I., Galbács, G., et al. (2009). Chloroplastic glutamine synthetase is activated by direct binding of aluminium. *Physiol. Plant.* 135, 43–50. doi: 10.1111/j.1399-3054.2008.01167.x

Peuke, A. D., and Tischner, R. (1991). Nitrate uptake and reduction of aseptically cultivated spruce seedlings, *Picea abies* (L.) Karst. *J. Exp. Bot.* 239, 723–728. doi: 10.1093/jxb/42.6.723

Piña, R. G., and Cervantes, C. (1996). Microbial interactions with aluminium. *Biometals* 9, 311–316. doi: 10.1007/BF00817932

Pintro, J., Barloy, J., and Fallavier, P. (1996). Aluminum effects on the growth and mineral composition of corn plants cultivated in nutrient solution at low aluminum activity. *J. Plant Nutr.* 19, 729–741. doi: 10.1080/01904169609365156

Purcino, A. A. C., Alves, V. M. C., Parentoni, S. N., Belele, C. L., and Loguercio, L. L. (2003). Aluminum effects on nitrogen uptake and nitrogen assimilating enzymes in maize genotypes with contrasting tolerance to aluminum toxicity. *J. Plant Nutr.* 26, 31–61. doi: 10.1081/PLN-120016496

Rengel, Z., and Zhang, W. H. (2003). Role of dynamics of intracellular calcium in aluminium-toxicity syndrome. *New Phytol.* 159, 295–314. doi: 10.1046/j.1469-8137.2003.00821.x

Rorison, I. H. (1985). Nitrogen source and the tolerance of *Deschampsia flexuosa*, *Holcus lanatus* and *Bromus erectus* to aluminium during seedling growth. *J. Ecol.* 73, 83–90.

Rousk, J., Brookes, P. C., and Bååth, E. (2010). Investigating the mechanisms for the opposing pH relationships of fungal and bacterial growth in soil. *Soil Biol. Biochem.* 42, 926–934. doi: 10.1016/j.soilbio.2010.02.009

Ruan, J., Gerendás, J., Hardter, R., and Sattelmacher, B. (2007). Effect of nitrogen form and root zone pH on growth and nitrogen uptake of tea (*Camellia sinensis*) plants. *Ann. Bot.* 99, 301–310. doi: 10.1093/aob/mcl258

Rufty, T. W., MacKnown, C. T., Lazof, D. B., and Carter, T. E. (1995). Effects of aluminium on nitrate uptake and assimilation. *Plant Cell Environ.* 18, 1325–1331. doi: 10.1111/j.1365-3040.1995.tb00192.x

Rufyikiri, G., Dufey, J. E., Nootens, D., and Delvaux, B. (2001). Effect of aluminium on bananas (*Musa* spp.) cultivated in acid solutions. II. Water and nutrient uptake. *Fruits* 56, 5–16. doi: 10.1051/fruits:2001107

Ruiz, J. M., Rivero, R. M., and Romero, L. (2007). Comparative effect of Al, Se, and Mo toxicity on NO_3^- assimilation in sunflower (*Helianthus annuus* L.) plants. *J. Environ. Manage.* 83, 207–212. doi: 10.1016/j.jenvman.2006.03.001

Ryan, P. R., Ditomaso, J. M., and Kochian, L. V. (1993). Aluminum toxicity in roots: an investigation of spatial sensitivity and the role of the root cap. *J. Exp. Bot.* 44, 437–446. doi: 10.1093/jxb/44.2.437

Ryan, P. R., Tyerman, S. D., Sasaki, T., Furuichi, T., Yamamoto, Y., Zhang, W. H., et al. (2011). The identification of aluminium-resistance genes provides opportunities for enhancing crop production on acid soils. *J. Exp. Bot.* 62, 9–20. doi: 10.1093/jxb/erq272

Schier, G. A., and McQuattie, C. J. (1999). Effect of nitrogen source on aluminum toxicity in nonmycorrhizal and ectomycorrhizal pitch pine seedling. *J. Plant Nutr.* 22, 951–965. doi: 10.1080/01904169909365685

Schroeder, J. I., Delhaize, E., Frommer, W. B., Guerinot, M. L., Harrison, M. J., Herrera-Estrella, L., et al. (2013). Using membrane transporters to improve crops for sustainable food production. *Nature* 497, 60–66. doi: 10.1038/nature11909

Shahnawaz, M. D., Chouhan, R., and Sanadhya, D. (2017). Impact of aluminum toxicity on physiological aspects of barley (*Hordeum vulgare* L.) cultivars and its alleviation through ascorbic acid and salicylic acid seed priming. *Int. J. Curr. Microbiol. Appl. Sci.* 6, 875–891. doi: 10.20546/ijcmas.2017.605.098

Sharma, P., and Dubey, R. S. (2005). Modulation of nitrate reductase activity in rice seedlings under aluminium toxicity and water stress: role of osmolytes as enzyme protectant. *J. Plant Physiol.* 162, 854–864. doi: 10.1016/j.jplph.2004.09.011

Souza, L. C., Nogueira, D. C. S., Machado, L. C., Costa, T. C., Martins, J. T. S., Mendes, C. A. P., et al. (2016). Nitrogen compounds, proteins and amino acids in corn subjected to doses of aluminum. *Afr. J. Agric. Res.* 11, 1519–1524. doi: 10.5897/AJAR2015.10758

Sun, C., Lu, L., Liu, L., Liu, W., Yu, Y., Liu, X., et al. (2014). Nitrate reductase-mediated early nitric oxide burst alleviates oxidative damage induced by aluminum through enhancement of antioxidant defenses in roots of wheat (*Triticum aestivum*). *New Phytol.* 201, 1240–1250. doi: 10.1111/nph.12597

Tan, K., Keltjens, W. G., and Findenegg, G. R. (1992). Effect of nitrogen form on aluminum toxicity in sorghum genotypes. *J. Plant Nutr.* 15, 1383–1394. doi: 10.1080/01904169209364405

Taylor, G. J. (1988a). Aluminum tolerance is independent of rhizosphere pH in *Triticum aestivum* L. *Commun. Soil Sci. Plant Anal.* 19, 1217–1227. doi: 10.1080/00103628809368007

Taylor, G. J. (1988b). Mechanisms of aluminum tolerance in *Triticum aestivum* (wheat). V. Nitrogen nutrition, plant-induced pH, and tolerance to aluminum; correlation without causality? *Can. J. Bot.* 66, 694–699. doi: 10.1139/cjb-66-4-694

Taylor, G. J., and Foy, C. D. (1985a). Mechanisms of aluminum tolerance in *Triticum aestivum* L. (wheat). I. Differential pH induced by winter cultivars in nutrient solutions. *Am. J. Bot.* 72, 695–701. doi: 10.2307/2443681

Taylor, G. J., and Foy, C. D. (1985b). Mechanisms of aluminum tolerance in *Triticum aestivum* L. (wheat). II. Differential pH induced by spring cultivars in nutrient solutions. *Am. J. Bot.* 72, 702–706. doi: 10.2307/2443682

Taylor, G. J., and Foy, C. D. (1985c). Mechanisms of aluminum tolerance in *Triticum aestivum* (wheat). IV. The role of ammonium and nitrate nutrition. *Can. J. Bot.* 63, 2181–2186. doi: 10.1139/b85-309

Thornton, B. (1998). Influence of pH and aluminum on nitrogen partitioning in defoliated grasses. *Grass Forage Sci.* 53, 170–178. doi: 10.1046/j.1365-2494.1998.5320170.x

Tischner, R. (2000). Nitrate uptake and reduction in higher and lower plants. *Plant Cell Environ.* 23, 1005–1024. doi: 10.1046/j.1365-3040.2000.00595.x

Tomioka, R., Takenaka, C., Maeshima, M., Tezuka, T., Kojima, M., and Sakakibara, H. (2012). Stimulation of root growth induced by aluminum in *Quercus serrata* Thunb. is related to activity of nitrate reductase and maintenance of IAA concentration in roots. *Am. J. Plant Sci.* 3, 1619–1624. doi: 10.4236/ajps.2012.311196

Tomioka, R., Uchida, A., Takenaka, C., and Tezuka, T. (2007). Effect of aluminum on nitrate reductase and photosynthetic activities in *Quercus serrata* seedlings. *Environ. Sci.* 14, 157–165.

Townsend, L. R. (1966). Effect of nitrate and ammonium nitrogen on the growth of the lowbush blueberry. *Can. J. Plant Sci.* 46, 209–210. doi: 10.4141/cjps66-033

Townsend, L. R., and Blatt, C. R. (1966). Lowbush blueberry: evidence for the absence of a nitrate reducing system. *Plant Soil* 25, 456–460. doi: 10.1007/BF01394468

van Breemen, N., Burrough, P. A., Velthorst, E. J., van Dobben, H. F., de Wit, T., Ridder, T. B., et al. (1982). Soil acidification from atmospheric ammonium sulphate in forest canopy throughfall. *Nature* 299, 548–550. doi: 10.1038/299548a0

van Hai, T., Nga, T. T., and Laudelout, H. (1989). Effect of aluminium on the mineral nutrition of rice. *Plant Soil* 114, 173–185. doi: 10.1007/BF02220796

Van Praag, H. J., Weissen, F., Sougnez-Remy, S., and Carletti, G. (1985). Aluminum effects on spruce and beech seedlings. II. Statistical analysis of sand culture experiments. *Plant Soil* 83, 339–356. doi: 10.1007/BF02184446

Vitousek, P. M., and Howarth, R. W. (1991). Nitrogen limitation on land and in the sea: how can it occur? *Biogeochemistry* 13, 87–115. doi: 10.1007/BF00002772

von Uexküll, H. R., and Mutert, E. (1995). Global extent, development and economic impact of acid soils. *Plant Soil* 171, 1–15. doi: 10.1007/BF00009558

Wagatsuma, T., and Yamasaku, K. (1985). Relationship between differential aluminium tolerance and plant induced pH change of medium among barley cultivars. *Soil Sci. Plant Nutr.* 31, 521–535. doi: 10.1080/00380768.1985.10557461

Wang, H., Li, Y., Hou, J., Huang, J., and Liang, W. (2017). Nitrate reductase-mediated nitric oxide production alleviates Al-induced inhibition of root elongation by regulating the ascorbate-glutathione cycle in soybean roots. *Plant Soil* 410, 453–465. doi: 10.1007/s11104-016-3045-4

Wang, H. H., Huang, J. J., and Bi, Y. R. (2010). Nitrate reductase-dependent nitric oxide production is involved in aluminum tolerance in red kidney bean roots. *Plant Sci.* 179, 281–288. doi: 10.1016/j.plantsci.2010.05.014

Wang, W., Zhao, X. Q., Chen, R. F., Dong, X. Y., Lan, P., Ma, J. F., et al. (2015). Altered cell wall properties are responsible for ammonium-reduced aluminum accumulation in rice roots. *Plant Cell Environ.* 38, 1382–1390. doi: 10.1111/pce.12490

Watanabe, T., and Osaki, M. (2002). Mechanisms of adaptation to high aluminum condition in native plant species growing in acid soils: a review. *Commun. Soil Sci. Plant Anal.* 33, 1247–1260. doi: 10.1081/CSS-120003885

Watanabe, T., Osaki, M., and Tadano, T. (1998). Effects of nitrogen source and aluminum on growth of tropical tree seedlings adapted to low pH soils. *Soil Sci. Plant Nutr.* 44, 655–666. doi: 10.1080/00380768.1998.10414489

Yandow, T. S., and Klein, R. M. (1986). Nitrate reductase of primary roots of red spruce seedlings. Effects of acidity and metal ions. *Plant Physiol.* 81, 723–725. doi: 10.1104/pp.81.3.723

Zhao, X. Q., Aizawa, T., Schneider, J., Wang, C., Shen, R. F., and Sunairi, M. (2013a). Complete mitochondrial genome of the aluminum-tolerant fungus *Rhodotorula taiwanensis* RS1 and comparative analysis of *Basidiomycota* mitochondrial genomes. *Microbiologyopen* 2, 308–317. doi: 10.1002/mbo3.74

Zhao, X. Q., Bao, X. M., Wang, C., Xiao, Z. Y., Hu, Z. M., Zheng, C. L., et al. (2017). Hydroxy-Al and cell-surface negativity are responsible for the enhanced sensitivity of *Rhodotorula taiwanensis* to aluminum by increased medium pH. *Arch. Microbiol.* 199, 1185–1194. doi: 10.1007/s00203-017-1387-9

Zhao, X. Q., Chen, R. F., and Shen, R. F. (2014). Coadaptation of plants to multiple stresses in acidic soils. *Soil Sci.* 179, 503–513. doi: 10.1097/SS.0000000000000086

Zhao, X. Q., Guo, S. W., Shinmachi, F., Sunairi, M., Noguchi, A., Hasegawa, I., et al. (2013b). Aluminum tolerance in rice is antagonistic with nitrate preference and synergistic with ammonium preference. *Ann. Bot.* 111, 69–77. doi: 10.1093/aob/mcs234

Zhao, X. Q., and Shen, R. F. (2013). Interactive regulation of nitrogen and aluminum in rice. *Plant Signal. Behav.* 8:e24355. doi: 10.4161/psb.24355

Zhao, X. Q., Shen, R. F., and Sun, Q. B. (2009). Ammonium under solution culture alleviates aluminum toxicity in rice and reduces aluminum accumulation in roots compared with nitrate. *Plant Soil* 315, 107–121. doi: 10.1007/s11104-008-9736-8

Zhou, X., Gu, Z., Xu, H., Chen, L., Tao, G., Yu, Y., et al. (2016). The effects of exogenous ascorbic acid on the mechanism of physiological and biochemical responses to nitrate uptake in two rice cultivars (*Oryza sativa* L.) under aluminum stress. *J. Plant Growth Regul.* 35, 1013–1024. doi: 10.1007/s00344-016-9599-9

Conflict of Interest Statement: The authors declare that the research was conducted in the absence of any commercial or financial relationships that could be construed as a potential conflict of interest.

frontiers in Plant Science

ORIGINAL RESEARCH
published: 07 May 2018
doi: 10.3389/fpls.2018.00606

Bioinformatic and Functional Analysis of a Key Determinant Underlying the Substrate Selectivity of the Al Transporter, Nrat1

Muxue Lu†, Guangzhe Yang†, Peifang Li†, Zhigang Wang, Shan Fu, Xiang Zhang, Xi Chen, Mingxing Shi, Zhenhua Ming and Jixing Xia**

State Key Laboratory of Conservation and Utilization of Subtropical Agro-Bioresources, College of Life Science and Technology, Guangxi University, Nanning, China

OPEN ACCESS

Edited by:
Wei Fan,
Yunnan Agricultural University, China

Reviewed by:
He Qiang Lou,
Zhejiang Agriculture and Forestry University, China
Dezhi Wu,
Zhejiang University, China
Miguel A. Pineros,
United States Department of Agriculture (USDA), United States

***Correspondence:**
Jixing Xia
xiajx@gxu.edu.cn
Zhenhua Ming
zhming@gxu.edu.cn

† These authors have contributed equally to this work.

Specialty section:
This article was submitted to Plant Abiotic Stress, a section of the journal Frontiers in Plant Science

Received: *23 December 2017*
Accepted: *17 April 2018*
Published: *07 May 2018*

Citation:
Lu M, Yang G, Li P, Wang Z, Fu S, Zhang X, Chen X, Shi M, Ming Z and Xia J (2018) Bioinformatic and Functional Analysis of a Key Determinant Underlying the Substrate Selectivity of the Al Transporter, Nrat1. Front. Plant Sci. 9:606. doi: 10.3389/fpls.2018.00606

Nrat1 is a member of the natural resistance-associated macrophage protein (Nramp) family of metal ion transporters in all organisms. Different from other Nramp members capable of transporting divalent metals, Nrat1 specifically transports trivalent aluminum (Al) ion. However, molecular mechanism underlying the Al transport selectivity of Nrat1 remains unknown. Here, we performed structure-function analyses of Nrat1 and other Nramp members to gain insights into the determinants of ion selectivity. A phylogenetic analysis showed that plant Nramp transporters could be divided into five groups. OsNrat1 was found in one of the individual clades and clustered with SbNrat1 and ZmNrat1 on the evolutionary tree. Structural modeling revealed that Nrat1 transporters adopted a common LeuT fold shared by many Nramp-family transporters that likely employed an identical transport mechanism. Sequence alignment and evolutionary conservation analysis of amino acids identified a metal-permeation pathway of Nrat1 centered at the metal binding site. The metal binding site of Nrat1 was characterized by two conserved sequence motifs, i.e., the Asp-Pro-Ser-Asn motif (motif A) and the Ala-Ile-Ile-Thr motif (motif B). Replacement of the Ala-Met-Val-Met motif B of the OsNramp3 manganese (Mn) transporter to that of Nrat1 resulted in a partial gain of Al transport activity and a total loss of Mn in yeast. Conversely, substitution of the motif B of OsNrat1 with that of OsNramp3 altered the Al transport activity. These observations indicated the metal binding site, particularly the motif B, as a key determinant of Al selectivity of Nrat1.

Keywords: Nrat1, aluminum, Al transporter, selectivity, bioinformatic analysis

INTRODUCTION

The natural resistance-associated macrophage proteins (Nramps) are widely presented in bacteria, fungi, plants, and mammals (Curie et al., 2000; Nevo and Nelson, 2006). They function as metal ion transporters for a wide range of divalent metal substrates such as Fe^{2+}, Mn^{2+}, Cd^{2+}, Zn^{2+}, Co^{2+}, Ca^{2+}, Cu^{2+}, Ni^{2+}, and Pb^{2+} (Gunshin et al., 1997). In higher plants, Nramp proteins play major roles in the transport of mineral elements from soil to different organs and tissues of plants. For example, AtNramp1 is found to be localized at the plasma membrane of root cells and functions as a high-affinity transporter for Mn uptake in *Arabidopsis* (Cailliatte et al., 2010). AtNramp3 and

AtNramp4 function redundantly to release Fe and Mn from the vacuole (Thomine et al., 2000; Lanquar et al., 2005, 2010). In rice, OsNramp1 transports Fe and Cd in yeast and is suggested to be involved in Cd uptake (Takahashi et al., 2011). OsNramp3 is localized at the plasma membrane of node cells and is involved in distribution of Mn, but not Fe and Cd (Yamaji et al., 2013). The plasma membrane-localized transporter OsNramp5 is the major contributor for Mn and Cd uptake (Sasaki et al., 2012).

Recently, OsNrat1, an Nramp member, was reported to specifically transport Al^{3+} but not divalent metal ions such as Fe^{2+}, Mn^{2+}, and Cd^{2+}, and required for Al tolerance in rice (Xia et al., 2010). In sorghum, SbNrat1, a close homolog of rice OsNrat1, also was shown to selectively transport Al^{3+} (Lu et al., 2017). However, the molecular mechanisms underlying the Al transport selectivity of Nrat1 remain unknown.

Several studies have investigated the relationships between the structure and the function in Nramp proteins. For instance, mutational analysis of the first external loop (Loop I) of NRAMP2/DCT1/DMT1 suggested that Loop I is involved in metal ion binding and specificity (Cohen et al., 2003). The mutation (G185R) in NRAMP2/DCT1/DMT1 not only resulted in a decrease in iron transport but increased the permeability to calcium (Xu et al., 2004). In *Arabidopsis*, three residues (L67, E401, F413) of AtNramp4 have been also shown to play important roles in metal selectivity (Pottier et al., 2015). On the other hand, the crystal structural studies have revealed that Nramp proteins shared a conserved protein fold that was previously found in the amino acid transporter LeuT (Cellier, 2012; Ehrnstorfer et al., 2014). The ScaNramp structure also revealed that a metal binding site consists of conserved aspartate, asparagines, and methionine residues, and a backbone carbonyl from transmembrane segments (TMs) 1 and 6 (Ehrnstorfer et al., 2014). Moreover, the conserved metal-binding site methionine was shown to confer selectivity against the abundant alkaline earth metals calcium and magnesium (Bozzi et al., 2016a). However, the role of the conserved metal-binding site in controlling substrate selectivity is still poorly understood.

In this study, we compared the structure and function of Nrat1 and other initially reported Nramp members in plants by phylogenetic analysis and homology modeling. Furthermore, we performed the site-direct mutagenesis analysis of the conserved metal binding motif in two Nramp proteins, OsNrat1 and OsNramp3, which are known as transporters for Al and Mn (Xia et al., 2010; Yamaji et al., 2013), respectively, and examined their transport activities for Al and Mn. Our results identified a key determinant of Al selectivity of Nrat1, which is essential for Mn selectivity of OsNramp3. It provides novel insights into the molecular basis of Al transport selectivity of Nrat1 and valuable clues to investigate Mn transport selectivity of OsNramp3.

MATERIALS AND METHODS

Sequence and Structure Collection

The amino acid sequences of OsNrat1 homologs from four types of plants, *Oryza sativa*, *Arabidopsis thaliana*, *Sorghum bicolor,* and *Zea mays*, were obtained by BLAST (Johnson et al., 2008) using the OsNrat1 sequence as a query in the U.S. National Center for Biotechnology Information (NCBI) reference sequence (RefSeq) database. After eliminating the repetitive sequences, we collected a total of 24 sequences. The structures of prokaryotic Nramp transporters were downloaded from the Protein Data Bank (PDB) database. The 25 Nramp transporters and their NCBI accession numbers are as follows: OsNramp1, XP_015647629; OsNramp2, XP_015632573; OsNramp3, XP_015644306; OsNrat1, XP_015625418; OsNramp5, XP_015645014; OsNramp6, XP_015620405; OsNramp7, XP_015618209; AtNramp1, NP_178198; AtNramp2, NP_175157; AtNramp3, NP_179896; AtNramp4, NP_201534; AtNramp5, NP_193614; AtNramp6, NP_173048; SbNramp1, XP_002459640; SbNramp2, XP_002465667; SbNramp3, XP_002438846; SbNramp4, XP_021317241; SbNramp5, XP_002461772; SbNramp6, XP_002464246; SbNrat1, XP_002451480; ZmNramp1, XP_008670084; ZmNramp4, XP_008670762; ZmNramp5, XP_008652227; ZmNramp6, XP_008665146; ZmNrat1, NP_001334019.

Sequence Alignment and Phylogenetic Analysis

Multiple-sequence alignment (MSA) was performed by using the T-Coffee server (Di Tommaso et al., 2011). The alignment was produced by combining multiple methods, including mafft_msa, clustalw_msa and t_coffee_msa. Results were subjected to figure production by ESPript version 3.0 (Robert and Gouet, 2014), evolutionary tree building by MEGA6 (Tamura et al., 2013), or evolutionary conservation analysis by ConSurf (Ashkenazy et al., 2010).

Phylogenetic analysis was conducted in MEGA version 6 by the bootstrap neighbor joining method (Saitou and Nei, 1987). Bootstrap method (Felsenstein, 1985) was used for test of phylogeny and the number of bootstrap replications was set to 1000. The evolutionary distances were calculated using the Poisson correction method (Zuckerkandl and Pauling, 1965) and were in the units of the number of amino acid substitutions per site. The analysis involved all 25 amino acid sequences of the Nramp family transporters in the four types of plants. All positions containing gaps and missing data were eliminated. There was a total of 450 positions in the final dataset.

Evolutionary Conservation Analysis

MSA of the 25 plant Nramp transporters constructed by T-Coffee and the I-TASSER model for the core domain of OsNrat1 (45–502) was used to calculate the position-specific conservation scores by the empirical Bayesian algorithms (Mayrose et al., 2004) in ConSurf (Ashkenazy et al., 2010). The continuous conservation scores are divided into a discrete scale of nine grades for visualization, from the most variable positions (grade 1) colored turquoise, through intermediately conserved positions (grade 5) colored white, to the most conserved positions (grade 9) colored maroon. Scripts for visualizing the protein colored with ConSurf scores were generated and the colored protein was shown in PyMOL (DeLano, 2002).

Normalized conservation scores were also extracted and used to calculate the average conservation score for each structural element and produce figures in GraphPad Prim version 5.

Vector Construction

The coding region of OsNrat1 and OsNramp3 was amplified from rice (*Oryza sativa*, Nipponbare) root cDNA with high-fidelity PCR (KOD Fx polymerase, Toyobo), and the amplified fragments were cloned into the HindIII/EcoRI, BamHI/EcoRI restriction sites of yeast expression vector pYES2 (Invitrogen), respectively. Site-directed mutagenesis of *OsNrat1* and *OsNramp3* was performed by overlapping PCR (Ho et al., 1989). The wild-type and mutated *OsNrat1* or *OsNramp3* CDS were verified by sequencing. All the PCR primers used are listed in Supplementary Table S1.

Yeast Assays

The yeast strains used in this study were BY4741 (*MATa his2Δ0 met15Δ0 ura3Δ0*) and *smf1* (*MATa his2Δ0 met15Δ0 ura3Δ0 YOL122c::KanMX4*). Al sensitivity test on agar and complementation of the *smf1* phenotype were performed as described by Xia et al. (2010). For Al sensitivity evaluation, *OsNrat1, OsNramp3*, *mutated OsNrat1,* or *OsNramp3,* and vector control pYES2 were introduced into yeast strain BY4741 and then spotted on solid media (LPM with 2% galactose for induction of the GAL promoter) containing 0, 200, or 300 μM $AlCl_3$ buffered with 5 mM succinic acid. For Al uptake in liquid culture, transformants were selected on uracil-deficient medium and grown in synthetic complete (SC-uracil) yeast solution containing 2% glucose. Cells at mid-exponential phase were harvested and transferred to LPM medium containing 2% galactose. Cells were cultured for 2 h. Then $AlCl_3$ was added to the cell culture at the final concentration of 50 μM $AlCl_3$. After 6 h incubation with shaking, cells were harvested by centrifugation at 12000 × *g* for 5 min, and washed three times with deionized water (MilliQ; Millipore), dried and then digested with 65% HNO_3. Al concentration was measured by inductively coupled plasma optical emission spectrometry.

RESULTS

Plant Nramp Transporters Fall Into Five Groups on the Phylogenetic Tree

The amino acid sequence of OsNrat1 was used to retrieve Nramp homologs in four plant species by BLAST (Johnson et al., 2008). Twenty-four protein sequences were selected for phylogenetic analysis, including six from *Oryza sativa* (OsNrat1, OsNramp1-3, and 5-7), six from *Arabidopsis thaliana* (AtNramp1-6), seven from *Sorghum bicolor* (SbNrat1 and SbNramp1-6), and five from *Zea mays* (ZmNrat1, ZmNramp1, and ZmNramp4-6). The resulting phylogenetic tree includes five main clades corresponding to five distinctive Nramp groups (**Figure 1**). Notably, two known transporters for trivalent Al ion, OsNrat1 (Xia et al., 2010, 2014; Li et al., 2014) and SbNrat1 (Lu et al., 2017), an Nrat1-like transporter of *Zea mays* (ZmNrat1) as well, are located in the same clade (group III) but separated from other divalent ion transporters on the evolutionary tree.

Nrat1 Transporter Adopts a Conserved LeuT Fold

Sequence alignment of the 25 plant Nramp transporters and the *Staphylococcus Capitis* Divalent Metal Ion Transporter (ScaDMT) reveals that they contain a conserved core domain (amino acid sequence 45–502 in OsNrat1, see Supplementary Figure S1). The available structural information on the Nramp family is limited to the prokaryotic homologues of divalent metal transporters. To understand the mechanism in which trivalent Al is recognized by Nrat1 transporter, we modeled the protein structures of core domain of OsNrat1 and OsNramp3 through an iterative threading algorithm using the I-TASSER server (Roy et al., 2010), as the terminal N- and C- regions with unknown functionality are not as important as the core domain that is highly conserved and constitutes a part of the molecular determinants for ion permeation. To compare the architecture of metal binding sites in the ionic binding state of these two proteins, the Mn-binding structure of ScaDMT (PDBID: 5M95), which showed the highest sequence similarities with OsNrat1 (59%) and OsNramp3 (62%), was used as a template. The estimated TM-score and C-score of OsNrat1 are 0.95 ± 0.05 and 1.68, respectively; while those of OsNramp3 are 0.92 ± 0.06 and 1.50, respectively. Hence, these two models appear to be acceptable.

OsNrat1 adopts a common LeuT fold (**Figure 2**) that is associated with many prokaryotic Nramp-family transporters, including the *Staphylococcus* divalent metal transporter ScaDMT (59% sequence similarity, PDBID: 5M95), the *Deinococcus radiodurans* Nramp homolog (DraNramp, 56% similarity, PDBID: 5KTE), and the *Eremococcus coleocola* Manganese Transporter (EcoDMT, 56% similarity, PDBID: 5M87). OsNrat1 contains a compact globular domain of 12 transmembrane segments (TMs), of which TMs 1–5 and 6–10 form two inverted repeats of the LeuT fold. Like other LeuT-type transporters, the first TM in each of the two inverted repeats (TM1 and TM6) of OsNrat1 contains two α-helices disrupted by a short discontinuous stretch in the middle (Supplementary Figure S1). Overall, a helical bundle comprising TMs 3–5 and 8–10 forms a semicircular (letter C shaped) structure that wraps partway around a second helical bundle formed by TMs 1, 2, 6, and 7. Substrate transport of the LeuT-type transporters is likely to be coupled with a switch from outward-open to inward-open conformation, through a rigid-body rotation (Shi, 2013) of the moving portion (corresponding to the latter α helical bundle) related to the non-moving portion (corresponding to the former helical bundle).

The Metal Transport Mechanism of Nrat1 Is Conserved

Evolutionary conservation analysis by the ConSurf server (Ashkenazy et al., 2010) reveals an overwhelming conservation of residues that make up the interior of the Nrat1 cylinder structure (**Figure 2A**), which contains a substrate transport path along the central axis that is perpendicular to the lipid

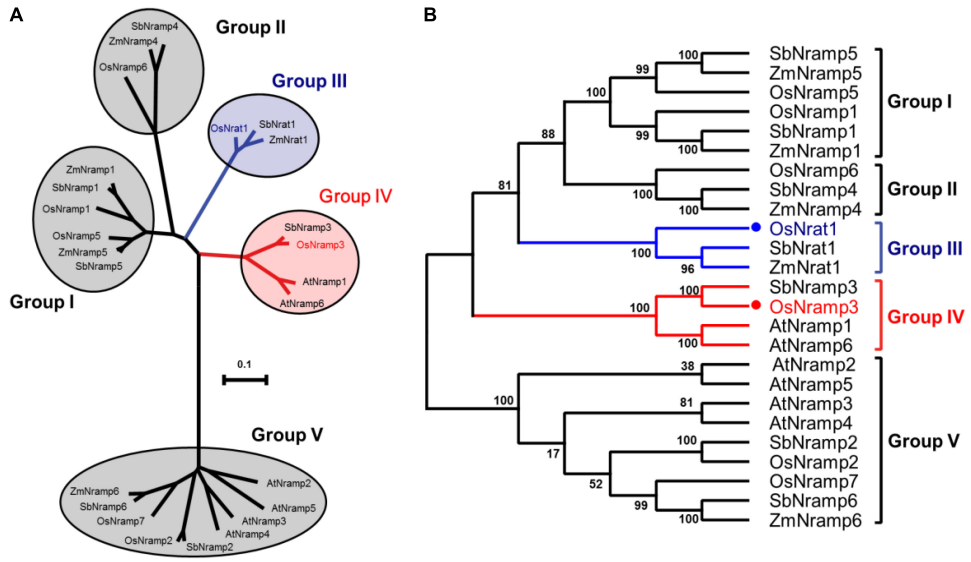

FIGURE 1 | Evolutionary relationships of the plant Nramp family transporters. **(A)** An unrooted phylogenetic tree for the 25 plant metal transporters of the Nramp family was built by MEGA6. The five clades of the evolutionary tree are indicated by circles, with the OsNrat1 containing group (group III) and the OsNramp3 containing group (group IV) colored in blue and red, respectively. The tree is drawn to scale, with branch lengths in the same units as those of the evolutionary distances used to infer the phylogenetic tree. **(B)** Related to **(A)**, the evolutionary tree is shown in a squarish-corner style. The percentages of replicate trees in which the associated taxa clustered together in the bootstrap test (1000 replicates) are shown next to the branches.

membrane plane. A detailed conservation analysis for each structural element was performed by calculating the normalized evolutionary conservation scores on all amino acid residues. As shown in **Figure 2B**, TMs 1-3, 6, 8-10, along with the L23 loop are highly conserved across all 25 Nramp transporters in plants, suggesting that these conserved elements may play important roles in metal transport. On the contrary, structural elements of NT, CT, TM11 and TM12 in the Nramp family are variable. These observations are consistent with structural and functional analysis of other LeuT-type transporters, indicating a conserved substrate transport mechanism. Similar to other known LeuT-type transporters, the five TMs (TMs 1, 3, 6, 8, and 10) may participate directly in substrate binding and transport. TM2 and TM9, which connect the functional helices TM1/TM3 and TM8/TM10, respectively, may confer transport activity through control of the local conformation. The L23 linker that connects neighboring helices of TM2 and TM3 may parallel the roles of TM2 and TM9.

The Nrat1 Transporter Contains a Unique Ion Binding Site

The metal recognition site of prokaryotic Nramp transporters is known to be characterized by two structural motifs (**Figure 3** and Supplementary Figure S1), motifs A and B. The highly conserved Asp-Pro-[Gly/Ser]-Asn motif (motif A) occurs in the loop between TM1a and TM1b, as well as the N-terminal portion of TM1b; while the moderate conserved motif (motif B) occurs in the C-terminal portion of TM6a and the loop between TM6a and TM6b. Only four residues, i.e., the first and fourth residues in each motif, are required to coordinate the central metal ion (**Figure 3D**). The Asp and Asn residues in motif A (locating at the first and fourth position, respectively), as well as the fourth residue in motif B, use their side chains to contact the metal ion. By contrast, the first residue in motif B contributes to metal binding by its main-chain carbonyl oxygen. In support of the structural and functional importance of the metal coordination ligands, the Asp and Asn residues in motif A are invariant within the Nramp family and across plant species (**Figure 3A** and Supplementary Figure S1). Notably, the metal ligands in motif B are only moderately conserved (**Figure 3A** and Supplementary Figure S1), suggesting that this motif may contribute to ion-subtype specificity. It is also worth noting that, through refining the proper conformation of terminal residues in each motif, interspace residues of the two motifs may be important for ion binding and selectivity as well.

Sequence alignment results for the two signature motifs show good agreement with the phylogenetic analysis of plant Nramp transporters (**Figure 3A**). Transporters of the Nrat1 group and group II have an Asp-Pro-Ser-Asn sequence pattern of motif A, while other groups consist of a motif A with a uniform Asp-Pro-Gly-Asn sequence. The characteristic sequence patterns of motif B can be clearly divided into five sets, each corresponding to one of the five phylogenetic groups. Among the five sets of motif B, sequences of groups I, III, and IV have the highest conservation. Motif B of group III transporters has an invariant sequence of Ala-Ile-Ile-Thr, while motif B of group I and IV has an identical sequence of Ala-Leu-Val-Met and Ala-Met-Val-Met, respectively. Together, these data indicated that Nrat1 transporters contain a unique pair of sequence motifs which may be critical for mediating metal recognition.

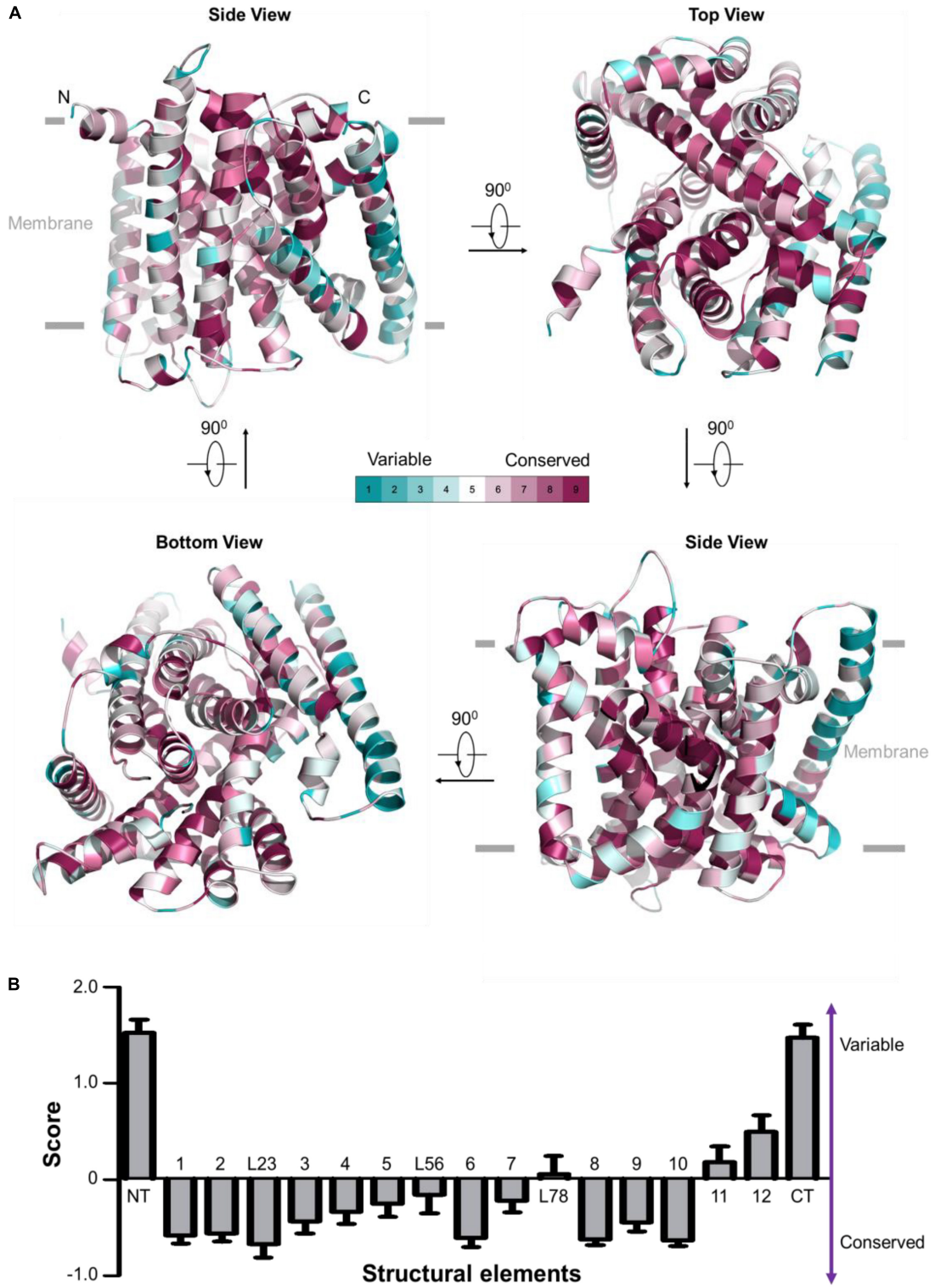

FIGURE 2 | Evolutionary conservation analysis for OsNrat1. The 25 plant Nramp family transporters were used to perform evolutionary conservation analysis by ConSurf. **(A)** Mapping of evolutionary conservation scales for amino acid positions in the core structure of OsNrat1 (45–502). Residues are colored by their conservation grades (1–9) using the color-coding bar, from turquoise to maroon indicating variable to conserved. The structure is shown in four orientations in cartoon representation. **(B)** Normalized evolutionary conservation score for each structural element of OsNrat1. The lowest score indicates that this position is the most conserved in this specific protein calculated using a specific multiple sequence alignment (MSA). Error bars represent SEMs. The NT and CT regions of OsNrat1 are not shown in **(A)**.

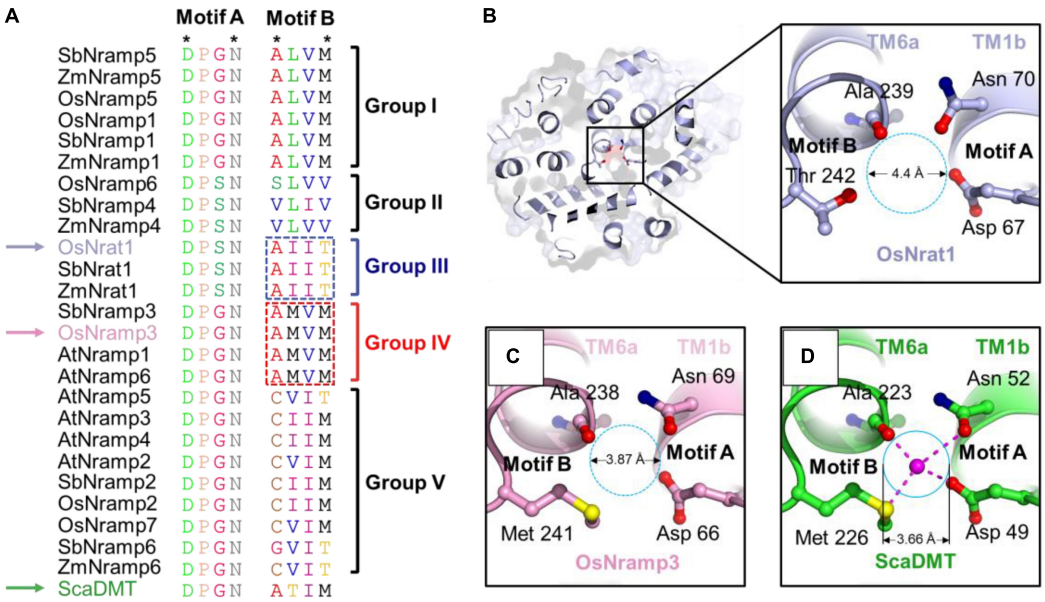

FIGURE 3 | OsNrat1 has a unique metal binding site. **(A)** Sequence alignment of the two signature motifs of the 25 plant Nramp transporters and a bacteria Nramp transporter ScaDMT. The variations of amino acids in the two motifs were marked with different colors. The four residues involved in metal coordination are indicated as stars above the alignment. OsNrat1, OsNramp3, and ScaDMT are indicated by arrows in light blue, pink and green, respectively. The five phylogenetic groups are labeled to the right of the alignment. The amino acids being swapped in Nrat1 and OsNramp3 are marked by dotted rectangles. **(B)** A top view of OsNrat1 from the extracellular side of the membrane **(Left)** with a cartoon representation. The four metal binding residues are shown as colored sticks. The carbon, oxygen, and nitrogen atoms are colored in light blue, red, and tv_blue, respectively. A close-up view of the metal binding site is given in the right panel. **(C)** A close-up view of the metal binding site of OsNramp3 shown with the same orientation as OsNrat1. The coloring code for the atoms are the same as that in **(B)**, except for carbon (pink) and sulfur (yellow). **(D)** A close-up view of the binding site of ScaDMT shown with the same orientation as OsNrat1. The coloring pattern for the atoms is the same as that in **(C)**, except for carbon colored green. The proposed metal binding sites of OsNrat1 and OsNramp3 are indicated by dotted circles, while the metal binding site of ScaDMT is indicated by a solid circle. The approximate diameters of the binding sites are calculated by the equation: *D1 = D2*d1/d2*. *D1* is the diameter of the binding site circle to be calculated. *D2* is the spatial distance between the main-chain oxygen of Ala223 and the side-chain oxygen of Asn52 measured in the crystal structure of ScaDMT by the software PyMOL. *d1* is the diameter of the binding site circle measured in the figure. *d2* is the distance between the main-chain oxygen of Ala223 and the side-chain oxygen of Asn52 of ScaDMT measured in the figure.

We proceeded to compar the putative metal binding sites from the core domain structural models of OsNrat1 and OsNramp3, with that of the crystal structure of ScaDMT. As shown in **Figures 3B–D**, the architecture of the divalent ion recognition site in OsNramp3 is identical to that observed in ScaDMT. By contrast, the trivalent metal binding site in OsNrat1 appears to be slightly larger than those in OsNramp3 and ScaDMT, as calculated in the two models and the ScaDMT crystal structure (**Figures 3B–D**). These differences are likely caused by a replacement of the Met with a Thr, which contains a shorter side-chain compared to that of a Met, at the fourth residue of motif B.

The Nrat1 Specific Motif B Is a Key Determinant for Al Transport

To determine the functional importance of the signature motifs, we generated several mutations for OsNrat1 and OsNramp3 (OsNrat1^{I240M,I241V,T242M}, OsNrat1^{T242M}, OsNramp3^{M239I,V240I,M241T}, OsNramp3^{M241T}, see Supplementary Table S2) by exchanging corresponding residues of one protein with another and examined their capabilities on Al and Mn transport as well as OsNrat1 or OsNramp3 as a positive control, respectively.

In the absence of Al, all the transformants showed similar growth on the plate (**Figure 4A**). However, in the presence of Al, the growth of yeast cells carrying *OsNrat1*^{T242M}, *OsNramp3*^{M239I,V240I,M241T}, or *OsNrat1* was significantly inhibited compared with that of the vector control, while that of *OsNrat1*^{I240M,I241V,T242M}, *OsNramp3*^{M241T}, or *OsNramp3* was not (**Figure 4A**). Al uptake also significantly increased in the yeast carrying *OsNrat1*^{T242M}, *OsNramp3*^{M239I,V240I,M241T}, or *OsNrat1* and was not affected in the yeast carrying *OsNrat1*^{I240M,I241V,T242M}, *OsNramp3*^{M241T}, or *OsNramp3* (**Figure 4B**). Furthermore, the Al uptake ability of *OsNrat1*^{T242M} or *OsNramp3*^{M239I,V240I,M241T} was lower than that of *OsNrat1* (**Figure 4B**). These results suggested that substitution of the intact motif B of OsNrat1 (OsNrat1^{I240M,I241V,T242M}) with that of OsNramp3 completely deprived the Al transport activity of OsNrat1, while a single mutation on the fourth residue Thr242Met (OsNrat1^{T242M}) resulted in a decrease in Al uptake of OsNrat1, and that replacement of the intact motif B of OsNramp3 (OsNramp3^{M239I,V240I,M241T}) with that of OsNrat1, but not a single mutation on the fourth residue Met241Thr (OsNramp3^{M241T}), rendered the Mn specific divalent transporter to gain a function of Al transport.

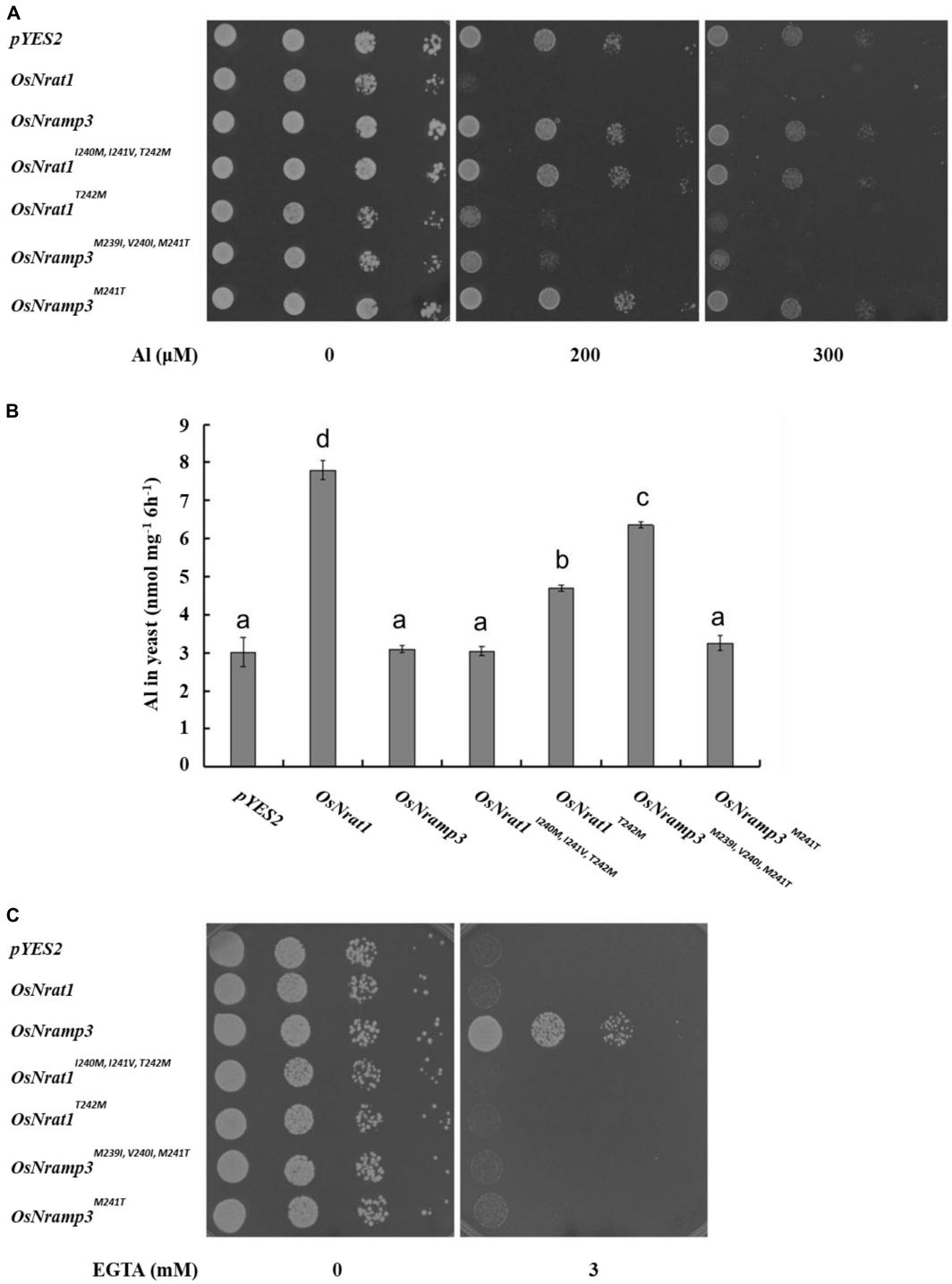

FIGURE 4 | Influence of the signature motif substitution of OsNrat1 or OsNramp3 on transport activity for Al and Mn. **(A)** Effect of mutated OsNrat1 or OsNramp3 on Al tolerance. Yeast strain (BY4741) transformed with empty vector *pYES2*, *OsNrat1*, *OsNramp3*, *OsNrat1*^{I240M,I241V,T242M}, *OsNrat1*^{T242M}, *OsNramp3*^{M239I,V240I,M241T}, *OsNramp3*^{M241T} were spotted on LPM without uracil medium (pH 4.2) buffered with 5 mM succinic acid with or without $AlCl_3$ at serial dilutions (from left to right: 10 μl cell suspension with OD 0.2, 0.02, 0.002, and 0.0002) and incubated at 30°C for 3 days. **(B)** Transport activity of mutated OsNrat1 or OsNramp3 for Al. Yeast cells expressing different mutants were exposed to a solution containing 50 μM $AlCl_3$ (pH 4.2) for 6 h. Data are mean ± SD of three biological replicates. Different letters above the bars indicate significant differences ($P < 0.05$, Tukey's test). **(C)** Complementation of manganese uptake. Transformed *smf1* were grown on a medium (pH 6.0) buffered with 50 mM MES in the presence or absence of EGTA. The plates were incubated at 30°C for 3 days.

Subsequently, we performed a complementation test in the Δ*smf1* yeast strain to examine whether mutants of OsNrat1 and OsNramp3 could have transport activity for Mn. As expected, OsNramp3 could restore the growth of a yeast mutant (*smf1*) defective in Mn uptake, while OsNrat1 could not (**Figure 4C**). Surprisingly, as shown in **Figure 4C**, all of the four above mentioned mutations failed to complement the manganese uptake phenotype of the Δ*smf1* mutant yeast. These observations collectively indicate that the Nrat1 specific motif B is both sufficient and required for Al transport, while the OsNramp3 specific motif B, especially the fourth ionic coordination ligand, is only required but not sufficient for Mn transport.

We also studied the functional importance of residues in close vicinity of the signature motifs by sequence exchange between OsNrat1 and OsNramp3 (OsNrat1$^{A59F,\ G64A}$, OsNrat1^{Y244H}, OsNramp3$^{F58A,\ A63G}$, OsNramp3^{H243Y}, see Supplementary Table S2). As shown in the Supplementary Figure S2, the expression of *OsNrat1*^{A59F,G64A}, *OsNrat1*^{Y244H}, or *OsNrat1* increased the sensitivity of yeast to Al toxicity and the Al uptake in yeast compared with that of the vector control, while that of *OsNramp3*^{F58A,A63G}, *OsNramp3*^{H243Y}, or *OsNramp3* did not (Supplementary Figures S2A,B). Furthermore, the Al uptake ability of *OsNrat1*^{A59F,G64A} or *OsNrat1*^{Y244H} was lower than that of *OsNrat1* (Supplementary Figure S2B). On the other hand, in contrast to *OsNramp3*, the expression of *OsNrat1*^{A59F,G64A}, *OsNrat1*^{Y244H}, *OsNramp3*^{F58A,A63G}, or *OsNramp3*^{H243Y} was not able to complement the growth of the yeast mutant Δ*smf1* under the Mn-limited condition controlling by EGTA (Supplementary Figure S2C). These results indicated that flanking residues of the characteristic motifs are dispensable for Al selectivity but required, at least in part, for Al transport activity. These data also suggested that residues near the metal binding motifs of OsNramp3, but not OsNrat1, are essential for Mn uptake of the transporter.

DISCUSSION

A number of reported variations in the Nrat1 coding region affect transport activity (Li et al., 2014; Xia et al., 2014; Lu et al., 2017) but not selectivity of Nrat1. We reasoned that careful examination of the metal binding site may facilitate to understand the selectivity of the transporter. The Nramp family of transporters utilizes two separate motifs, each from one of the two discontinuous TMs, to coordinate metal ions (Ehrnstorfer et al., 2014, 2017; Bozzi et al., 2016b). Our bioinformatic and functional analyses demonstrate that the metal binding site, particularly the motif B with a sequence of Ala-Ile-Ile-Thr, is a prominent determinant of Al selectivity for Nrat1.

Motif B of OsNramp3 is probably essential for the selectivity of the transporter. However, the interpretation for selectivity of Nrat1 cannot be directly applied to give a simplified explanation for the selectivity of the Mn specific transporters of the Nramp family, as substitution of mere motif B in OsNrat1 by that of OsNramp3 is not sufficient for the former to gain Mn transport activity. This is consistent with the experimental observations for divalent Nramp transporters reported by Bozzi et al. (2016a). The conserved metal-binding methionine (Met230) of motif B is dispensable in the bacterial DraNramp, as the Met-to-Ala mutant can still enable robust transport of the physiological manganese substrate and similar divalent iron and cobalt. In sharp contrast to the DraNramp, the corresponding Met265Ala mutant of human Nramp2 did not transport any of the tested divalent metals, including Co, Mn, Cd, and Ca. These results indicate a dependency of the functional divergence on sequence and structure context (Bozzi et al., 2016a). Supporting this hypothesis, whereas the single mutation (corresponding to Gln76 of OsNrat1) in TM1b of the mammalian transporter DCT1 (Slc11a2) completely blocked Mn transport, a double mutation (corresponding to Asp74 and Gln76 of OsNrat1) in TM1b restored the activity and altered the metal ion specificity in favor of Fe (Cohen et al., 2003). Moreover, random mutagenesis studies revealed that three residues, Leu67 (in the immediate vicinity of motif A) from TM1a and Glu401/Phe413 from TM10, contributed to the selectivity of AtNramp4 for the uptake of another divalent metal Cd (Pottier et al., 2015).

Our work identified that the Nrat1-type motif B is both sufficient and required for Al transport in Nrat1 and OsNramp3, as one of the key determinants for the Al selectivity. Our results also suggested that the OsNramp3-type motif B is necessary, though not sufficient, for the Mn selectivity of OsNramp3. Identification of the important functions of motif B in substrate selectivity of Nrat1 and OsNramp3 may help further elucidate the selectivity of other Nramp transporters.

AUTHOR CONTRIBUTIONS

ZM and JX conceived and designed the experiments. ML, GY, PL, ZW, XZ, XC, SF, and MS performed the experiments. ML, GY, ZM, and JX analyzed the data. ZM and JX wrote the paper.

FUNDING

This work was supported by Guangxi Natural Science Foundation (2015GXNSFCB139001, 2016GXNSFFA380013, 2016GXNSFBA380176), National Natural Science Foundation of China (31670253, 31700052), the Project of High Level Innovation Team and Outstanding Scholar in Guangxi Colleges and Universities (2016), and China Postdoctoral Science Foundation (2017M612863).

ACKNOWLEDGMENTS

We thank Zheng Zhang (Shandong University) for helpful discussion.

SUPPLEMENTARY MATERIAL

The Supplementary Material for this article can be found online at: https://www.frontiersin.org/articles/10.3389/fpls.2018.00606/full#supplementary-material

REFERENCES

Ashkenazy, H., Erez, E., Martz, E., Pupko, T., and Ben-Tal, N. (2010). ConSurf 2010: calculating evolutionary conservation in sequence and structure of proteins and nucleic acids. *Nucleic Acids Res.* 38, W529–W533. doi: 10.1093/nar/gkq399

Bozzi, A. T., Bane, L. B., Weihofen, W. A., Mccabe, A. L., Singharoy, A., Chipot, C. J., et al. (2016a). Conserved methionine dictates substrate preference in Nramp-family divalent metal transporters. *Proc. Natl. Acad. Sci. U.S.A.* 113, 10310–10315. doi: 10.1073/pnas.1607734113

Bozzi, A. T., Bane, L. B., Weihofen, W. A., Singharoy, A., Guillen, E. R., Ploegh, H. L., et al. (2016b). Crystal structure and conformational change mechanism of a bacterial nramp-family divalent metal transporter. *Structure* 24, 2102–2114. doi: 10.1016/j.str.2016.09.017

Cailliatte, R., Schikora, A., Briat, J. F., Mari, S., and Curie, C. (2010). High-affinity manganese uptake by the metal transporter NRAMP1 is essential for *Arabidopsis* growth in low manganese conditions. *Plant Cell* 22, 904–917. doi: 10.1105/tpc.109.073023

Cellier, M. F. (2012). Nramp: from sequence to structure and mechanism of divalent metal import. *Curr. Top. Membr.* 69, 249–293. doi: 10.1016/B978-0-12-394390-3.00010-0

Cohen, A., Nevo, Y., and Nelson, N. (2003). The first external loop of the metal ion transporter DCT1 is involved in metal ion binding and specificity. *Proc. Natl. Acad. Sci. U.S.A.* 100, 10694–10699. doi: 10.1073/pnas.1934572100

Curie, C., Alonso, J. M., Le Jean, M., Ecker, J. R., and Briat, J. F. (2000). Involvement of NRAMP1 from Arabidopsis thaliana in iron transport. *Biochem. J.* 347(Pt 3), 749–755. doi: 10.1042/bj3470749

DeLano, W. (2002). *The PyMOL Molecular Graphics System*. San Carlos, CA: Delano Scientific.

Di Tommaso, P., Moretti, S., Xenarios, I., Orobitg, M., Montanyola, A., Chang, J. M., et al. (2011). T-Coffee: a web server for the multiple sequence alignment of protein and RNA sequences using structural information and homology extension. *Nucleic Acids Res.* 39, W13–W17. doi: 10.1093/nar/gkr245

Ehrnstorfer, I. A., Geertsma, E. R., Pardon, E., Steyaert, J., and Dutzler, R. (2014). Crystal structure of a SLC11 (NRAMP) transporter reveals the basis for transition-metal ion transport. *Nat. Struct. Mol. Biol.* 21, 990–996. doi: 10.1038/nsmb.2904

Ehrnstorfer, I. A., Manatschal, C., Arnold, F. M., Laederach, J., and Dutzler, R. (2017). Structural and mechanistic basis of proton-coupled metal ion transport in the SLC11/NRAMP family. *Nat. Commun.* 8:14033. doi: 10.1038/ncomms14033

Felsenstein, J. (1985). Confidence limits on phylogenies: an approach using the bootstrap. *Evolution* 39, 783–791. doi: 10.1111/j.1558-5646.1985.tb00420.x

Gunshin, H., Mackenzie, B., Berger, U. V., Gunshin, Y., Romero, M. F., Boron, W. F., et al. (1997). Cloning and characterization of a mammalian proton-coupled metal-ion transporter. *Nature* 388, 482–488. doi: 10.1038/41343

Ho, S. N., Hunt, H. D., Horton, R. M., Pullen, J. K., and Pease, L. R. (1989). Site-directed mutagenesis by overlap extension using the polymerase chain reaction. *Gene* 77, 51–59. doi: 10.1016/0378-1119(89)90358-2

Johnson, M., Zaretskaya, I., Raytselis, Y., Merezhuk, Y., Mcginnis, S., and Madden, T. L. (2008). NCBI BLAST: a better web interface. *Nucleic Acids Res.* 36, W5–W9. doi: 10.1093/nar/gkn201

Lanquar, V., Lelievre, F., Bolte, S., Hames, C., Alcon, C., Neumann, D., et al. (2005). Mobilization of vacuolar iron by AtNRAMP3 and AtNRAMP4 is essential for seed germination on low iron. *EMBO J.* 24, 4041–4051. doi: 10.1038/sj.emboj.7600864

Lanquar, V., Ramos, M. S., Lelievre, F., Barbier-Brygoo, H., Krieger-Liszkay, A., Kramer, U., et al. (2010). Export of vacuolar manganese by AtNRAMP3 and AtNRAMP4 is required for optimal photosynthesis and growth under manganese deficiency. *Plant Physiol.* 152, 1986–1999. doi: 10.1104/pp.109.150946

Li, J. Y., Liu, J., Dong, D., Jia, X., Mccouch, S. R., and Kochian, L. V. (2014). Natural variation underlies alterations in Nramp aluminum transporter (NRAT1) expression and function that play a key role in rice aluminum tolerance. *Proc. Natl. Acad. Sci. U.S.A.* 111, 6503–6508. doi: 10.1073/pnas.1318975111

Lu, M., Wang, Z., Fu, S., Yang, G., Shi, M., Lu, Y., et al. (2017). Functional characterization of the SbNrat1 gene in sorghum. *Plant Sci.* 262, 18–23. doi: 10.1016/j.plantsci.2017.05.010

Mayrose, I., Graur, D., Ben-Tal, N., and Pupko, T. (2004). Comparison of site-specific rate-inference methods for protein sequences: empirical Bayesian methods are superior. *Mol. Biol. Evol.* 21, 1781–1791. doi: 10.1093/molbev/msh194

Nevo, Y., and Nelson, N. (2006). The NRAMP family of metal-ion transporters. *Biochim. Biophys. Acta* 1763, 609–620. doi: 10.1016/j.bbamcr.2006.05.007

Pottier, M., Oomen, R., Picco, C., Giraudat, J., Scholz-Starke, J., Richaud, P., et al. (2015). Identification of mutations allowing Natural Resistance Associated Macrophage Proteins (NRAMP) to discriminate against cadmium. *Plant J.* 83, 625–637. doi: 10.1111/tpj.12914

Robert, X., and Gouet, P. (2014). Deciphering key features in protein structures with the new ENDscript server. *Nucleic Acids Res.* 42, W320–W324. doi: 10.1093/nar/gku316

Roy, A., Kucukural, A., and Zhang, Y. (2010). I-TASSER: a unified platform for automated protein structure and function prediction. *Nat. Protoc.* 5, 725–738. doi: 10.1038/nprot.2010.5

Saitou, N., and Nei, M. (1987). The neighbor-joining method: a new method for reconstructing phylogenetic trees. *Mol. Biol. Evol.* 4, 406–425.

Sasaki, A., Yamaji, N., Yokosho, K., and Ma, J. F. (2012). Nramp5 is a major transporter responsible for manganese and cadmium uptake in rice. *Plant Cell* 24, 2155–2167. doi: 10.1105/tpc.112.096925

Shi, Y. (2013). Common folds and transport mechanisms of secondary active transporters. *Annu. Rev. Biophys.* 42, 51–72. doi: 10.1146/annurev-biophys-083012-130429

Takahashi, R., Ishimaru, Y., Senoura, T., Shimo, H., Ishikawa, S., Arao, T., et al. (2011). The OsNRAMP1 iron transporter is involved in Cd accumulation in rice. *J. Exp. Bot.* 62, 4843–4850. doi: 10.1093/jxb/err136

Tamura, K., Stecher, G., Peterson, D., Filipski, A., and Kumar, S. (2013). MEGA6: molecular evolutionary genetics analysis version 6.0. *Mol. Biol. Evol.* 30, 2725–2729. doi: 10.1093/molbev/mst197

Thomine, S., Wang, R., Ward, J. M., Crawford, N. M., and Schroeder, J. I. (2000). Cadmium and iron transport by members of a plant metal transporter family in Arabidopsis with homology to Nramp genes. *Proc. Natl. Acad. Sci. U.S.A.* 97, 4991–4996. doi: 10.1073/pnas.97.9.4991

Xia, J., Yamaji, N., Che, J., Shen, R. F., and Ma, J. F. (2014). Differential expression of Nrat1 is responsible for Al-tolerance QTL on chromosome 2 in rice. *J. Exp. Bot.* 65, 4297–4304. doi: 10.1093/jxb/eru201

Xia, J., Yamaji, N., Kasai, T., and Ma, J. F. (2010). Plasma membrane-localized transporter for aluminum in rice. *Proc. Natl. Acad. Sci. U.S.A.* 107, 18381–18385. doi: 10.1073/pnas.1004949107

Xu, H., Jin, J., Defelice, L. J., Andrews, N. C., and Clapham, D. E. (2004). A spontaneous, recurrent mutation in divalent metal transporter-1 exposes a calcium entry pathway. *PLoS Biol.* 2:E50. doi: 10.1371/journal.pbio.0020050

Yamaji, N., Sasaki, A., Xia, J. X., Yokosho, K., and Ma, J. F. (2013). A node-based switch for preferential distribution of manganese in rice. *Nat. Commun.* 4:2442. doi: 10.1038/ncomms3442

Zuckerkandl, E., and Pauling, L. (1965). "Evolutionary divergence and convergence in proteins," in *Evolving Genes and Proteins*, eds V. Bryson and H. J. Vogel (New York, NY: Academic Press), 97–166. doi: 10.1016/B978-1-4832-2734-4.50017-6

Conflict of Interest Statement: The authors declare that the research was conducted in the absence of any commercial or financial relationships that could be construed as a potential conflict of interest.

frontiers in Plant Science

ORIGINAL RESEARCH
published: 26 April 2018
doi: 10.3389/fpls.2018.00570

Functional Conservation and Divergence of Soybean GmSTOP1 Members in Proton and Aluminum Tolerance

Weiwei Wu[1], Yan Lin[1], Qianqian Chen[1], Wenting Peng[2], Junchu Peng[1], Jiang Tian[1], Cuiyue Liang[1] and Hong Liao[2]*

[1] *Root Biology Center, State Key Laboratory for Conservation and Utilization of Subtropical Agro-bioresources, South China Agricultural University, Guangzhou, China,* [2] *Root Biology Center, Fujian Agriculture and Forestry University, Fuzhou, China*

Proton (H^+) and aluminum (Al) rhizotoxicity are two major factors limiting crop production in acid soils. Orthologs of the zinc-finger transcription factor, Sensitive To Proton Rhizotoxicity1 (STOP1), have been found to play an essential role in the tolerance to both stresses by regulating the transcription of multiple H^+ and Al tolerant genes. In the present study, color three *GmSTOP1* homologs were identified in the soybean genome. All three *GmSTOP1* exhibited similar properties as reflected by the harboring of four potential zinc finger domains, localizing in the nucleus, and having transactivation activity. Expression profiling showed that H^+ stress slightly modulated transcription of all three *GmSTOP1*s, while Al significantly up-regulated *GmSTOP1-1* and *GmSTOP1-3* in root apexes and *GmSTOP1-3* in basal root regions. Furthermore, complementation assays in an Arabidopsis *Atstop1* mutant line overexpressing these *GmSTOP1*s demonstrated that all three GmSTOP1s largely reverse the H^+ sensitivity of the *Atstop1* mutant and restore the expression of genes involved in H^+ tolerance. In contrast, only GmSTOP1-1 and GmSTOP1-3 could partially recover Al tolerance in the *Atstop1* mutant. These results suggest that the function of three GmSTOP1s is evolutionarily conserved in H^+ tolerance, but not in Al tolerance.

Keywords: GmSTOP1, proton rhizotoxicity, Al rhizotoxicity, soybean, transcription factor

OPEN ACCESS

Edited by:
Jian Li Yang,
Zhejiang University, China

Reviewed by:
Meiya Liu,
Tea Research Institute (CAAS), China
Jiangfeng You,
Jilin University, China

****Correspondence:***
Cuiyue Liang
liangcy@scau.edu.cn

Specialty section:
This article was submitted to Plant Abiotic Stress, a section of the journal Frontiers in Plant Science

Received: *27 December 2017*
Accepted: *11 April 2018*
Published: *26 April 2018*

Citation:
Wu W, Lin Y, Chen Q, Peng W, Peng J, Tian J, Liang C and Liao H (2018) Functional Conservation and Divergence of Soybean GmSTOP1 Members in Proton and Aluminum Tolerance. Front. Plant Sci. 9:570. doi: 10.3389/fpls.2018.00570

INTRODUCTION

Agricultural production is limited on acid soils, which comprise approximately 50% of the world's potentially arable lands (von Uexküll and Mutert, 1995). There are several constraints limiting plant growth on acid soils, including deficiency of mineral nutrients, such as phosphorus (P), calcium (Ca), and magnesium (Mg), as well as, toxicity of excessive ions, including aluminum (Al^{3+}), hydrogen (H^+), and manganese (Mn^{2+}) (Ishitani et al., 2004).

Among these stresses, Al toxicity has been widely acknowledged as a major constraint on crop production (Kochian et al., 2004; Ma, 2007; Bojórquez-Quintal et al., 2017). The Al^{3+} ion can cause rapid and severe impairment of root apical development by damaging cell walls (Horst et al., 1999) and cytoskeletons (Chang et al., 1999; Sivaguru et al., 1999), disturbing DNA and plasma membrane processes (Elstner et al., 1988; Yamaguchi et al., 1999; Meriga et al., 2004), blocking

production of callose (Sivaguru et al., 2000), and impeding stress-signaling pathways (Ramos-Díaz et al., 2007). Consequently, plant root growth and nutrient acquisition are inhibited, which leads to significant reductions in crop yields (Ryan et al., 2001; Kochian et al., 2004; Ma, 2007; Bojórquez-Quintal et al., 2017).

Often combined with Al toxicity, H^+ rhizotoxicity has also been recognized as a major limiting factor for crop production on acid soils (Kochian et al., 2004). When exposed to strong acid conditions, plant root cells will be structurally and functionally damaged (Foy, 1984). For example, obviously swollen root hairs and cracks between cells in root meristems have been observed in Arabidopsis (Koyama et al., 1995, 2001; Iyer-Pascuzzi et al., 2011) and yorkshire-fog grass (*Holcus lanatus*) subjected to acid treatments (Kidd and Proctor, 2001). Moreover, a pH drop from 5.5 to 4.0 is associated with significant membrane depolarization, destruction of epidermal and cortical cells, and, ultimately, inhibition of root growth in *Lotus corniculatus* (Pavlovkin et al., 2009; Paláve-Balang et al., 2012). Similar symptom caused by proton rhizotoxicity have also been observed in many other plant species, such as alfalfa (*Medicago sativa*) (Yokota and Ojima, 1995), spinach (*Spinacia oleracea*) (Yang et al., 2005), common bean (*Phaseolus vulgaris*) (Rangel et al., 2005), and barley (*Hordeum vulgare*) (Song et al., 2011). Besides direct toxicity, low pH can also increase the solubility of other toxic ions, such as Al^{3+}, in soil, and thus adversely influence plant root growth. In this aspect, Al and H^+ toxicities are physiologically linked to one another.

Over the past few decades, mechanisms of plant tolerance to Al and H^+ rhizotoxicities have been elucidated in many studies. Among them, identification of the C2H2-type zinc finger transcription factor family, STOP1 (Sensitive to Proton Rhizotoxicity1), contributed considerably to understanding of regulatory mechanisms underlying the integration of Al and H^+ tolerance *in planta* (Iuchi et al., 2007; Yamaji et al., 2009; Ohyama et al., 2013; Sawaki et al., 2014; Fan et al., 2015).

The first *STOP1* gene, *AtSTOP1*, was identified in Arabidopsis (Iuchi et al., 2007). Transcriptome analyses and genetic characterization showed that AtSTOP1 regulates the expression of a set of genes, including three major Al tolerance genes, *AtALMT1* (*Aluminum activated Malate Transporter1*), *AtMATE* (*Multidrug and Toxic Compound Extrusion*), and *AtALS3* (*Aluminum Sensitive3*), along with other genes apparently involved in the regulation of cytosolic pH, such as *GAD1* (*Glutamate Decarboxylase1*), *ME1/2* (*Malic Enzyme1/2*), and *GDH1/2* (*Glutamate Dehydrogenase 1/2*) (Liu et al., 2009; Sawaki et al., 2009; Kobayashi et al., 2014). Interestingly, the STOP1 homolog AtSTOP2, which partially accounts for tolerance to Al and H^+ rhizotoxicities, is also regulated by AtSTOP1 (Kobayashi et al., 2014). Moreover, a STOP1 ortholog in rice bean (*Vigna umbellata*), *VuSTOP1*, was isolated by suppression subtractive hybridization (Fan et al., 2014). In contrast to the constitutive expression exhibited by *AtSTOP1*, the expression of *VuSTOP1* was inducible by both of Al and H^+ stresses (Fan et al., 2014). However, the assay of *planta* complementation in *Atstop1* mutant showed that VuSTOP1 could fully restore the transcription of several H^+-tolerance related genes, but only partially restores the expression of *AtMATE* and *ALS3*, indicating that VuSTOP1 might play a major role in H^+ tolerance, but only a minor role in Al tolerance (Fan et al., 2015). Similarly, other STOP1 homologs, including NtSTOP1 in tobacco (*Nicotiana tabacum*), LjSTOP1 in *Lotus japonicas*, PnSTOP1 in black poplar (*Populus nigra*), CsSTOP1 in tea (*Camellia sinensis*) and EguSTOP1 in *Eucalyptus* also reportedly possess similar functions in H^+ tolerance, and only partial or even no functionality in Al tolerance (Ohyama et al., 2013; Sawaki et al., 2014). On the other hand, the mutation of *ART1* (*Al Resistance Transcription Factor1*), a *STOP1* homolog in rice (*Oryza sativa*), appears to only affect Al hypersensitivity (Yamaji et al., 2009). In short, previous studies suggest that STOP1 transcription factors are ubiquitous in plants and have conserved functions in plant stress (Al and/or H^+) tolerance, though specific responses vary among plant species.

Soybean (*Glycine max*) is one of the most important leguminous crops globally, comprising approximately 68% of crop legume production in the world and 57% of the global oilseed production (Herridge et al., 2008). Though many studies have elucidated the functions of STOP1 orthologs in other plant species, no information is available on whether GmSTOP family members are also involved in H^+ and Al tolerance in soybean. In the present study, three GmSTOP1 homologs were isolated and characterized from soybean. The function of each *GmSTOP1* gene was analyzed in terms of Al and H^+ tolerance in Arabidopsis. The results demonstrate that all three *GmSTOP1*s play important roles in H^+ tolerance, while only GmSTOP1-1 and GmSTOP1-3 could partially recover Al tolerance in Arabidopsis *Atstop1* mutant. Taken together, these results strongly suggest that the three *GmSTOP1*s in soybean share evolutionary conservation of H^+ tolerance, but not of Al tolerance.

MATERIALS AND METHODS

Plant Material and Growth Conditions

The soybean genotype YC03-3 was chosen as the plant material in this study. Soybean seeds were germinated in paper rolls moistened with modified one-half-strength nutrient solution as previously described (Liang et al., 2013). The resultant seedlings were then gown in full strength nutrient solution for 24 h before being used for various treatments. For the low pH treatment, soybean seedlings were subjected to 0.5 mM $CaCl_2$ (pH 4.2) for 0, 2, 4, 6, and 12 h. After low pH treatment, root tips (0–2 cm) were harvested for gene expression assays. For the tissue specific expression experiment, soybean root tips (0–2 cm), which was further divided into two segments (0–1 cm and 1–2 cm), basal roots (>2 cm) and leaves were harvested after 4 h of Al (0 or 50 μM $AlCl_3$ in 0.5 mM $CaCl_2$, pH 4.2) treatment. For the Al dose experiment, soybean seedlings were treated with 0, 10, 50, and 100 μM $AlCl_3$ in 0.5 mM $CaCl_2$ solution (pH 4.2) for 4 h. For the time-course experiment, soybean seedlings were transplanted to Al (50 μM $AlCl_3$ in 0.5 mM $CaCl_2$, pH 4.2) treatments for 0, 2, 4, 6, and 12 h. In both of the concentration response experiment and time-course experiment, root tips (0–2 cm) were separately harvested for gene expression assays. All experiments had four biological replicates.

Phylogenetic Analysis and Characterization of GmSTOP1 Proteins in Soybean

TBLASTN analysis using the AtSTOP1 proteins sequence (accession number: Q9C8N5.1) as the query sequences was conducted at the Phytozome website[1]. Consequently, three STOP1 homologs with high similarity to AtSTOP1 were identified and designated as GmSTOP1-1 (Glyma10g35940), GmSTOP1-2 (Glyma16g27280), and GmSTOP1-3 (Glyma20g31650). Subsequently, multiple sequence alignment and phylogenetic tree construction were conducted using the deduced protein sequences of all three GmSTOP1s together with other STOP1 homologs, including AtSTOP1 from Arabidopsis, NtSTOP1 from tobacco, LjSTOP1 from *Lotus japonicas*, PnSTOP1 from black poplar (*Populus nigra*), CsSTOP1 from tea, EguSTOP1 from *Eucalyptus*, OsART1 from rice, PpSTOP1 from *Physcomitrella patens*, and TaSTOP1-A, TaSTOP1-B, TaSTOP1-D from wheat (*Triticum aestivum*). ClustalX2 and MEGA4.1 were used for the multiple sequence alignment and phylogenetic tree construction, respectively. The phylogenetic tree was constructed using the Neighbor-Joining method with 1,000 bootstrap replicates.

RNA Extraction and Quantitative Real-Time PCR

Total RNA was extracted from plant tissues using RNA-solve reagent (OMEGA Bio-Tek, Norcross, GA, United States). Genomic DNA in the RNA samples was eliminated with RNase-free DNase I (Invitrogen, Carlsbad, CA, United States). The resulting extracts were then used to conduct the reverse transcription via MMLV-reverse transcriptase (Promega, Madison, WI, United States) following the manufacturer's instructions. Subsequently, SYBR Green monitored qRT-PCR (quantitative real-time PCR) analysis was performed using a ABI Step-one Plus real-time PCR system (Thermo Fisher Scientific, Waltham, MA, United States). The primer pairs used for expression analysis are listed in Supplementary Table S1.

Subcellular Localization of GmSTOP1s

The full length cDNAs of the three identified *GmSTOP1* genes were amplified from first strand cDNA derived from soybean roots using gene specific primer pairs as listed in Supplementary Table S1. The PCR products were then cloned into the pMD18-T vector (Takara, Japan) for sequence confirmation.

Full-length cDNA of the three *GmSTOP1*s was fused with enhanced green fluorescent protein (GFP) to construct *35S::GmSTOP1s-GFP* plasmids. Each construct was introduced into tobacco (*Nicotiana tabacum*) leaf cells according to previously described methods (Liang et al., 2010; Liu et al., 2016). The *35S::GFP* construct was used as the control. Fluorescence signals of GFP were detected at 488 nm by confocal scanning microscope (LSM780; Zeiss, Germany).

[1]https://phytozome.jgi.doe.gov/pz/portal.html

Transcriptional Activation Activity of GmSTOP1s

Gene specific primers with terminal *Sfi*I and *Sal*I restriction sites were used to amplify full-length cDNA of GmSTOP1-1 and GmSTOP1-3, whereas, primers with *BamH*I and *Pst*I restriction sites were used to amplify full-length cDNA of GmSTOP1-2. Sequence fragments were digested by the corresponding restriction enzymes and inserted into the pGBKT7 vector (Clontech, Japan), producing *pGBKT7-GmSTOP1*s plasmids. The resultant plasmids and the *pGBKT7* empty vector were then transformed into yeast strain AH109. After verification by PCR, transformed AH109 cells were cultured on either SD-Trp or SD-His medium for 3 days. The yeast cells grown on SD-Trp were then printed onto filter paper moistened with X-gal solution. Subsequently, the filter paper was freeze-thawed with liquid nitrogen and moistened again with X-gal solution. The appearance of blue areas on the filter paper was used to determine β-galactosidase activity.

Complementation of GmSTOP1s in *Atstop1* Mutant Plants

The three identified *GmSTOP1*s were separately introduced into the modified *pBEGFP* binary vector under the control of a *35S CaMV* promoter to produce an over-expression construct that was then transformed into *A. tumefaciens* strain Gv3101. Subsequently, the constructs were transformed into Arabidopsis *Atstop1* mutant plants via the floral dip method (Clough and Bent, 1998). Two independent over-expression lines for each gene were verified by qRT-PCR and used for further analysis as complemented lines.

To investigate the functions of *GmSTOP1*s in resistance to H^+ and Al toxicity, wild type, *Atstop1* mutant and the complemented lines overexpressing *GmSTOP1* were germinated on solid Murashige and Skoog (MS) medium for 5 days. Uniform seedlings with ∼1.5 cm root lengths were transferred to modified 1/30 strength Hoagland nutrient solution (without $NH_4H_2PO_4$ and plus 1 mM $CaCl_2$) with different treatments as described (Fan et al., 2015). Control plants were grown in media with pH adjusted to 5.8, while treated plants were grown in low pH media (pH 4.7) or media containing 2 μM $AlCl_3$ (pH 5.0) for 7 days (Fan et al., 2015). Upon harvest, roots of each plant were scanned and analyzed in Image J (National Institutes of Health, United States). All experiments had four biological replicates, each of which contains two plants.

For analysis of H^+ and Al genes expression responses, uniform Arabidopsis seedlings were treated with 1/30 strength Hoagland nutrient solution containing 2 μM $AlCl_3$ (pH 5.0) and low pH (pH 4.7) for 24 h (Fan et al., 2015). All experiments were conducted in a growth incubator running a 24°C, 12h/22°C, 12 h day/night cycle. The whole roots were harvested for gene expression assays. The primer pairs of target genes for qRT-PCR analysis are listed in Supplementary Table S1. Arabidopsis *UBQ1* was used as housekeeping gene control to normalize the expression of the corresponding genes. All experiments had four biological replicates.

Statistical Analysis

All data were analyzed by Student's *t*-tests using SPSS 13.0 (SPSS Institute, Chicago, IL, United States).

RESULTS

Identification of STOP1 Homologs in Soybean

A homolog search resulted in retrieval of three STOP1 homologs in the soybean genome, which were named GmSTOP1-1 (Glyma.10G215200), GmSTOP1-2 (Glyma.16G156400) and GmSTOP1-3 (Glyma.20G176500) based on genome localization. A phylogenetic tree showed that the STOP1 homologs in dicots were differentiated from those in monocots (**Figure 1A**). Moreover, GmSTOP1-1 and GmSTOP1-3 present as duplicated pair and display high similarity with VuSTOP from rice bean, while GmSTOP1-2 clusters in another sub-clade with LjSTOP1 from *Lotus japonicus* (**Figure 1A**). Moreover, the deduced amino acid sequences of all three GmSTOP1s contain four putative C2H2 zinc finger domains that are highly conserved in STOP1 orthologs from other plant species (**Figure 1B**).

Subcellular Localization and Transcription Activation Activity of GmSTOP1s

To determine the subcellular localization of the three identified GmSTOP1s, *GmSTOP1-GFP* fusion constructs were assayed for transient expression in tobacco leaf cells. The results showed that control GFP fluorescence was detectable in both the nucleus and cytoplasm. In contrast, fluorescence derived from GmSTOP1-GFP constructs was exclusively localized within the nucleus (**Figure 2A**), strongly suggesting that the three GmSTOP1 members are all nucleus localized proteins.

Transcription activity of the three GmSTOP1 members was determined in a one-hybridization expression system in yeast. The results showed that the yeast strain AH109 transformed with either a *pGBKT7-GmSTOP1* or the *pGBKT7* empty vector could grow well on the SD-Trp medium (**Figure 2B**). However, only the three AH109 strains transformed with *pGBKT7-GmSTOP1*s grew well on the SD-His medium (**Figure 2B**). Furthermore, all three of the AH109 strains transformed with a *pGBKT7-GmSTOP1* showed high β-galactosidase activity as indicated by the blue color on filter paper using X-gal as a substrate (**Figure 2B**). Therefore, the ability of all three GmSTOP1 homologs to activate *lacZ* expression strongly suggests that each one functions as a transcription factor.

Expression Patterns of *GmSTOP1*s in Response to Al and Low pH Stress

Quantitative real-time PCR was used to analyze *GmSTOP1* expression patterns in soybean seedlings. Expression levels of the three *GmSTOP1*s were hardly affected by low pH stress during the 12 h treatment period (Supplementary Figure S2). On the other hand, transcriptional responses varied among the three *GmSTOP1* genes in response to Al stress. As shown in **Figure 3A**, transcription of *GmSTOP1-2* was not significantly affected after 4 h of Al treatment in any tissues, including root tips (0–2 cm), basal regions of roots (>2 cm) and leaves, (**Figure 3A**). In contrast to the constitutive expression of *GmSTOP1-2* in roots, transcript levels of *GmSTOP1-1* and *GmSTOP1-3* increased by more than 6- and 11-fold, respectively, in root tips after 4 h of Al treatment (**Figure 3A**). However, in root basal regions, only transcription of *GmSTOP1-3* increased by more than 1.7-fold in response to Al stress, while no detectable change was observed for *GmSTOP1-1*.

Dose-responses of *GmSTOP1*s to Al stress were further analyzed in soybean root tips after 4 h of Al treatment. Transcript accumulations of both *GmSTOP1-1* and *GmSTOP1-3* were strictly dependent on Al concentration in the medium (**Figure 3B**), with transcript abundances enhanced for both *GmSTOP1-1* and *GmSTOP1-3* in 50 and 100 μM Al treatments (**Figure 3B**). The expression of *GmSTOP1-2* was constitutively expressed at relatively high levels regardless the external Al concentrations (**Figure 3B**).

Results from time-course experiments showed that the expression of both *GmSTOP1-1* and *GmSTOP1-3* were quickly enhanced in response to Al stress by more than twofold after 2 h of Al treatment, and remained high over 12 h (**Figure 3C**). Meanwhile, the expression of *GmSTOP1-2* did not vary during the period of Al treatment (**Figure 3C**).

Functional Analysis of GmSTOP1s in the Arabidopsis *Atstop1* Mutant

In order to examine their functions in plant H^+ and Al tolerance, all three *GmSTOP1*s were overexpressed in the Arabidopsis *Atstop1* mutant. The expression of all three of the *GmSTOP1* genes in the *Atstop1* mutant was verified by qRT-PCR. Under normal growth conditions, no significant differences were observed among wild type, *Atstop1* mutant and complemented lines overexpressing any of the *GmSTOP1*s (**Figures 4A,B**). However, under low pH condition (pH 4.7), root elongation of wild type and *Atstop1* mutant was inhibited by 51% and 80%, respectively (**Figures 4A,C**). In each of two complemented lines of *GmSTOP1-1* (#5 and #6), *GmSTOP1-2* (#12 and #15) and *GmSTOP1-3* (#47 and #54), root elongation was inhibited much less than that of the *Atstop1* mutant (**Figures 4A,C**). These results suggest that all three *GmSTOP1*s are able to confer H^+ tolerance in *Atstop1* mutant plants.

Addition of Al to the low pH culture solution slightly decreased root elongation of wild type plants, but significantly inhibited root elongation of *Atstop1* mutants as indicated by a 90% decrease in root elongation compared to root elongation in wild type plants (**Figures 4A,D**). Unlike the role of *GmSTOP1*s in H^+ tolerance, the functions of *GmSTOP1*s in Al tolerance varied. Each of the lines complemented with *GmSTOP1-1* (#5 and #6) and *GmSTOP1-3* (#47 and #54) overexpression recovered elongation to 28% and 32%, and 29% and 19% of that of wild type, respectively (**Figures 4A,D**). In contrast, lines complemented with *GmSTOP1-2* overexpression

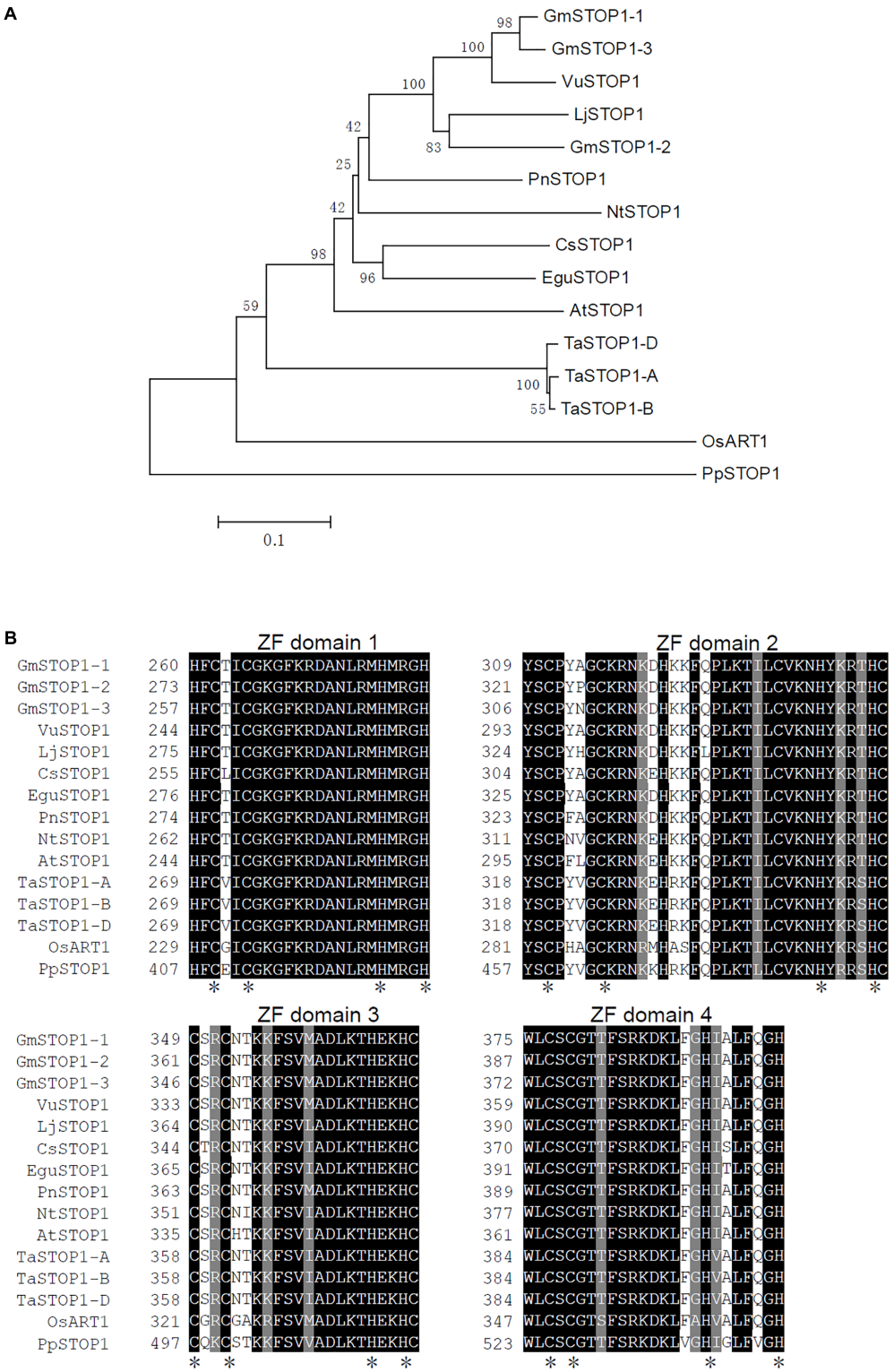

FIGURE 1 | Phylogenetic tree and amino acid alignments of predicted C_2H_2 zinc finger domains in plant STOP1s. **(A)** Phylogenetic tree was generated based on an amino-acid alignment with STOP1 orthologs from several plant species. **(B)** Alignment of the amino acid sequences of predicted C2H2 zinc finger domains in STOP1 proteins. Black background indicates identical residues. Asterisks indicate conserved Cys and His residues of C2H2 motifs. The plant STOP1 proteins aligned include representatives from *Glycine max* (GmSTOP1-1, XP_006588359.1; GmSTOP1-2, XP_006598713.1; GmSTOP1-3, XP_014628358.1), *Arabidopsis thaliana* (AtSTOP1, NP_174697.1), *Nicotiana tabacum* (NtSTOP1, AB811781), *Lotus japonicus* (LjSTOP1, BAN67817.1), *Vigna umbellata* (VuSTOP1, KP637172), *Camellia sinensis* (CsSTOP1, BAN67815.1), *Populus nigra* (PnSTOP1, BAN67813.1), *Eucalyptus* (EguSTOP1, BAO56822.1), *Triticum aestivum* (TaSTOP1-A, AGS15201.1; TaSTOP1-B, AGS15202.1; TaSTOP1-D, AGS15195.1), *Oryza sativa* (OsART1, AB379846), and *Physcomitrella patens* (PpSTOP1, BAN67814.1).

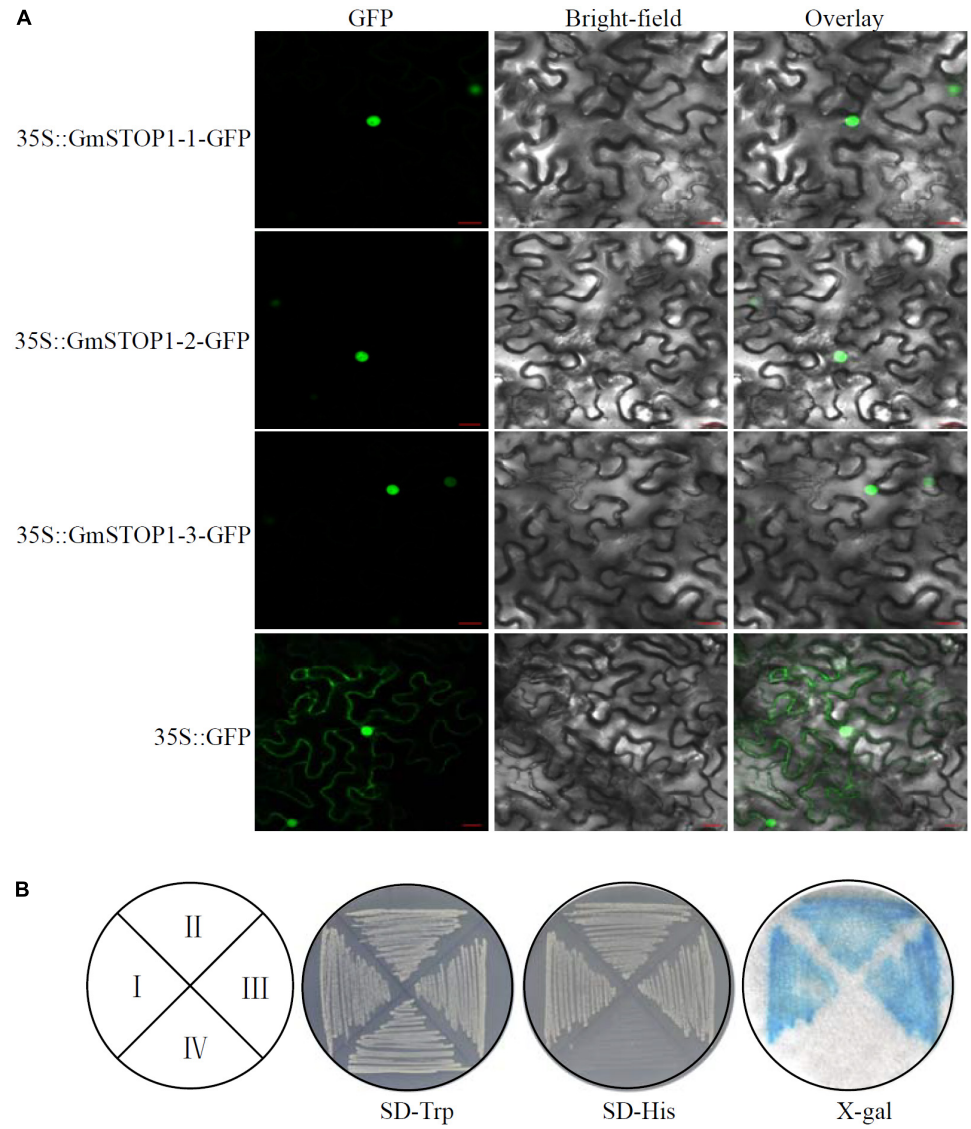

FIGURE 2 | Subcellular localization and transactivation assay of GmSTOP1s. **(A)** *35S::GmSTOP1*s-*GFP* and *35S::GFP* (control) constructs were introduced individually into *Nicotiana benthamiana* leaves. Scale bars: 20 μm. **(B)** Transactivation assay of GmSTOP1-1 (I), GmSTOP1-2 (II), GmSTOP1-3 (III), and control (IV). β-galactosidase activity is indicated by blue color on the filter paper using X-gal as the substrate.

did not recover root elongation. These results indicate that *GmSTOP1-1* and *GmSTOP1-3*, but not *GmSTOP1-2* can partially reverse the Al hypersensitivity of *Atstop1* mutant plants.

Transcription of STOP1 Down-Stream Genes in *GmSTOP1* Complemented *Atstop1* Mutants

The differential contributions of *GmSTOP1*s to H^+ and Al tolerance were further determined by investigating the transcript levels of several related down-stream genes in *GmSTOP1* complemented *Atstop1* mutants. The results showed that expression of several H^+ tolerance genes were significantly restored in all of the complemented *Atstop1* mutant lines (**Figure 5**). Among responsive genes, the expression of *GDH2* (At5g07440) was restored the most, with transcription returning to at least 50% of transcript levels in WT plants (**Figure 5**). Although restored to lesser extents, the expression of three other H^+ tolerance genes, *GDH1* (At5g18170), *GABA-T* (At3g22200) and *NADP-malate enzyme* 2 (*NADP-ME2*), was restored nonetheless by 37, 25, and 20%, respectively, over expression in the *Atstop1* mutant (**Figure 5**).

Unlike expression patterns of H^+ tolerance related genes, expression responses of Al tolerance related genes varied among *GmSTOP1* complemented lines. These Al tolerance related genes included *pectin methylesterase inhibitor superfamily protein* (*PMI*, *At2g45220*), *AtTDT* (At5g47560), *NADP-ME2* (At5g11670), and

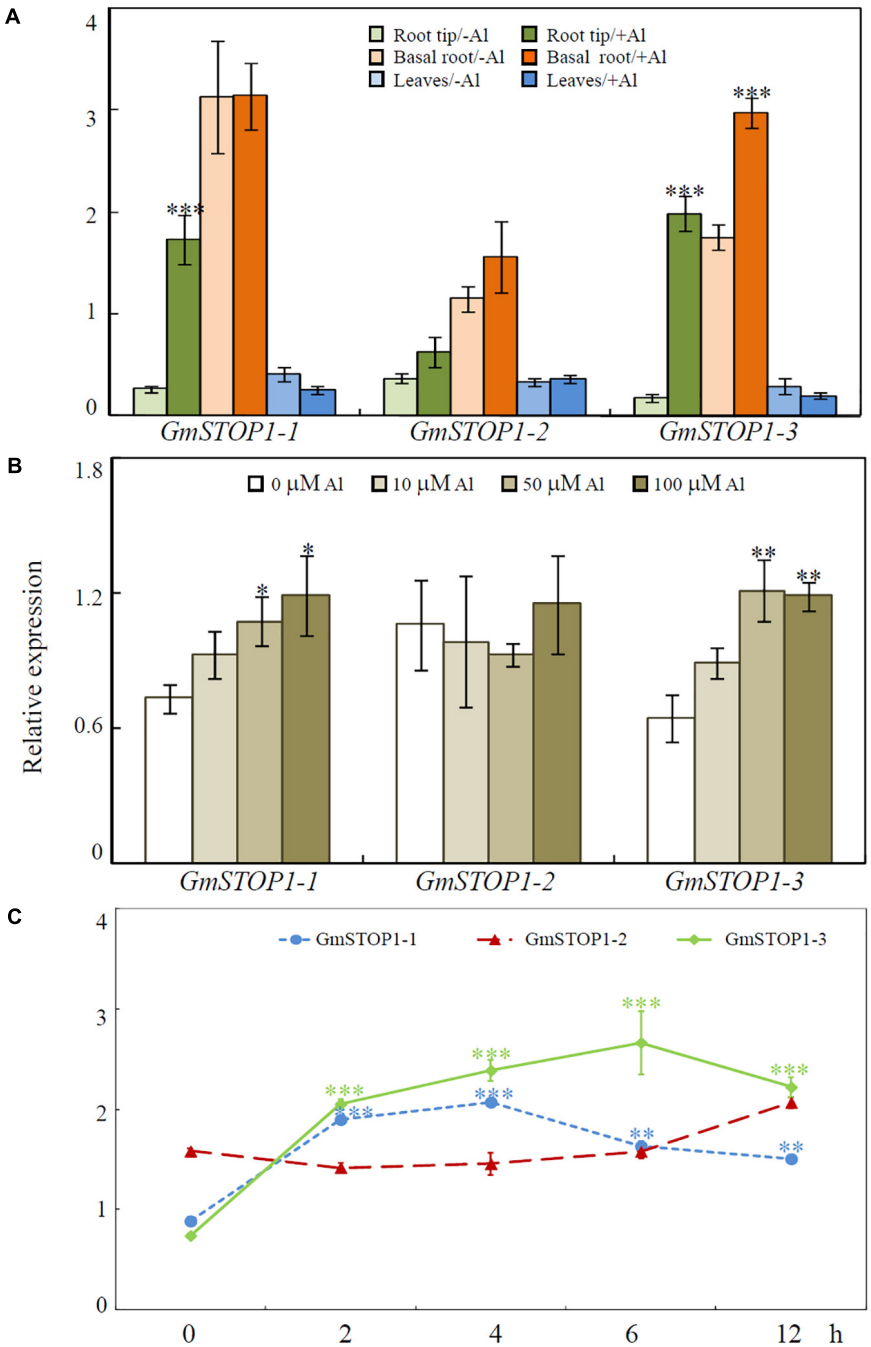

FIGURE 3 | Expression patterns of *GmSTOP1*s in response to Al toxicity. **(A)** Relative expression of *GmSTOP1*s in root tips (0–2 cm), basal roots (>2 cm) and leaves after 4 h of –Al (0 μM) or +Al (50 μM) treatment. **(B)** Relative expression of *GmSTOP1*s in soybean root tips (0–2 cm) treated with different concentrations of Al for 4 h. **(C)** Relative expression of *GmSTOP1*s in soybean roots tips (0–2 cm) in response to Al (50 μM) for different treatment times. Asterisks indicate significant differences between the +Al treatment and –Al control (*0.01 < *P* < 0.05; **0.001 < *P* < 0.01; ***$P < 0.001$).

AtMATE (At1g51340). In both *GmSTOP1-1* and *GmSTOP1-3* complemented lines, the expression of *AtPMI*, *AtTDT*, *NADP-ME2,* and *AtMATE* were partially restored. Yet, in *GmSTOP1-2* complemented lines, the expression of each of these four genes was not affected relative to expression in *Atstop1* mutants (**Figure 5**).

DISCUSSION

Proton and Al rhizotoxicities are two of the major constraints of plant growth and development on acid soil (Kochian et al., 2004). Plants have adapted to these stresses by developing a variety of coping strategies involving a number of genes (Liu

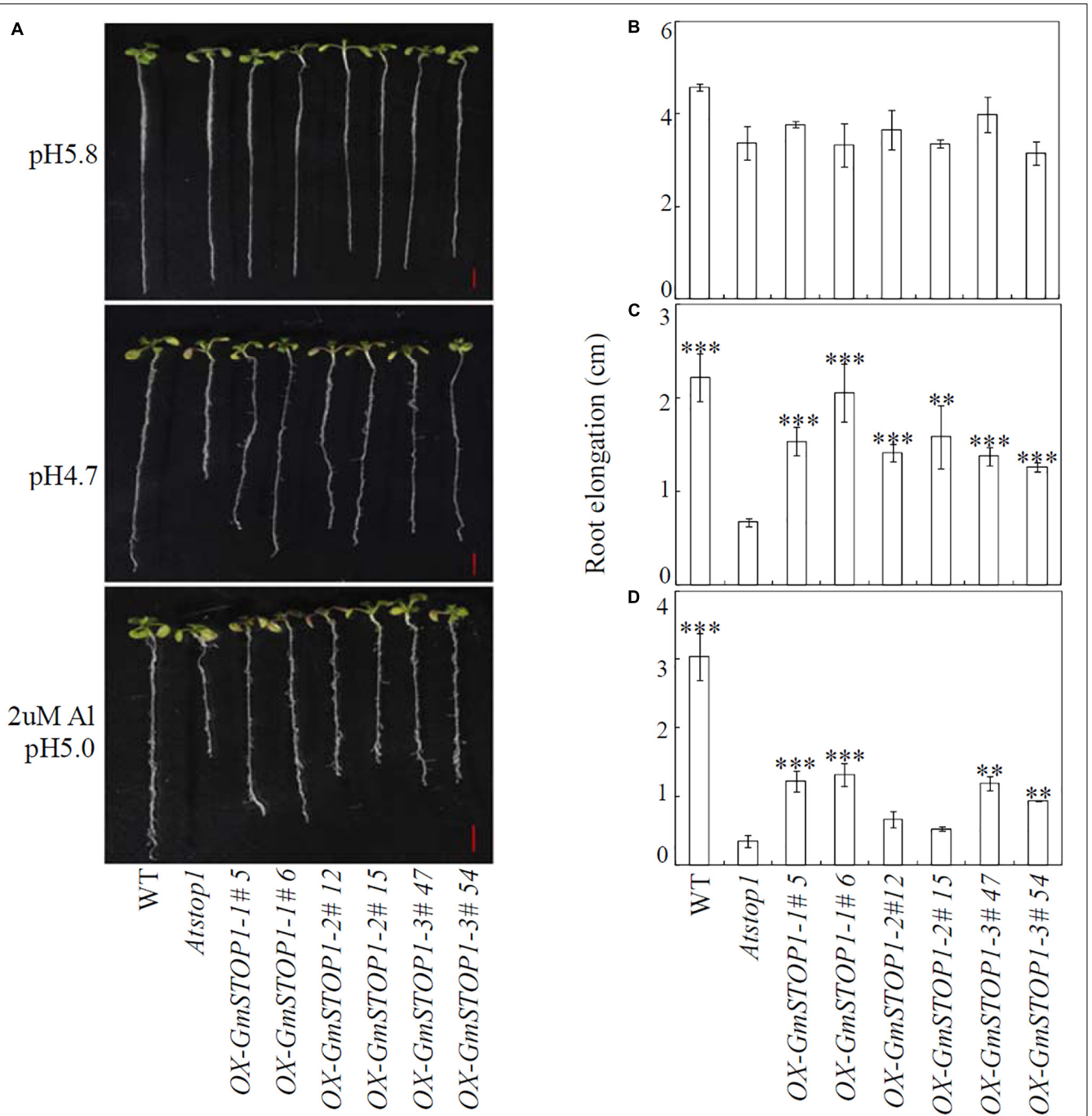

FIGURE 4 | Effects of low pH and Al stresses on the growth of Arabidopsis *Atstop1* mutant plants overexpressing *GmSTOP1*s. Uniform seedlings with ∼1.5 cm root lengths were treated with low pH (pH 4.7) and Al stresses (2 μM Al and pH 5.0) for 7 days. The phenotypes of wild-type (WT), *Atstop1* and *GmSTOP1* overexpressing *Atstop1* lines in response to H^+ and Al were photographed **(A)**. Root elongation for each line was measured under control **(B)**, low pH **(C)**, and Al **(D)** treatments. Each bar represents the mean of four biological replicates with standard error. Asterisks indicate significant differences in comparison to the *Atstop1* mutant (*$0.01 < P < 0.05$; **$0.001 < P < 0.01$; ***$P < 0.001$). Scale bars: 5 mm.

et al., 2014; Kochian et al., 2015). Recent studies have revealed that H^+ and Al tolerance mechanisms are regulated by STOP1 transcription factors in many plant species (Iuchi et al., 2007; Sawaki et al., 2009, 2014; Yamaji et al., 2009; Garcia-Oliveira et al., 2013; Ohyama et al., 2013; Fan et al., 2015). However, few studies have attempted to systematically dissect the possible roles of all STOP1 members in a single species responding to H^+ stress, Al toxicity, or both.

In the present study, a total of three *GmSTOP1* genes were identified in the soybean genome. All of these GmSTOP1

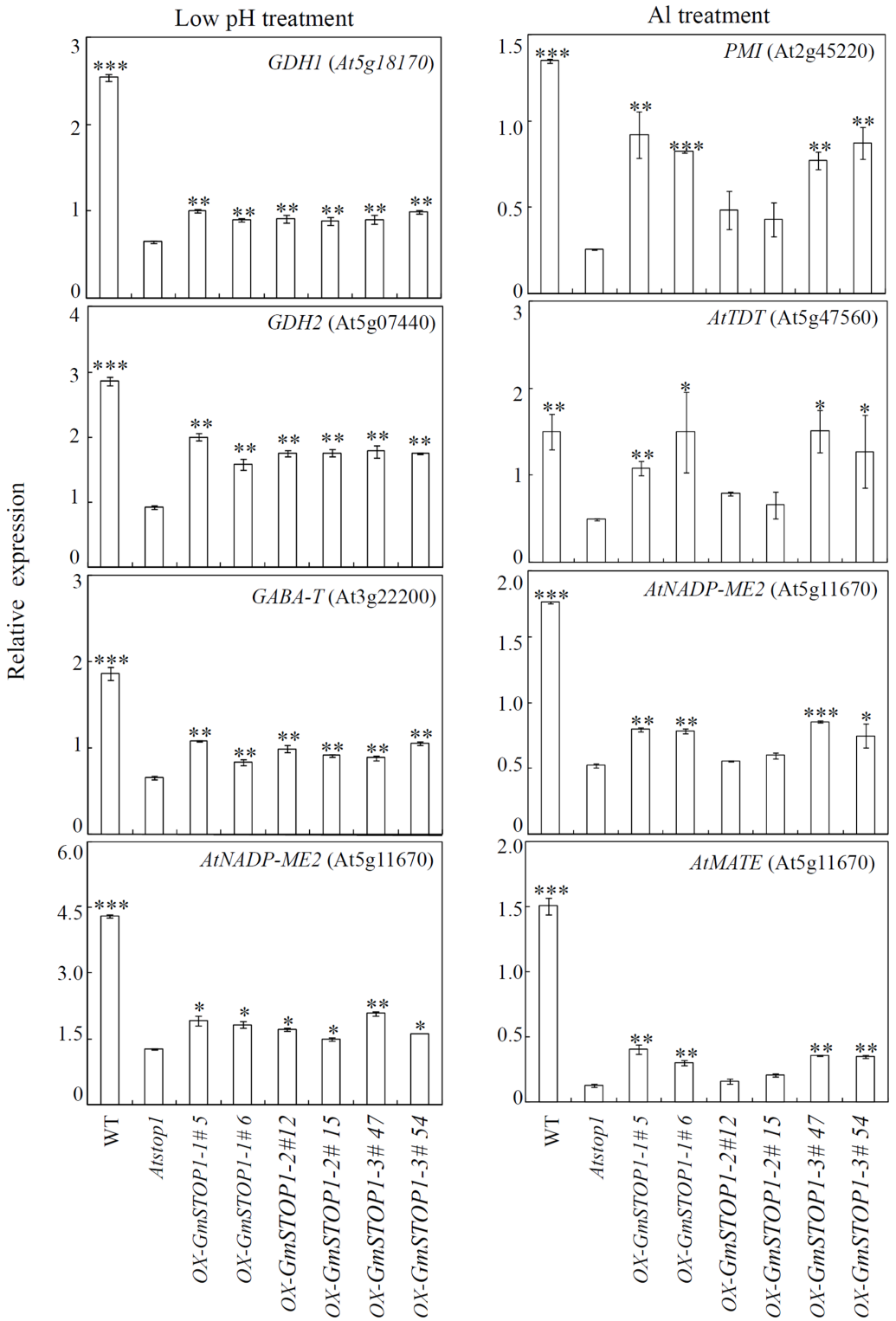

FIGURE 5 | Transcriptional accumulation of genes regulated by *GmSTOP1*s under low pH and Al stresses. Wild-type (WT), *Atstop1* mutant and complemented lines overexpressing *GmSTOP1-1* (#5 and #6), *GmSTOP1-2* (#12 and #15), and *GmSTOP1-3* (#47 and #54) were exposed to low pH (pH 4.7) and Al treatments ($AlCl_3$: 2 μM; pH 5.0) for 24 h. Transcript abundances of *GDH1*, *GDH2*, *GABA-T* and *AtNADP-ME2* were quantified from plants grown in the low pH treatment, while expression levels of *PMI* (At2g45220), *AtTDT* (At5g47560), *AtNADP-ME2* (At5g11670), and *AtMATE* (At1g51340) were quantified in Al treated samples. UBQ1 transcript levels were used as the internal standard. Data are expressed as means of four replicates. Asterisks indicate significant differences in comparison to the *Atstop1* mutant (*$0.01 < P < 0.05$; **$0.001 < P < 0.01$; ***$P < 0.001$).

homologs are localized to the nucleus, and exhibit transcription activity (**Figure 2**). Sequence analysis revealed that GmSTOP1-2 is phylogenetically distinct from GmSTOP1-1 and GmSTOP1-3, which appear to be a duplicated pair (**Figure 1**). As gene duplication provides opportunities for functional divergence (Force et al., 1999; Lynch et al., 2001; Flagel and Wendel, 2009; Libault et al., 2010; Schmutz et al., 2010), we hypothesize that the three *GmSTOP1* genes might have divergent functions in regard to H^+ and Al tolerance even though they are highly conserved in some features (**Figures 1**, **2**).

To dissect the differential contributions of *GmSTOP1*s in H^+ tolerance, expression analysis was conducted. The results showed that similar to *AtSTOP1* in Arabidopsis (Iuchi et al., 2007), all three *GmSTOP1* genes were constitutively expressed and hardly affected by H^+ treatment (Supplementary Figure S2). Further complementation assays showed that all three *GmSTOP1* genes are able to confer H^+ tolerance to the Arabidopsis *Atstop1* mutant (**Figure 4C**). These results are consistent with the previous studies reporting that *STOP1* orthologs in dicots are able to confer H^+ tolerance to the H^+ sensitive *Atstop1* mutant (Ohyama et al., 2013; Sawaki et al., 2014; Fan et al., 2015). Furthermore, the H^+ hypersensitivity of the *Atstop1* mutant is the result of down-regulation of genes in several pH regulation pathways caused by the dysfunction of AtSTOP1 (Sawaki et al., 2009).

The expression of several H^+ tolerance genes, including *STOP2, CIPK23,* and *PGIP1*, has been restored *in planta* in complementation assays of *Atstop1* by *STOP1* orthologs from rice bean (*VuSTOP1*), *Eucalyptus* (*EguSTOP1*), tobacco (*NtSTOP1*), black poplar (*PnSTOP1*), tea (*CsSTOP1*), *Lotus japonicus* (*LjSTOP1*), or *Physcomitrella patens* (PpSTOP1) (Ohyama et al., 2013; Sawaki et al., 2014; Fan et al., 2015). However, none of these genes were affected by complementation with any of the *GmSTOP1* homologs in the *Atstop1* mutant (Supplementary Figure S4). Instead, *GmSTOP1* complementation restored the transcription of several other H^+ tolerance relative genes, including *GDH1*, *GDH2*, *GABA-T,* and *AtNADP-ME2*, which are considered to play roles in maintaining pH homeostasis in plants. For example, *AtNADP-ME2* has been reported to function in the pH stat pathway through consumption of cytosolic H^+ (Roberts et al., 1992; Sakano, 1998). Meanwhile, *GDH1*, *GDH2* and *GABA-T* are the major isoforms in the "GABA shunt" pathway, which contributes largely to cytosolic pH homeostasis in plant cells (Crawford et al., 1994; Bown and Shelp, 1997). These results strongly suggest that all three *GmSTOP1* homologs participate in conserved functions in H^+ tolerance mainly through regulation of similar pH stat pathways that are distinct from the pH stat pathways regulated by other plant *STOP1* orthologs (Ohyama et al., 2013; Sawaki et al., 2014; Fan et al., 2015).

Interestingly, in the presence of Al, expression of both *GmSTOP1-1* and *GmSTOP1-3* quickly escalated in root tips, while expression of *GmSTOP1-2* was not significantly affected (**Figure 3** and Supplementary Figure S3). Similar results have also been reported for bread wheat, in which expression of *TaSTOP1-A* was found to be responsive to H^+ and Al stresses and divergent from the responses of *TaSTOP1-B* and *TaSTOP1-D* (Garcia-Oliveira et al., 2013). It has been suggested that this divergence might be mainly due to the presence of a pyrimidine-rich stretch and the absence of a light responsive element in the 5′ UTR of TaSTOP1-A compared to its homologs TaSTOP1-B and TaSTOP1-D (Garcia-Oliveira et al., 2013). Consistent with this, our investigation revealed that the 5′-UTR is more similar between *GmSTOP1-1* and *GmSTOP1-3* than it is between either of these genes and *GmSTOP1-2* (Supplementary Figure S1). Therefore, there is a possibility that the differential expression between *GmSTOP1-2* and the other two *GmSTOP1*s in response to Al stress might be due to divergence in the 5′-UTR. Thereby, divergence between *GmSTOP1-2* and the other two *GmSTOP1*s in both transcriptional regulation and protein sequence further suggests that *GmSTOP1-2* functions differently than *GmSTOP1-1* and *GmSTOP1-3* in Al tolerance responses.

Even more evidence in support of divergence among *GmSTOP1*s in Al tolerance functionality was gathered in complementation assays (**Figure 4**). The results strongly indicate that *GmSTOP1-1* and *GmSTOP1-3* are involved at least partially in *AtSTOP1* related Al tolerance responses, whereas GmSTOP1-2 is not. It has been reported that AtSTOP1 regulates transcription of three major Al tolerance genes in Arabidopsis, namely *AtALMT1*, *ALS3,* and *AtMATE* (Kobayashi et al., 2007; Liu et al., 2009; Sawaki et al., 2009; Tokizawa et al., 2015). Among them, *AtALMT1* accounts for more than 70% of the Al tolerance phenotype in Arabidopsis (Iuchi et al., 2007; Liu et al., 2012). In the current study, it was interesting to find that none of the *GmSTOP1* homologs restores the expression of *AtALMT1* or *ALS3* in the *Atstop1* mutant, while *AtMATE* expression was recovered slightly in both *GmSTOP1-1* and *GmSTOP1-3* complemented lines, but not in *GmSTOP1-2* complemented lines (**Figure 5** and Supplementary Figure S4). Similar results were also reported in other plant species, where most STOP1 orthologs are not able to restore the expression of all three Al tolerance genes in the *Atstop1* mutant. For example, LjSTOP1, CsSTOP1, and PnSTOP1 can slightly restore the expression of *AtALMT1*, but not the expression of *ALS3* or *AtMATE*, while VuSTOP1 can partially restore the expression of *ALS3* and *AtMATE*, but not the expression of *AtALMT1* (Ohyama et al., 2013; Fan et al., 2015). Placing the current results in the context of previous reports suggests that the regulatory functions of *AtSTOP1* in Al tolerance is not entirely conserved among plant *STOP1* orthologs.

Potential phenotypic effects of GmSTOP1-1/GmSTOP1-3 in the *Atstop1* mutant in response to Al toxicity are revealed by considering functions of *PMI*, *AtTDT,* and *NADP-ME2*, which are down-regulated in *Atstop1* mutants subjected to Al stress (Sawaki et al., 2009), and which had expression restored in the complementation experiments herein. Members of the PMI family have been reported to inhibit pectin methylesterase activity, and thereby increasing Al tolerance (Sénéchal et al., 2015; Geng et al., 2017). The other two genes, *AtTDT* and *NADP-ME2*, are involved in malate homeostasis and metabolism in the vacuole and cytosol, respectively (Hurth et al., 2005; Badia et al., 2015). Results in the present study showed that all of these genes were partially restored in both

GmSTOP1-1 and *GmSTOP1-3* complemented lines, but not in *GmSTOP1-2* complemented lines (**Figure 5**). These expression responses are in accord with the variation in Al tolerance observed among *GmSTOP1*s complemented lines (**Figure 4D**). Therefore, it appears that GmSTOP1-1/GmSTOP1-3 might function in Al tolerance through the regulation of cell wall modifications and malate metabolism.

Overall, the present study identifies three *GmSTOP1* homologs in the soybean genome, all of which localize in the nucleus and have the transactivation potential. Complementation assays suggest that all three *GmSTOP1* homologs play major roles in H^+ tolerance through transcriptional regulation of H^+ tolerance genes, whereas, only GmSTOP1-1 and GmSTOP1-3 function in Al tolerance. Taken together, the results herein suggest that the functions of the three identified *GmSTOP1*s are evolutionarily conserved in H^+ tolerance responses, but not in Al tolerance responses.

AUTHOR CONTRIBUTIONS

WW, YL, QC, WP, JP, and CL performed the experiments and collected the data. CL, JT, and HL designed the research, analyzed the data, and wrote the manuscript.

FUNDING

This work was supported by grants from National Natural Science Foundation of China (31672220 and 31422046), the National Key Research and Development Program (2016YFD0100700), Guangdong Natural Science Funds for Distinguished Young Scholars (2015A030306034), Guangdong High-level Personnel of Special Support Program (2015TQ01N078, 2015TX01N042, and YQ201530) and Research Team Project of the Natural Science Foundation of Guangdong Province (2016A030312009).

ACKNOWLEDGMENTS

The authors thank Dr. Thomas Walk of Golden Fidelity LLC for critical reading.

SUPPLEMENTARY MATERIAL

The Supplementary Material for this article can be found online at: https://www.frontiersin.org/articles/10.3389/fpls.2018.00570/full#supplementary-material

REFERENCES

Badia, M. B., Arias, C. L., Tronconi, M. A., Maurino, V. G., Andreo, C. S., Drincovich, M. F., et al. (2015). Enhanced cytosolic NADP-ME2 activity in *A. thaliana* affects plant development, stress tolerance and specific diurnal and nocturnal cellular processes. *Plant Sci.* 240, 193–203. doi: 10.1016/j.plantsci.2015.09.015

Bojórquez-Quintal, E., Escalante-Magaña, C., Echevarría-Machado, I., and Martínez-Estévez, M. (2017). Aluminum, a friend or foe of higher plants in acid soils. *Front. Plant Sci.* 8:1767. doi: 10.3389/fpls.2017.01767

Bown, A. W., and Shelp, B. J. (1997). The metabolism and functions of g-aminobutyric acid. *Plant Physiol.* 115, 1–5. doi: 10.1104/pp.115.1.1

Chang, Y. C., Yamamoto, Y., and Matsumoto, H. (1999). Accumulation of aluminium in the cell wall pectin in cultured tobacco (*Nicotiana tabacum* L.) cells treated with a combination of aluminium and iron. *Plant Cell Environ.* 22, 1009–1017. doi: 10.1046/j.1365-3040.1999.00467.x

Clough, S. J., and Bent, A. F. (1998). Floral dip: a simplified method for Agrobacterium-mediated transformation of *Arabidopsis thaliana*. *Plant J.* 16, 735–743. doi: 10.1046/j.1365-313x.1998.00343.x

Crawford, L. A., Bown, A. W., Breitkreuz, K. E., and Guinel, F. C. (1994). The synthesis of g-aminobutyric acid in response to treatments reducing cytosolic pH. *Plant Physiol.* 104, 865–871. doi: 10.1104/pp.104.3.865

Elstner, E. F., Wagner, G. A., and Schutz, W. (1988). Activated oxygen in green plants in relation to stress situations. *Curr. Top. Plant Biochem. Physiol.* 7, 159–187.

Fan, W., Lou, H. Q., Gong, Y. L., Liu, M. Y., Cao, M. J., Liu, Y., et al. (2015). Characterization of an inducible C2H2-type zinc finger transcription factor VuSTOP1 in rice bean (*Vigna umbellata*) reveals differential regulation between low pH and aluminum tolerance mechanisms. *New Phytol.* 208, 456–468. doi: 10.1111/nph.13456

Fan, W., Lou, H. Q., Gong, Y. L., Liu, M. Y., Wang, Z. Q., Yang, J. L., et al. (2014). Identification of early Al-responsive genes in rice bean (*Vigna umbellata*) roots provides new clues to molecular mechanisms of Al toxicity and tolerance. *Plant Cell Environ.* 37, 1586–1597. doi: 10.1111/pce.12258

Flagel, L. E., and Wendel, J. F. (2009). Gene duplication and evolutionary novelty in plants. *New Phytol.* 183, 557–564. doi: 10.1111/j.1469-8137.2009.02923.x

Force, A., Lynch, M., Pickett, F. B., Amores, A., Yan, Y. L., and Postlethwait, J. (1999). Preservation of duplicate genes by complementary, degenerative mutations. *Genetics* 151, 1531–1545.

Foy, C. D. (1984). "Physiological effects of hydrogen, aluminium and manganese toxicities in acid soil," in *Soil Acidity and Liming*, 2nd Edn, ed. F. Adams (Madison, WI: American Society of Agronomy), 57–97.

Garcia-Oliveira, A. L., Benito, C., Prieto, P., de Andrade Menezes, R., Rodrigues-Pousada, C., Guedes-Pinto, H., et al. (2013). Molecular characterization of TaSTOP1 homoeologues and their response to aluminium and proton (H+) toxicity in bread wheat (*Triticum aestivum* L.). *BMC Plant Biol.* 13:134. doi: 10.1186/1471-2229-13-134

Geng, X., Horst, W. J., Golz, J. F., Lee, J. E., Ding, Z., and Yang, Z. B. (2017). LEUNIG_HOMOLOG transcriptional co-repressor mediates aluminium sensitivity through PECTIN METHYLESTERASE46-modulated root cell wall pectin methylesterification in Arabidopsis. *Plant J.* 90, 491–504. doi: 10.1111/tpj.13506

Herridge, D. F., Peoples, M. B., and Boddey, R. M. (2008). Global inputs of biological nitrogen fixation in agricultural systems. *Plant Soil* 311, 1–18. doi: 10.1007/s11104-008-9668-3

Horst, W. J., Schmoh, N., Kollmeier, M., Baluška, F., and Sivaguru, M. (1999). Does aluminium affect root growth of maize through interaction with the cell wall-plasma membrane-cytoskeleton continuum? *Plant Soil* 215, 163–174. doi: 10.1023/A:1004439725283

Hurth, M. A., Suh, S. J., Kretzschmar, T., Geis, T., Bregante, M., Gambale, F., et al. (2005). Impaired pH homeostasis in Arabidopsis lacking the vacuolar dicarboxylate transporter and analysis of carboxylic acid transport across the tonoplast. *Plant Physiol.* 137, 901–910. doi: 10.1104/pp.104.058453

Ishitani, M., Rao, I., Wenzl, P., Beebe, S., and Tohme, J. (2004). Integration of genomics approach with traditional breeding towards improving abiotic stress adaptation: drought and aluminum toxicity as case studies. *Field Crop Res.* 90, 35–45. doi: 10.1016/j.fcr.2004.07.004

Iuchi, S., Koyama, H., Iuchi, A., Kobayashi, A., Kitabayashi, S., Kobayashi, Y., et al. (2007). Zinc finger protein STOP1 is critical for proton tolerance in Arabidopsis and coregulates a key gene in aluminum tolerance. *Proc. Natl. Acad. Sci. U.S.A.* 104, 9900–9905. doi: 10.1073/pnas.0700117104

Iyer-Pascuzzi, A. S., Jackson, T., Cui, H., Petricka, J. J., Busch, W., Tsukagoshi, H., et al. (2011). Cell identity regulators link development and stress responses in the Arabidopsis root. *Dev. Cell* 21, 770–782. doi: 10.1016/j.devcel.2011.09.009

Kidd, P. S., and Proctor, J. (2001). Why plants grow poorly on very acid soils: are ecologists missing the obvious? *J. Exp. Bot.* 52, 791–799. doi: 10.1093/jexbot/52.357.791

Kobayashi, Y., Hoekenga, O. A., Itoh, H., Nakashima, M., Saito, S., Shaff, J. E., et al. (2007). Characterization of AtALMT1 expression in aluminum-inducible malate release and its role for rhizotoxic stress tolerance in Arabidopsis. *Plant Physiol.* 145, 843–852. doi: 10.1104/pp.107.102335

Kobayashi, Y., Ohyama, Y., Kobayashi, Y., Ito, H., Iuchi, S., Fujita, M., et al. (2014). STOP2 activates transcription of several genes for Al- and low pH-tolerance that are regulated by STOP1 in Arabidopsis. *Mol. Plant* 7, 311–322. doi: 10.1093/mp/sst116

Kochian, L. V., Hoekenga, O. A., and Piñeros, M. A. (2004). How do crop plants tolerate acid soils? Mechanisms of aluminum tolerance and phosphorus efficiency. *Annu. Rev. Plant Biol.* 55, 459–493. doi: 10.1146/annurev.arplant.55.031903.141655

Kochian, L. V., Piñeros, M. A., Liu, J., and Magalhaes, J. V. (2015). Plant adaptation to acid soils: the molecular basis for crop aluminum resistance. *Annu. Rev. Plant Biol.* 66, 571–598. doi: 10.1146/annurev-arplant-043014-114822

Koyama, H., Toda, T., and Hara, T. (2001). Brief exposure to low-pH stress causes irreversible damage to the growing root in *Arabidopsis thaliana*: pectin–Ca interaction may play an important role in proton rhizotoxicity. *J. Exp. Bot.* 52, 361–368.

Koyama, H., Toda, T., Yokota, S., Zuraida, D., and Hara, T. (1995). Effects of aluminium and pH on root growth and cell viability in *Arabidopsis thaliana* strain Landsberg in hydroponic culture. *Plant Cell Physiol.* 36, 201–205.

Liang, C., Piñeros, M. A., Tian, J., Yao, Z., Sun, L., Liu, J., et al. (2013). Low pH, aluminum, and phosphorus coordinately regulate malate exudation through GmALMT1 to improve soybean adaptation to acid soils. *Plant Physiol.* 161, 1347–1361. doi: 10.1104/pp.112.208934

Liang, C., Tian, J., Lam, H. M., Lim, B. L., Yan, X., and Liao, H. (2010). Biochemical and molecular characterization of PvPAP3, a novel purple acid phosphatase isolated from common bean enhancing extracellular ATP utilization. *Plant Physiol.* 152, 854–865. doi: 10.1104/pp.109.147918

Libault, M., Farmer, A., Joshi, T., Takahashi, K., Langley, R. J., Franklin, L. D., et al. (2010). An integrated transcriptome atlas of the crop model Glycine max, and its use in comparative analyses in plants. *Plant J.* 63, 86–99. doi: 10.1111/j.1365-313X.2010.04222.x

Liu, J., Luo, X., Shaff, J., Liang, C., Jia, X., Li, Z., et al. (2012). A promoter-swap strategy between the AtALMT and AtMATE genes increased Arabidopsis aluminum resistance and improved carbon-use efficiency for aluminum resistance. *Plant J.* 71, 327–337. doi: 10.1111/j.1365-313X.2012.04994.x

Liu, J., Magalhaes, J. V., Shaff, J., and Kochian, L. V. (2009). Aluminum-activated citrate and malate transporters from the MATE and ALMT families function independently to confer Arabidopsis aluminum tolerance. *Plant J.* 57, 389–399. doi: 10.1111/j.1365-313X.2008.03696.x

Liu, J., Piñeros, M. A., and Kochian, L. V. (2014). The role of aluminum sensing and signaling in plant aluminum resistance. *J. Integr. Plant Biol.* 56, 221–230. doi: 10.1111/jipb.12162

Liu, P. D., Xue, Y. B., Chen, Z. J., Liu, G. D., and Tian, J. (2016). Characterization of purple acid phosphatases involved in extracellular dNTP utilization in *Stylosanthes*. *J. Exp. Bot.* 67, 4141–4154. doi: 10.1093/jxb/erw190

Lynch, M., O'Hely, M., Walsh, B., and Force, A. (2001). The probability of preservation of a newly arisen gene duplicate. *Genetics* 159, 1789–1804. doi: 10.1093/jxb/erw190

Ma, J. F. (2007). Syndrome of aluminum toxicity and diversity of aluminum resistance in higher plants. *Int. Rev. Cytol.* 264, 225–252. doi: 10.1016/S0074-7696(07)64005-4

Meriga, B., Reddy, B. K., Rao, K. R., Reddy, L. A., and Kishor, P. B. (2004). Aluminium induced production of oxygen radicals, lipid peroxidation and DNA damage in seedlings of rice (*Oryza sativa*). *J. Plant Physiol.* 161, 63–68. doi: 10.1078/0176-1617-01156

Ohyama, Y., Ito, H., Kobayashi, Y., Ikka, T., Morita, A., Kobayashi, M., et al. (2013). Characterization of *AtSTOP1* orthologous genes in tobacco and other plant species. *Plant Physiol.* 162, 1937–1946. doi: 10.1104/pp.113.218958

Palóve-Balang, P., ćiamporová, M., Zelinová, V., Pavlovkin, J., Gurinová, E., and Mistrík, I. (2012). Cellular responses of two Latin-American cultivars of *Lotus corniculatus* to low pH and Al stress. *Cent. Eur. J. Biol.* 7, 1046–1054. doi: 10.2478/s11535-012-0098-0

Pavlovkin, J., Palóve-Balang, P., Kolarović, L., and Zelinová, V. (2009). Growth and functional responses of different cultivars of *Lotus corniculatus* to aluminum and low pH stress. *J. Plant Physiol.* 166, 1479–1487. doi: 10.1016/j.jplph.2009.03.005

Ramos-Díaz, A., Brito-Argáez, L., Munnik, T., and Hernández-Sotomayor, S. M. T. (2007). Aluminum inhibits phosphatidic acid formation by blocking the phospholipase C pathway. *Planta* 225, 393–401. doi: 10.1007/s00425-006-0348-3

Rangel, A. F., Mobin, M., Rao, I. M., and Horst, W. J. (2005). Proton toxicity interferes with the screening of common bean (*Phaseolus vulgaris* L.) genotypes for aluminium resistance in nutrient solution. *J. Plant. Nutr. Soil Sci.* 168, 607–616. doi: 10.1002/jpln.200520509

Roberts, J. K., Hooks, M. A., Miaullis, A. P., Edwards, S., and Webster, C. (1992). Contribution of malate and amino acid metabolism to cytoplasmic pH regulation in hypoxic maize root tips studied using nuclear magnetic resonance spectroscopy. *Plant Physiol.* 98, 480–487. doi: 10.1104/pp.98.2.480

Ryan, P. R., Delhaize, E., and Jones, D. L. (2001). Function and mechanism of organic anion exudation from plant roots. *Annu. Rev. Plant Physiol. Mol. Biol.* 52, 527–560. doi: 10.1146/annurev.arplant.52.1.527

Sakano, K. (1998). Revision of biochemical pH-stat: involvement of alternative pathway metabolisms. *Plant Cell Physiol.* 39, 467–473. doi: 10.1093/oxfordjournals.pcp.a029393

Sawaki, Y., Iuchi, S., Kobayashi, Y., Kobayashi, Y., Ikka, T., Sakurai, N., et al. (2009). STOP1 regulates multiple genes that protect Arabidopsis from proton and aluminum toxicities. *Plant Physiol.* 150, 281–294. doi: 10.1104/pp.108.134700

Sawaki, Y., Kobayashi, Y., Kihara-Doi, T., Nishikubo, N., Kawazu, T., Kobayashi, M., et al. (2014). Identification of a STOP1-like protein in *Eucalyptus* that regulates transcription of Al tolerance genes. *Plant Sci.* 223, 8–15. doi: 10.1016/j.plantsci.2014.02.011

Schmutz, J., Cannon, S. B., Schlueter, J., Ma, J., Mitros, T., Nelson, W., et al. (2010). Genome sequence of the palaeopolyploid soybean. *Nature* 463, 178–183. doi: 10.1038/nature08670

Sénéchal, F., Mareck, A., Marcelo, P., Lerouge, P., and Pelloux, J. (2015). Arabidopsis PME17 activity can be controlled by pectin methylesterase inhibitor4. *Plant Signal. Behav.* 10:e983351. doi: 10.4161/15592324.2014.983351

Sivaguru, M., Baluska, F., Volkmann, D., Felle, H. H., and Horst, W. J. (1999). Impacts of aluminum on the cytoskeleton of the maize root apex. short-term effects on the distal part of the transition zone. *Plant Physiol.* 119, 1073–1082. doi: 10.1104/pp.119.3.1073

Sivaguru, M., Fujiwara, T., Šamaj, J., Baluska, F., Yang, Z., Osawa, H., et al. (2000). Aluminum-induced 1-3- b-D-glucan inhibits cell-to-cell trafficking of molecules through plasmodesmata: a new mechanism of aluminum toxicity in plants. *Plant Physiol.* 124, 991–1006. doi: 10.1104/pp.124.3.991

Song, H., Xu, X., Wang, H., and Tao, Y. (2011). Protein carbonylation in barley seedling roots caused by aluminum and proton toxicity is suppressed by salicylic acid. *Russ. J. Plant Physiol.* 58, 653–659. doi: 10.1134/S1021443711040169

Tokizawa, M., Kobayashi, Y., Saito, T., Kobayashi, M., Iuchi, S., Nomoto, M., et al. (2015). SENSITIVE TO PROTON RHIZOTOXICITY1, CALMODULIN BINDING TRANSCRIPTION ACTIVATOR2, and other transcription factors are involved in ALUMINUM-ACTIVATED MALATE TRANSPORTER1 expression. *Plant Physiol.* 167, 991–1003. doi: 10.1104/pp.114.256552

von Uexküll, H. R., and Mutert, E. (1995). "Global extent, development and economic impact of acid soils," in *Plant-Soil Interactions at Low pH: Principles and Management*, eds R. A. Date, N. J. Grundon, G. E. Raymet, and M. E. Probert (Dordrecht: Kluwer Academic), 5–19. doi: 10.1007/978-94-011-0221-6_1

Yamaguchi, Y., Yamamoto, Y., and Matsumoto, H. (1999). Cell death process initiated by a combination of aluminium and iron in suspension cultures of tobacco cells (*Nicotiana tabacum*): apoptosis-like cell death mediated by calcium and proteinase. *Soil Sci. Plant Nutr.* 45, 647–657. doi: 10.1080/00380768.1999.10415828

Yamaji, N., Huang, C. F., Nagao, S., Yano, M., Sato, Y., Nagamura, Y., et al. (2009). A zinc finger transcription factor ART1 regulates multiple genes implicated in aluminum tolerance in rice. *Plant Cell* 21, 3339–3349. doi: 10.1105/tpc.109.070771

Yang, J. L., Zheng, S. J., He, Y. F., and Matsumoto, H. (2005). Aluminium resistance requires resistance to acid stress: a case study with spinach that exudes oxalate rapidly when exposed to Al stress. *J. Exp. Bot.* 56, 1197–1203. doi: 10.1093/jxb/eri113

Yokota, S., and Ojima, K. (1995). Physiological response of root tip of alfalfa to low pH and aluminium stress in water culture. *Plant Soil* 171, 163–165. doi: 10.1007/BF00009581

Conflict of Interest Statement: The authors declare that the research was conducted in the absence of any commercial or financial relationships that could be construed as a potential conflict of interest.

frontiers in Plant Science

ORIGINAL RESEARCH
published: 28 February 2018
doi: 10.3389/fpls.2018.00258

Identification of STOP1-Like Proteins Associated With Aluminum Tolerance in Sweet Sorghum (*Sorghum bicolor* L.)

*Sheng Huang†, Jie Gao†, Jiangfeng You, Yanan Liang, Kexing Guan, Siqi Yan, Meiqi Zhan and Zhenming Yang**

Jilin Province Engineering Laboratory of Plant Genetic Improvement, College of Plant Science, Jilin University, Changchun, China

Aluminum (Al) toxicity in acidic soils affects crop production worldwide. C_2H_2-type zinc finger transcription factor STOP1/ART1-mediated expression of Al tolerance genes has been shown to be important for Al resistance in *Arabidopsis*, rice and other crop plants. Here, we identified and characterized four STOP1-like proteins (SbSTOP1a, SbSTOP1b, SbSTOP1c, and SbSTOP1d) in sweet sorghum, a variant of grain sorghum (*Sorghum bicolor* L.). Al induced the transcription of the four *SbSTOP1* genes in both time- and Al concentration-dependent manners. All SbSTOP1 proteins localized to the cell nucleus, and they showed transcriptional activity in a yeast expression system. In the HEK 293 coexpression system, SbSTOP1d showed transcriptional regulation of *SbSTAR2* and *SbMATE*, indicating the possible existence of another SbSTOP1 and SbSTAR2-dependent Al tolerance mechanism in sorghum apart from the reported SbMATE-mediated Al exclusion mechanism. A transgenic complementation assay showed that *SbSTOP1d* significantly rescued the Al-sensitivity characteristic of the *Atstop1* mutant. Additionally, yeast two-hybrid and bimolecular fluorescence complementation (BiFC) assays showed that SbSTOP1d interacted with SbSTOP1b and SbSTOP1d itself, suggesting that SbSTOP1 may function as a homodimer and/or heterodimer. These results indicate that STOP1 plays an important role in Al tolerance in sweet sorghum and extend our understanding of the complex regulatory mechanisms of STOP1-like proteins in response to Al toxicity.

Keywords: aluminum toxicity, STOP1, transcriptional regulation, Al tolerance genes, sweet sorghum

OPEN ACCESS

Edited by:
Wei Fan,
Yunnan Agricultural University, China

Reviewed by:
Jian Li Yang,
Zhejiang University, China
Chao-Feng Huang,
Shanghai Institutes for Biological Sciences (CAS), China
Fernando Carlos Gómez-Merino,
Inicio COLPOS, Mexico

****Correspondence:***
Zhenming Yang
zmyang@jlu.edu.cn
†Co-first authors

Specialty section:
This article was submitted to Plant Abiotic Stress, a section of the journal Frontiers in Plant Science

Received: *27 November 2017*
Accepted: *12 February 2018*
Published: *28 February 2018*

Citation:
Huang S, Gao J, You J, Liang Y, Guan K, Yan S, Zhan M and Yang Z (2018) Identification of STOP1-Like Proteins Associated With Aluminum Tolerance in Sweet Sorghum (Sorghum bicolor L.). Front. Plant Sci. 9:258. doi: 10.3389/fpls.2018.00258

INTRODUCTION

Acid soils are widespread and limit crop production all over the world. Aluminum (Al) toxicity is a primary limiting factor in acid soils. At pH below 5, Al (the most abundant form, Al^{3+}) inhibits root elongation within a few minutes, which leads to subsequent water and nutrient deficiency (Kochian et al., 2004; Ma, 2007; Bojórquez-Quintal et al., 2017).

To cope with Al stress, plants develop a series of strategies that have been categorized into two main types of Al resistance mechanisms. Al exclusion mechanisms, which are external strategies, aim at preventing toxic Al from entering root cells by exuding organic compounds (e.g., organic acids or phenolics) into the rhizosphere to chelate Al. Al tolerance mechanisms, which are internal strategies, sequester and detoxify Al that enters the plant (Ma, 2000; Ryan et al., 2001;

Kochian et al., 2015). The mechanisms of Al-meditated root exudation of organic acids (citrate, malate or oxalate) are well characterized, with involvement of transporters from the Al-activated malate transporter (ALMT) family and the multidrug and toxic compound extrusion (MATE) family (Sasaki et al., 2004; Furukawa et al., 2007; Magalhaes et al., 2007). *SbMATE* in sorghum (and *MATE* in barley, *HvAACT1*) was the first Al resistance gene to be identified. It encodes a citrate transporter that is primarily responsible for Al resistance in sorghum via citrate release (Furukawa et al., 2007; Magalhaes et al., 2007). Subsequently, homologs of MATE were isolated in other species, including AtMATE1 in *Arabidopsis thaliana*, VuMATE1 in *Vigna umbellata* and OsFRD1 in *Oryza sativa* (Liu et al., 2009; Yang et al., 2011; Yokosho et al., 2011). Once Al traverses the external organic compound barrier, it reaches the root cells. In response, plants develop Al tolerance mechanisms that involve other membrane transporters, including Nramps, ABC transporters and aquaporins (Huang et al., 2009, 2010; Negishi et al., 2012, 2013; Li et al., 2014). The cell wall constitutes the first barrier against Al in cells, while some ABC transporters (such as OsSTAR1/OsSTAR2 protein complex) are thought to mediate the efflux of UDP-glucose into the cell wall, which presumably alters the cell wall composition, limiting Al accumulation and reducing Al toxicity (Huang et al., 2009).

Al induces the coordinated expression of multiple Al tolerance genes in plants. Sensitive to proton rhizotoxicity 1 (STOP1) in *Arabidopsis* was isolated and further shown to be a key transcription factor that regulates the expression of a range of Al tolerance genes (including *AtALMT1*, *AtMATE,* and *AtALS3*) and some proton tolerance genes (Liu et al., 2009; Sawaki et al., 2009). Al resistance transcription factor 1 (ART1) was also identified in rice. In contrast to AtSTOP1, the rice homolog regulates only Al tolerance genes (such as *OsNrat1*, *OsSTAR1*, and *OsSTAR2*) but not proton tolerance genes (Yamaji et al., 2009). Homologous *STOP1*-like genes have also been characterized in other plant species. These genes all encode a Cys_2His_2 (C_2H_2) zinc finger protein, but their expression patterns vary. *AtSTOP1* in *A. thaliana*, *OsART1* in *O. sativa,* and *NtSTOP1* in *Nicotiana tabacum* are constitutively expressed in roots, whereas *VuSTOP1* in *V. umbellata* is upregulated by Al toxicity in a dosage-dependent manner (Yamaji et al., 2009; Ohyama et al., 2013; Fan et al., 2015). AtSTOP2, a homolog of AtSTOP1, was identified in *Arabidopsis* recently. AtSTOP2 activates the expression of some genes for Al- and low pH-tolerance that are regulated by AtSTOP1 (Kobayashi et al., 2014). The distinct roles and/or consociation of AtSTOP1 and AtSTOP2 in Al signaling and regulatory pathways, however, have not yet been clarified.

In this study, four *STOP1*-like genes (*SbSTOP1a*, *SbSTOP1b*, *SbSTOP1c,* and *SbSTOP1d*) with diverse expression profiles were identified in sweet sorghum, a variant of grain sorghum (*Sorghum bicolor* L.). SbSTOP1d, which shares the highest identity with AtSTOP1 and OsART1, regulated the transcription of *SbSTAR2*, suggesting the existence of a SbSTOP1-mediated Al tolerance mechanism aside from the previously reported SbMATE-dependent Al exclusion mechanism in sorghum. SbSTOP1d interacted with itself and SbSTOP1b in plants, implying that SbSTOP1d might form a homo- and/or heterodimer to function. Taken together, we characterized homologous SbSTOP1s in sweet sorghum and examined the association between diverse SbSTOP1s, which may help to further clarify the complex signal transduction pathways of STOP1-like proteins in response to Al toxicity.

MATERIALS AND METHODS

Plant Materials, Culture Conditions, and Al Treatments

The sweet sorghum (*S. bicolor* L.) cultivar POTCHETSTRM was used in this study (Zhang et al., 2015). Seeds were surface sterilized with 1% (v/v) NaClO for 20 min, rinsed with deionized water five times, spread on wet filter paper in a Petri dish and germinated for 2 days in darkness at 28°C. The germinated seeds were transplanted into 0.5 mM $CaCl_2$ solution at pH 4.5 or 5.8 depending on the treatment. The seedlings were grown in an environmentally controlled growth chamber with a 14 h light (400 μmol m^{-2} s^{-1})/10 h dark photoperiod, 26°C day/22°C night temperatures and 80% relative humidity.

For gene expression pattern analysis, seedlings cultured for 3 days in 0.5 mM $CaCl_2$ solution (pH 4.5) were then exposed to a different treatment. For the time-course assay, seedlings were exposed to 0.5 mM $CaCl_2$ solution with 15 μM $AlCl_3$ for 0, 3, 6, 9, or 24 h (pH 4.5), then the root apices (0–1 cm) were excised. For the Al concentration-dependent assay, seedlings were exposed to 0.5 mM $CaCl_2$ solution with 0, 5, 10, 15, or 30 μM $AlCl_3$ for 24 h (pH 4.5), then the root apices (0–1 cm) were cut. For the tissue expression pattern assay, seedlings were exposed to 0.5 mM $CaCl_2$ solution with 0 or 15 μM $AlCl_3$ for 24 h (pH 4.5) with roots (0–1 cm, 1–2 cm, or 2–3 cm) and shoots excised. For the different metal treatments, seedlings were exposed to 15 μM $AlCl_3$, 10 μM $CdCl_2$, 0.5 μM $CuCl_2$ or 10 μM $LaCl_3$ for 24 h (pH 4.5), then the root apices (0–1 cm) were excised. For the low pH treatments, seedlings were cultured in 0.5 mM $CaCl_2$ solution (pH 5.8) for 3 days, then exposed to the same solution at pH 5.8, 5.0, 4.5, 4.0, or 3.5 for 24 h. Then, the root apices (0–1 cm) were excised for RNA isolation. Each treatment was analyzed using three biological replicates.

Sequence Analysis

All sequences were analyzed using BLAST in the sorghum genome database[1] and NCBI. Sequence alignment was performed using Vector NTI and modified in GeneDoc. The phylogenetic tree was constructed according to the neighbor-joining method using MEGA 5.1.

RNA Isolation and Quantitative Real-Time PCR

Total RNA isolation, cDNA preparation and quantitative real-time PCR (qRT-PCR) were performed as previously described

[1]http://pgsb.helmholtz-muenchen.de/plant/sorghum/

(Zhang et al., 2015). The gene-specific primers were designed using Primer 5.0 software (Supplementary Table 1). The house-keeping gene β-*actin* (GenBank ID: X79378) was used as an internal control (Zhang et al., 2015). The qRT-PCR was performed using SYBR Premix ExTaq (Takara) in an Mx3005P qPCR system (Stratagene, United States). Thermocycling proceeded as follows: 1 cycle of 30 s at 95°C, 30 cycles of 5 s at 95°C and 20 s at 60°C, and 1 cycle of 60 s at 95°C, 30 s at 55°C, and 30 s at 95°C for the melting curve analysis. The relative expression level of the genes was calculated using the $2^{-\Delta\Delta C_T}$ method (Livak and Schmittgen, 2001). The experiment was conducted using three biological replicates.

Subcellular Localization of SbSTOPs

Arabidopsis protoplasts were isolated from 4-week-old plants. Leaves were cut into strips and transferred quickly into the enzyme solution [1% (w/v) cellulase R10, 0.25% (w/v) macerozyme R10, 0.4 M D-mannitol, 20 mM KCl, 20 mM MES pH 5.7 and 10 mM $CaCl_2$] for 1 h digestion at room temperature in darkness. Protoplasts were filtered through a 100-micron nylon mesh and centrifuged for 2 min at 100 *g*, rinsed with ice-cold W5 buffer [154 mM NaCl, 125 mM $CaCl_2$, 5 mM KCl and 2 mM MES, pH 5.7], and suspended in MMg buffer [0.4 M mannitol, 15 mM $MgCl_2$, 4 mM MES, pH 5.7]. Afterward, the protoplasts were ready for transformation. The PEG-mediated protoplast transformation method was used in this study. 10 μl of *35S::YFP-SbSTOP1a* (or *35S::YFP-SbSTOP1b*, *35S::YFP-SbSTOP1c* and *35S::YFP-SbSTOP1d*) was mixed with 100 μl protoplasts and 110 μl PEG solution [40% (w/v) PEG4000, 0.2 M mannitol, 100 mM $CaCl_2$]. The protoplast/DNA mixture was incubated at room temperature in darkness for 15 min, washed twice with W5 buffer, and incubated in darkness at room temperature for 12–16 h. The fluorescence images were captured using a fluorescence microscope (Axio Observer A1, Zeiss).

Transcriptional Activity Detection and Yeast Two-Hybrid Assay

To detect the transcriptional activity of SbSTOP1s, the bait vector pBridge expressing SbSTOP1a, SbSTOP1b, SbSTOP1c, SbSTOP1d, SbSTOP1d-NT (1–275 aa) or SbSTOP1d-CT (276–519 aa) fused to the GAL4 DNA-binding domain (BD) was used to transform the yeast strain Y2HGold. Colonies were selected on SD/-Trp-His medium (with or without 3-AT) and cultured for 3 days at 30°C. For the yeast two-hybrid assay, the prey vector pGADT7 expressing SbSTOP1b or SbSTOP1d fused to the GAL4 activation domain (AD) and the bait vector pBridge expressing SbSTOP1d-NT (1–275 aa) fused to the BD were used to co-transform the yeast strain Y2HGold (or the Y190 yeast strain for the β-galactosidase assay). Colonies were selected on SD/-Trp-Leu-His medium and cultured for 3 days at 30°C. The β-galactosidase assay was performed using chlorophenol red-β-D-galactopyranoside (CPRG) as substrate, and Miller units were calculated according to the Yeast Protocols Handbook (Clontech, PT3024-1). The experiment was conducted using three biological replicates.

HEK293 Coexpression System and Dual-Luciferase Reporter Assay

To examine the transcriptional regulation of *SbMATE* or *SbSTAR2* by SbSTOP1d, the reporter plasmid (*pSbMATE::LUC-SV40::REN* or *pSbSTAR2::LUC-SV40::REN*) and effector plasmid (*CMV::SbSTOP1d-Myc*) were co-transfected into HEK293 (human embryonic kidney) cells.

HEK293 cells were cultured as previously described (Gao et al., 2015). Cells were maintained in Dulbecco's modified Eagle's medium (DMEM) with FBS (10%) and penicillin/streptomycin (1%) in a cell culture flask, T75 (Eppendorf), which was incubated in a 37°C incubator with a humidified atmosphere of 5% CO_2 in air. When the cell count reached 2×10^7, cells were subcultured in a 6-well plate the night before and grown to 60–70% confluence by the day of transfection. HEK293 cells were transfected with the constructed plasmids (reporter and effector) using the calcium phosphate transfection method as reported (Gao et al., 2015). After 30–48 h, the transfected cells were ready for the dual-luciferase reporter assay.

The dual-luciferase reporter assay was conducted according to the technical manual of the Dual-luciferase Reporter Assay System (Promega, E1910). After removing the growth medium, the transfected cells were gently rinsed with 1 × PBS (pH 7.2, Thermo, 20012050) and lysed in 1 × Passive Lysis Buffer (PLB). The PLB lysate was plated in a 96-well plate with volume ≤20 μl/well. The firefly luciferase activity was measured by adding 100 μl of Luciferase Assay Reagent II (LAR II) to generate a luminescent signal that was measured with a luminometer (Berthold LB960). This reaction was then quenched, and the *Renilla* luciferase reaction is simultaneously initiated by adding 100 μl of Stop & Glo® Reagent to the same well. The Stop & Glo® Reagent also produced a luminescent signal from the *Renilla* luciferase, which served as an internal control. The experiment was conducted using three biological replicates.

Bimolecular Fluorescence Complementation Assay

Different pairs of plasmids encoding nYFP-SbSTOP1d and cCFP-SbSTOP1b, or encoding nYFP-SbSTOP1d and cCFP-SbSTOP1d were co-transformed into *Arabidopsis* protoplasts. The protoplast preparation and transformation method are described above. The reconstituted YFP fluorescence images were examined by a fluorescence microscope (Axio Observer A1, Zeiss), and the percentage of cells that exhibited bimolecular fluorescence complementation (BiFC) fluorescence signals were calculated. The experiment was conducted using three biological replicates.

Overexpression of *SbSTOP1d* in the *Atstop1* Mutant

The open reading frame (ORF) of *SbSTOP1d* was amplified and cloned into the pEGAD vector (*35S::LUC-SbSTOP1d*) using the In-Fusion enzyme. The construct was transformed into *Agrobacterium tumefaciens* strain AGL0, which was further introduced into the *Atstop1* mutant using the floral dip method (Clough and Bent, 1998). The transgenic seedlings were first screened with the Basta herbicide, then

confirmed by a three-primer PCR-based genotyping using the following primers: LP, 5′- TTCATTGGTGAGAACGACT CC -3′, RP, 5′- ATCTTCTTGTTGGTCGTGGTG -3′, LB, 5′- AT TTTGCCGATTTCGGAAC -3′. An immunoblot assay was performed to examine the expression of the fusion protein LUC-SbSTOP1d. After seeds were surface sterilized and germinated on solid MS medium vertically for 5 days, uniform seedlings were transferred to solid medium containing 4.3 mM $CaCl_2$ and 3% sucrose at pH 4.5, with or without 50 μM $AlCl_3$ for 2 days, and their root growth was measured. At least 20 seedlings were measured for each treatment and independent experiments were performed three times.

RESULTS

Sequence Analysis of SbSTOP1s

Using the amino acid sequences of AtSTOP1 and OsART1 as queries, four sweet sorghum *STOP1*-like genes, named *SbSTOP1a* (Sb01g001950.1), *SbSTOP1b* (Sb04g023670.1), *SbSTOP1c* (Sb07g023890.1), and *SbSTOP1d* (Sb03g041170.1), were identified in the sorghum genome database. The *SbSTOP1a, SbSTOP1b, SbSTOP1c,* and *SbSTOP1d* coding regions are 795, 1185, 1290, and 1560 bp, respectively, and they encode proteins of 264, 394, 429, and 519 amino acids, respectively. All SbSTOP1s contain four putative Cys_2His_2 zinc finger domains that resemble those of AtSTOP1, OsART1 and other homologs in different species (**Figure 1A**). SbSTOP1d shows the highest similarity to AtSTOP1 and OsART1, with identities of 54.9 and 48.5%, respectively, while SbSTOP1a, SbSTOP1b, and SbSTOP1c share relatively lower identities with AtSTOP1 and OsART1 (**Figure 1A**). Phylogenetic analysis revealed that SbSTOP1d clusters closely with AtSTOP1 and OsART1 compared to the other three SbSTOP1s. SbSTOP1b and SbSTOP1c cluster more closely with AtSTOP2 (**Figure 1B**).

Detection of *SbSTOP1* Expression Patterns

The expression patterns of the SbSTOP1s were investigated using quantitative real-time PCR. A time-course experiment indicated that Al induced a gradual increase in *SbSTOP1a*, *SbSTOP1b*, *SbSTOP1c,* and *SbSTOP1d* expression in root apices (0–1 cm) during the entire 24 h Al treatment, though with different transcript abundances (**Figure 2A**). In addition, the four *SbSTOP1s* showed increased transcriptional abundances in a dosage-dependent manner when the roots were exposed to increasing external Al concentrations for 24 h (**Figure 2B**). All *SbSTOP1s* were mainly expressed in roots rather than shoots, and their expression levels in basal roots (1–2 cm) and roots (2–3 cm) were higher than that detected in root apices (0–1 cm) regardless of Al stress (**Figure 2C**). Al stress induced increasing *SbSTOP1s* expression in roots (especially in root apices), but there was no detectable effect on the expression of *SbSTOP1s* in shoots (**Figure 2C**). We also compared the expression of the four *SbSTOP1s* under Al stress with their expression under other metal and proton stress. The expression of *SbSTOP1c* was specifically induced by Al stress, while the expression of *SbSTOP1a*, *SbSTOP1b,* and *SbSTOP1d* was induced only by Al and Cd stress but not by other metals (Supplementary Figures 1A–D). In addition, as shown in Supplementary Figure 2, the expression of *SbSTOP1a*, *SbSTOP1b,* and *SbSTOP1c* was increased when the pH value of the treatment solution decreased. A notable exception was the expression of *SbSTOP1d*, which was relatively unaffected by low pH stress, similar to *OsART1* (Yamaji et al., 2009).

The Subcellular Localization and Transcriptional Ability of SbSTOP1s

The main transcriptional characteristics of the SbSTOP1s were examined, including the subcellular localization, transcriptional activity and DNA-binding property. *YFP-SbSTOP1a*, *YFP-SbSTOP1b*, *YFP-SbSTOP1c,* and *YFP-SbSTOP1d* fusion genes under the control of the cauliflower mosaic virus *35S* promoter were transiently introduced into *Arabidopsis* protoplasts. As shown in **Figure 3**, the YFP-SbSTOP1a, YFP-SbSTOP1b, YFP-SbSTOP1c, and YFP-SbSTOP1d fusion proteins were strictly localized to the nucleus, while the control YFP protein was distributed throughout the cytosol and nucleus.

The transcriptional activity of SbSTOP1s was assessed in the yeast expression system. SbSTOP1a, SbSTOP1b, SbSTOP1c, and SbSTOP1d were fused to the GAL4 DNA-BD. The resulting plasmids were transformed into the Y2HGold yeast strain with a His auxotrophic marker. As observed in **Figure 4A**, yeast cells carrying BD-SbSTOP1a, BD-SbSTOP1b, BD-SbSTOP1c, and BD-SbSTOP1d grew well in SD medium without His. In contrast, yeast cells containing the GAL4 DNA-BD alone did not. These results indicated that all four SbSTOP1s have transcriptional activity.

We further investigated the DNA-binding property of SbSTOP1d due to its high similarity to AtSTOP1 and OsART1 (**Figure 1**). *SbMATE* (*Sb03g043890*), the first and also one of the few reported Al tolerance genes in sorghum (Magalhaes et al., 2007), and *SbSTAR2* (*Sb09g001990*), an ortholog of *OsSTAR2* that is transcriptionally regulated by OsART1 (Yamaji et al., 2009; Tsutsui et al., 2011), were both examined as potential downstream genes using the HEK293 coexpression system (Gao et al., 2015) and a dual-luciferase reporter assay. We introduced the *SbMATE*/*SbSTAR2* promoter to drive the firefly luciferase reporter gene with the *Renilla* luciferase gene as an internal control (**Figure 4B**). As an effector, full-length SbSTOP1d under the control of the cytomegalovirus (CMV) promoter (**Figure 4B**) was co-transformed with the above reporter into HEK293 cells, and luciferase activity was detected. Both the *SbMATE* and *SbSTAR2* promoter-driven reporters showed higher luciferase activity in the presence of the SbSTOP1d effector compared to the vector-only effector, though the *SbSTAR2* promoter-driven reporter showed higher absolute value and significant differences at $P < 0.01$ compared with the *SbMATE* promoter-driven reporter (**Figures 4C,D**). SbSTOP1a, SbSTOP1b, and SbSTOP1c also showed weak or positive effects on the expression of *SbMATE* (Supplementary Figure 3). These results demonstrated that SbSTOP1d interacts with the *SbSTAR2* and *SbMATE* promoters to act as a transcriptional activator.

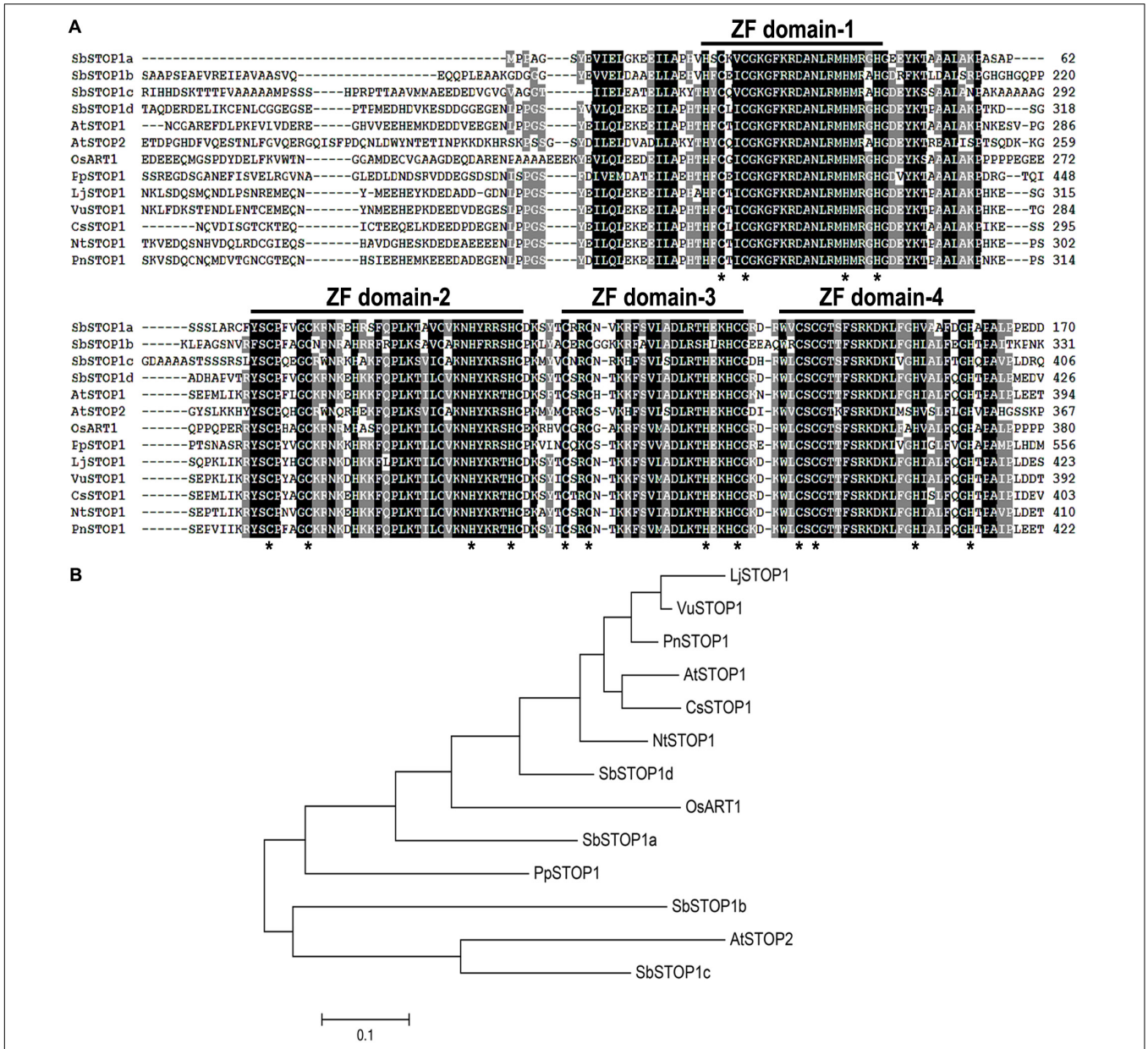

FIGURE 1 | Identification of SbSTOP1s. **(A)** Sequence alignment of the zinc finger domains of SbSTOP1s and homologous proteins from other species, including *Arabidopsis thaliana* (AtSTOP1, At1g34370, and AtSTOP2, At5g22890), *Physcomitrella patens* (PpSTOP1, AB811779), *Nicotiana tabacum* (NtSTOP1, AB811781), *Oryza sativa* (OsART1, AB379846), *Camellia sinensis* (CsSTOP1, AB811780), *Populus nigra* (PnSTOP1, AB811778), *Lotus japonicus* (LjSTOP1, AB811782) and *Vigna umbellata* (VuSTOP1, KP637172). Horizontal lines indicate zinc finger (ZF) domains, and asterisks show conserved Cys_2His_2 or Cys_2His_2-Cys motifs as predicted (Iuchi et al., 2007). **(B)** Phylogenic analysis of SbSTOP1s and the above homologous proteins. The phylogenetic tree was constructed according to the neighbor-joining method using MEGA 5.1.

SbSTOP1d Interacts With Itself or SbSTOP1b in Plants

We performed a yeast two-hybrid assay to screen for proteins that interact with SbSTOP1d, with the N-terminal fragment of SbSTOP1d [SbSTOP1d-NT, 1-275 aa, truncated before the zinc finger (ZF) domain] as bait, since its autoactivation could be readily suppressed by adding 3 mM 3-AT in SD medium (Supplementary Figure 4). Interestingly, the potential interaction proteins of SbSTOP1d included SbSTOP1d itself and SbSTOP1b. Yeast two-hybrid validation indicated that yeast cells co-transformed with SbSTOP1d-NT and SbSTOP1b grew well on SD/-Trp-Leu-His medium (**Figure 5A**). In addition, yeast cells containing SbSTOP1d-NT and SbSTOP1d showed similar result as the above (**Figure 5B**). Moreover, β-galactosidase assays showed that the β-galactosidase activities of yeast cells co-transformed with SbSTOP1d-NT and SbSTOP1b,

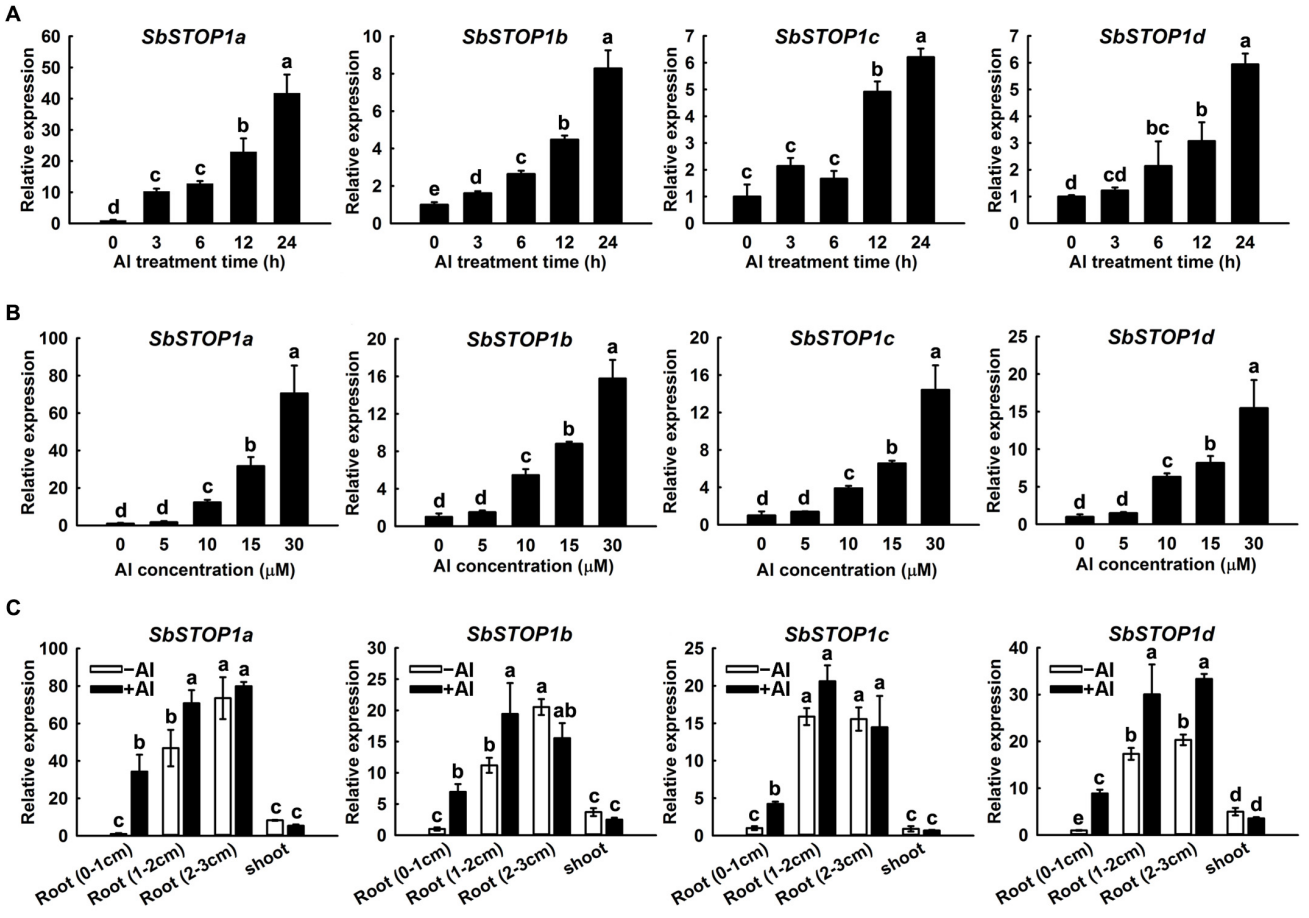

FIGURE 2 | Quantitative real-time PCR analysis of *SbSTOP1s* expression profiles. **(A)** Relative expression of *SbSTOP1a*, *SbSTOP1b*, *SbSTOP1c,* and *SbSTOP1d* in sweet sorghum (*Sorghum bicolor*) root apices (0–1 cm) in response to 15 μM Al for different treatment times. **(B)** Relative expression of *SbSTOP1a*, *SbSTOP1b*, *SbSTOP1c,* and *SbSTOP1d* in root apices (0–1 cm) exposed to different Al concentrations for 24 h. **(C)** Relative expression of *SbSTOP1a*, *SbSTOP1b*, *SbSTOP1c,* and *SbSTOP1d* in root apices (0–1 cm), basal roots (1–2 cm), roots (2–3 cm) and shoots in the absence (–Al) or presence (+Al, 15 μM) of Al stress for 24 h. Data represent the means ± SD from three independent biological replicates. Columns with different letters are significantly different at $P < 0.05$.

and with SbSTOP1d-NT and SbSTOP1d were approximately 80 times and 450 times that of the control (**Figure 5C**). These results demonstrated that SbSTOP1d can interact with SbSTOP1d itself and SbSTOP1b at the N-terminal region (1–275 aa, not include ZF domain). SbSTOP1a and SbSTOP1c, nevertheless, showed no interaction with SbSTOP1d (Supplementary Figure 5). We further tested whether SbSTOP1d could interact with SbSTOP1b or itself in plant cells using the BiFC assay as described previously (Meng et al., 2013). SbSTOP1d was fused to the N-terminal fragment of YFP or to the C-terminal fragment of CFP, and SbSTOP1b was fused to the C-terminal fragment of CFP. Different pairs of constructs were co-transformed into *Arabidopsis* protoplasts while the protein–protein interaction was observed under a microscope (**Figure 5D**) and analyzed semi-quantitatively by measuring the percentage of cells that showed reconstituted YFP activity (**Figure 5E**). These results demonstrated that SbSTOP1d interacted with SbSTOP1d itself (self-association) as well as with SbSTOP1b in plants (**Figures 5D,E**), suggesting that SbSTOP1d might function as a homo- and/or heterodimer in plants. The homo- and/or heterodimerization of SbSTOP1d might facilitate its specificity and DNA-binding affinity, since this is a strategy used by other transcription factors (Crossley et al., 1995; Jakoby et al., 2002; Xu et al., 2015).

SbSTOP1d Overexpression in *Arabidopsis* Confers Aluminum Tolerance

The primary symptom of Al toxicity is a rapid inhibition of root growth (Foy, 1988; Kochian et al., 2004). The *Atstop1* mutant showed a root inhibition phenotype under Al stress, while the overexpression of *PpSTOP1*, *PnSTOP1,* or *NtSTOP1* in the *Atstop1* mutant could recover the Al- sensitive phenotype to varying extents (Ohyama et al., 2013; Fan et al., 2015). To further examine the function of SbSTOP1d, we introduced *LUC-SbSTOP1d* under the control of the CaMV 35S promoter

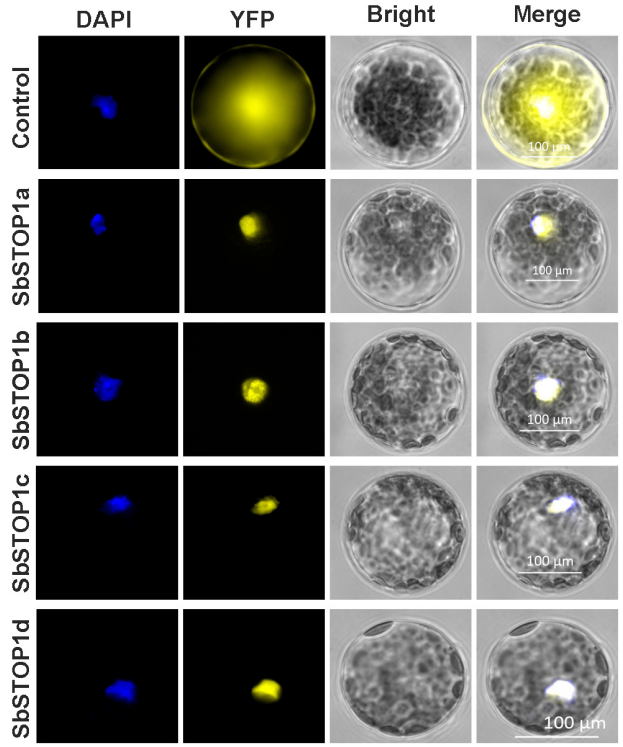

FIGURE 3 | Subcellular localization of SbSTOP1s. Transient expression of YFP-SbSTOP1a, YFP-SbSTOP1b, YFP-SbSTOP1c, and YFP-SbSTOP1d fusion proteins and YFP control in *Arabidopsis* protoplast. DAPI, nuclear signal; YFP, YFP fluorescence; Bright, bright field. Scale bar indicates 100 μm.

in the *Atstop1* mutant background (SALK 114108). After a three-primer PCR-based genotyping (Supplementary Figure 6) and an immunoblot analysis for the LUC-SbSTOP1d fusion protein (**Figure 6A**), two independent complemented lines expressing SbSTOP1d were selected for phenotypic analysis. As shown in **Figures 6B,C**, the root growth of the WT, *Atstop1*, and two complemented lines was similar in the absence of Al. In the presence of Al, the root growth of WT was inhibited, with a relative root elongation (RRE) of 65%. *Atstop1*, which is sensitive to Al, had only 35% RRE, and in contrast, the two SbSTOP1d complemented lines greatly recovered the Al sensitivity characteristic of the *Atstop1* mutant, with 55 and 60% RRE, respectively. These results indicated that heterologous expression of *SbSTOP1d* improved the Al tolerance of the transgenic plants.

DISCUSSION

Aluminum can be a beneficial element for some plant species at low concentrations. At pH values below 5, aluminum concentration (Al^{3+}) rises sharply, inhibiting root growth and function, which leads to significant reductions in crop yields (Foy, 1983; Liu et al., 2014; Bojórquez-Quintal et al., 2017; Moreno-Alvarado et al., 2017). Transcription factors, such as STOP1 and WRKY46 in *Arabidopsis*, ART1 and ASR5 in rice play important roles in Al signal perception and transduction (Sawaki et al., 2009; Yamaji et al., 2009; Ding et al., 2013; Arenhart et al., 2014; Xu et al., 2017). Moreno-Alvarado et al. (2017) recently reported for the first time the induction of transcription factor *NAC* gene expression in Al-treated rice plants. Among them, STOP1-like proteins have been shown to be key transcription factors and investigated in many plant species, including *Arabidopsis* (AtSTOP1, AtSTOP2), rice (OsART1), tobacco (NtSTOP1), eucalyptus (EguSTOP1), and rice bean (VuSTOP1) (Iuchi et al., 2007; Yamaji et al., 2009; Ohyama et al., 2013; Kobayashi et al., 2014; Sawaki et al., 2014; Fan et al., 2015), yet a STOP1-like protein has never been characterized in sorghum. We isolated four sweet sorghum genes, *SbSTOP1a*, *SbSTOP1b*, *SbSTOP1c,* and *SbSTOP1d*, encoding proteins containing four conserved C_2H_2 zinc finger domains, similar to other homologous proteins (**Figure 1**). Compared with the other three SbSTOP1s, SbSTOP1d shares higher similarity with AtSTOP1/OsART1 (**Figure 1**), its expression level was relatively higher under Al stress (data not shown) and it was specifically affected by Al stress but not low pH stress (Supplementary Figure 2D), thus, SbSTOP1d was further investigated and confirmed to be effective for Al tolerance in plants (**Figure 6**).

As previously reported, the expression levels of *AtSTOP1* and *OsART1* were not significantly affected by Al (Iuchi et al., 2007; Yamaji et al., 2009). However, in this study, the expression of *SbSTOP1a*, *SbSTOP1b*, *SbSTOP1c,* and *SbSTOP1d* in roots was significantly induced by Al in a time- and Al concentration-dependent manner (**Figure 2**). These results suggested that SbSTOP1s could respond to Al toxicity as early as transcriptional regulation and that different Al response mechanisms may exist between SbSTOP1s and AtSTOP1/OsART1. *VuSTOP1* shares similar expression patterns with the *SbSTOP1s*, since its expression is induced by Al stress, but VuSTOP1 expression is also affected by low pH (Fan et al., 2015). In sweet sorghum, *SbSTOP1a*, *SbSTOP1b*, and *SbSTOP1c* expression were induced by low pH (pH 3.5), but *SbSTOP1d* expression showed little change under proton stress (Supplementary Figure 2). Thus, it is possible that different STOP1-like proteins from various species or even from the same species differ in function. In addition, Al- and low pH- tolerance seem to be regulated by different gene groups that belong to the STOP1-regulated system (Kobayashi et al., 2014). Therefore, in this study, we focused on SbSTOP1d for further functional analysis due to its high sequence identity to AtSTOP1 and OsART1 and because its expression was specifically affected by Al toxicity but not proton stress. Further research could be conducted to investigate the detailed characterizations of different SbSTOP1s in sweet sorghum.

All SbSTOP1s localized to the nucleus (**Figure 3**), and this agreed with the expectation for transcription factors. The four SbSTOP1s displayed transcriptional activity. SbSTOP1d-CT (276–519 aa, including ZF domains) showed stronger transcriptional activity than that of SbSTOP1d-NT (1–275 aa), which could not be inhibited with 15 mM 3-AT in SD medium (Supplementary Figure 4).

STOP1-like proteins generally regulate the transcription of Al tolerance genes by binding to the *cis*-acting element of the

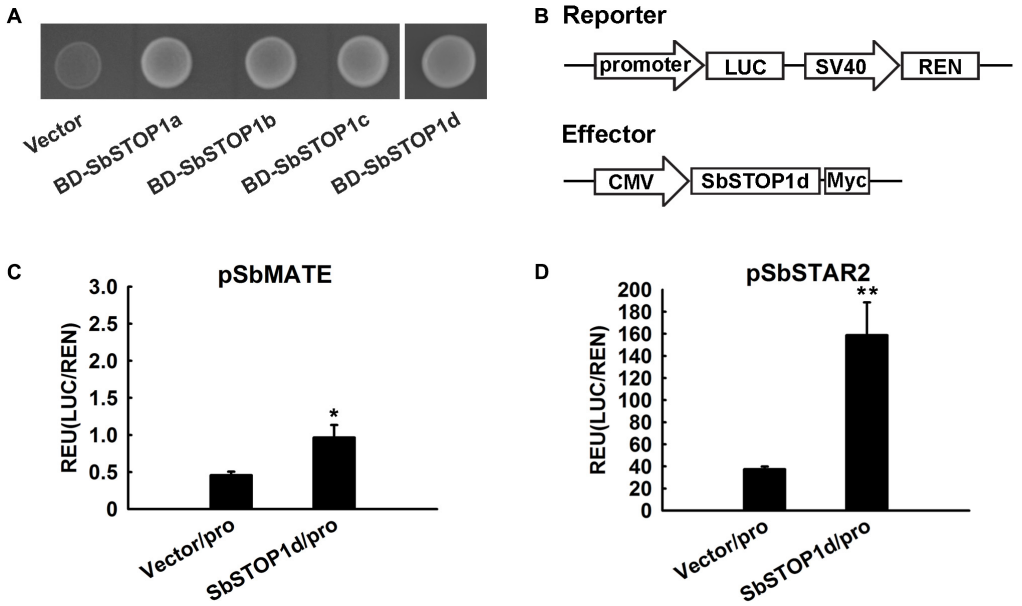

FIGURE 4 | Transcriptional characteristic analysis of SbSTOP1s. **(A)** Transcriptional activity of SbSTOP1s in yeast. Y2HGold yeast strain carrying fused protein of GAL4 DNA-binding domain and SbSTOP1a (BD-SbSTOP1a), BD-SbSTOP1b, BD-SbSTOP1c, BD-SbSTOP1d or BD alone (vector) were cultured on SD-Trp-His medium. **(B)** Schematic diagram of the reporter and effector used in the HEK293 coexpression system. Promoter, *SbMATE* or *SbSTAR2* promoter (–2039 bp and –1963 bp, respectively); LUC, firefly luciferase reporter; REN, *Renilla* luciferase reporter as internal control; SV40 and cytomegalovirus (CMV), two promoters commonly used in mammalian expression vectors to drive gene expression; Myc, protein tag. **(C,D)** Transcriptional regulation of *SbMATE* **(C)** and *SbSTAR2* **(D)** by SbSTOP1d in HEK293 cells. Luciferase activity of reporter (LUC) driven by the promoters (pro) of *SbMATE* **(C)** and *SbSTAR2* **(D)** was normalized to the internal control reporter (REN). Data represent the means ± SD from three independent biological replicates. Asterisk (*) represents significant differences from the vector-only control at $P < 0.05$. Asterisks (**) represent significant differences from the vector-only control at $P < 0.01$.

promoter. OsART1 regulates multiple genes implicated in Al tolerance, and most of these genes (e.g., *OsSTAR1*, *OsSTAR2*) possess a *cis*-acting element as GGN(T/g/a/C)V(C/A/g)S(C/G) in their promoter (Yamaji et al., 2009; Tsutsui et al., 2011). AtSTOP1 also regulates several genes such as *AtALMT1* and *AtMATE1* in response to Al toxicity (Liu et al., 2009; Sawaki et al., 2009). Therefore, we tested whether SbSTOP1d regulates the transcription of two typical Al-associated genes, *SbMATE* (involved in Al exclusion mechanisms) and *SbSTAR2* (involved in Al tolerance mechanisms). Both genes contain the above putative *cis*-acting element in their promoters. SbSTOP1d showed a positive effect on the expression of *SbMATE* and *SbSTAR2* (**Figures 4C,D**), though the *SbMATE* promoter-driven reporter showed relatively lower luciferase activity than the *SbSTAR2* promoter-driven reporter did. Similarly, VuSTOP1 can bind only weakly to the promoter of *VuMATE* (Fan et al., 2015). It was reported that the promoter of *SbMATE* harbored a tourist like miniature inverted repeat transposable element (MITE). The copy number (sequence repeats) of this MITE, which varied in different sorghum accessions, was positively correlated with Al tolerance (Magalhaes et al., 2007). Thus, the expression level of *SbMATE* in the sweet sorghum cultivar we used may also be regulated by this transposable element. It is unlikely, but we cannot exclude the possibility that there are some other *cis*-acting elements away from the tested promoter (−2039 bp) of *SbMATE*, since VuSTOP1 can also interact with a DNA sequence lacking the putative GGN(T/g/a/C)V(C/A/g)S(C/G) *cis*-acting element (Fan et al., 2015). In addition, even though an increasing expression level of SbSTOP1s was induced by Al (**Figure 2**), some post-translational modifications may restrict the transcriptional activity of SbSTOP1. These modifications, such as protein phosphorylation, are frequently involved in the activation of transcription factors in response to biotic and abiotic stress, e.g., tomato *PSEUDOMONAS* TOMATO RESISTANCE (PTO) kinase phosphorylates PTI4 to increases the DNA-binding ability of PTI4 (Singh et al., 2002); Phosphorylation of ABA-responsive element binding proteins (AREB) was suggested to be involved in their activation (Uno et al., 2000). Thus, complex SbMATE regulation pathways may exist in sorghum. SbMATE-dependent citrate excretion is an important Al exclusion mechanism in sorghum (Magalhaes et al., 2007), while our study suggested that the SbSTOP1-dependent Al tolerance mechanism may blaze another trail, i.e., SbSTOP1 transcriptionally regulates *SbSTAR2* (**Figure 4D**) to fulfill its Al resistance function.

Homo- and/or heterodimerization of transcription factors occurs frequently to facilitate their function at diverse promoters or bring together/stabilize two regulatory elements. Plant basic-leucine zipper (bZIP) transcription factors form homodimers or heterodimers to bind DNA and *trans*-activate downstream gene expression (Schindler et al., 1992; Jakoby et al., 2002). Several types of zinc-finger motifs in transcription factors function as parts of DNA-binding and protein–protein interaction domains,

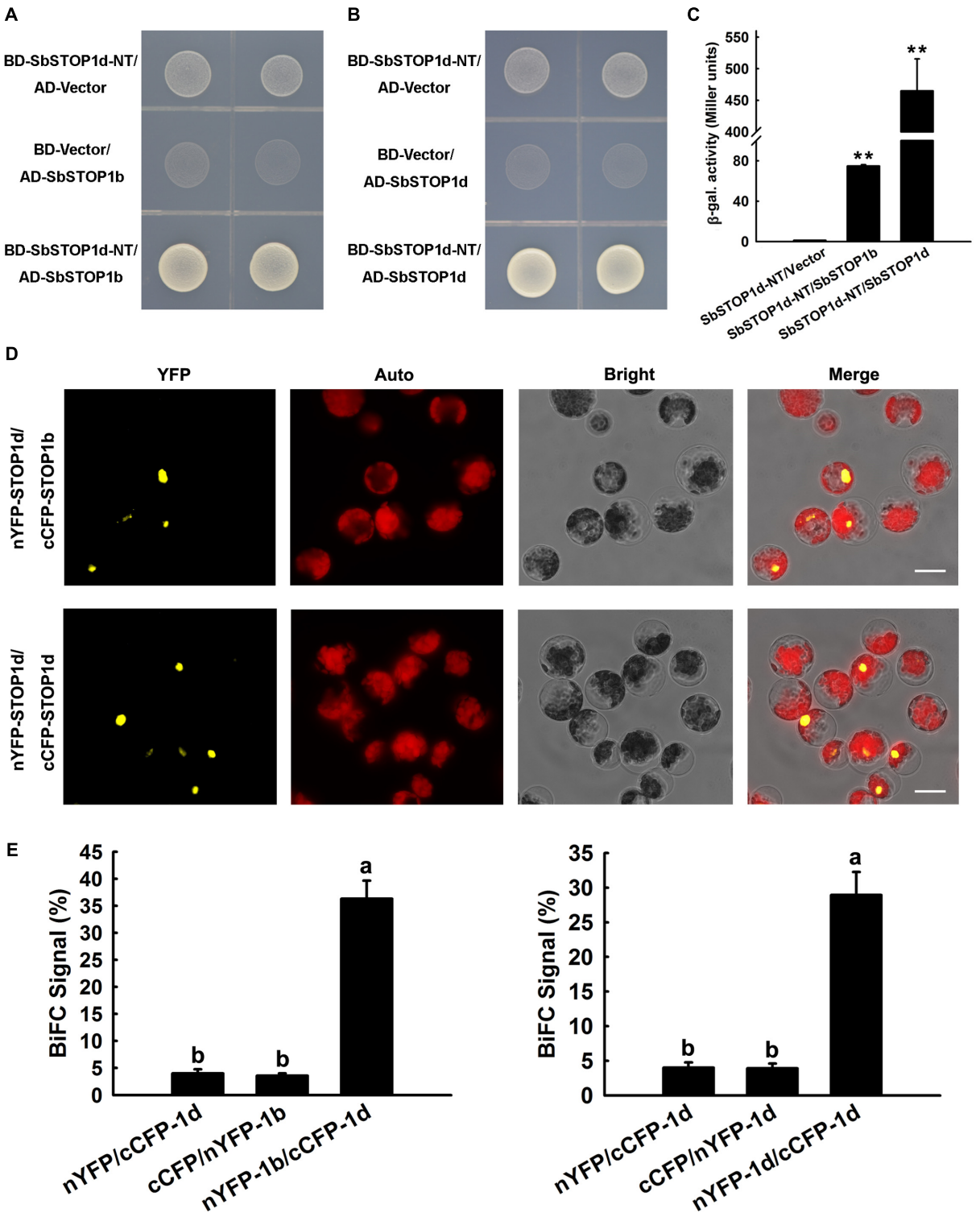

FIGURE 5 | SbSTOP1d interacted with SbSTOP1b and SbSTOP1d itself. **(A,B)** Yeast Two-hybrid assays showing the interactions of BD-SbSTOP1d-NT with AD-SbSTOP1b **(A)** and BD-SbSTOP1d-NT with AD-SbSTOP1d **(B)**. **(C)** β-galactosidase assays showing the above protein interactions quantitatively. Data represent the means ± SD from three independent biological replicates. Asterisks (**) represent significant differences in comparison to control at $P < 0.01$. **(D)** BiFC assays showing the association of SbSTOP1d and SbSTOP1b and the self-association of SbSTOP1d in *Arabidopsis* protoplasts. YFP, YFP fluorescence; Auto, autofluorescence; Bright, bright field. Scale bar indicates 100 μm. **(E)** The percentage of protoplasts that exhibit BiFC fluorescence signals was calculated. 1b, SbSTOP1b; 1d, SbSTOP1d. Data represent the means ± SD from three independent biological replicates. Columns with different letters are significantly different at $P < 0.05$.

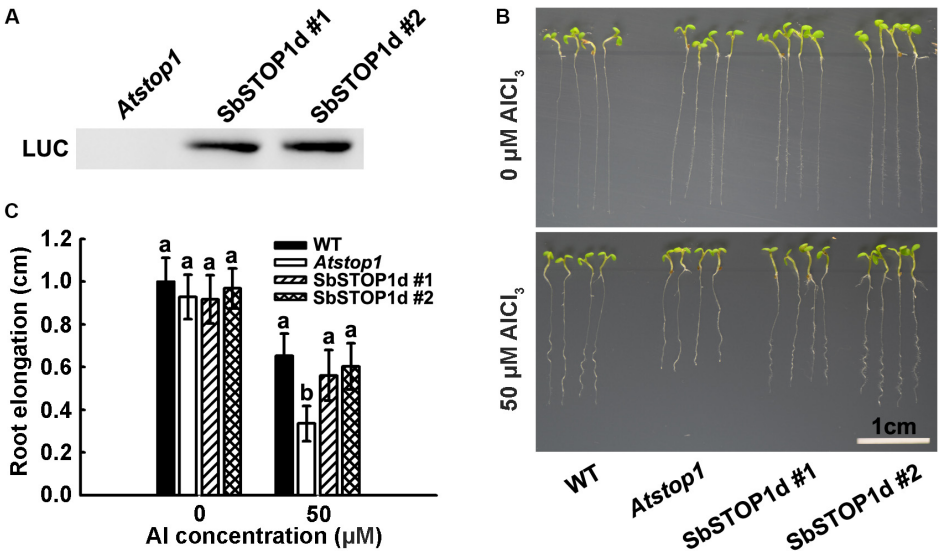

FIGURE 6 | Transgenic *Arabidopsis* expressing *SbSTOP1d* shows improved tolerance to Al stress. **(A)** Immunoblot analysis of LUC-SbSTOP1d fusion protein in two independent complemented lines. **(B)** Al-sensitive phenotype of WT (Col4), *Atstop1* and *SbSTOP1d* complemented lines. Five-day-old seedlings were precultured on solid MS medium, then transferred to solid medium containing 4.3 mM $CaCl_2$ and 3% sucrose at pH 4.5, with or without 50 μM $AlCl_3$. **(C)** Root elongation of WT (Col4), *Atstop1* and *SbSTOP1d* complemented lines with or without Al treatment. Data are means of 20 replicates ± SD. Columns with different letters indicate significant differences between various plants under each Al treatment at $P < 0.05$.

e.g., GATA-1 in erythroid cells self-associates mediated by its zinc finger domain to influence transcription (Crossley et al., 1995). These studies provide a clue that the self-association of SbSTOP1d and association of SbSTOP1d and SbSTOP1b may also be beneficial for the DNA-binding property of SbSTOP1d. Differing from those of other zinc finger TFs, the association of SbSTOP1d itself (or with SbSTOP1b) in the yeast assays occurred at the N-terminal region, which lacks zinc finger domains (**Figures 5A–C**). In addition, SbSTOP1b shows the highest identity with AtSTOP2, except for SbSTOP1c in the sorghum genome database, and closely clusters with AtSTOP2 (**Figure 1B**). AtSTOP2, a homolog of AtSTOP1, was reported to activate transcription of some of the genes regulated by AtSTOP1 (Kobayashi et al., 2014), while the regulatory roles (individual roles or possible partnership) of AtSTOP1 and AtSTOP2 in Al- and low pH-tolerance have not yet been clarified. In the present study, SbSTOP1d and SbSTOP1b, as the homologous proteins of AtSTOP1 and AtSTOP2, respectively, displayed protein-protein interaction (**Figures 5A,C**). This result may help to further clarify the complex signal transduction pathways of STOP1-like proteins in response to Al and/or proton stress.

Complementation assays were conducted introducing multiple *AtSTOP1* orthologous genes in the *Atstop1* mutant background, and the results varied. Overexpression of *PpSTOP1* and *PnSTOP1* could almost fully or partially rescue the Al-sensitive phenotype of *Atstop1*, while CsSTOP1 was somewhat effective in transgenic lines (Ohyama et al., 2013; Sawaki et al., 2014). Here, SbSTOP1d greatly recovered the Al-sensitive phenotype of the *Atstop1* mutant, with nearly 90% of the root elongation of WT, demonstrating the Al tolerance function of SbSTOP1d in plants (**Figure 6**).

In summary, we have identified four STOP1-like genes (*SbSTOP1a*, *SbSTOP1b*, *SbSTOP1c,* and *SbSTOP1d*) in sweet sorghum that encode C_2H_2 zinc finger transcription factors. The expression of all four genes in roots was upregulated by Al stress. Heterologous expression of *SbSTOP1d* in *Atstop1* enhanced the Al tolerance of transgenic plants. SbSTOP1d interacted with itself (self-association) and SbSTOP1b in plants. These results provide a complete characterization of the SbSTOP1s in sweet sorghum and extend the understanding of STOP1-like transcription factors regulating Al tolerance in different plant species.

AUTHOR CONTRIBUTIONS

ZY designed the research and revised the manuscript. SH, JG, YL, KG, SY, and MZ conducted the experiments. SH and JY analyzed the data. JG wrote the manuscript.

FUNDING

This work was supported by the National Natural Science Foundation of China (31572192 and 31701982) and the China Postdoctoral Science Foundation (2017M611327).

SUPPLEMENTARY MATERIAL

The Supplementary Material for this article can be found online at: https://www.frontiersin.org/articles/10.3389/fpls.2018.00258/full#supplementary-material

REFERENCES

Arenhart, R. A., Bai, Y., de Oliveira, L. F., Bucker Neto, L., Schunemann, M., Maraschin Fdos, S., et al. (2014). New insights into aluminum tolerance in rice: the ASR5 protein binds the *STAR1* promoter and other aluminum-responsive genes. *Mol. Plant* 7, 709–721. doi: 10.1093/mp/sst160

Bojórquez-Quintal, E., Escalante-Magaña, C., Echevarría-Machado, I., and Martínez-Estévez, M. (2017). Aluminum, a friend or foe of higher plants in acid soils. *Front. Plant Sci.* 8:1767. doi: 10.3389/fpls.2017.01767

Clough, S. J., and Bent, A. F. (1998). Floral dip: a simplified method for *Agrobacterium*-mediated transformation of *Arabidopsis thaliana*. *Plant J.* 16, 735–743. doi: 10.1046/j.1365-313x.1998.00343.x

Crossley, M., Merika, M., and Orkin, S. H. (1995). Self-association of the erythroid transcription factor GATA-1 mediated by its zinc finger domains. *Mol. Cell. Biol.* 15, 2448–2456. doi: 10.1128/MCB.15.5.2448

Ding, Z. J., Yan, J. Y., Xu, X. Y., Li, G. X., and Zheng, S. J. (2013). WRKY46 functions as a transcriptional repressor of *ALMT1*, regulating aluminum-induced malate secretion in *Arabidopsis*. *Plant J.* 76, 825–835. doi: 10.1111/tpj.12337

Fan, W., Lou, H. Q., Gong, Y. L., Liu, M. Y., Cao, M. J., Liu, Y., et al. (2015). Characterization of an inducible C2H2-type zinc finger transcription factor VuSTOP1 in rice bean (*Vigna umbellata*) reveals differential regulation between low pH and aluminum tolerance mechanisms. *New Phytol.* 208, 456–468. doi: 10.1111/nph.13456

Foy, C. D. (1983). The physiology of plant adaptation to mineral stress. *Iowa State J. Res.* 57, 355–391.

Foy, C. D. (1988). Plant adaptation to acid, aluminum-toxic soils. *Commun. Soil Sci. Plant Anal.* 19, 959–987. doi: 10.1080/00103628809367988

Furukawa, J., Yamaji, N., Wang, H., Mitani, N., Murata, Y., Sato, K., et al. (2007). An aluminum-activated citrate transporter in barley. *Plant Cell Physiol.* 48, 1081–1091. doi: 10.1093/pcp/pcm091

Gao, J., Wang, X., Zhang, M., Bian, M., Deng, W., Zuo, Z., et al. (2015). Trp triad-dependent rapid photoreduction is not required for the function of *Arabidopsis* CRY1. *Proc. Natl. Acad. Sci. U.S.A.* 112, 9135–9140. doi: 10.1073/pnas.1504404112

Huang, C. F., Yamaji, N., and Ma, J. F. (2010). Knockout of a bacterial-type ATP-binding cassette transporter gene, *AtSTAR1*, results in increased aluminum sensitivity in *Arabidopsis*. *Plant Physiol.* 153, 1669–1677. doi: 10.1104/pp.110.155028

Huang, C. F., Yamaji, N., Mitani, N., Yano, M., Nagamura, Y., and Ma, J. F. (2009). A bacterial-type ABC transporter is involved in aluminum tolerance in rice. *Plant Cell* 21, 655–667. doi: 10.1105/tpc.108.064543

Iuchi, S., Koyama, H., Iuchi, A., Kobayashi, Y., Kitabayashi, S., Kobayashi, Y., et al. (2007). Zinc finger protein STOP1 is critical for proton tolerance in *Arabidopsis* and coregulates a key gene in aluminum tolerance. *Proc. Natl. Acad. Sci. U.S.A.* 104, 9900–9905. doi: 10.1073/pnas.0700117104

Jakoby, M., Weisshaar, B., Dröge-Laser, W., Vicente-Carbajosa, J., Tiedemann, J., Kroj, T., et al. (2002). bZIP transcription factors in *Arabidopsis*. *Trends Plant Sci.* 7, 106–111. doi: 10.1016/S1360-1385(01)02223-3

Kobayashi, Y., Ohyama, Y., Kobayashi, Y., Ito, H., Iuchi, S., Fujita, M., et al. (2014). STOP2 activates transcription of several genes for Al- and low pH-tolerance that are regulated by STOP1 in *Arabidopsis*. *Mol. Plant* 7, 311–322. doi: 10.1093/mp/sst116

Kochian, L. V., Hoekenga, O. A., and Piñeros, M. A. (2004). How do crop plants tolerate acid soils? Mechanisms of aluminum tolerance and phosphorous efficiency. *Annu. Rev. Plant Biol.* 55, 459–493. doi: 10.1146/annurev.arplant.55.031903.141655

Kochian, L. V., Piñeros, M. A., Liu, J., and Magalhaes, J. V. (2015). Plant adaptation to acid soils: the molecular basis for crop aluminum resistance. *Annu. Rev. Plant Biol.* 66, 571–598. doi: 10.1146/annurev-arplant-043014-114822

Li, J. Y., Liu, J., Dong, D., Jia, X., Mccouch, S. R., and Kochian, L. V. (2014). Natural variation underlies alterations in Nramp aluminum transporter (*NRAT1*) expression and function that play a key role in rice aluminum tolerance. *Proc. Natl. Acad. Sci. U.S.A.* 111, 6503–6508. doi: 10.1073/pnas.1318975111

Liu, J., Magalhaes, J. V., Shaff, J., and Kochian, L. V. (2009). Aluminum-activated citrate and malate transporters from the MATE and ALMT families function independently to confer *Arabidopsis* aluminum tolerance. *Plant J.* 57, 389–399. doi: 10.1111/j.1365-313X.2008.03696.x

Liu, J., Piñeros, M. A., and Kochian, L. V. (2014). The role of aluminum sensing and signaling in plant aluminum resistance. *J. Integr. Plant Biol.* 56, 221–230. doi: 10.1111/jipb.12162

Livak, K. J., and Schmittgen, T. D. (2001). Analysis of relative gene expression data using real-time quantitative PCR and the $2^{-\Delta\Delta C_T}$ method. *Methods* 25, 402–408. doi: 10.1006/meth.2001.1262

Ma, J. F. (2000). Role of organic acids in detoxification of aluminum in higher plants. *Plant Cell Physiol.* 41, 383–390. doi: 10.1093/pcp/41.4.383

Ma, J. F. (2007). Syndrome of aluminum toxicity and diversity of aluminum resistance in higher plants. *Int. Rev. Cytol.* 264, 225–252. doi: 10.1016/s0074-7696(07)64005-4

Magalhaes, J. V., Liu, J., Guimarães, C. T., Lana, U. G. P., Alves, V. M. C., Wang, Y. H., et al. (2007). A gene in the multidrug and toxic compound extrusion (MATE) family confers aluminum tolerance in sorghum. *Nat. Genet.* 39, 1156–1161. doi: 10.1038/ng2074

Meng, Y., Li, H., Wang, Q., Liu, B., and Lin, C. (2013). Blue light-dependent interaction between Cryptochrome2 and CIB1 regulates transcription and leaf senescence in soybean. *Plant Cell* 25, 4405–4420. doi: 10.1105/tpc.113.116590

Moreno-Alvarado, M., García-Morales, S., Trejo-Téllez, L. I., Hidalgo-Contreras, J. V., and Gómez-Merino, F. C. (2017). Aluminum enhances growth and sugar concentration, alters macronutrient status and regulates the expression of *NAC* transcription factors in rice. *Front. Plant Sci.* 8:73. doi: 10.3389/fpls.2017.00073

Negishi, T., Oshima, K., Hattori, M., Kanai, M., Mano, S., Nishimura, M., et al. (2012). Tonoplast- and plasma membrane-localized aquaporin-family transporters in blue hydrangea sepals of aluminum hyperaccumulating plant. *PLoS One* 7:e43189. doi: 10.1371/journal.pone.0043189

Negishi, T., Oshima, K., Hattori, M., and Yoshida, K. (2013). Plasma membrane-localized Al-transporter from blue hydrangea sepals is a member of the anion permease family. *Genes Cells* 18, 341–352. doi: 10.1111/gtc.12041

Ohyama, Y., Ito, H., Kobayashi, Y., Ikka, T., Morita, A., Kobayashi, M., et al. (2013). Characterization of *AtSTOP1* orthologous genes in tobacco and other plant species. *Plant Physiol.* 162, 1937–1946. doi: 10.1104/pp.113.218958

Ryan, P. R., Delhaize, E., and Jones, D. L. (2001). Function and mechanism of organic anion exudation from plant roots. *Annu. Rev. Plant Physiol. Plant Mol. Biol.* 52, 527–560. doi: 10.1146/annurev.arplant.52.1.527

Sasaki, T., Yamamoto, Y., Ezaki, B., Katsuhara, M., Ahn, S. J., Ryan, P. R., et al. (2004). A wheat gene encoding an aluminum-activated malate transporter. *Plant J.* 37, 645–653. doi: 10.1111/j.1365-313X.2003.01991.x

Sawaki, Y., Iuchi, S., Kobayashi, Y., Kobayashi, Y., Ikka, T., Sakurai, N., et al. (2009). STOP1 regulates multiple genes that protect *Arabidopsis* from proton and aluminum toxicities. *Plant Physiol.* 150, 281–294. doi: 10.1104/pp.108.134700

Sawaki, Y., Kobayashi, Y., Kihara-Doi, T., Nishikubo, N., Kawazu, T., Kobayashi, M., et al. (2014). Identification of a STOP1-like protein in *Eucalyptus* that regulates transcription of Al tolerance genes. *Plant Sci.* 223, 8–15. doi: 10.1016/j.plantsci.2014.02.011

Schindler, U., Menkens, A. E., Beckmann, H., Ecker, J. R., and Cashmore, A. R. (1992). Heterodimerization between light-regulated and ubiquitously expressed Arabidopsis GBF bZIP proteins. *EMBO J.* 11, 1261–1273.

Singh, K. B., Foley, R. C., and Oñate-Sánchez, L. (2002). Transcription factors in plant defense and stress responses. *Curr. Opin. Plant Biol.* 5, 430–436. doi: 10.1016/S1369-5266(02)00289-3

Tsutsui, T., Yamaji, N., and Ma, J. F. (2011). Identification of a cis-acting element of ART1, a C2H2-type zinc-finger transcription factor for aluminum tolerance in rice. *Plant Physiol.* 156, 925–931. doi: 10.1104/pp.111.175802

Uno, Y., Furihata, T., Abe, H., Yoshida, R., Shinozaki, K., and Yamaguchi-Shinozaki, K. (2000). *Arabidopsis* basic leucine zipper transcription factors involved in an abscisic acid-dependent signal transduction pathway under drought and high-salinity conditions. *Proc. Natl. Acad. Sci. U.S.A.* 97, 11632–11637. doi: 10.1073/pnas.190309197

Xu, J. M., Fan, W., Jin, J. F., Lou, H. Q., Chen, W. W., Yang, J. L., et al. (2017). Transcriptome analysis of Al-induced genes in buckwheat (*Fagopyrum esculentum* Moench) root apex: new insight into Al toxicity and resistance mechanisms in an Al accumulating species. *Front. Plant Sci.* 8:1141. doi: 10.3389/fpls.2017.01141

Xu, L., Xu, Z., Liu, X., Huang, Y., He, X., Ma, H., et al. (2015). The subcellular localization and ectopic expression analysis in *Arabidopsis* of

soybean *GmbZIP60* gene. *J. Plant Biochem. Biotechnol.* 24, 9–17. doi: 10.1007/s13562-013-0228-4

Yamaji, N., Huang, C. F., Nagao, S., Yano, M., Sato, Y., Nagamura, Y., et al. (2009). A zinc finger transcription factor ART1 regulates multiple genes implicated in aluminum tolerance in rice. *Plant Cell* 21, 3339–3349. doi: 10.1105/tpc.109.070771

Yang, X. Y., Yang, J. L., Zhou, Y., Piñeros, M. A., Kochian, L. V., Li, G. X., et al. (2011). A *de novo* synthesis citrate transporter, *Vigna umbellata* multidrug and toxic compound extrusion, implicates in Al-activated citrate efflux in rice bean (*Vigna umbellata*) root apex. *Plant Cell Environ.* 34, 2138–2148. doi: 10.1111/j.1365-3040.2011.02410.x

Yokosho, K., Yamaji, N., and Ma, J. F. (2011). An Al-inducible MATE gene is involved in external detoxification of Al in rice. *Plant J.* 68, 1061–1069. doi: 10.1111/j.1365-313X.2011.04757.x

Zhang, H., Shi, W. L., You, J. F., Bian, M. D., Qin, X. M., Yu, H., et al. (2015). Transgenic *Arabidopsis thaliana* plants expressing a beta-1,3-glucanase from sweet sorghum (*Sorghum bicolor* L.) show reduced callose deposition and increased tolerance to aluminium toxicity. *Plant Cell Environ.* 38, 1178–1188. doi: 10.1111/pce.12472

Conflict of Interest Statement: The authors declare that the research was conducted in the absence of any commercial or financial relationships that could be construed as a potential conflict of interest.

frontiers in Plant Science

ORIGINAL RESEARCH
published: 14 February 2018
doi: 10.3389/fpls.2018.00118

The Cell Cycle Checkpoint Regulator ATR Is Required for Internal Aluminum Toxicity-Mediated Root Growth Inhibition in *Arabidopsis*

Yang Zhang[1,2†], Jinliang Guo[1,2†], Mo Chen[1], Lun Li[1,2], Lihua Wang[3] and Chao-Feng Huang[1,2]*

[1] College of Resources and Environmental Sciences, Nanjing Agricultural University, Nanjing, China, [2] Shanghai Center for Plant Stress Biology, National Key Laboratory of Plant Molecular Genetics, CAS Center for Excellence in Molecular Plant Sciences, Chinese Academy of Sciences, Shanghai, China, [3] Flower Research Institute, Yunnan Academy of Agricultural Sciences, Kunming, China

OPEN ACCESS

Edited by:
Jian Li Yang,
Zhejiang University, China

Reviewed by:
He Qiang Lou,
Zhejiang A & F University, China
Wei Fan,
Yunnan Agricultural University, China
Cuiyue Liang,
South China Agricultural University, China

***Correspondence:**
Chao-Feng Huang
cfhuang@sibs.ac.cn

[†] These authors have contributed equally to this work.

Specialty section:
This article was submitted to Plant Nutrition, a section of the journal Frontiers in Plant Science

Received: 13 November 2017
Accepted: 22 January 2018
Published: 14 February 2018

Citation:
Zhang Y, Guo J, Chen M, Li L, Wang L and Huang C-F (2018) The Cell Cycle Checkpoint Regulator ATR Is Required for Internal Aluminum Toxicity-Mediated Root Growth Inhibition in Arabidopsis. Front. Plant Sci. 9:118. doi: 10.3389/fpls.2018.00118

Aluminum (Al) can target multiple sites of root cells for toxicity, including the cell wall, the plasma membrane and symplastic components. Previous work revealed that the cell cycle checkpoint regulator (ATR) Ataxia Telangiectasia-mutated and Rad3-related is required for Al toxicity-induced root growth inhibition in *als3* and that the symplastic component DNA is an important target site of Al for the toxicity. However, whether monitoring DNA integrity through ATR-regulated pathway is required for Al-induced root growth inhibition in other Al-sensitive mutants remains unknown. In this study, we demonstrated that the *atr* mutation could also rescue the Al hypersensitivity and Al-induced cell cycle arrest in *star1*, which supports the hypothesis that ALS3 and STAR1 function together to be involved in the detoxification of Al in *Arabidopsis*. However, mutation of *ATR* could not rescue the Al-sensitive phenotype of *almt1* or *stop1*, both of which are defective in external detoxification mechanisms of Al. We further showed that the Al hypersensitivity and Al-induced quiescent center (QC) differentiation in *als1* could also be rescued by the *atr* mutation. Therefore, our results suggest that ATR-regulated pathway is involved in the modulation of internal Al toxicity-mediated root growth inhibition in *Arabidopsis*.

Keywords: aluminum toxicity, *Arabidopsis thaliana*, ATR, cell cycle checkpoint, DNA damage, external, internal

INTRODUCTION

Aluminum (Al) comprises about 7% of the earth's crust and is the most abundant metallic element. In neutral or alkaline soils, Al exists as insoluble aluminosilicates or oxides, which are non-toxic to plants. However, in acid soils with a pH of 5.5 or lower, solubilization of Al is enhanced and phytotoxic forms of Al are released into soil to levels that affect root growth. As a consequence, Al toxicity on acid soils becomes one of the most severe global problems since these soils comprise approximately 50% of the world's potentially arable land (von Uexkull and Mutert, 1995; Kochian et al., 2004).

In acidic soils, Al exists as the octahedral hexahydrate $Al(H_2O)_6^{3+}$, which is more commonly referred to as Al^{3+}. The phytotoxic Al^{3+} is the hardest Lewis acid, which is characterized by

a low covalent and a high ionic index. Hard metal ions have strong interactions with organic molecules bearing oxygen groups (Poschenrieder et al., 2008). Therefore, Al^{3+} preferentially binds to phosphate, sulfate, and carboxyl groups for toxicity. Considering the components of a plant cell, Al is believed to target multiple sites for toxicity, including the cell wall, the plasma membrane and inside the cells. Cell walls and intercellular spaces are the first sites of the root in contact with Al when the roots are exposed to Al. Many studies have shown that most of the Al is bound to the cell wall. The ratio of cell wall Al to the total Al has been reported to range from 85 to 99.9% (Ma, 2007). Al can also bind to the plasma membrane and alter the membrane fluidity and surface potential (Kinraide, 2001), block ion channel activity (Pineros and Kochian, 2001), and induce the reactive oxygen species (ROS) as well as lipid peroxidation on the plasma membrane (Yamamoto et al., 2001). Furthermore, a small portion of Al can enter the symplasm rapidly and may interact with a number of symplastic targets (Lazof et al., 1996; Silva et al., 2000). For example, Al disrupts the cytoskeleton by interacting with both microtubules and actin filaments (Grabski and Schindler, 1995; Blancaflor et al., 1998), and blocks signal transduction pathways, particularly in Ca^{2+} homeostasis and signaling (Jones and Kochian, 1995; Jones et al., 1998; Zhang and Rengel, 1999). Al can also interact with DNA (Karlik et al., 1980; Karlik and Eichhorn, 1989), which is expected to have serious effects on gene expression and chromosome structure.

To cope with Al toxicity, plants have evolved Al-resistance mechanisms, including external and internal detoxification of Al (Ma et al., 2001; Kochian et al., 2004). In *Arabidopsis thaliana*, external detoxification of Al is primarily achieved through AtALMT1-mediated secretion of malate to form a non-toxic form of Al-malate in the apoplast (Hoekenga et al., 2006), and the citrate transport AtMATE play a minor role in the external detoxification of Al (Liu et al., 2009). STOP1, a C2H2 transcription factor, is involved in the detoxification of Al mainly through the regulation of *AtALMT1* expression (Iuchi et al., 2007). For the internal detoxification of Al, the tonoplast-localized ATP-binding cassette (ABC) transporter ALS1 is required, which tolerates Al presumably via the transport of cytosolic Al into vacuoles (Larsen et al., 2007). STAR1 and STAR2/ALS3 encode a nucleotide-binding domain and transmembrane domain of a bacterial-type ABC transporter, respectively, and are suggested to be involved in Al tolerance through modification of cell wall or redistribution of Al from Al-sensitive root tips to other less Al-sensitive tissues (Larsen et al., 2005; Huang et al., 2009, 2010). Recently, Dong et al. (2017) reported that unlike rice STAR1 and STAR2, *Arabidopsis* ALS3 interacts with AtASTAR1 to be localized to the tonoplast, suggesting that AtSTAR1/ALS3 might be also required for the internal detoxification of Al.

Through the screening of the suppressors of the Al hypersensitivity of *als3* mutant, Gabrielson et al. (2006) identified a dozen of suppressor mutants, and two of them had different mutations on the same gene *ATR* (Rounds and Larsen, 2008). ATR (Ataxia Telangiectasia-mutated and Rad3-related) is a cell cycle checkpoint regulator that functions in detecting DNA damage and then halting cell division (Culligan et al., 2004). *atr* mutant is hypersensitive to clastogenic and genotoxic stresses, but shows increased tolerance to Al because of failure to halt cell cycle progression. Together with the recovery of the Al hypersensitivity of *als3* by the *atr* mutation, the results suggest that Al acts as a mild genotoxic agent and can target DNA to arrest root growth through ATR-regulated pathway (Rounds and Larsen, 2008).

In this study, to determine whether ATR-dependent pathway is required for the Al hypersensitivity in all Al-sensitive mutants, we created a series of double mutants between Al-sensitive mutants and *atr* mutant and then evaluated their sensitivity to Al in *Arabidopsis*. Our results revealed that the *atr* mutation could rescue the Al-sensitive phenotype of *als3*, *star1* and *als1*, but not that of *almt1* and *stop1*. These findings suggest that ATR-regulated pathway is required for internal Al toxicity-induced root growth inhibition.

MATERIALS AND METHODS

Plant Materials and Growth Conditions

Arabidopsis thaliana (Columbia ecotype, Col-0) was used for all the control experiments. The T-DNA insertion lines *atr* (SALK_032841C), *star1* (GABI_762A06), *als3* (SALK_004094), *stop1* (SALK_114108), *almt1* (SALK_00962) and the mutant *als1-1* (CS3847) were all derived from uNASC[1]. Plants were grown in a growth chamber or controlled room at 22–25°C with 14 h of light and 10 h of darkness.

Mutant Genotyping

To select homozygous mutants of *atr*, *als3*, *star1*, *stop1*, and *almt1*, primer pairs flanked each T-DNA insertion were used as follows: *ATR* (5′-ACTGCATGCCAT TTACTCCTAC-3′ and 5′-GATCAGCTTGATCATCCAAACT-3′), *ALS3* (5′- CAA TGTTCTTGCTCGTCCTCCT-3′ and 5′-TGGTTCACGTAGTG GGCCATCG-3′), *STAR1* (5′-TCGTAGAGTTGGAATGCTTTT TC-3′ and 5′-GTTGAAGAAACCTCTGTGCCATT-3′), *ALMT1* (5′-TTGAGAGAGCTGAGTGACCA-3′ and 5′-ACAAC GA TATCAGCGCGAAC-3′), and *STOP1* (5′-TCTTAAAGCGG CCATTGGTG-3′ and 5′-TTAGAGACTAGTATCTGAAACAG ACTCAC-3′). For *als1-1* mutant, a dCAPS (derive Cleaved Amplified Polymorphic sequences) marker was developed by using a primer pair (5′-TGTGAAACAGTTTGGTCGCT-3′ and 5′-TGCGTTTAGTCCTCCGAAGA-3′) and a restriction endonuclease TfiI. To generate double or triple mutants, crosses were made between *atr* and each Al-sensitive mutant or between *als3atr* and *star1* and then the derived F2 plants were genotyped and selected. For genotyping of *CyclinB1;1* and *QC46* marker lines, a primer pair for the *GUS* gene was used (5′-ATGTTACGTCCTGTAGAAACC-3′ and 5′-TCATTGTTTGCCTCCC TGCTGC-3′).

RNA Isolation and Expression Analysis

Seeds were sterilized and stratified at 4°C for 2 days and then sowed on a 0.3% Gellan gum (G1910; Sigma–Aldrich) nutrient

[1]http://szlapncs01.nottingham.ac.uk/

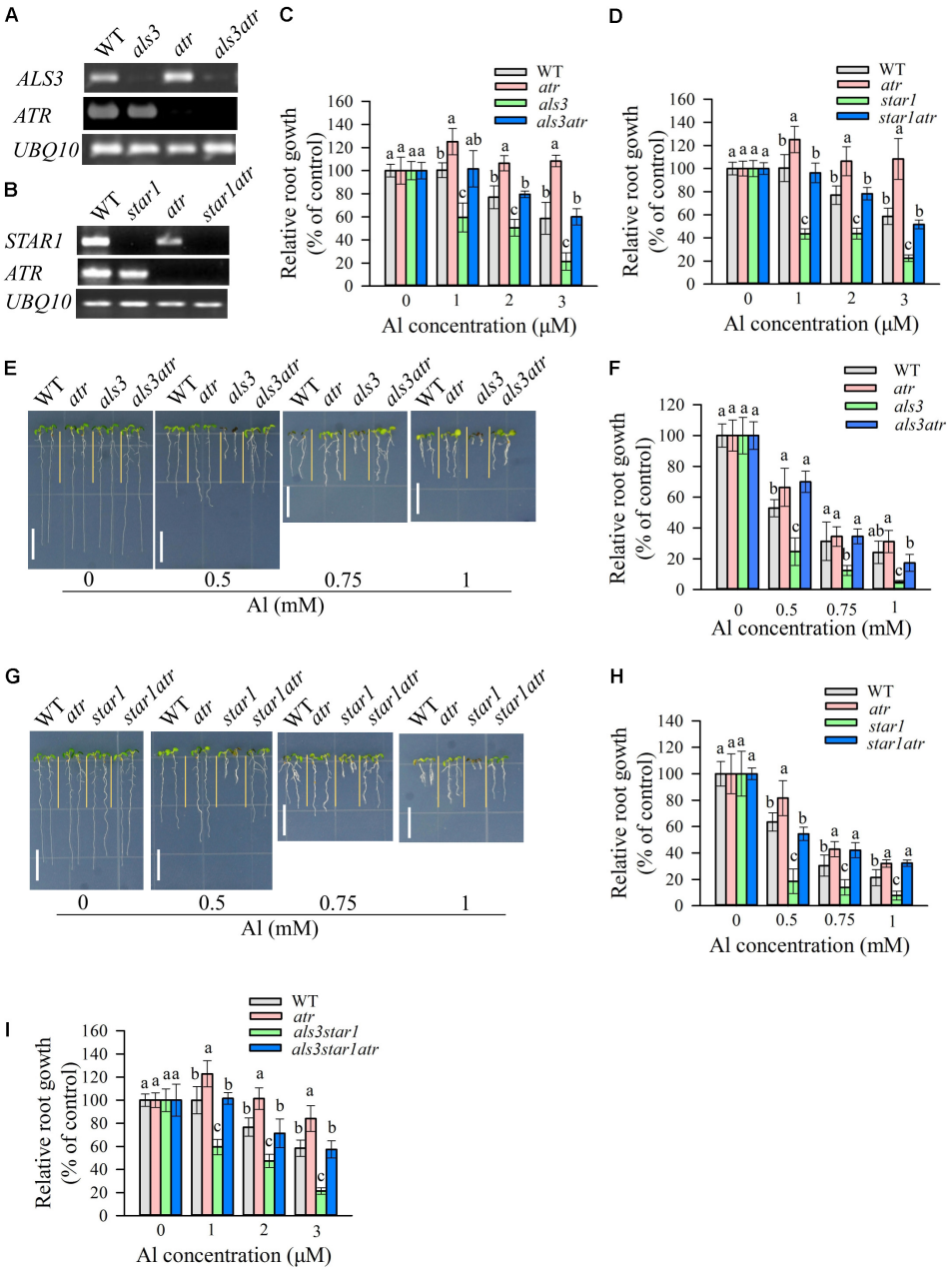

FIGURE 1 | Rescue of the Al-sensitive phenotype of *als3* and *star1* by *atr* mutation. **(A,B)** RT-PCR analysis of *ATR*, *ALS3,* or *STAR1* in WT and different single or double mutants. UBQ10 was used as internal control. **(C,D)** Evaluation of Al tolerance in *als3* **(C)** or *star1* **(D)**-related mutants in hydroponic conditions. Seedlings were grown on a nutrient solution containing 0, 1, 2, or 3 μM Al at pH 5.0 for 7 days and then root length was measured and compared. Data are means ± SD (n = 15–20). **(E–H)** Evaluation of Al tolerance in soaked gel conditions. Seedlings were grown on a soaked gel medium containing 0, 0.5, 0.75, or 1 mM Al for 7 days. Data are means ± SD (n = 10–15). **(E,F)** Rescue of the Al-sensitive phenotype of *als3* by *atr*. **(G,H)** Rescue of the Al-sensitive phenotype of *star1* by *atr*. **(I)** Rescue of the Al-sensitive phenotype of *als3star1* by *atr* in hydroponic conditions. Means with different letters are significantly different ($P < 0.05$, Tukey's test). Scale bar = 1 cm.

medium consisting of 1 mM KNO_3, 0.2 mM KH_2PO_4, 2 mM $MgSO_4$, 0.25 mM $(NH_4)_2SO_4$, 1 mM $Ca(NO_3)2$, 1 mM $CaSO_4$, 1 mM K_2SO_4, 1 μM $MnSO_4$, 5 μM H_3BO_3, 0.05 μM $CuSO_4$, 0.2 μM $ZnSO_4$, 0.02 μM $NaMoO_4$, 0.1 μM $CaCl_2$, 0.001 μM $CoCl_2$ and 1% sucrose. After 7 days growth, the seedlings were transferred to a 0.5 mM $CaCl_2$ solution for 6 h pretreatment at pH 4.8 and then exposed to a 0.5 mM $CaCl_2$ solution (pH 4.8) with or without 20 μM $AlCl_3$ for 12 h. Total RNA was extracted using TaKaRa MiniBEST plant RNA Extraction Kit (Cat # 9769). Around one microgram total RNA was first digested with DNase I and then subjected for the synthesis of first-strand cDNAs by using HiScript® 1st Strand cDNA Synthesis Kit (Vazyme Biotech

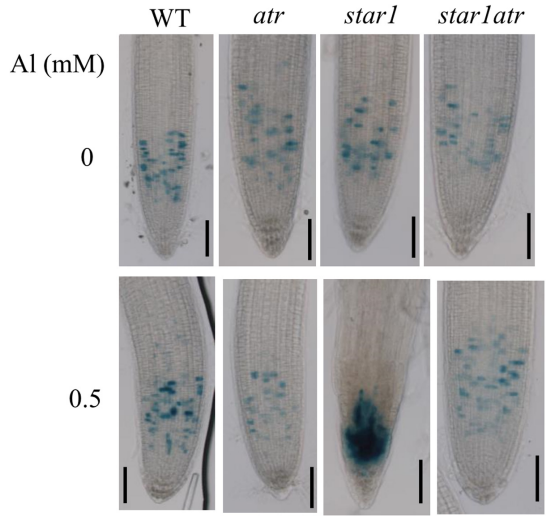

FIGURE 2 | Rescue of cell cycle progression defects in *star1* by *atr* mutation under Al stress conditions. Seedlings of WT, *atr*, *star1,* and *star1atr* harboring *CycB1;1:GUS* marker were grown on a soaked gel medium containing 0 or 0.5 mM Al for 7 days and the roots were stained and observed under a microscope. Scale bar = 50 μm.

Co., Ltd., Nanjing, China). One twentieth of the cDNA products and the SYBR® Green Master Mix kit (Vazyme Biotech Co., Ltd., Nanjing, China) were used for RT-PCR and real-time RT-PCR analysis. The primers for RT-PCR analysis of *ATR*, *ALS3*, *STAR1*, *ALMT1,* and *STOP1* were same to those primers for genotyping as shown above. The primers for real-time RT-PCR analysis were as follows: *ATR* (5′-CTGACTGAGGACTGTGGTCTGGT-3′ and 5′-GACGGTCACCAAGCCCAACA-3′), *ALS3* (5′-CGTATCTC TTCATGGTCTCTGTCG-3′ and 5′-GTAACTCCGGTGACGGT CATG-3′), *STAR1* (5′-TTCAAGGGACTGTTGCGGATA-3′ and 5′-AAGAGCACTTGTTGGTTCATCG-3′), *ALS1* (5′-GCCTCA CAGTTGGTTCATCGG-3′ and 5′-GTCGTTTTTCCTCCACCG CT-3′), *ALMT1* (5′-TGCAAGCTGCGTTGTCGAC-3′ and 5′-CAAAATCTTGAAGGAAGTGGGAG-3′) and *STOP1* (5′-TCACATAGCTCTGTTCCAGGGA-3′ and 5′-ATCAGTCATTC CAGGCTGTGT-3′). *UBQ10* was used as an internal control and the forward and reverse prime sequences of *UBQ10* are 5′-CGTCTTCGTGGTGGTTTCTAA-3′ and 5′-GGATTATACA AGGCCCCAAAA-3′, respectively.

Evaluation of Sensitivity to Al

For assessment of Al sensitivity in hydroponic conditions, we referred to a previous method with slight modifications (Huang et al., 2010). Briefly, seeds of each line were stratified at 4°C for 2 days and then sowed on a plastic mesh floating on a 1/30 strength Hoagland nutrient solution ($NH_4H_2PO_4$ omitted) plus 1 mM $CaCl_2$ and different concentrations of $AlCl_3$ at pH 5.0 for 7 days. The solution was renewed every 3 days. After the treatment, the seedlings were photographed and root length was measured by ImageJ. Relative root growth expressed as (root length with Al treatment/root length without Al) × 100 was used to evaluate the Al sensitivity. For soaked gel experiments, we adopted the method developed by Larsen et al. (2005). Nutrient agar medium was first prepared, which consisted of 50 ml of 1 mM KNO_3, 0.2 mM KH_2PO_4, 2 mM $MgSO_4$, 0.25 mM $(NH_4)_2SO_4$, 1 mM $Ca(NO_3)_2$, 1 mM $CaSO_4$, 1 mM K_2SO_4, 1 μM $MnSO_4$, 5 μM H_3BO_3, 0.05 μM $CuSO_4$, 0.2 μM $ZnSO_4$, 0.02 μM $NaMoO_4$, 0.1 μM $CaCl_2$, 0.001 μM $CoCl_2$, 1% sucrose, and 0.3% Gellan gum (G1910; Sigma–Aldrich). The agar medium was then soaked with 25 ml of the same nutrient medium containing 0, 0.5, 0.75, or 1 mM $AlCl_3$. After 2 days soaking, the solution was removed and seeds were grown on the agar medium plates for 7 days. The seedlings were then pictured and compared and the root length was measured by ImageJ.

GUS Activity Assay

To investigate the effect of Al on Cyclin B1;1 accumulation, seeds of *CycB1;1:GUS* –containing WT, *atr*, *star1*, and *star1atr* were grown on a soaked gel medium containing 0 or 0.5 mM $AlCl_3$ for 7 days. The seedlings were then stained with a commercialized GUS staining solution (161031; O'Biolab Co., Ltd., Beijing, China) for 2 h at 37°C. For determination of the status of the quiescent center (QC) after Al treatment, seeds of QC46 (GUS-based QC marker)-containing WT, *atr*, *als1*, and *als1atr* were grown on a soaked gel medium containing 0 or 1.5 mM $AlCl_3$. After growth for 7 days, the seedlings were stained with the GUS staining solution overnight at 37°C. Stained tissues were observed and photographed with a microscope (Olympus BX53F, Japan).

RESULTS

Mutation of *ATR* Rescued the Al-Sensitive Phenotype of Both *als3* and *star1* Mutants

To confirm the previous observation that mutation of *ATR* could rescue the Al-sensitive phenotype of *als3* (Rounds and Larsen, 2008), we generated *als3atr* double mutant through a genetic cross between *atr* and *als3* single mutants. RT-PCR analysis revealed that *ATR* and *ALS3* were knocked out in respective single or double mutants (**Figure 1A**). We evaluated the tolerance of WT, *atr*, *als3,* and *als3atr* mutants to Al in both hydroponic and soaked gel conditions. Consistent with previous results, *atr* mutant showed more tolerance to Al than WT, and the *atr* mutation was able to reduce the sensitivity of *als3* to Al at all Al concentrations (**Figures 1C,E,F**). Nevertheless, mutation of *ATR* was not able to fully rescue the Al-sensitive phenotype of *als3*, especially at high Al concentrations (**Figures 1C,E,F**), suggesting that other Al toxicity mechanisms are also required for Al-induced growth inhibition in *als3* mutant. As STAR1 interacts with ALS3 to be involved in the regulation of Al tolerance in *Arabidopsis* (Huang et al., 2010; Dong et al., 2017), we investigated whether the *atr* mutation could also rescue the Al-sensitive phenotype of *star1*. We generated *star1atr* double mutant through crossing and genotyping and RT-PCR analysis confirmed that both *STAR1* and *ATR* were knocked out in the double mutant (**Figure 1B**). Evaluation of Al tolerance in the

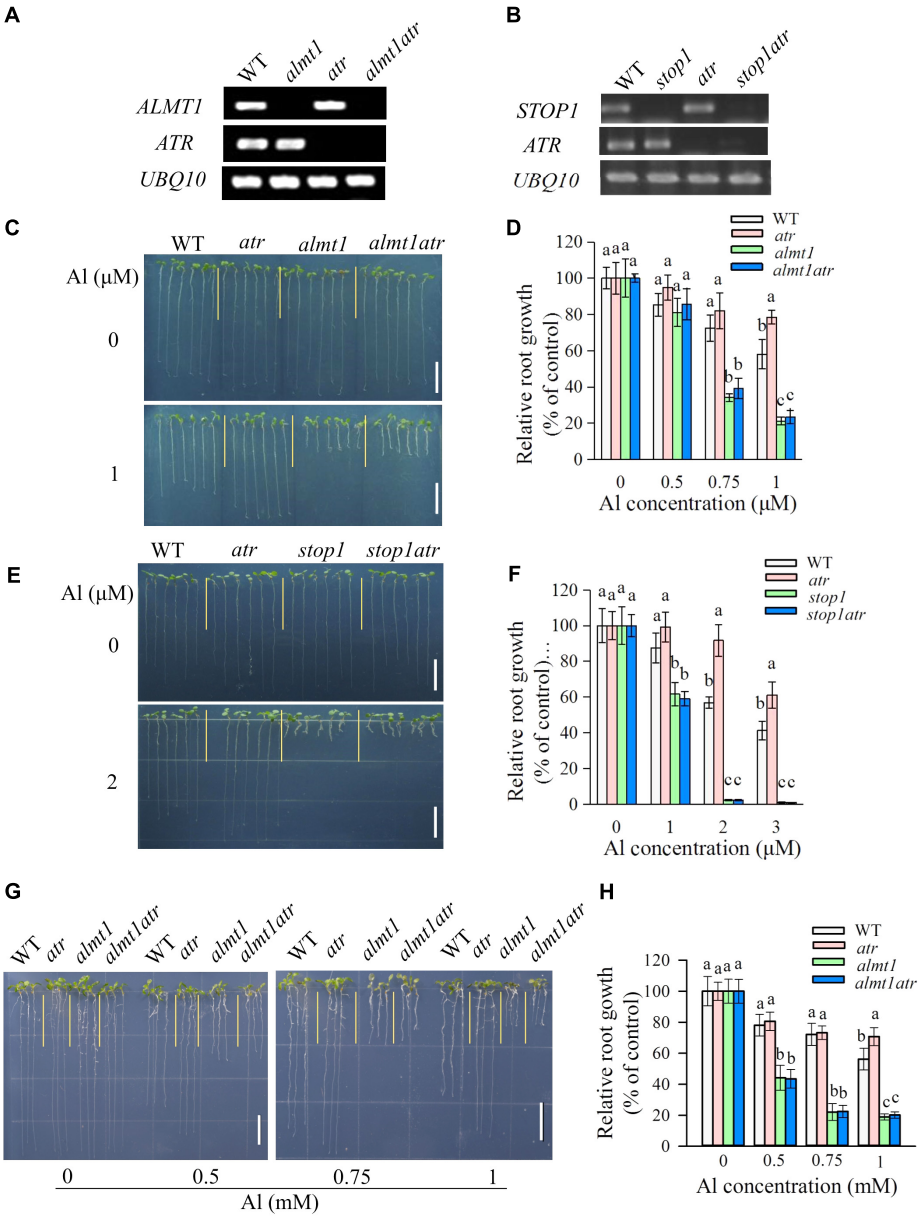

FIGURE 3 | The Al hypersensitivity defects in *almt1* and *stop1* could not be rescued by the *atr* mutation. **(A,B)** RT-PCR analysis of *ATR*, *ALMT1*, or *STOP1* in WT and different single or double mutants. UBQ10 was used as internal control. **(C–F)** Evaluation of Al tolerance in *almt1* **(C,D)** or *stop1* **(E,F)**-related mutants in hydroponic conditions. Seedlings were grown on a nutrient solution with different concentrations of Al at pH 5.0 for 7 days and then root length was measured and compared. Data are means ± SD (n = 15–20). **(G,H)** Evaluation of Al tolerance in *almt1*-related mutants in soaked gel conditions. Seedlings were grown on a soaked gel medium containing 0, 0.5, 0.75, or 1 mM Al for 7 days. Data are means ± SD (n = 10–15). Means with different letters are significantly different ($P < 0.05$, Tukey's test). Scale bar = 1 cm.

double mutant showed that *star1atr* was more tolerant to Al than *star1* at all Al concentrations (**Figures 1D,G,H**), indicating that ATR is required for Al-induced growth inhibition in *star1* mutant. Additionally, similar to that in *als3atr* mutant, mutation of *ATR* did not fully rescue the Al-sensitive phenotype of *star1* (**Figures 1D,G,H**). We also generated *star1als3* and *star1als3atr* mutants to further investigate whether mutation of *ATR* could rescue the Al sensitivity in *star1als3* double mutant. Results showed that the Al-sensitive phenotype of *star1als3* could also be rescued by the introduction of the *atr* mutation (**Figure 1I**). Together, these results confirm that STAR1 and ALS3 regulate Al tolerance through the same pathway and indicate that ATR-dependent pathway is also required for Al-induced growth inhibition in *star1* mutant.

Al-induced inhibition of root growth was correlated with the increase in the number of cells trapped in the G2 stage,

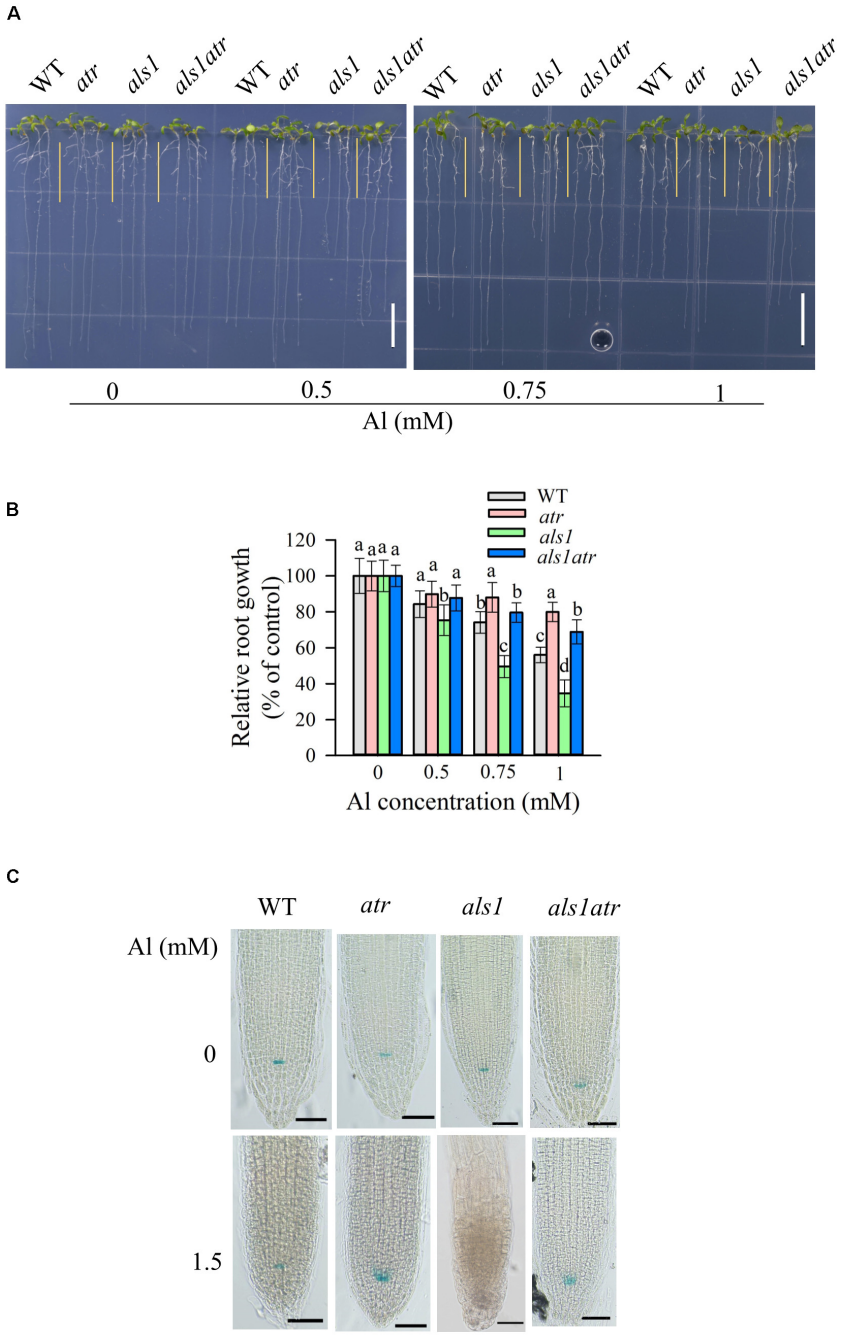

FIGURE 4 | Rescue of the Al-sensitive phenotype of *als1* by *atr* mutation. **(A,B)** Seedlings of WT, *atr*, *als1,* and *als1atr* were grown on a soaked gel medium containing 0, 0.5, 0.75, or 1 mM Al for 7 days. Data are means ± SD (n = 10–15). Means with different letters are significantly different ($P < 0.05$, Tukey's test). Scale bar = 1 cm. **(C)** Rescue of QC differentiation of *als1* by *atr* mutation. Seedlings of WT, *atr*, *als1,* and *als1atr* harboring *QC46* (QC-specific marker) were grown on a soaked gel medium containing 0 or 1.5 mM Al for 7 days and the roots were stained with GUS staining solution and observed under a microscope. Scale bar = 50 μm.

which causes the hyperaccumulation of Cyclin B1;1 in root tips (Rounds and Larsen, 2008). To examine the effect of Al on the accumulation of Cyclin B1;1 in *star1* mutant background, we introduced *CycB1;1:GUS* into *atr*, *star1* and *star1atr* through crossing. In the absence of Al, GUS expression was detected at relatively low levels in all the materials (**Figure 2**). After exposure to a low toxic level of Al, while GUS activity was slightly increased in WT, GUS expression in *star1* was dramatically increased in root tips, suggesting that cell cycle progression was halted in *star1* (**Figure 2**). In *star1atr*, GUS activity was detected at similar low

levels to that in WT and *atr*, which suggested that the arrest of cell cycle progression in *star1* was rescued by the *atr* mutation. The Cyclin B1;1 expression results support the conclusion that knockout of *ATR* is able to rescue the Al hypersensitivity in *star1*.

The *atr* Mutation Could Not Rescue the Al Hypersensitivity in Either *almt1* or *stop1* Mutants

To investigate whether mutation of *ATR* could rescue the hypersensitivity of *almt1* and *stop1* to Al, we introduced the *atr* mutation into *stop1* and *almt1* mutants by crossing and genotyping, respectively. RT-PCR analysis confirmed that *ALMT1* or *STOP1* were knocked out in the corresponding mutants (**Figures 3A,B**). Phenotypic analysis of Al tolerance showed that the tolerance of *almt1atr* to Al did not differ from that of *almt1* at all Al concentrations in both hydroponic and soaked gel conditions (**Figures 3C,D,G,H**), indicating that mutation of *ATR* could not rescue Al-sensitive phenotype of *almt1*. Similarly, Al tolerance in *stop1atr* was also not different from that in *stop1* under all Al treatment (**Figures 3E,F**), demonstrating that the *atr* mutation was not able to rescue the Al-sensitive phenotype of *stop1* either. These results suggest that ATR is not required for Al-induced growth inhibition in those Al-sensitive mutants that are defective in the external detoxification of Al.

The Al-Sensitive Phenotype of *als1* Could Also Be Rescued by the *atr* Mutation

Since ATR is localized in the nucleus and required for Al-induced halting cell division in *als3* or *star1* (**Figures 1**, **2**), there are two possibilities that ATR might detect general internal Al toxicity signal or *star1*/*als3*-specific Al toxicity signal. To distinguish these two, we utilized another Al-sensitive mutant *als1*, which is deficient in the sequestration of Al into vacuoles (Larsen et al., 2007). Introduction of *atr* mutation into *als1* mutant could also rescue its Al-sensitive phenotype at various Al concentrations (**Figures 4A,B**). These results imply that ATR is required for internal Al toxicity-mediated root growth inhibition.

We also determined the status of the QC after Al treatment by introduction of a GUS-based QC marker, QC46 (Sabatini et al., 2003), into *atr*, *als1* and *als1atr*. Without Al treatment, GUS expression was well detected in all the materials (**Figure 4C**). However, in the presence of high levels of Al, GUS activity was lost in *als1*, suggesting that the essential stem cells required for maintenance of root growth was destroyed by Al toxicity in *als1* mutant. In contrast, *als1atr* double mutant displayed normal GUS activity in the QC after Al treatment (**Figure 4C**). These results indicate that the *atr* mutation could help *als1* mutant to maintain the QC integrity for root growth when exposure to highly toxic levels of Al.

Expression Pattern of *ATR* and Al-Resistance Genes

To examine whether *ATR* expression was altered in Al-sensitive mutants, we compared the expression level of *ATR* between WT and the Al-sensitive mutants. Results showed that there was no significant difference in *ATR* expression between WT and the mutants in the absence of Al (**Figure 5A**). Al treatment slightly decreased the expression of *ATR*, but no significant difference in *ATR* expression was found in WT and the mutants. This result suggests that increased Al sensitivity of the mutants was not due to altered *ATR* expression. The expression of Al-resistance genes in *atr* mutant was also determined. The expression levels of the Al-resistance genes including *ALS3*, *STAR1*, *ALS1*, *ALMT1,* and *STOP1* in *atr* mutant were similar to those in WT under both –Al and –Al conditions (**Figure 5B**), suggesting that increased Al tolerance in *atr* mutant was not caused by elevated expression of Al-resistance genes.

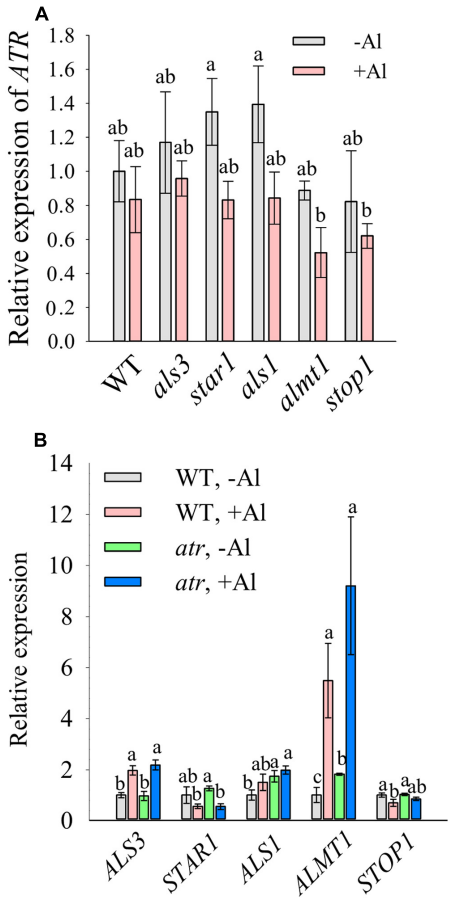

FIGURE 5 | Expression analysis of *ATR* and Al-resistance genes. Seven-day-old seedlings grown on a nutrient agar medium were pretreated with a 0.5 mM $CaCl_2$ solution for 6 h at pH 4.8 and then exposed to the same solution containing 0 or 20 μM Al at pH 4.8 for 12 h. The roots were sampled for expression analysis of *ATR* **(A)** or Al-resistance genes **(B)**. Data are means ± SD ($n = 3$). Means with different letters are significantly different ($P < 0.05$, Tukey's test).

DISCUSSION

ATR functions as a cell cycle checkpoint to detect DNA damage and subsequently prevent cell division (Culligan et al., 2004).

Since knockout of *ATR* is able to rescue the Al hypersensitivity in *als3* mutant (Gabrielson et al., 2006; Rounds and Larsen, 2008), two possible mechanisms exist for the increased sensitivity to Al in *als3*. One possible mechanism is that mutation of *ALS3* results in the increased Al accumulation in nucleus and consequently activates ATR-regulated pathway to halt cell division and ultimately inhibit root growth. The other is that Al toxicity-induced specific signal in *als3* activates ATR-regulated pathway to cause root growth inhibition. Our results showed that in addition to *als3*, mutation of *ATR* can also rescue Al-sensitive phenotype of *star1* and *als1*, indicating that rescue of Al-sensitive phenotype by *atr* mutation is not specific to *als3* mutant. Thus, we prefer the former hypothesis that elevated Al accumulation in the nucleus induces ATR-regulated pathway to inhibit root growth in *als3* mutant.

In contrast to its hypersensitivity to clastogenic and genotoxic stresses, *atr* mutant shows increased tolerance to Al. Al in nucleus might bind to DNA non-covalently and induce a conformational alteration from the B-form to Z-DNA, which affects DNA unwinding during DNA replication (Anitha and Rao, 2002). Nevertheless, unlike other genotoxic stresses, Al is thought to be a mild DNA damage agent and its binding to DNA is likely to be reversible (Rounds and Larsen, 2008; Nezames et al., 2012). This unique interaction of Al with DNA can activate ATR-, ALT2-, and SOG1-regualted transcriptional response to halt cell division and cause the inhibition of root growth (Sjogren et al., 2015). However, it remains unknown about how the interaction of Al with DNA activates the ATR-regulated pathway and what the ATR-regulated downstream transcriptional events that lead to the cease of cell division are.

The inhibition of root growth can be attributed to the disruption of cell division and/or cell elongation. Rapid reduction in root growth suggests an initial impact of Al on cell elongation instead of cell division (Sharp et al., 1988; Kopittke et al., 2015). However, when roots are exposed to Al for a long period of time, inhibition of cell division might also contribute to the reduction of root growth. Al-activated ATR-regulated cease of cell division in *als3*/*star1* or *als1* suggests that inhibition of cell division plays a critical role in Al-induced inhibition of root growth in these Al-sensitive mutants. Further work is required to determine whether mutation of *atr* could rescue the Al-sensitive phenotype of these mutants after a short-term exposure to Al.

Numerous studies have suggested that Al can target multiple sites for toxicity, including apoplastic and symplastic components (Kochian, 1995; Ma, 2007). Nevertheless, it remains debatable about which sites play more important roles in Al-induced inhibition of root growth. We found that the *atr* mutation could not rescue the Al hypersensitivity in *almt1* and *stop1*, which are defective in the capacity to detoxify Al externally. These results indicate that ATR is not required for Al-induced inhibition of root growth in all Al-sensitive mutants and suggest that both symplastic components such as DNA and apoplastic components including cell wall are important Al target sites that lead to root growth inhibition by Al toxicity. Additionally, our data showed that the *atr* mutation could not fully rescue the Al hypersensitivity in *als3*, suggesting that Al also targets other symplastic sites to cause root growth inhibition in *als3* mutant.

In rice, OsSTAR1 interacts with OsSTAR2, the rice ortholog of ALS3, to form a functional complex that is suggested to be involved in the modification of cell wall that is required for Al detoxification (Huang et al., 2009). Although *Arabidopsis* AtSTAR1 can also interact with ALS3 to be involved in the detoxification of Al, AtSTAR1 and ALS3 are localized to tonoplast (Larsen et al., 2005; Huang et al., 2010; Dong et al., 2017), which are different from OsSTAR1 and OsSTAR2 that are localized to vesicle membranes (Huang et al., 2009). We found that in addition to *als3*, knockout of *ATR* also rescues the Al-sensitive phenotype of *star1*. Furthermore, the *atr* mutation can even rescue Al hypersensitivity in *als3star1* double mutant. These results indicate that *als3* and *star1* share the same mechanism for their hypersensitivity to Al, i.e., ATR-regulated pathway required for Al-induced inhibition of root growth. The results also support the view that STAR1 and STAR2/ALS3 function together to be involved in the same pathway of Al detoxification. We further found that the Al hypersensitivity in *als1* was rescued by the *atr* mutation. *als1* has defects in the internal detoxification of Al (Larsen et al., 2007). Together, our results suggest that ATR is required for internal Al toxicity-induced inhibition of root growth and that STAR1 and ALS3 might be involved in the internal detoxification of Al in *Arabidopsis*. We propose that under Al stress conditions, internal Al detoxification-deficient mutants accumulate high levels of Al in the nucleus, which induces DNA damage and consequently activates ATR-regulated pathway and arrest cell cycle, finally leading to the inhibition of root growth.

AUTHOR CONTRIBUTIONS

All authors conceived the project. C-FH drafted the manuscript. YZ, JG, MC, LL, and LW performed the experiments. YZ and JG helped to analyze the data and write the manuscript. All authors read and approved the final manuscript.

FUNDING

This work was supported by Jiangsu Science Fund for Distinguished Young Scholars (Grant No. BK20150027), National Natural Science Foundation of China (Grant No. 31570253 to C-FH), the Strategic Priority Research Program (Grant No. XDPB0404) of the Chinese Academy of Sciences, and the Shanghai Center for Plant Stress Biology, Chinese Academy of Sciences.

ACKNOWLEDGMENTS

We thank Prof. Philip N. Benfey from Duke University for kindly providing the QC46 marker.

REFERENCES

Anitha, S., and Rao, K. S. J. (2002). The complexity of aluminum-DNA interactions: relevance to Alzheimer's and other neurological diseases. *Struct. Bond.* 104, 79–97. doi: 10.1007/3-540-45425-X_3

Blancaflor, E. B., Jones, D. L., and Gilroy, S. (1998). Alterations in the cytoskeleton accompany aluminum-induced growth inhibition and morphological changes in primary roots of maize. *Plant Physiol.* 118, 159–172. doi: 10.1104/pp.118.1.159

Culligan, K., Tissier, A., and Britt, A. (2004). ATR regulates a G2-phase cell-cycle checkpoint in *Arabidopsis thaliana*. *Plant Cell* 16, 1091–1104. doi: 10.1105/Tpc.018903

Dong, J. S., Pineros, M. A., Li, X. X., Yang, H. B., Liu, Y., Murphy, A. S., et al. (2017). An *Arabidopsis* ABC transporter mediates phosphate deficiency-induced remodeling of root architecture by modulating iron homeostasis in roots. *Mol. Plant* 10, 244–259. doi: 10.1016/j.molp.2016.11.001

Gabrielson, K. M., Cancel, J. D., Morua, L. F., and Larsen, P. B. (2006). Identification of dominant mutations that confer increased aluminium tolerance through mutagenesis of the Al-sensitive *Arabidopsis* mutant, *als3-1*. *J. Exp. Bot.* 57, 943–951. doi: 10.1093/jxb/erj080

Grabski, S., and Schindler, M. (1995). Aluminum induces rigor within the actin network of soybean cells. *Plant Physiol.* 108, 897–901. doi: 10.1104/pp.108.3.897

Hoekenga, O. A., Maron, L. G., Pineros, M. A., Cancado, G. M., Shaff, J., Kobayashi, Y., et al. (2006). *AtALMT1*, which encodes a malate transporter, is identified as one of several genes critical for aluminum tolerance in *Arabidopsis*. *Proc. Natl. Acad. Sci. U.S.A.* 103, 9738–9743. doi: 10.1073/pnas.0602868103

Huang, C. F., Yamaji, N., and Ma, J. F. (2010). Knockout of a bacterial-type ATP-binding cassette transporter gene, *AtSTAR1*, results in increased aluminum sensitivity in *Arabidopsis*. *Plant Physiol.* 153, 1669–1677. doi: 10.1104/pp.110.155028

Huang, C. F., Yamaji, N., Mitani, N., Yano, M., Nagamura, Y., and Ma, J. F. (2009). A bacterial-type ABC transporter is involved in aluminum tolerance in rice. *Plant Cell* 21, 655–667. doi: 10.1105/tpc.108.064543

Iuchi, S., Koyama, H., Iuchi, A., Kobayashi, Y., Kitabayashi, S., Ikka, T., et al. (2007). Zinc finger protein STOP1 is critical for proton tolerance in *Arabidopsis* and coregulates a key gene in aluminum tolerance. *Proc. Natl. Acad. Sci. U.S.A.* 104, 9900–9905. doi: 10.1073/pnas.0700117104

Jones, D. L., and Kochian, L. V. (1995). Aluminum inhibition of the inositol 1,4,5-trisphosphate signal transduction pathway in wheat roots: a role in aluminum toxicity? *Plant Cell* 7, 1913–1922. doi: 10.1105/tpc.7.11.1913

Jones, D. L., Kochian, L. V., and Gilroy, S. (1998). Aluminum induces a decrease in cytosolic calcium concentration in BY-2 tobacco cell cultures. *Plant Physiol.* 116, 81–89. doi: 10.1104/pp.116.1.81

Karlik, S. J., and Eichhorn, G. L. (1989). Polynucleotide cross-linking by aluminum. *J. Inorg. Biochem.* 37, 259–269. doi: 10.1016/0162-0134(89)85001-9

Karlik, S. J., Eichhorn, G. L., Lewis, P. N., and Crapper, D. R. (1980). Interaction of aluminum species with deoxyribonucleic acid. *Biochemistry* 19, 5991–5998. doi: 10.1021/Bi00567a008

Kinraide, T. B. (2001). Ion fluxes considered in terms of membrane-surface electrical potentials. *Aust. J. Plant Physiol.* 28, 605–616. doi: 10.1071/PP01019

Kochian, L. V. (1995). Cellular mechanisms of aluminum toxicity and resistance in plants. *Annu. Rev. Plant Physiol. Plant Mol. Biol.* 46, 237–260. doi: 10.1146/annurev.arplant.46.1.237

Kochian, L. V., Hoekenga, O. A., and Pineros, M. A. (2004). How do crop plants tolerate acid soils? Mechanisms of aluminum tolerance and phosphorous efficiency. *Annu. Rev. Plant Biol.* 55, 459–493. doi: 10.1146/annurev.arplant.55.031903.141655

Kopittke, P. M., Moore, K. L., Lombi, E., Gianoncelli, A., Ferguson, B. J., Blamey, F. P., et al. (2015). Identification of the primary lesion of toxic aluminum in plant roots. *Plant Physiol.* 167, 1402–1411. doi: 10.1104/pp.114.253229

Larsen, P. B., Cancel, J., Rounds, M., and Ochoa, V. (2007). *Arabidopsis ALS1* encodes a root tip and stele localized half type ABC transporter required for root growth in an aluminum toxic environment. *Planta* 225, 1447–1458. doi: 10.1007/s00425-006-0452-4

Larsen, P. B., Geisler, M. J. B., Jones, C. A., Williams, K. M., and Cancel, J. D. (2005). *ALS3* encodes a phloem-localized ABC transporter-like protein that is required for aluminum tolerance in *Arabidopsis*. *Plant J.* 41, 353–363. doi: 10.1111/j.1365-313X.2004.02306.x

Lazof, D. B., Goldsmith, J. G., Rufty, T. W., and Linton, R. W. (1996). The early entry of Al into cells of intact soybean roots - A comparison of three developmental root regions using secondary ion mass spectrometry imaging. *Plant Physiol.* 112, 1289–1300. doi: 10.1104/pp.112.3.1289

Liu, J. P., Magalhaes, J. V., Shaff, J., and Kochian, L. V. (2009). Aluminum-activated citrate and malate transporters from the MATE and ALMT families function independently to confer *Arabidopsis* aluminum tolerance. *Plant J.* 57, 389–399. doi: 10.1111/j.1365-313X.2008.03696.x

Ma, J. F. (2007). Syndrome of aluminum toxicity and diversity of aluminum resistance in higher plants. *Int. Rev. Cytol.* 264, 225–252. doi: 10.1016/S0074-7696(07)64005-4

Ma, J. F., Ryan, P. R., and Delhaize, E. (2001). Aluminium tolerance in plants and the complexing role of organic acids. *Trends Plant Sci.* 6, 273–278. doi: 10.1016/S1360-1385(01)01961-6

Nezames, C. D., Sjogren, C. A., Barajas, J. F., and Larsen, P. B. (2012). The *Arabidopsis* cell cycle checkpoint regulators TANMEI/ALT2 and ATR mediate the active process of aluminum-dependent root growth inhibition. *Plant Cell* 24, 608–621. doi: 10.1105/tpc.112.095596

Pineros, M. A., and Kochian, L. V. (2001). A patch-clamp study on the physiology of aluminum toxicity and aluminum tolerance in maize. Identification and characterization of Al3+-induced anion channels. *Plant Physiol.* 125, 292–305. doi: 10.1104/pp.125.1.292

Poschenrieder, C., Gunse, B., Corrales, I., and Barcelo, J. (2008). A glance into aluminum toxicity and resistance in plants. *Sci. Total Environ.* 400, 356–368. doi: 10.1016/j.scitotenv.2008.06.003

Rounds, M. A., and Larsen, P. B. (2008). Aluminum-dependent root-growth inhibition in *Arabidopsis* results from AtATR-regulated cell-cycle arrest. *Curr. Biol.* 18, 1495–1500. doi: 10.1016/j.cub.2008.08.050

Sabatini, S., Heidstra, R., Wildwater, M., and Scheres, B. (2003). SCARECROW is involved in positioning the stem cell niche in the *Arabidopsis* root meristem. *Genes Dev.* 17, 354–358. doi: 10.1101/gad.252503

Sharp, R. E., Silk, W. K., and Hsiao, T. C. (1988). Growth of the maize primary root at low water potentials.1. spatial-distribution of expansive growth. *Plant Physiol.* 87, 50–57. doi: 10.1104/Pp.87.1.50

Silva, I. R., Smyth, T. J., Moxley, D. F., Carter, T. E., Allen, N. S., and Rufty, T. W. (2000). Aluminum accumulation at nuclei of cells in the root tip. Fluorescence detection using lumogallion and confocal laser scanning microscopy. *Plant Physiol.* 123, 543–552. doi: 10.1104/pp.123.2.543

Sjogren, C. A., Bolaris, S. C., and Larsen, P. B. (2015). Aluminum-dependent terminal differentiation of the Arabidopsis root tip is mediated through an ATR-, ALT2-, and SOG1-regulated transcriptional response. *Plant Cell* 27, 2501–2515. doi: 10.1105/tpc.15.00172

von Uexkull, H. R., and Mutert, E. (1995). Global extent, development and economic-impact of acid soils. *Plant Soil* 171, 1–15. doi: 10.1007/BF00009558

Yamamoto, Y., Kobayashi, Y., and Matsumoto, H. (2001). Lipid peroxidation is an early symptom triggered by aluminum, but not the primary cause of elongation inhibition in pea roots. *Plant Physiol.* 125, 199–208. doi: 10.1104/Pp.125.1.199

Zhang, W. H., and Rengel, Z. (1999). Aluminium induces an increase in cytoplasmic calcium in intact wheat root apical cells. *Aust. J. Plant Physiol.* 26, 401–409. doi: 10.1071/PP98149

Conflict of Interest Statement: The authors declare that the research was conducted in the absence of any commercial or financial relationships that could be construed as a potential conflict of interest.

frontiers in Plant Science

ORIGINAL RESEARCH
published: 23 January 2018
doi: 10.3389/fpls.2017.02156

BoALMT1, an Al-Induced Malate Transporter in Cabbage, Enhances Aluminum Tolerance in *Arabidopsis thaliana*

Lei Zhang[1†], Xin-Xin Wu[1†], Jinfang Wang[1†], Chuandong Qi[1], Xiaoyun Wang[1], Gongle Wang[1], Mingyue Li[1], Xingsheng Li[2] and Yang-Dong Guo[1]*

[1] *Beijing Key Laboratory of Growth and Developmental Regulation for Protected Vegetable Crops, College of Horticulture, China Agricultural University, Beijing, China,* [2] *Shandong Huasheng Agriculture Co. Ltd, Shandong, China*

Aluminum (Al) is present in approximately 50% of the arable land worldwide and is regarded as the main limiting factor of crop yield on acidic soil. Al-induced root malate efflux plays an important role in the Al tolerance of plants. Here, the aluminum induced malate transporter *BoALMT1* (KF322104) was cloned from cabbage (*Brassica oleracea*). *BoALMT1* showed higher expression in roots than in shoots. The expression of *BoALMT1* was specifically induced by Al treatment, but not the trivalent cations lanthanum (La), cadmium (Cd), zinc (Zn), or copper (Cu). Subcellular localization studies were performed in onion epidermal cells and revealed that BoALMT1 was localized at the plasma membrane. Scanning Ion-selective Electrode Technique was used to analyze H^+ flux. *Xenopus* oocytes and *Arabidopsis thaliana* expressing *BoALMT1* excreted more H^+ under Al treatment. Overexpressing *BoALMT1* in transgenic *Arabidopsis* resulted in enhanced Al tolerance and increased malate secretion. The results suggested that *BoALMT1* functions as an Al-resistant gene and encodes a malate transporter. Expressing *BoALMT1* in *Xenopus* oocytes or *A. thaliana* indicated that BoALMT1 could increase malate secretion and H+ efflux to resist Al tolerance.

Keywords: aluminum tolerance, *BoALMT1*, cabbage, malates, SIET

OPEN ACCESS

Edited by:
Wei Fan,
Yunnan Agricultural University, China

Reviewed by:
Qi Chen,
Kunming University of Science and Technology, China
Jiang Tian,
South China Agricultural University, China

***Correspondence:**
Yang-Dong Guo
yaguo@cau.edu.cn

†These authors have contributed equally to this work.

Specialty section:
This article was submitted to Plant Abiotic Stress, a section of the journal Frontiers in Plant Science

Received: *24 July 2017*
Accepted: *06 December 2017*
Published: *23 January 2018*

Citation:
Zhang L, Wu X-X, Wang J, Qi C, Wang X, Wang G, Li M, Li X and Guo Y-D (2018) BoALMT1, an Al-Induced Malate Transporter in Cabbage, Enhances Aluminum Tolerance in Arabidopsis thaliana. Front. Plant Sci. 8:2156. doi: 10.3389/fpls.2017.02156

INTRODUCTION

Al is the most abundant metal and the third most abundant element, making up around 7% of the earth's crust (Tesfaye et al., 2001). When the soil pH value is lower than 5.0, the soluble aluminum in soil solutions is mostly present as the toxic Al^{3+}, which inhibits root growth at micromolar concentrations in many species (Kochian et al., 2005). Micromole levels of Al^{3+} can remarkably inhibit root elongation, and impair the absorption, of water and nutrients (Kochian et al., 2005). The well-known mechanism of plant Al tolerance is the Al-induced secretion of organic acids (OA) from the root tips. The OAs chelate Al^{3+} and form the non-toxic compound OA-Al (Kochian et al., 2004; Horst et al., 2010; Ryan et al., 2011). The most common OAs involved in the Al detoxification process are malate, citrate, and oxalate, depending on the plant. For example, malate is used in wheat (Delhaize et al., 1993) and *Arabidopsis* (Hoekenga et al., 2003), citrate is secreted in maize (Pellet et al., 1995), and oxalate is used in buckwheat (Zheng et al., 2005) and tomato (Yang et al., 2008).

Wheat *TaALMT1* (ALMT, for Al-activated Malate Transporter) encoding a malate transporter was the first plant gene involved in Al tolerance and the first ALMT family gene. In Al-tolerant wheat genotypes, *TaALMT1* is specifically expressed in the root tips (Sasaki et al., 2004; Raman et al., 2005). Overexpression of *TaALMT1* in wheat, barley, and tobacco-cell suspension increases the efflux of Al-activated malate and enhances tolerance to Al stress (Delhaize et al., 2004; Sasaki et al., 2004; Pereira et al., 2010). *TaALMT1* homologs have now been isolated in *Arabidopsis* (Hoekenga et al., 2006), oilseed rape (Ligaba et al., 2006), rye (Collins et al., 2008), soybean (Liang et al., 2013), and *Medicago sativa* (Chen et al., 2013). Multi-antimicrobial extrusion (MATE) proteins are a family of proteins that function as drug/sodium or proton antiporters. MATE proteins can secrete organic anions to contribute to the Al tolerance in plants (Furukawa et al., 2007; Magalhaes et al., 2007; Wang et al., 2007; Liu et al., 2009). In *Arabidopsis*, the zinc finger transcription factor *STOP1* (known as ART1 in rice) plays a critical role in plant Al tolerance by regulating the Al-inducible expression of *ALMT* and *MATE* (Liu et al., 2009). In rice, multiple genes implicated in Al tolerance, including MATE transporter family members, are regulated by the transcription factor ART1 (Yamaji et al., 2009).

Cabbage (*Brassica oleracea*) is one of the most important vegetable crops around the world (Wu et al., 2014). Our previous study has shown that *BoMATE* encodes a citrate transporter and is induced by Al and enhances aluminum tolerance in *Arabidopsis* (Wu et al., 2014). Here we report that cabbage BoALMT1 is located in the plasma membrane and induced by Al. A reverse genetic approach was used to characterize the functions of *BoALMT1*. Overexpressing *BoALMT1* in *Xenopus oocytes and Arabidopsis* facilitated H^+ efflux. Overexpressing *BoALMT1* in *Arabidopsis* resulted in enhanced Al tolerance and increased malate secretion. These results suggested that BoALMT1 has an important role in Al tolerance in cabbage.

RESULTS

Sequence Analysis of *BoALMT1* in Cabbage

The ALMT gene was the first Al^{3+} tolerance gene identified in plants (Sasaki et al., 2004; Delhaize et al., 2007; Meyer et al., 2010). Membrane protein ALMTs possess 5–7 predicted transmembrane domains and a UPF0005 domain with unknown function (Delhaize et al., 2007). *BoALMT1* (KF322104) cloned from cabbage contains an open reading frame of 1,497 bp, encoding a polypeptide of 498 amino acids. BLAST analysis revealed that the sequence of BoALMT1 was a 99% match to BnALMT1 from rape, 73% match to AtALMT1 from *Arabidopsis*, and 33% match to TaALMT1 from wheat. The HMMTOP transmembrane topology prediction server was used to predict the localization of helical transmembrane segments and the analysis indicated that BoALMT1 contained 5 predicted transmembrane domains (**Figure 1A**). Analysis of BoALMT1 and other reported ALMTs in plants indicated that BoALMT1 was most closely clustered with the BnALMT1 from *Brassica napus* (**Figure 1B**).

Expression Pattern of *BoALMT1*

We performed real-time reverse transcription (RT)-PCR analysis to measure the expression of *BoALMT1* in the roots and shoots, and found that *BoALMT1* expression was primarily localized to the roots (**Figure 2A**). Al treatment enhanced its expression in all tissues (**Figure 2A**). Cabbage plants were exposed to a variety of trivalent cations, and the expression of *BoALMT1* was not induced by lanthanum (La), cadmium (Cd), zinc (Zn), or copper (Cu), but was severely induced by aluminum (**Figure 2B**). A dose-response experiment and a time-course experiment indicated that increasing the external Al concentration and treatment time did not further increase the *BoALMT1* transcript level (**Figures 2C,D**).

Subcellular Localization of BoALMT1

The subcellular localization of BoALMT1 was determined via localization of the GFP::BoALMT1 protein transiently expressed in onion epidermal cells (**Figure 3**). The GFP::BoALMT1 green fluorescence was only observed at the outer layer of the cell (**Figures 3a,b**), and the cells expressing GFP showed green fluorescence in the whole cell (**Figures 3e,f**). We induced plasmolysis by the addition of 0.8 M mannitol to distinguish localization in the plasma membrane and observed that the fluorescence of GFP::BoALMT1 was exclusively located in the plasma membrane in the plasmolysis cells (**Figures 3c,d**). These localization results were similar to those of some ALMTs identified in other species [TaALMT1 (Yamaguchi et al., 2005), BnALMT1 (Ligaba et al., 2006), ZmALMT1 (Piñeros et al., 2008), ZmALMT2 (Ligaba et al., 2008), and GmALMT1 (Liang et al., 2013)].

Pattern of Malate Secretion

To investigate whether the secretion of malate was induced by Al treatment, we characterized malate exudation from cabbage roots. Cabbage roots secreted a low level of malate under normal conditions. After 3 h treatment with 50 μM Al, malate exudation was remarkably induced (**Figure 4**).

Heterologous Expression of *BoALMT1* Reduced Al-Induced H^+ Efflux in *Xenopus* Oocytes

By treated the *Arabidopsis* mutant with Al stress, Degenhardt et al. (1998) observed that the pH of the root surface increased, while Bose et al. (2010) further confirmed Al stress correlated with lower H^+ influx. So in our study, we used the non-invasive Scanning Ion-selective Electrode Technique (SIET) system to measure H^+ fluxes crossing the surface of *Xenopus* oocytes with or without the per-injected malate (**Figure 5A**). We noticed that the H^+ flux had no difference in the control oocytes under the absence or the present of Al. Furthermore, compared with the control cells, *BoALMT1*-expressing oocytes also secreted similar amount of H^+ without pretreated with malate. However, when the malate was fed, the *BoALMT1*-expressing oocytes secreted more H^+ compared with the control oocytes under the absence

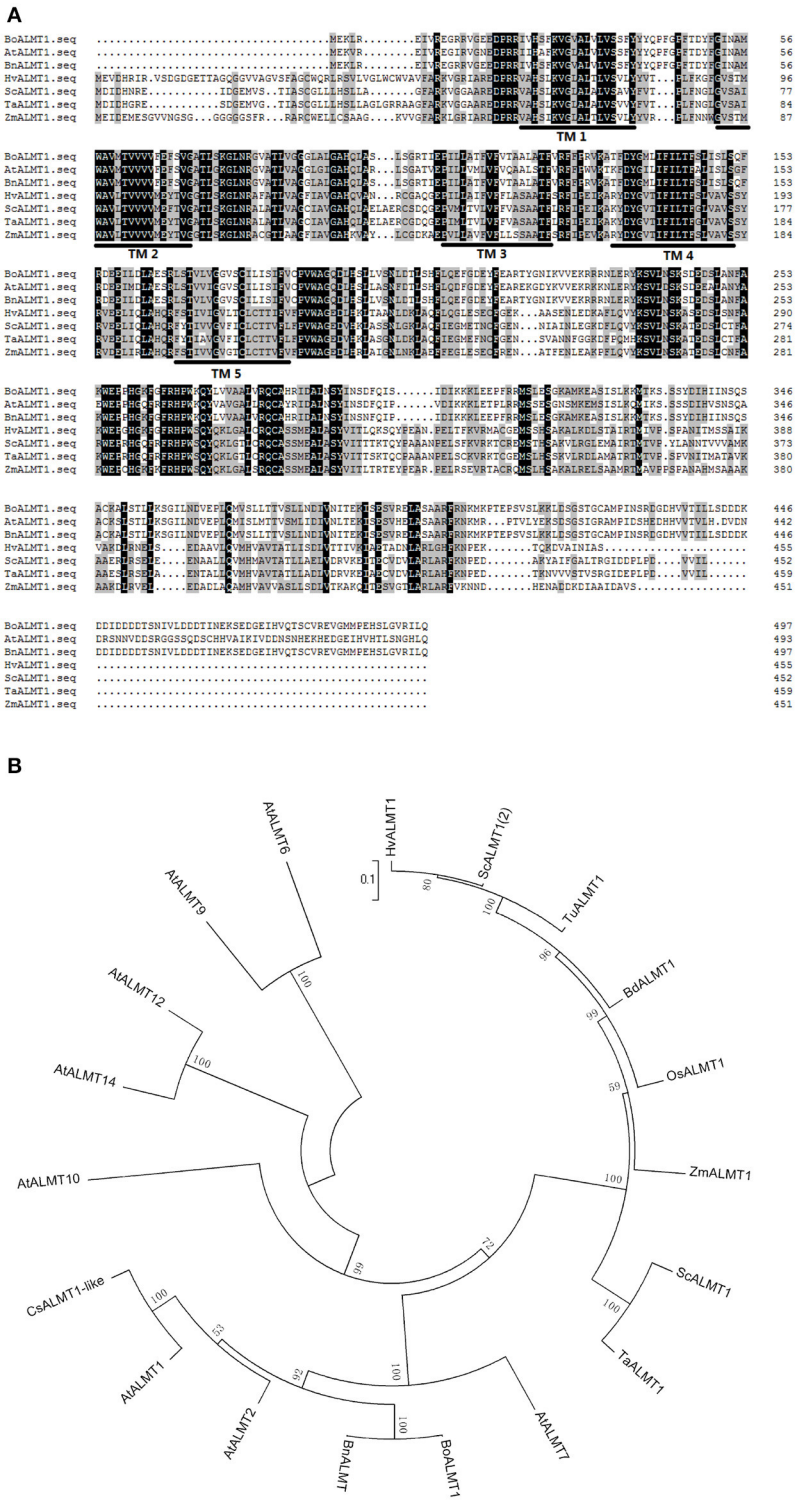

FIGURE 1 | Amino acid sequence **(A)** and phylogenetic **(B)** analysis of *Brassica oleracea BoALMT1*. **(A)** Multiple sequence alignment of cabbage *BoALMT1*, maize *ZmALMT1*, wheat *TaALMT1*, *Arabidopsis AtALMT1*, rape *BnALMT1*, rye *ScALMT1,* and Barley *HvALMT1*. Identical amino acids and similar amino acids were indicated by dark shading and light shading, respectively. Lines depict the 5 predicted transmembrane domains in BoALMT1 as predicted by HMMTOP. **(B)** Phylogenetic relationship of BoALMT1 and other known Al-activated malate transporters (ALMT). The amino acid sequences were aligned by ClustalW.

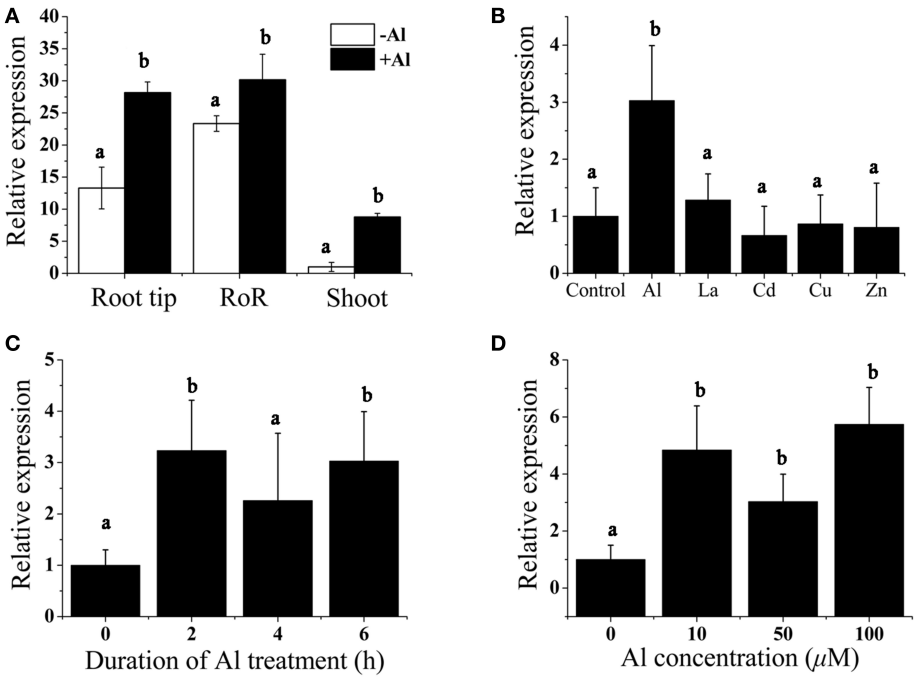

FIGURE 2 | Analysis of *BoALMT1* expression in cabbage seedlings by quantitative real-time PCR. **(A)** Tissue-specific expression of *BoALMT1*. Seedlings were exposed to a 0.5 mM $CaCl_2$ solution (pH 4.5) containing 50 μM $AlCl_3$ for 6 h. Expression of *BoALMT1* gene in the root tip, rest of root (RoR) and shoots were determined. **(B)** Effect of Al, La, Cd, Cu, and Zn on *BoALMT1* expression. Seedlings were exposed to a 0.5 mM $CaCl_2$ solution (pH 4.5) containing 50 μM $AlCl_3$, 25 μM Cd, 10 μM La, 0.5 μM Cu, or 2.0 μM Zn. **(C)** Time-dependent expression of *BoALMT1*. Cabbage seedlings were exposed to a solution containing 50 μM $AlCl_3$ for different time. **(D)** Dose-response expression analysis of *BoALMT1* gene in cabbage roots. The roots were exposed to a 0.5 mM $CaCl_2$ solution (pH 4.5) containing 0, 10, 50, and 100 μM $AlCl_3$ for 6 h. Actin expression was used as an internal control. Bars represent means ± *SD* of three replicates and independent experiments were performed at least three times. Different letters above the columns indicate significant differences ($P < 0.05$) between treatments.

or the present of Al condition (**Figure 5A**). To further elucidate BoALMT1 served as a malate efflux transporter, we fed the control and the *BoALMT1*-expressing oocytes with ^{14}C-labeled malate and then measured the efflux of radioactively labeled malate (**Figure 5B**). The *BoALMT1*-expressing oocytes excreted more labeled malate than the control cells. These results indicated that BoALMT1 was a malate efflux transporter and enhanced the H^+ efflux according to malate secretion in *Xenopus* oocytes.

Overexpressing *BoALMT1* in *A. thaliana* Enhanced Al Tolerance

Al-activated membrane transporters, which mediate organic acid release from the root apex, are the primary physiological mechanism of plant Al tolerance (Kochian et al., 2004). Plant ALMTs that have been implicated in malate transport and Al tolerance are TaALMT1 in wheat (Sasaki et al., 2004), AtALMT1 in *Arabidopsis* (Hoekenga et al., 2006), BnAMLT1 and BnALMT2 in oilseed rape (Ligaba et al., 2006), GmALMT1 in soybean (Liang et al., 2013), and MsALMT1 in *M. sativa* (Chen et al., 2013).

In this study, to investigate whether the overexpression of *BoALMT1* enhances malate exudation and Al tolerance, we induced expression of *BoALMT1* driven by the CaMV 35S promoter in *Arabidopsis* plants. Successful introduction of *BoALMT1* in two transgenic lines, but not the control line, was confirmed by RT-PCR (**Figure 6A**). Root malate exudation was then measured in the plants expressing *BoALMT1* and demonstrating increased Al tolerance (**Figure 6B**). Plants expressing *BoALMT1* showed a remarkable increase in root malate exudation rates in the presence of Al, but no difference was observed in the absence of Al. When grown in in agar plates without Al, the transgenic plants expressing *BoALMT1* showed root growth similar to that of wild-type (**Figure 6C**). When grown in agar plates with 400 μM $AlCl_3$, root elongation of plants expressing *BoALMT1* showed less root growth inhibition than that of the plants without expression (**Figures 6C,D**). To further determine the effect on H^+ flow caused by overexpressing *BoALMT1* in *Arabidopsis*, we performed SIET to detect the H^+ flux at the root DEZ with 0 or 50 μM Al (pH = 4.5). Under low pH condition, the pattern of H^+ influx exhibited no statistic difference between WT lines and *BoALMT1* transgenic lines. However, treated with 50 μM Al, the H^+ influx was inhibited in the WT lines, while the H^+ was secreted from the roots *BoALMT1* transgenic lines (**Figure 6E**).

DISCUSSION

Al-activated malate transporters (ALMT) have been reported to be involved in Al tolerance and have been isolated from *Arabidopsis*, *M. sativa*, oil seed rape, rye, wheat, and soybean (Sasaki et al., 2004; Hoekenga et al., 2006; Ligaba et al.,

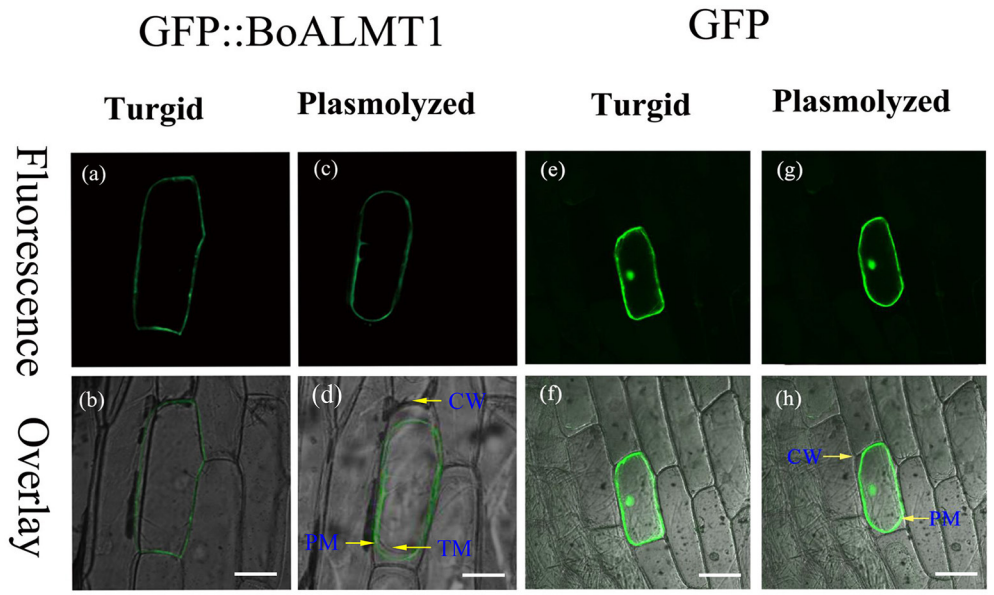

FIGURE 3 | Cellular localization of the BoALMT1 protein by transient expression of the GFP::BoALMT1 fusion protein in epidermal onion cells. **(a–d)** The plasma membrane localization of BoALMT1 in onion epidermal cells before **(a,b)** and after cell plasmolysis with 0.8 M mannitol **(c,d)**. **(e–h)** GFP protein in onion epidermal cells before **(e,f)** and after cell plasmolysis with 0.8M manitol **(g,h)**. PM, CW, and TM labels denote the plasma membrane cell wall and tonoplast membrane localization, respectively. White bars = 100 μm.

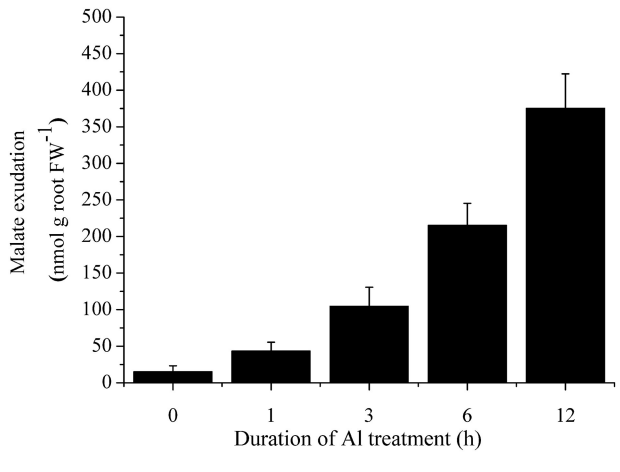

FIGURE 4 | Time course of malate secretion after exposure of 50 μM Al in cabbage roots. Data are means ± *SD* ($n = 5$).

2006; Collins et al., 2008; Liang et al., 2013). Here we reported that Al-induced cabbage BoALMT1 enhanced malate secretion under Al stress in *Arabidopsis*. BoALMT1 contains five predicted transmembrane domains (**Figure 1A**) and was most closely clustered with BnALMT1 (**Figure 1B**). The expression of *BoALMT1* was rapidly induced by aluminum and was primarily localized to the root (**Figure 2**). Some *ALMTs* are Al-induced but not Al-activated, such as *GmALMT1*, but *AtALMT1* is both induced and activated by Al (Hoekenga et al., 2006; Liang et al., 2013). If *BoALMT1* is activated by Al requires further studies.

BoALMT1 was heterologously expressed in oocytes and *Arabidopsis* to analyze its function (**Figures 5**, **6**). In oocytes, under the absence of Al condition, cells expressing BoALMT1 secreted more H^+ compared with control cells. After Al treatment, H^+ influx diminished in the wild type cells and slightly reduced in the *BoALMT1*-expressing cells (**Figure 5A**). In *Arabidopsis*, the *BoALMT1* overexpression lines exhibited longer root elongation and more malate exudation under Al treatment compared with WT lines, but there no difference between WT and transgenic lines (**Figures 6B–D**). These results demonstrate that *BoALMT1* increase malate secretion to resist Al tolerance in *Arabidopsis*. This was similar with the reported homologous *ALMT*s in *Arabidopsis* and *B. napus* (Hoekenga et al., 2006; Ligaba et al., 2006). In **Figure 6E**, compared with the low pH condition, *BoALMT1* expressing plants secreted H^+ form root tips while the WT plants only diminished the H^+ influx. As described by Ahn and Matsumoto, the activity of H^+-ATPase of Al-tolerance wheat lines was higher than that of Al-sensitive wheat under Al treatment (Ahn and Matsumoto, 2006). In faba bean, the activity of PM H^+-ATPase was increased and positively associated with citrate exudation under Al stress (Chen et al., 2015). The similar results were also found in our previous study about *BoMATE* (Wu et al., 2014). Our results might imply that BoALMT1 mediate malate transport instead of directly mediate H^+ flux, and the H^+ efflux might associate with the secretion of malate (**Figures 5**, **6**). However, the causes of these different H^+ flux patterns between *Xenopus* oocytes and *Arabidopsis* are unclear. Expressing *ALMTs* in yeast and bacteria did not show their functions (Ryan et al., 2011). *BoALMT1* may behave differently in these two heterologous expressing systems.

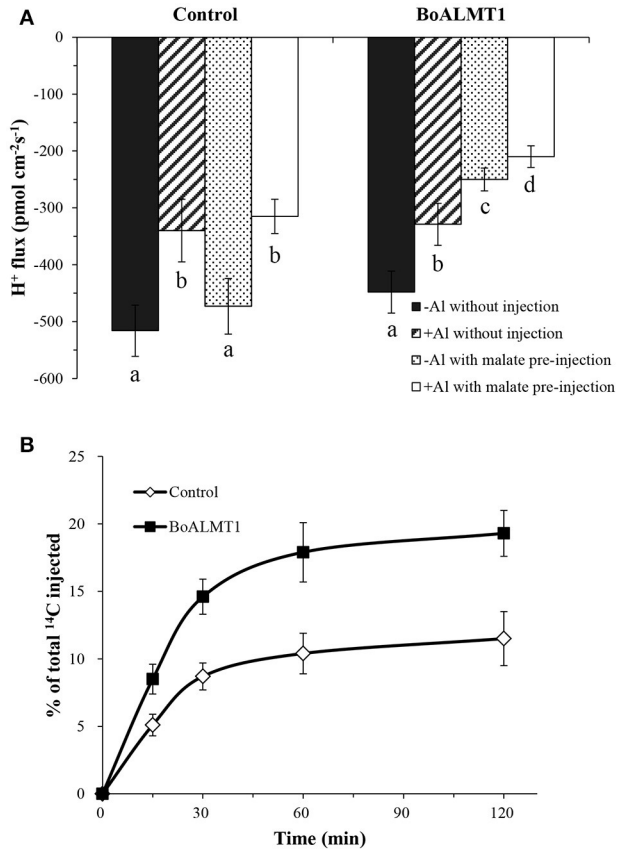

FIGURE 5 | Characterization of BoALMT1 in *Xenopus* oocytes. **(A)** Mean values of H^+ fluxes in the absence or presence of 50 μM Al with pretreated malate or water. Each value represents the average of at least 3 different cells, the error bars represent *SD* ($n = 4$–6). **(B)** Malate efflux transport activity. Control and *BoALMT1*-expressing oocytes injected with ^{14}C-labeled malate were kept in OCM solution. The radioactivity in the bathing solution was measured at the indicated time points; values are expressed as a percentage of the total radioactivity injected. Data was given as means ± *SD* ($n = 3$). Different letters above the columns indicate significant differences ($P < 0.05$) between treatments.

So combining the previous studies by Wu et al. (2014) and Chen et al. (2015) with our findings, we speculated that the secretions of organic acids such as citrate and malate was associated with the activity of PM H^+-ATPase to resist Al stress.

A C2H2-type zinc finger transcription factor STOP1 plays a key role in plant Al tolerance. Multiple Al-induced genes such as *ALMTs* and *MATEs* are regulated by STOP1 (Liu et al., 2009; Yamaji et al., 2009). To uncover the Al tolerance mechanism in cabbage and determine if STOP1 or a similar regulator participate in this mechanims, further studies are required.

In addition to the external Al detoxification, ALMTs may also have other uncharacterized functions. Recently, Kobayashi et al. demonstrated that *ALMT1* responds to multiple signals such as abscisic acid (ABA), indole-3-acetic acid (IAA), low pH, and hydrogen peroxide, but does not respond to methyl jasmonate and salicylic acid (Kobayashi et al., 2013). A few reports found that aluminum-induced malate efflux is negatively regulated by ethylene by inhibition of the expression of *TaALMT1* (Tian et al., 2014), this process can be alleviated by the inhibition of ACS activity (Yu et al., 2016). Furthermore, TAA1 regulates local auxin biosynthesis and influences the aluminum-induced inhibition of root growth (Yang et al., 2014). Further work should examine the complex regulation of *BoALMT1* during the resistance of multiple stresses and the mechanism by which plants can sense external Al (Kobayashi et al., 2013).

Our results illustrated that the cabbage BoALMT1 localized to the plasma membrane, and the expression of *BoALMT1* was specifically induced by Al treatment. Expression of *BoALMT1* in *Xenopus* oocytes and *Arabidopsis* could enhance Al tolerance. We identified that *BoALMT1* can function as an Al-induced gene, and the BoALMT1 protein is involved in H^+ flux in response to Al stress.

MATERIALS AND METHODS

Plant Cultivars and Growth Conditions

Cabbage (*B. oleracea* cv. Zhonggan-11) was seeded at 25°C on moist filter paper in the dark for 2 days. The seedlings were then moved to a complete nutrient solution (Ligaba et al., 2006). After 5 days of culture, the uniform seedlings were moved to a new plastic pot wetted with 0.5 mM $CaCl_2$ (pH 4.5) solution and pre-incubated for ∼24 h. To measure the spatial expression patterns of *BoALMT1* in root tips (0–1 cm), after 6 h of 50 μM Al exposure, the roots and shoots were separately collected and subjected to qRT-PCR analysis. To test the specificity of Al-induced *BoALMT1* gene expression, we exposed seedlings in a 0.5 mM $CaCl_2$ solution (pH 4.5) containing 50 μM $AlCl_3$, 25 μM $CdCl_2$, 10 μM $LaCl_3$, 0.5 μM $CuCl_2$, or 2.0 μM $ZnCl_2$ for 6 h. To investigate the dose effects of Al on *BoALMT1* expression, the seedlings were exposed to a 0.5 mM $CaCl_2$ solution (pH 4.5) containing 0, 10, 50, or 100 μM $AlCl_3$ for 6 h. To analyze time-course effects of Al toxicity on *BoALMT1* expression, the seedlings were exposed to a 0.5 mM $CaCl_2$ solution (pH 4.5) containing 50 μM $AlCl_3$ for 0, 2, 4, and 6 h.

Gene Cloning and Sequencing

To clone *BoALMT1*, RNA was isolated from cabbage seedlings roots treated with Al. To identify cabbage *BoALMT1*, we performed a BLAST search with the known *AtALMT1* and *BnALMT1* sequences on the NCBI website (http://www.ncbi.nlm.nih.gov/). For further amplification, two expressed sequence tags (ESTs) (DK499842 and DY012377) were selected. The two nucleotide sequences were combined to generate a full-length cDNA. The full-length cDNA of *BoALMT1* was amplified with sense primer 5′-ATGGAGAAAGTGAGAGA GATAGTGAG-3′ and anti-sense primer 5′-TCAAATCTGA AGTATACGAACACCC-3′, and then constructed into the pMD18-T vector (Takara, Japan). HMMTOP was used for transmembrane protein prediction analysis. Multiple amino acid alignment was conducted by using ClustalX and MEGA4.1 software.

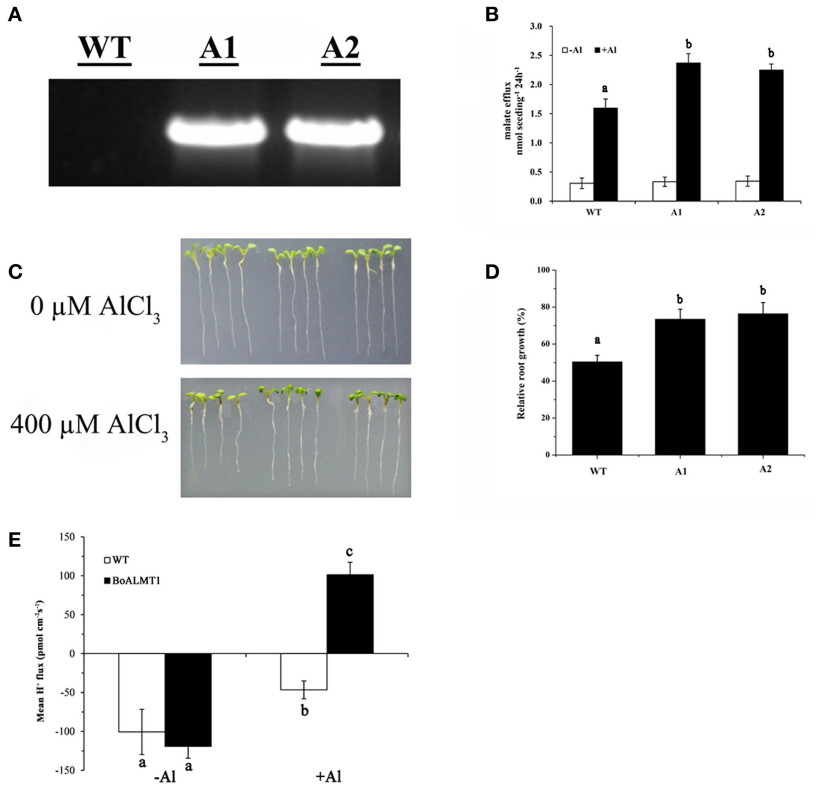

FIGURE 6 | Expression of *BoALMT1* in transgenic *Arabidopsis* plants results in enhanced citrate release and Al tolerance. **(A)** *BoALMT1* expression in the two transgenic lines (A1 and A2) and a control line (WT). **(B)** Root malate exudation in the absence and presence of 50 μM $AlCl_3$. Experiments were repeated at least three times ($n = 100$). **(C)** Root growth of representative plants from two independent transgenic lines grown in agar medium in the absence or presence of Al for 2 days. **(D)** Relative root growth of the plants subjected to 400 μM Al for 2 d. Each bar represents the mean of three replicates ± *SD* ($n = 4$). **(E)** Comparison H^+ flux at the DEZ of 4- to 5-day-old *Arabidopsis thaliana* seedlings in the presence and absence of Al. Data are given as means ± *SD* ($n = 3$–5). Different letters above the columns indicate significant differences ($P < 0.05$) between treatments.

Characterization of *BoALMT1* Expression via qPCR

BoALMT1 expression was evaluated using quantitative real-time RT-PCR techniques. Primers for qPCR were designed using Primer 3.0. The first-strand cDNA synthesis was performed by using the Primescript reverse transcriptase (Takara, Japan). We performed real-time PCR with a SYBR Premix Ex Taq™ (perfect real time) kit (Takara, Japan) and using the Applied Biosystems 7500 Real-Time PCR System (ABI) using a relative standard curve method with the following primers: *BoALMT1*, 5′-AGAGAAGGAAGGAGGGTAGGAG AA-3′ (forward) and 5′-GAAGACAACAACGACGGTCA-3′ (reverse); *Actin* (LOC106327159), 5′-TAACAGGGAGAAGATG ACTCAGATCA-3′ (forward) and 5′-AAGATCAAGACGAAGG ATAGCATGAG-3′ (reverse). Quantitative PCR was performed with conditions of 95°C for 3 min, and then 40 cycles of 95°C for 10 s, 60°C for 30 s, and 72°C for 30 s. Expression data were normalized to the expression level of *Actin* by the ΔΔCt method.

Subcellular Localization of BoALMT1

The subcellular localization of BoALMT1 was determined in onion (*Allium cepa*) epidermal cells. We constructed a vector as 35S:BoALMT1::GFP. The coding region of *BoALMT1* was subcloned into the expression vector pCAMBIA1302 using primers: 5′-CATGCCATGGTAATGGAGAAACTGAGAGAGA TAGTG-3′ (forward) and 5′-GGACTAGTAATCTGAAGTAT ACGAACACCC-3′ (reverse). We transferred the chimera by particle bombardment. The gold particles (1 μm, 1.5 mg) were coated with 5 μg of plasmid DNA in a solution of 2.5 M $CaCl_2$ and 0.1 M spermidine (Sigma). We bombarded the epidermal onion peels at a helium pressure of 25–30 Mpa (Bio-rad, U.S.), and then incubated the tissue in MS medium at room temperature in the dark for 24 h. Confocal laser scanning microscopy (Leica DMI 6000B-CS, Germany) with a 488 nm excitation wavelength was used to detect the GFP fluorescence. We induced cell plasmolysis by adding 0.8 M mannitol for 3–5 min.

BoALMT1 Expression in *Xenopus laevis* Oocytes

We cloned the coding regions (cDNA) of *BoALMT1* into the MCS of a pCS107 vector. According to the manufacturer's (Ambion) recommendations, we synthesized the cRNA from 1 μg of *Asc*I-linearized plasmid DNA template. We harvested

stage V–VI *Xenopus laevis* oocytes as described previously (Golding, 1992; Hoekenga et al., 2006). We injected 50 nl RNase-free water containing 15 ng of cRNA encoding *BoALMT1* or 50 nl RNase-free water into oocytes using a micro-injector and then incubated the injected oocytes at 18°C for 2 d in oocyte culture medium, OCM; 1L OCM contains 600 ml L-15 (Sigma L4386), 400 mg BSA (Sigma A4919), 5 ml Penicillin-Streptomycin (Gibco 15140-122), and 400 ml H_2O). Before flux measurements of H^+, we preloaded malate in the *Xenopus* oocytes by injection of 50 nl of 0.1 M sodium malate or water. Two hours after preloading, the H^+ fluxes were measured 30 μm away from *X. laevis* oocytes in a solution of 2 mM KCl, 96 mM NaCl, 1 mM $MgCl_2$, 0.3 mM MES, 1.8 mM $CaCl_2$ with or without 0.1 mM $AlCl_3$ and with the pH 4.5. Net H^+ fluxes were measured using SIET (Xuyue Science and Technology Co., Ltd., Beijing, China) under steady conditions for 8–10 min to insure that no fluctuation was present. We used the OCM bath solution (pH = 4.5) to perform the ^{14}C-labeled malate experiment as our previous study (Wu et al., 2014).

Heterologous Expression of *BoALMT1* in *Arabidopsis thaliana*

The coding region (cDNA) of *BoALMT1* was amplified with primers (5′-GCTCTAGAATGGAGAAACTGAGAGAGATAGTG-3′ and 5′-CGCCCCGGGTCAAATCTGAAGTATACGAACACCC-3′) and was cloned into pBI121. We transformed the construct into *Arabidopsis* using *Agrobacterium tumefaciens* via the floral dip method (Clough and Bent, 1998). We used RT-PCR to measure the expression level of *BoALMT1* in the transgenic plants. Root malate release and Al tolerance were analyzed in two independent homozygous transgenic T3 lines as follows. *Arabidopsis* seeds, stratified at 4°C for 3 days, were surface-sterilized and sown onto solid MS medium for 4 days. After germination, we removed uniform seedlings to 0.5 mM $CaCl_2$-agar plates containing 0 or 400 μM $AlCl_3$ (pH = 4.5). The seedlings were kept on agar plates for 2 days, and then the roots were scanned and the primary root length was measured by the Image J program (Liu et al., 2009). For malate exudation assays, two transgenic *Arabidopsis* and wild-type lines were surface sterilized and germinated on solid MS medium for 1 week. Next, we transferred the seedlings to a 25 ml solution with 0.5 mM $CaCl_2$ (pH 4.5) and without Al for 24 h. After this 24 h pre-incubation step, we then transfered the plants to 25 ml exudation medium (pH 4.5) with or without Al (50 μM $AlCl_3$). We collected the sample for malate assay by capillary electrophoresis, as described by Hoekenga et al. (2006). We measured the fluxes of H^+ by using the non-invasive Scanning Ion-selective Electrode Technique (SIET) (Xuyue Science and Technology Co., Ltd., Beijing, China) as described by Bose et al. (2010). The 4- to 5-day-old wild type and BoALMT1 expressing *Arabidopsis* seedlings were equilibrated in a solution (0.1 mM CaCl2, 0.1 mM KCl, 0.3 mM MES, pH 4.5) with or without 50 mM Al for 5–10 min. H^+ fluxes were measured 200 mm from the root tip for 6–10 min. The H^+ fluxes were calculated by the JCal V3.1 (a free MS Excel spreadsheet, youngerusa.com or ifluxes.com). The H^+ flux assay was replicated independently 4–6 times and the data were averaged.

Statistical Analysis

All the statistical analysis was performed by one-way ANOVA and the *t*-test to determine the significance at the $P < 0.05$ level.

AUTHOR CONTRIBUTIONS

LZ, X-XW, and Y-DG: designed research; X-XW, LZ, JW, CQ, XW, GW, ML, and XL: performed research; JW, X-XW, LZ, and Y-DG: analyzed the data; X-XW, LZ, JW, and Y-DG: wrote the paper.

ACKNOWLEDGMENTS

We thank Prof. S Ren and Dr. S Weeda (Virginia State University) for critical reading of the manuscript and Prof. Q Tao (Tsinghua University, Beijing) for providing Xenopus oocytes test system. This work was supported by the grants to Y-DG (2016YFD0101007, BLVT-03) and to XL (tszy20140808).

REFERENCES

Ahn and Matsumoto, H. (2006). The role of the plasma membrane in the response of plant roots to aluminum toxicity. *Plant Signal. Behav.* 1, 37–45. doi: 10.4161/psb.1.2.2588

Bose, J., Babourina, O., Shabala, S., and Rengel, Z. (2010). Aluminum-dependent dynamics of ion transport in *Arabidopsis*: specificity of low pH and aluminum responses. *Physiol. Plantarum* 139, 401–412. doi: 10.1111/j.1399-3054.2010.01377.x

Chen, Q., Kan, Q., Wang, P., Yu, W., Yu, Y., Zhao, Y., et al. (2015). Phosphorylation and interaction with the 14-3-3 protein of the plasma membrane H^+-ATPase are involved in the regulation of magnesium-mediated increases in aluminum-induced citrate exudation in broad bean (*Vicia faba*. L). *Plant Cell Physiol.* 56, 1144–1153. doi: 10.1093/pcp/pcv038

Chen, Q., Wu, K. H., Wang, P., Yi, J., Li, K. Z., Yu, Y., et al. (2013). Overexpression of MsALMT1, from the aluminum-sensitive *Medicago sativa*, enhances malate exudation and aluminum resistance in tobacco. *Plant Mol. Biol. Rep.* 31, 769–774. doi: 10.1007/s11105-012-0543-2

Clough, S. J., and Bent, A. F. (1998). Floral dip: a simplified method for Agrobacterium-mediated transformation of *Arabidopsis thaliana*. *Plant J.* 16, 735–743. doi: 10.1046/j.1365-313x.1998.00343.x

Collins, N. C., Shirley, N. J., Saeed, M., Pallotta, M., and Gustafson, J. P. (2008). An ALMT1 gene cluster controlling aluminum tolerance at the Alt4 locus of rye (*Secale cereal* L.). *Genetics* 179, 669–692. doi: 10.1534/genetics.107.083451

Degenhardt, J., Larsen, P. B., Howell, S. H., and Kochian, L. V. (1998). Aluminum resistance in the *Arabidopsis* mutant alr-104 is caused by an aluminum-induced increase in rhizosphere pH. *Plant Physiol.* 117, 19–27. doi: 10.1104/pp.117.1.19

Delhaize, E., Gruber, B. D., and Ryan, P. R. (2007). The roles of organic anion permeases in aluminium resistance and mineral nutrition. *FEBS Lett.* 581, 2255–2262. doi: 10.1016/j.febslet.2007.03.057

Delhaize, E., Ryan, P. R., Hebb, D. M., Yamamoto, Y., Sasaki, T., and Matsumoto, H. (2004). Engineering high-level aluminum tolerance in barley with the ALMT1 gene. *Proc. Natl. Acad. Sci. U.S.A.* 101, 15249–15254. doi: 10.1073/pnas.0406258101

Delhaize, E., Ryan, P. R., and Randall, P. J. (1993). Aluminum tolerance in wheat (*Triticum aestivum* L.): II. Aluminum-stimulated excretion of malic acid from root apices. *Plant Physiol.* 103, 695–702. doi: 10.1104/pp.103.3.695

Furukawa, J., Yamaji, N., Wang, H., Mitani, N., Murata, Y., Sato, K., et al. (2007). An aluminum-activated citrate transporter in barley. *Plant Cell Physiol.* 48, 1081–1091. doi: 10.1093/pcp/pcm091

Golding, A. L., (1992). Maintenance of *Xenopus laevis* and oocyte injection. *Method Enzymol.* 207, 266–279. doi: 10.1016/0076-6879(92)07017-I

Hoekenga, O. A., Maron, L. G., Pineros, M. A., Cancado, G. M. A., Shaff, J., Kobayashi, Y., et al. (2006). AtALMT1, which encodes a malate transporter, is identified as one of several genes critical for aluminum tolerance in *Arabidopsis*. *Proc. Natl. Acad. Sci. U.S.A.* 103, 9738–9743. doi: 10.1073/pnas.0602868103

Hoekenga, O. A., Vision, T. J., Shaff, J. E., Monforte, A. J., Lee, G. P., Howell, S. H., et al. (2003). Identification and characterization of aluminum tolerance loci in *Arabidopsis* (*Landsberg erecta x Columbia*) by quantitative trait locus mapping. A physiologically simple but genetically complex trait. *Plant Physiol.* 132, 936–948. doi: 10.1104/pp.103.023085

Horst, W. J., Wang, Y., and Eticha, D. (2010). The role of the root apoplast in aluminium-induced inhibition of root elongation and in aluminium resistance of plants: a review. *Ann. Bot.* 106, 185–197. doi: 10.1093/aob/mcq053

Kobayashi, Y., Sugimoto, M., Lakshmanan, V., Iuchi, S., Kobayashi, M., et al. (2013). Characterization of the complex regulation of AtALMT1 expression in response to phytohormones and other inducers. *Plant Physiol.* 162, 732–740. doi: 10.1104/pp.113.218065

Kochian, L. V., Hoekenga, O. A., and Pineros, M. A. (2004). How do crop plants tolerate acid soils? Mechanisms of aluminum tolerance and phosphorous efficiency. *Annu. Rev. Plant Biol.* 55, 459–493. doi: 10.1146/annurev.arplant.55.031903.141655

Kochian, L. V., Pineros, M. A., and Hoekenga, O. A. (2005). The physiology, genetics and molecular biology of plant aluminum resistance and toxicity. *Plant Soil* 274, 175–195. doi: 10.1007/s11104-004-1158-7

Liang, C., Piñeros, M. A., Tian, J., Yao, Z., Sun, L., Liu, J., et al. (2013). Low pH, aluminum and phosphorus coordinately regulate malate exudation through GmALMT1 to improve soybean adaptation to acid soils. *Plant Physiol.* 161, 1347–1361. doi: 10.1104/pp.112.208934

Ligaba, A., Katsuhara, M., Ryan, P. R., Shibasaka, M., and Matsumoto, H. (2006). The BnALMT1 and BnALMT2 genes from rape encode aluminum-activated malate transporters that enhance the aluminum resistance of plant cells. *Plant Physiol.* 142, 1294–1303. doi: 10.1104/pp.106.085233

Ligaba, A., Maron, L. G., Shaff, J., Kochian, L. V., and Piñeros, M. A. (2008). Maize ZmALMT2 is a root anion transporter that mediates constitutive root malate efflux. *Plant Cell Environ.* 35, 1185–1200. doi: 10.1111/j.1365-3040.2011.02479.x

Liu, J., Magalhaes, J. V., Shaff, J., and Kochian, L. V. (2009). Aluminum-activated citrate and malate transporters from the MATE and ALMT families function independently to confer *Arabidopsis* aluminum tolerance. *Plant J.* 57, 389–399. doi: 10.1111/j.1365-313X.2008.03696.x

Magalhaes, J. V., Liu, J., Guimarães, C. T., Lana, U. G., Alves, V. M., Wang, Y. H., et al. (2007). A gene in the multidrug and toxic compound extrusion (MATE) family confers aluminum tolerance in sorghum. *Nat. Genet.* 39, 1156–1161. doi: 10.1038/ng2074

Meyer, S., De Angeli, A., Fernie, A. R., and Martinoia, E. (2010). Intra- and extra-cellular excretion of carboxylates. *Trends Plant Sci.* 15, 40–47. doi: 10.1016/j.tplants.2009.10.002

Pellet, D. M., Grunes, D. L., and Kochian, L. V. (1995). Organic acid exudation as an aluminum-tolerance mechanism in maize (*Zea mays* L.). *Planta* 196, 788–795. doi: 10.1007/BF01106775

Pereira, J. F., Zhou, G., Delhaize, E., Richardson, T., and Ryan, P. R. (2010). Engineering greater aluminium resistance in wheat by over-expressing TaALMT1. *Ann. Bot.* 106, 205–214. doi: 10.1093/aob/mcq058

Piñeros, M. A., Cancado, G. M. A., Maron, L. G., Lyi, S. M., Menossi, M., and Kochian, L. V. (2008). Not all ALMT1-type transporters mediate aluminum-activated organic acid responses: the case of ZmALMT1, an anion-selective transporter. *Plant J.* 53, 352–367. doi: 10.1111/j.1365-313X.2007.03344.x

Raman, H., Zhang, K., Cakir, M., Appels, R., Garvin, D. F., Maron, L. G., et al. (2005). Molecular characterization and mapping of ALMT1, the aluminium-tolerance gene of bread wheat (*Triticum aestivum* L.). *Genome* 48, 781–791. doi: 10.1139/g05-054

Ryan, P. R., Tyerman, S. D., Sasaki, T., Furuichi, T., Yamamato, Y., Zhang, W. H., et al. (2011). The identification of aluminium-resistance genes provides opportunities for enhancing crop production on acid soils. *J. Exp. Bot.* 62, 9–20. doi: 10.1093/jxb/erq272

Sasaki, T., Yamamoto, Y., Ezaki, B., Katsuhara, M., Ahn, S. J., Ryan, P. R., et al. (2004). A wheat gene encoding an aluminum-activated malate transporter. *Plant J.* 37, 645–653. doi: 10.1111/j.1365-313X.2003.01991.x

Tesfaye, M., Temple, S. J., Allan, D. L., Vance, C. P., and Samac, D. A. (2001). Overexpression of malate dehydrogenase in transgenic alfalfa enhances organic acid synthesis and confers tolerance to aluminum. *Plant Physiol.* 127, 1836–1844. doi: 10.1104/pp.010376

Tian, Q., Zhang, X., Sunita, R., Matthew, G., Stephen, D. T., and Zhang, W. H. (2014). Ethylene negatively regulates aluminum-induced malate efflux from wheat roots and tobacco cells transformed with TaALMT1. *J. Exp. Bot.* 65, 2415–2426. doi: 10.1093/jxb/eru123

Wang, J. P., Raman, H., Zhou, M. X., Ryan, P. R., Delhaize, E., Hebb, D. M., et al. (2007). High-resolution mapping of the Al locus and identification of a candidate gene HvMATE controlling aluminium tolerance in barley (*Hordeum vulgare* L.). *Theor. Appl. Genet.* 115, 265–276. doi: 10.1007/s00122-007-0562-9

Wu, X., Li, R., Shi, J., Wang, J., Sun, Q., Zhang, H., et al. (2014). *Brassica oleracea* MATE encodes a citrate transporter, and enhances aluminum tolerance in *Arabidopsis thaliana*. *Plant Cell Physiol.* 55, 1426–1436. doi: 10.1093/pcp/pcu067

Yamaguchi, M., Sasaki, T., Sivaguru, M., Yamamoto, Y., Osawa, H., Ahn, S. J, et al. (2005). Evidence for the plasma membrane localization of Al-activated malate transporter (ALMT1). *Plant Cell Physiol.* 46, 812–816. doi: 10.1093/pcp/pci083

Yamaji, N., Huang, C. F., Nagao, S., Yano, M., and Sato, Y. (2009). A zinc finger transcription factor ART1 regulates multiple genes implicated in aluminum tolerance in rice. *Plant Cell* 21, 3339–3349. doi: 10.1105/tpc.109.070771

Yang, J. L., Zhang, L., and Zheng, S. J. (2008). Aluminum-activated oxalate secretion does not associate with internal content among some oxalate accumulators. *J. Integr. Plant Biol.* 50, 1103–1107. doi: 10.1111/j.1744-7909.2008.00687.x

Yang, Z.-B., Geng, X., He, C., Zhang, F., Wang, R., Horst, W. J., et al. (2014). TAA1-regulated local auxin biosynthesis in the root-apex transition zone mediates the aluminum-induced inhibition of root growth in *Arabidopsis*. *Plant Cell* 26, 2889–2904. doi: 10.1105/tpc.114.127993

Yu, Y., Jin, C., Sun, C., Wang, J., Ye, Y., Zhou, W., et al. (2016). Inhibition of ethylene production by putrescine alleviates aluminum induced root inhibition in wheat plants. *Sci. Rep.* 6:18888. doi: 10.1038/srep18888

Zheng, S. J., Yang, J. L., He, Y. F., Yu, X. H., Zhang, L., You, J. L., et al. (2005). Immobilization of aluminum with phosphorous in roots is associated with high aluminum resistance in buckwheat. *Plant Physiol.* 138, 297–303. doi: 10.1104/pp.105.059667

Conflict of Interest Statement: The authors declare that the research was conducted in the absence of any commercial or financial relationships that could be construed as a potential conflict of interest.

frontiers in Plant Science

ORIGINAL RESEARCH
published: 10 January 2018
doi: 10.3389/fpls.2017.02246

Soybean NADP-Malic Enzyme Functions in Malate and Citrate Metabolism and Contributes to Their Efflux under Al Stress

*Ying Zhou, Zhenming Yang, Yuezi Xu, Haoran Sun, Zhitao Sun, Bao Lin, Wenjing Sun and Jiangfeng You**

Laboratory of Soil and Plant Molecular Genetics, College of Plant Science, Jilin University, Changchun, China

Malate accumulation has been suggested to balance Al-induced citrate synthesis and efflux in soybean roots. To test this hypothesis, characteristics of Al-induced accumulation and efflux of citrate and malate were compared between two soybean genotypes combining a functional analysis of *GmME1* putatively encode a cytosolic NADP-malic enzyme. Similar amounts of citrate were released, and root elongation was equally inhibited before 8 h of Al treatment of Jiyu 70 and Jiyu 62 cultivars. Jiyu 70 began to secrete more citrate and exhibited higher Al resistance than did Jiyu 62 at 12 h. A sustained increase in internal malate and citrate concentrations was observed in Jiyu 70 at 24 h of Al treatment. However, Jiyu 62 decreased its malate concentration at 12 h and its citrate concentration at 24 h of Al treatment. GmME1 localized to the cytoplast and clustered closely with cytosolic malic enzymes AtME2 and SgME1 and was constitutively expressed in the roots. Al treatment induced higher NADP-malic enzyme activities and *GmME1* expression levels in Jiyu 70 than in Jiyu 62 within 24 h. Compared with wild-type hairy roots, over-expressing *GmME1* in hairy roots (*GmME1*-OE) produced higher expression levels of *GmME1* but did not change the expression patterns of either of the putative citrate transporter genes *GmAACT1* and *GmFRDL* or the malate transporter gene *GmALMT1,* with or without Al treatment. *GmME1*-OE showed a higher internal concentration and external efflux of both citrate and malate at 4 h of Al stress. Lighter hematoxylin staining and lower Al contents in root apices of *GmME1*-OE hairy roots indicated greater Al resistance. Comprehensive experimental results suggest that sustaining Al-induced citrate efflux depends on the malate pool in soybean root apices. *GmME1* encodes a cytosolic malic enzyme that contributes to increased internal malate and citrate concentrations and their external efflux to confer higher Al resistance.

Keywords: aluminum toxicity, anaplerotic reaction, citrate efflux, malic enzyme, tricarboxylic acid cycle

OPEN ACCESS

Edited by:
Wei Fan,
Yunnan Agricultural University, China

Reviewed by:
Zhichang Chen,
Fujian Agriculture and Forestry University, China
Wei Hu,
Institute of Tropical Bioscience and Biotechnology (CATAS), China

****Correspondence:***
Jiangfeng You
youjf@jlu.edu.cn

Specialty section:
This article was submitted to Plant Abiotic Stress, a section of the journal Frontiers in Plant Science

Received: *21 July 2017*
Accepted: *21 December 2017*
Published: *10 January 2018*

Citation:
Zhou Y, Yang Z, Xu Y, Sun H, Sun Z, Lin B, Sun W and You J (2018) Soybean NADP-Malic Enzyme Functions in Malate and Citrate Metabolism and Contributes to Their Efflux under Al Stress. Front. Plant Sci. 8:2246. doi: 10.3389/fpls.2017.02246

INTRODUCTION

Aluminum (Al) toxicity seriously restricts crop yield in acidic soils, which cover almost 40% of the arable land worldwide (Ma et al., 2001). Al can significantly inhibit root growth and disrupt root function rapidly (Delhaize and Ryan, 1995). Fortunately, some plant species have developed Al resistance mechanisms to grow in acidic soils. Al-induced organic acid efflux has

been well established to detoxify Al internally and externally and thus far is the best-documented Al resistance mechanism in higher plants (Ma et al., 2001; Ryan et al., 2001; Kochian et al., 2004; Kochian et al., 2015). Two patterns have been classified according to the rapidity of organic acid release (Ma et al., 2001). In pattern I, some plant species, such as wheat (Ryan et al., 1995) and buckwheat (Ma and Miyasaka, 1998), can rapidly release malate or oxalate, respectively, after Al stress. In pattern II, some species, such as *Cassia tora* (Ma et al., 1997) and soybean (Yang et al., 2001), secrete citrate after at least 4 h of Al treatment. In both patterns, organic acid anion transporters are crucial for organic acid efflux under Al stress and for Al resistance (Ryan et al., 2011). Over-expression of *TaALMT1* (Aluminum-activated malate transporter) in barley (Liu et al., 2009) and wheat (Collins et al., 2008) increased Al resistance by 8-fold and 20-fold, respectively. The Al resistance of Arabidopsis can be increased by 2.5-fold and 3-fold by over-expression of MATE family citrate transporter genes *SbMATE* (Magalhaes et al., 2007) and *ZmMATE1* (Maron et al., 2013), respectively.

The strategies to over-express enzymes involved in organic acid metabolism have also been proven effective in regulating Al resistance in some plant species. Over-expression of citrate synthase genes in different plant species, including alfalfa, Arabidopsis, canola and tobacco, can increase their citrate efflux and Al^{3+} resistance in transgenic plants (Koyama et al., 1999; Anoop et al., 2003; Barone et al., 2008; Deng et al., 2009; Han et al., 2009). Malate dehydrogenase genes of different origins were over-expressed in alfalfa (Tesfaye et al., 2001) and tobacco (Wang et al., 2010) and showed enhanced malate efflux and improved Al^{3+} resistance. *SgME1* encoding NADP-dependent malic enzyme was found to functionally control malate synthesis and secretion and thus Al detoxification (Sun et al., 2014). Recently, over-expression of *VuFDH* encoding a mitochondrial formate dehydrogenase and *VuAAE3* encoding Acyl activating enzyme 3 in tobacco were found to increase Al tolerance by decreasing formate production and oxalate accumulation, respectively (Lou et al., 2016a,b).

Our previous study showed that Al-induced citrate secretion from soybean required almost 4 h of Al exposure (Yang et al., 2000, 2001), which was clearly classified as pattern II (Ma, 2000). Soybean mitochondrial enzymes, including increased citrate synthase and decreased aconitase, were found to contribute to the citrate efflux from roots under Al stress (Xu et al., 2010). Sustained Al-induced citrate efflux from common bean, the close relative of soybean, was reported to rely on the maintenance of high citrate synthase activity and citrate pool (Rangel et al., 2010). Cytosol phosphoenolpyruvate carboxylase (PEPC) and mitochondrial NAD malic enzyme were suggested to contribute to the accumulation and the secretion of citrate in common bean by fueling the tricarboxylic acid (TCA) cycle (Rangel et al., 2010).

Organic acid metabolism-related enzymes was proposed to contribute to detoxifying Al in some plant species (Rangel et al., 2010; Xu et al., 2010; Sun et al., 2014; Lou et al., 2016a,b). In soybean, during the process of citrate efflux from soybean, malate but not citrate significantly decreased with the increase in Al treatment duration (Yang et al., 2001). Thus, malate was hypothesized to maintain balance between the citrate pool and efflux in the soybean roots exposed to Al. However, there is no direct evidence to support this hypothesis until now. Malate is tightly controlled to affect a series of physiological processes because it is at the branching point of many metabolic pathways (Santelia and Lawson, 2016). The transcript level of NADP-malic enzyme was found by microarray assay to increase in soybean root apices under Al stress (You et al., 2011). In this study, in order to elucidate the role of malate pool in the Al-induced citrate efflux from soybean, *GmME1,* probably encoding NADP-dependent malic enzyme in soybean, was functionally characterized to evaluate its possible implications in organic acid pool and efflux. Al-induced accumulation and efflux of citrate and malate were also compared between two soybean genotypes in relation to GmME1 enzyme activities and gene expression patterns.

MATERIALS AND METHODS

Hydroponic Culture and Al Treatment Conditions

Our previous work has shown that soybean cultivar Jiyu 70 and Jiyu 62 exhibited contrast Al resistance capabilities, thus was used as Al tolerant and Al sensitive cultivars respectively in our lab. Seeds of soybean Jiyu 70 and Jiyu 62 cultivars were germinated in darkness for 3 days. Then, seedlings with roots 4–5 cm long were selected for transplant into 0.5 mM $CaCl_2$ solution. After 24 h of culture, seedlings were exposed to 0.5 mM $CaCl_2$ solution containing 0 or 30 μM $AlCl_3$ (pH 4.5). Root length was measured at 0, 8, 12, and 24 h. The relative root elongation (RRE) was calculated to evaluate Al sensitivity. The formula is root elongation with $AlCl_3$ treatment/root elongation, without $AlCl_3$ × 100.

The remaining germinated seedlings were grown in 1-L plastic pots filled with nutrient solution with composition, as described by Horst et al. (1992). The solutions were modified to pH 4.5 by HCl and aerated continually. After 14 days of culture, seedlings were pre-cultured in 0.5 mM $CaCl_2$ solution (pH 4.5) overnight and then transferred to 0.5 mM $CaCl_2$ solution containing 0 or 30 μM $AlCl_3$ (pH 4.5). Treatment solutions were refreshed at 2, 4, 8, 12, and 24 h and collected, respectively, for organic acid analysis. Root exudates were concentrated and purified, as described in Ma et al. (1997). Simultaneously, root apices were excised from the parallel Al-treated soybean seedlings at 0, 2, 4, 8, 12, and 24 h (∼0.5 g for each sample). Citrate and malate were extracted from the excised root apices, as described in Yang et al. (2001). Their concentrations were measured by high-performance liquid chromatography (HPLC) (LC 20AT, Shimadzu, Tokyo, Japan) with a Shodex RSpakKC-811 ion-exclusion column (300 × 8 mm, Shimadzu, Tokyo, Japan). NADP-malic enzyme (EC1.1.1.40) was extracted and quantified by an NADP-ME kit (Comin Biotechnology, Suzhou, China). The rate of increase of NADP was monitored at 340 nm.

The 7-day-old seedlings were transferred into 0.5 mM $CaCl_2$ solution (pH 4.5) overnight and then exposed to 0.5 mM $CaCl_2$ solution (pH 4.5) including 0 or 30 μM $AlCl_3$. Then, 0- to 1-cm root apices were excised at a treatment duration of 0, 2, 4, 8, 12,

and 24 h. The collected root apices were immediately placed in liquid nitrogen and stored at −80°C for RNA isolation.

Soybean seedlings were cultivated in a controlled environment with a 14 h/25°C day and 10 h/22°C night cycle. Light intensity was controlled as 300 μmol $m^{-2}s^{-1}$. Relative humidity was kept at 60%.

Jiyu 70 was sown in the field of the agricultural trial station of Jilin University at the end of April 2014. The soil contained 49.4 ± 4.8 g/kg available nitrogen, 11.8 ± 4.1 g/kg available P, 170 ± 6.2 g/kg K, and 21.8 ± 3.7 g/kg organic carbon at pH 6.5. After 18 days, the roots, shoots, leaves, flowers and pods were sampled in the field-grown soybean. The samples were stored at −80°C for RNA isolation.

Gene Transcriptional Expression

RNA was extracted from root apices by Trizol reagent (Invitrogen, Carlsbad, CA, United States). cDNA was obtained by reverse transcribing with M-MLV reverse transcriptase (TaKaRa Bio, Tokyo, Japan). The gene-specific primers were designed according to the CDS of *GmME1* (Glyma.06G087800) by Primer 3.0 online[1] and had the following sequences: forward primer 5′-AGCATCTGTGGTATTAGCA-3′; reverse primer 5′-GGAATAAGAAGGTATGGTCAAC-3′. The housekeeping gene β-*Tublin* (GenBank ID: 100811275) had the following primer: forward primer 5′-GGAAGGCTTTCTTGCATTGGTA-3′; reverse primer 5′-AGTGGCATCCTGGTACTGC-3′. Quantitative real-time PCR (qRT-PCR) was conducted in an Mx3005P machine (PRIMER Biosoft Company, Palo Alto, CA, United States). The 25 μl reaction system included 2 μl of cDNA template (50 ng), 1 μl of a mixture of forward and reverse primers (10 mM), 12.5 μl of 2× SYBR Taq (TaKaRa, Bio Inc.), and 9.5 μl of milli-Q water. The program was as follows: 95°C for 30 s; 30 cycles of 95°C for 5 s, 60°C for 20 s, 95°C for 60 s, 55°C for 30 s, and 95°C for 30 s. Relative expression was computed according to the $2^{-\Delta\Delta C_t}$ method (Livak and Schmittgen, 2001).

Gene Cloning and Sequence Analysis

PCR was performed with cDNA template prepared by root apices treated with Al for 4 h. The primers were designed according to the CDS of *GmME1* (Glyma.06G087800), considering the vector pCAMBIA3301 with BamHI with the following primer sequence: GmME1-NF5′-CATTCTGGCGGGATCCGCAGCAGCAGCAGCAATGTCGA GCGCTTCGTTGA-3, BamHI; GmME1-NR5′-GAGAAAGC TTGGATCCAACGGTAGCTTCGGTAGCCT-3′, BamHI. The PCR products were purified using the TransGen Biotech Kit according to the manufacturer's protocol, confirmed by sequencing, and aligned to vectors (pCAMBIA3301) by in-fusion enzyme. Phylogenetic tree construction and sequence comparison were conducted with MEGA 5.1 and Cluster. Other MATE family gene sequences were blasted at the NCBI website as follows: *Arabidopsis thaliana* (*AtNADP-ME1* GeneID:816509, *AtNADP-ME2* GeneID:831039, *AtNADP-ME3* GeneID:832657, *AtNADP-ME4* GeneID:844314), *Flaveria bidentis* (*FbNADP-ME* LOCUS: AAW56450), *Lycopersicon esculentum* (LeME2 LOCUS: AAB58728), *Medicago truncatula* (*MtNADP-ME* GeneID:25490143), *Nicotiana sylvestris* (*NtNADP-ME* GeneID:104247285), *Oryza sativa* (*OsNADP-ME* GeneID:4338007), *Stylosanthes guianensis* (*SgME1* LOCUS AGH32501), and *Vigna Umbellata* (*VuNADP-ME* LOCUS CAA56354).

The subcellular localization of GmME1 was determined as follows: The CDS of *GmME1* was cloned into pENSG-N-YFP vector with the cauliflower mosaic virus (CaMV) 35S as a promoter. The resulting constructs were fully sequenced to check the sequence accuracy. Plasmid DNA was transformed into Arabidopsis protoplast cells. The imaging of GFP fluorescence was conducted by microscopy (Zeiss 2012 Observer, Göttingen, Germany).

Agrobacterium-Mediated Over-expression of *GmME1* in Soybean Hairy Roots

With CaMV 35S as the promotor, PCR product was cloned into the modified pCamBIA3301 vector. After verification by sequence, the resulting construct was transformed into the K599 strain by electroporation. Soybean transformation in Jiyu 62 cotyledons and hairy root induction were performed according to Subramanian et al. (2005). Hairy roots with scanning luciferase activity greater than 3000 were considered successfully transformed. The hairy roots induced by only K599 were considered wild type (WT). Both transgenic and WT hairy roots were treated in 0.5 mM $CaCl_2$ solution (pH 4.5) including 0 or 30 μM $AlCl_3$ in a 5-ml plastic tube. Root exudates were collected at 4 h for citrate and malate efflux measurement. Root apices (0–1 cm) were cut, and three were stained by hematoxylin. The remaining root apices were stored at −80°C for RNA isolation, internal organic acid concentration measurement, or Al concentration examination. Internal citrate and malate were extracted according to Yang et al. (2000). Citrate and malate concentrations and efflux were measured by enzymatic method (Delhaize et al., 1993). The Al concentration in hairy root apices was determined by 2 M HCl and assayed by an atomic absorption spectrophotometer equipped with a graphite furnace atomizer (Perkin Elmer AAnalyst 700, United States).

RESULTS

Time Course of Relative Root Elongation and Citrate Efflux in Two Soybean Genotypes under Al Stress

Root elongation was nearly equally inhibited during 8 h of Al exposure for both genotypes, whereas recovery began at 12 h for Jiyu 70 and at 24 h for Jiyu 62 (**Figure 1A**). A significant difference in Al-induced citrate exudation (**Figure 1B**) was found between Jiyu 70 and Jiyu 62 at 12 h of Al treatment. The RRE of Jiyu 70 was approximately 1.7 fold greater than that of Jiyu 62 at 12 h (**Figure 1A**). In addition, an approximately 1.8 fold greater Al-induced citrate efflux was found in Jiyu 70 than in Jiyu 62 (**Figure 1B**). The higher Al resistance of Jiyu 70 depends on the

[1]http://primer3.ut.ee/

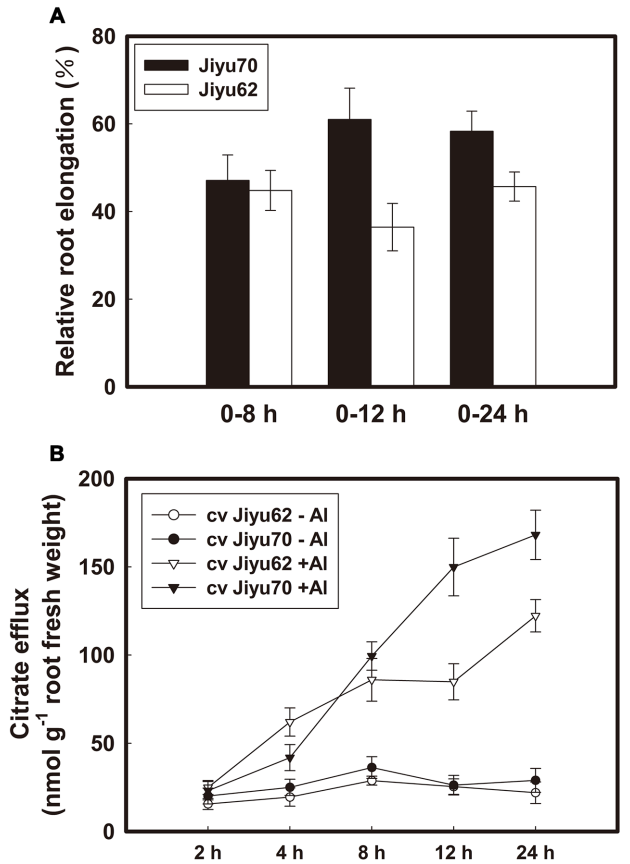

FIGURE 1 | Effect of Al on root elongation **(A)** and Al-induced citrate efflux **(B)** of two soybean genotypes. Seedlings with roots 4–5 cm long were exposed to 0 or 30 μM Al in 0.5 mM $CaCl_2$ solution. The root length was measured with a ruler at 0, 8, 12, and 24 h. Fourteen-day-old seedlings were exposed to 0 or 30 μM Al in 0.5 mM $CaCl_2$ solution. Root exudates were collected at 2, 4, 8, 12, and 24 h. Relative root elongation was calculated, and organic acid exudates were analyzed as described in Section "Materials and Methods." The values are the means of three independent experiments ± SDs.

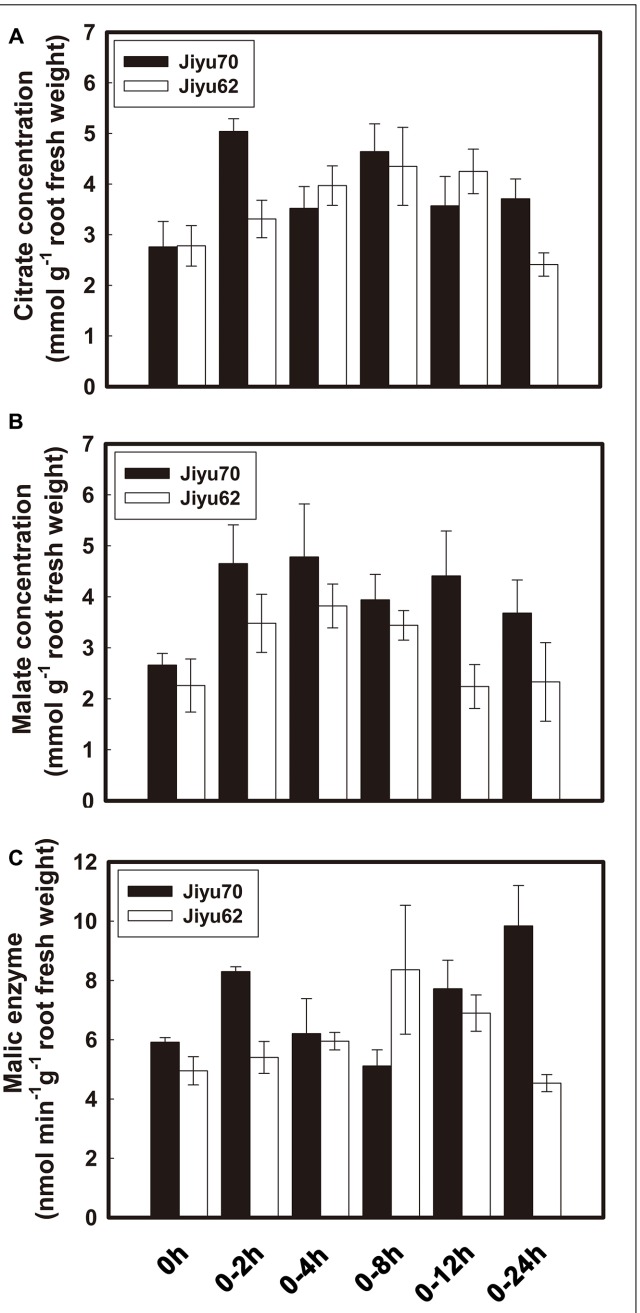

FIGURE 2 | The time course of internal citrate **(A)**, malate **(B)**, and NADP-malic enzyme **(C)** concentration in root apices of two soybean genotypes. Soybean seedlings were transferred to 0.5 mM $CaCl_2$ solution (pH 4.5) with or without 30 μM $AlCl_3$. The root apices of soybean were excised at 2, 4, 8, 12, and 24 h. Internal malate, citrate and malic enzyme were extracted and examined. Error bars represent ± SD (n = 3).

recovery from Al-induced root elongation inhibition, in which maintenance of continuous citrate efflux is necessary. Quimbaya, an Al-resistant common bean genotype, was also found to recover root elongation inhibition by sustaining Al-induced citrate efflux (Rangel et al., 2010).

Time Course of Internal Citrate and Malate Concentration and NADP-Mali Enzymes Activities in Two Soybean Genotypes under Al Stress

Al treatment increased the internal citrate and malate concentrations beginning at 2 h of Al exposure for both genotypes (**Figures 2A,B**). Higher citrate and malate concentrations were always found in Jiyu 70 during throughout the Al treatment duration. A great decrease in the malate concentration occurred at 12 h of Al treatment, followed by a decrease in the citrate concentration at 24 h in Jiyu 62 (**Figures 2A,B**). The exhaustion of malate (**Figure 2B**) might have a negative effect on the citrate concentration (**Figure 2A**) and efflux (**Figure 1B**) under Al stress. Compared with Jiyu 70, malate exhaustion at Jiyu 62 at 12 h was consistent with the lower citrate efflux at 24 h (**Figure 1B**). This result is consistent with our previous study in another soybean

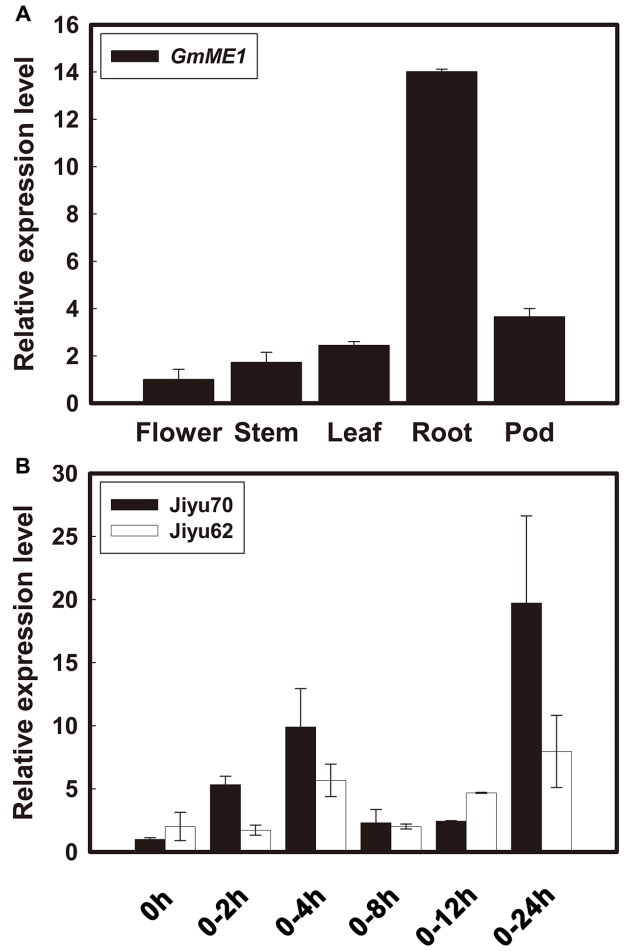

FIGURE 3 | Transcriptional expression patterns of *GmME1* in soybean. **(A)** Tissue localization expression of *GmME1*. After 18 days of growth in the field, the roots, shoots, leaves, flowers and pods were sampled from Jiyu 70 soybean seedlings. **(B)** Four-day-old seedlings were cultured in 0.5 mM $CaCl_2$ solution containing 30 μM $AlCl_3$ (pH 4.5) for 0, 2, 4, 8, 12, and 24 h. Total RNA was extracted from root apices (0–1 cm). qRT-PCR was performed using the β-tubulin gene as an internal standard with 0 h seedling root apices as a calibrator. Data are given as the mean ± SD (n = 3).

genotype, Shuzunari, in which the malate concentration but not the citrate concentration was found to decrease under Al stress (Yang et al., 2001). Malate might contribute to balance citrate synthesis and efflux. Al treatment increased the activities of NADP-malic enzymes beginning at 2 h of Al exposure for Jiyu 70. Activities of NADP-malic enzymes in Jiyu 62 increased at 4 h, peaked at 8 h and decreased in the remaining Al exposure duration (**Figure 2C**). The lower NADP-malic enzyme activities of Jiyu 62 were consistent with its lower malate concentration in root apices (**Figures 2B,C**).

The Transcriptional Expression of *GmME1*

GmME1 was constitutively expressed throughout the entire plant of Jiyu 70, especially in the roots (**Figure 3A**). Its transcriptional abundance fluctuated in Jiyu 70 and increased 10 fold and 20 fold at 4 and 24 h, respectively, under Al stress. Jiyu 62 also displayed higher expression at 4 and 24 h, albeit with less magnitude (**Figure 3B**).

The Bioinformatic Analysis of *GmME1*

Full-length *GmMe1* was isolated from soybean root apices (GenBank: 100778170). *GmMe1* encodes a protein with 619 amino acids. As predicted in http://prosite.expasy.org/scanprosite, GmMe1 contains a malic enzyme signature (Ps00331) at its 331-347 site. Sequence analysis at http://www.cbs.dtu.dk/services/SignalP/ showed that GmMe1 does not contain any predicted organelle sorting signal (data not shown).

The cloned *GmME1* showed high similarity to *AtME2* and *AtME3,* with identities of 77 and 76%, respectively. Arabidopsis NADP-malic enzyme isoforms shared high degrees of identity but have very different roles (Wheeler et al., 2008). With minimal structural differences, *AtME2* and *AtME3* display the forward (malate oxidative decarboxylation to decompose malate) and reverse (pyruvate reductive carboxylate ion to produce malate) reactions. GmME1 is conserved at the suggested critical regulatory regions of fumarate activation and malate inhibition (**Figure 4A**). Multiple isoforms of GmME1 might function redundantly or display different roles. GmNADP-ME homologues had identities between 35 and 96% (**Figure 4A**). Phylogenetic analysis showed that GmME1 exhibited high similarity to SgME1 (**Figure 4B**), which suggests contribution to more malate synthesis and efflux under Al stress (Sun et al., 2014). GmME1 also closely clustered with VuNADP-ME and OsNADP-ME (Chen et al., 2015).

Subcellular Localization of GmME1

Transiently expressed GmME1-YFP in Arabidopsis protoplast cells displayed fluorescence signal throughout the cytosol. The expressed YFP alone exhibited non-specific fluorescence within plasma membrane, cytosol and nucleus (**Figure 5**). Thus, GmME1 was suggested to localize at cytosol, which is similar to the cytosol localization of AtME2 and SgME1.

Agrobacterium Mediated Over-expression of *GmME1* in Soybean Hairy Roots

In comparison with the WT, *GmME1*-OE hairy roots contained higher internal malate (**Figure 6A**) and citrate (**Figure 6B**) concentrations and secreted more malate (**Figure 6C**) and citrate (**Figure 6D**) under either −Al or +Al stress. Compared with that of WT under −Al treatment, nearly 10-fold higher malate concentrations were found in the *GmME1*-OE hairy roots (**Figure 6A**). Malate concentrations were further increased by Al treatment of both transgenic and WT hairy roots (**Figure 6A**). A slight but significant increase in citrate concentration was found in *GmME1*-OE hairy roots (**Figure 6B**). Different from WT hairy roots, the citrate concentration in *GmME1*-OE hairy roots could not be increased by Al treatment (**Figure 6B**). By sensitive enzymatic assay, malate and citrate were detected in the

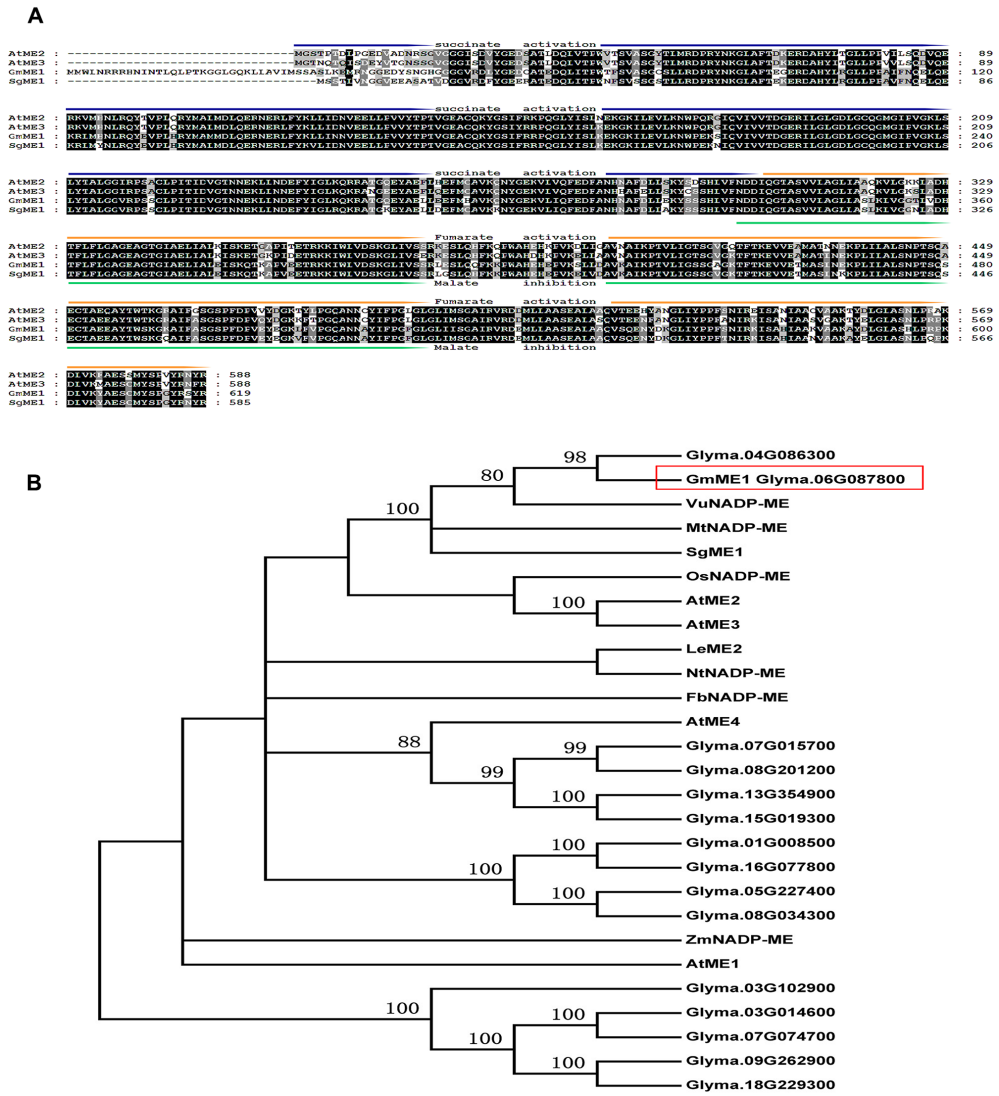

FIGURE 4 | Sequence **(A)** and phylogenetic tree **(B)** analysis of GmME1 and other known plant NADP-Malic enzymes. **(A)** Alignment of the amino acid sequences of GmME1 and orthologous proteins from other plant species, including AtME2 (GeneID:831039), AtME3 (GeneID:832657) and SgME1 (LOCUS AGH32501). Regions of the primary structure of each isoenzyme are labeled as follows: fumarate activation (orange), malate inhibition (green), and succinate activation of the reverse reaction (blue). **(B)** Phylogenetic relationship of GmME1 and other known Malic enzymes proteins. *Arabidopsis thaliana* (*AtNADP-ME1* GeneID:816509, *AtNADP-ME2* GeneID:831039, *AtNADP-ME3* GeneID:832657, *AtNADP-ME4* GeneID:844314), *Flaveria bidentis* (*FbNADP-ME* LOCUS: AAW56450), *Lycopersicon esculentum* (LeME2 LOCUS: AAB58728), *Medicago truncatula* (*MtNADP-ME* GeneID:25490143), *Nicotiana sylvestris* (*NtNADP-ME* GeneID:104247285), *Oryza sativa* (*OsNADP-ME* GeneID:4338007), *Stylosanthes guianensis* (*SgME1*LOCUS AGH32501), *Vigna umbellata* (*VuNADP-ME* LOCUS CAA56354), *Zea mays* (*ZmNADP-ME* GeneID:542209)*1*LOCUS AGH32501) and *GmME1 Glyma.06G087800*).

root exudates of both WT and *GmME1*-OE roots under either −Al or +Al treatment (**Figures 6C,D**). Compared with those of WT, 2.5-fold citrate efflux (**Figure 6D**) and 2.0-fold malate efflux (**Figure 6C**) increases were found in the root exudates of *GmME1*-OE hairy roots. The amount of malate efflux was approximately one-tenth that of citrate (**Figures 6C,D**).

Transcriptional expression analysis showed that *GmME1*-OE hairy roots had higher transcriptional abundance of *GmME1* (**Figure 7A**). 4 h Al treatment didn't cause significant changes of transcription abundance in *GmME1* in WT hairy roots, that was different from roots of Jiyu 62 response to Al stress (**Figure 3B**). The difference might result from distinct culture conditions or the different physiological properties between soybean roots and hairy roots. The over-expression of *GmME1* had less effect on the transcriptional patterns of either of the putative citrate transporters *GmAACT1* (**Figure 7B**) and *GmFRDL* (**Figure 7C**) or the malate transporter *GmALMT1* (**Figure 7D**).

Compared with the WT roots and in agreement with the higher organic acid concentration and exudation, lighter

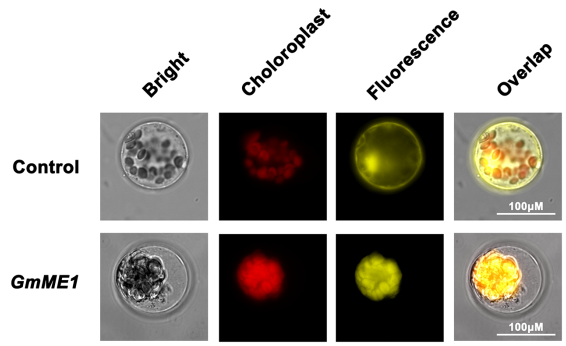

FIGURE 5 | Subcellular localization of *GmNADP-ME*. The YFP alone (above columns) and fusion protein GmME1:YFP (down columns) were transiently expressed in Arabidopsis protoplasts. The panels show the overlapped images of bright-field, chloroplast, fluorescence images from left to right. Scale bar = 100 μM.

hematoxylin staining was found in the *GmME1*-OE roots after 4 h of Al treatment (**Figure 8A**). The Al content in the WT hairy roots was almost 1.5 fold that in the *GmME1*-OE hairy roots (**Figure 8B**). Thus, *GmME1*-OE hairy roots successfully acquired higher Al resistance.

DISCUSSION

Al-induced citrate exudation has been well documented as the Al–exclusion mechanism in soybean (Yang et al., 2000, 2001; Silva et al., 2001). In the present study, both genotypes showed sensitivity to Al with similarly lower citrate efflux before 8 h of Al treatment, and significantly more citrate efflux was induced from Jiyu 70 at 12 h, which resulted in its higher RRE (**Figures 1A,B**). Thus, the capacity for maintaining higher citrate exudation is critical for Al resistance in soybean. Malate was hypothesized to maintain the balance between the citrate synthesis and release in soybean root exposed to Al because the internal root concentration of citrate increased, whereas malate dropped (Yang et al., 2001). The sharp decrease in malate preceded citrate under Al stress in the Al-sensitive genotype Jiyu 62 (**Figures 2A,B**). The exhaustion of internal malate in Jiyu 62 was more consistent with its lower malic enzyme activities (**Figure 2C**) than the less Al-induced citrate efflux in Jiyu 62 (**Figures 1B**, **2B**). Thus, malate was suggested to play a crucial role in the sustained Al-induced citrate release from soybean roots. It is necessary to elucidate how malate metabolism affects the Al-induced citrate efflux from soybean roots.

Malate is one of the essential carbon storage molecules in plants (Zell et al., 2010) and has long been thought to be involved in regulating and composing the root exudates or affecting stomatal function as an osmolyte (Fernie and Martinoia, 2009). Malic enzyme reversibly converses between malate and pyruvate, depending on the isoform, cellular conditions and available substrates (Sweetman et al., 2009). Mitochondrial NAD-malic enzyme has been suggested to supply pyruvate for the TCA cycle to increase the citrate pool in common bean under Al stress (Rangel et al., 2010). Cytosolic isoforms of NADP-dependent malic enzymes have been found to regulate the

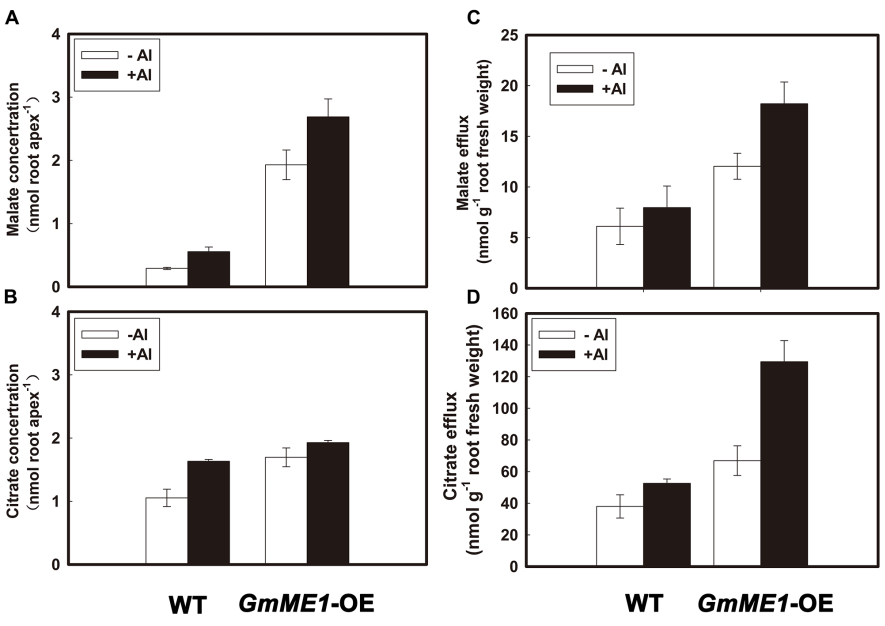

FIGURE 6 | Concentration and efflux of malate **(A,C)** and citrate **(B,D)** in soybean hairy roots of *GmME1*-OE under Al stress. Both transgenic and WT hairy roots were exposed to 0.5 mM $CaCl_2$ solution (pH 4.5) with or without 30 μM $AlCl_3$ for 4 h. Ten root apices were excised from each treatment for malate **(A)** and citrate **(B)** concentration analysis. Root exudates were collected for malate **(C)** and citrate **(D)** efflux measurement. Fresh root biomass was weighed immediately. Data are given as the mean ± SD (n = 3).

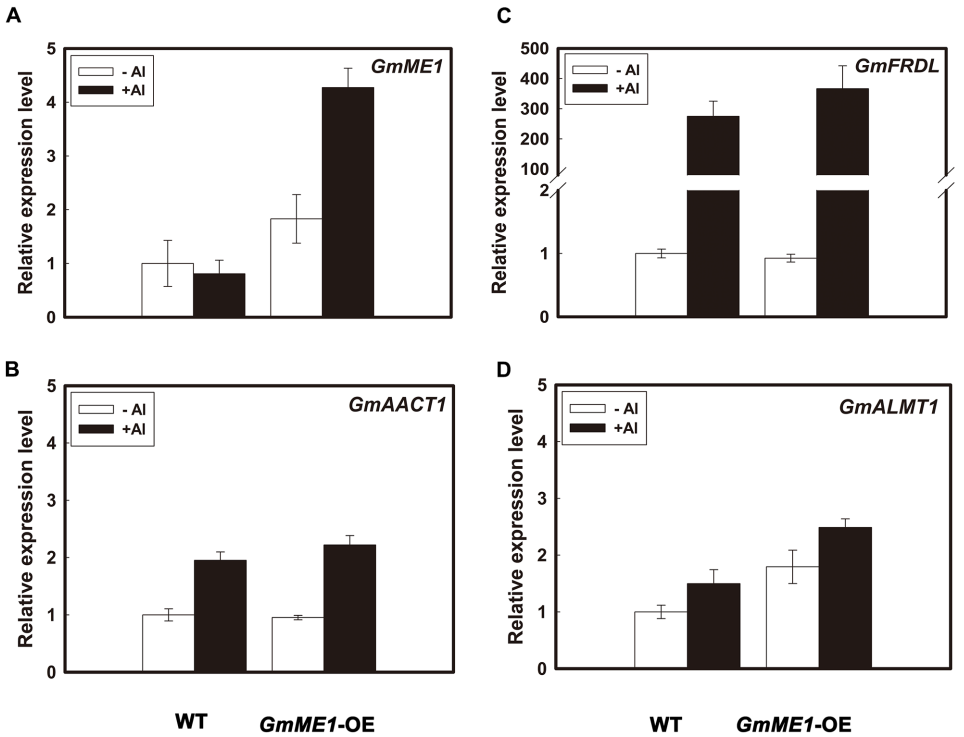

FIGURE 7 | The transcriptional levels of *GmME1* **(A)**, *GmFRDL* **(B)**, *GmAACT1* **(C)**, and *GmALMT1* **(D)** in transgenic hairy roots under Al stress. Both transgenic and WT hairy roots were exposed to 0.5 mM $CaCl_2$ solution (pH 4.5) with or without 30 μM $AlCl_3$. Ten 0- to 1-cm root apices were excised from each treatment at 4 h for RNA isolation. Quantitative real time PCR was performed to study the transcriptional expression of **(A)** *GmME1* **(B)**, *GmFRDL*, **(C)** *GmAACT1* and **(D)** *GmALMT1*. Data are given as the mean ± SD (n = 3).

cytosolic pH or stomatal closure by balancing malate synthesis and degradation (Martinoia and Rentsch, 1994; Laporte et al., 2002). Minimal changes in the primary structure of AtNADP-ME isoforms might result in very different kinetic behaviors of each AtNADP-ME isoform (Wheeler et al., 2008). Cytosol-localized NADP-ME2 and NADP-ME3 share 90% sequence identity but show distinct kinetic properties in their forward (malate oxidative decarboxylation) and reverse (pyruvate reductive carboxylation) reactions to regulation (Wheeler et al., 2009). SgME1 has been verified as a malic enzyme functioning in malate synthesis because of its over-expression in yeast, and *A. thaliana* and common bean hairy roots can significantly increase their malate concentrations (Sun et al., 2014). *GmME1* putatively encoding cytosolic NADP-dependent malic enzyme was revealed to increase its transcriptional abundance (You et al., 2011) and thus was chosen to study its contribution to Al-induced citrate efflux.

Fourteen homology genes putatively encoding cytosolic NADP-dependent malic enzyme existed in the soybean genome (**Figure 4B**). There have been no reports on their functional analysis until now. The transcription expression analysis in the present study revealed that *GmME1* was expressed throughout the whole soybean plant, at especially higher levels in the roots (**Figure 3A**). Al increased the transcription abundance of *GmME1* in soybean root apices of Jiyu 70 during 24 h (**Figure 3B**), which was consistent with its higher malate concentration (**Figure 2B**) and higher NADP-malic enzyme activities in the root apices (**Figure 2C**). GmME1 was localized to the cytosol (**Figure 5**) and displayed high similarity to AtME2 (77%), AtME3 (76%) and SgME1 (86%) (**Figure 4A**), which were conserved in the regions of suggested fumarate activation and malate inhibition (**Figure 4A**) (Wheeler et al., 2009). AtME3 is restricted to trichomes and pollen (Wheeler et al., 2009). According to sequence comparison (**Figures 4A,B**), subcellular localization (**Figure 5**), and spatial expression pattern (**Figure 3A**), GmME1 functions similarly to AtME2 and SgME1 as a malic enzyme contributing to malate metabolism.

Malate efflux from soybean under Al stress has been considered negligible because of several orders of lower magnitude and small variation between soybean genotypes (Yang et al., 2000; Silva et al., 2001). Soybean root malate exudation and concentrations were also reported to coordinately be influenced by pH changes, phosphorus deficiency, and Al toxicity (Liang et al., 2013). *GmALMT1* encoding a malate transporter was successfully cloned from soybean root apices, and GmALMT1-mediated root malate efflux was suggested to underlie soybean Al tolerance in soybean (Liang et al., 2013). The different conclusion in the role of Al-induced malate secretion might result from different experiment conditions and/or genotypes. Different from intact root treatment and HPLC detection in experiments from Yang et al. (2000, 2001), excised root apices and a sensitive enzyme assay were used in

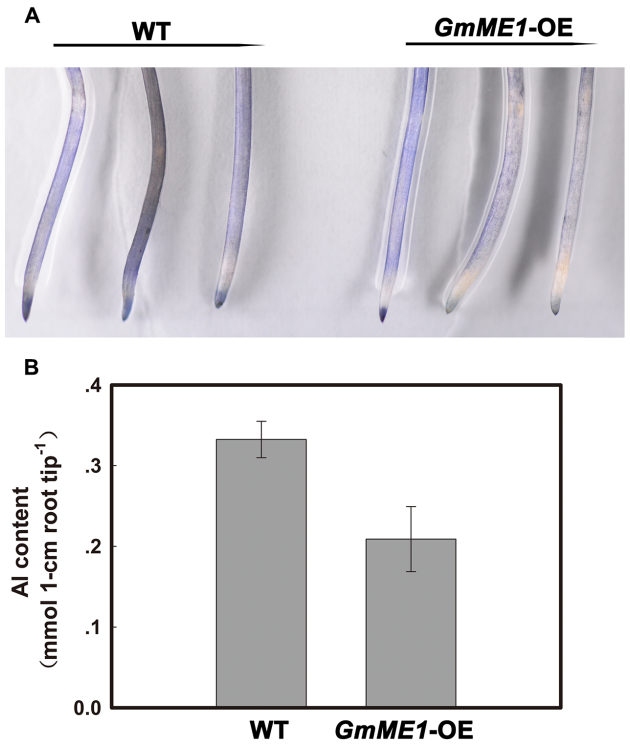

FIGURE 8 | The hematoxylin staining **(A)** and Al content **(B)** in hairy roots under Al stress. Both transgenic and WT hairy roots were exposed to 0.5 mM $CaCl_2$ solution (pH 4.5) with or without 30 μM $AlCl_3$. At 4 h, three Al-treated WT or transgenic hairy roots were soaked in hematoxylin solution for 30 min. Roots were rinsed by water three times before imaging with a Nikon camera **(A)**. Ten 0- to 1-cm root apices were excised at 4 h for Al concentration measurements **(B)**.

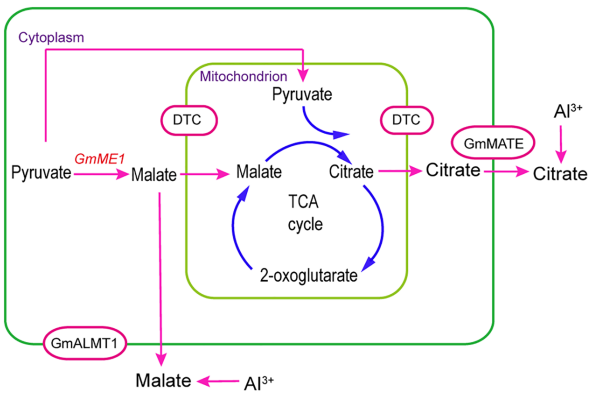

FIGURE 9 | A Model proposing the role of *GmME1* in the process of Al-induced malate and citrate efflux from soybean roots. Cytosolic malic enzyme, GmME1, was supposed to increase malate synthesis in cytosol and thus supply malate to the TCA cycle as an anaplerotic reaction to promote citrate pool over citrate exudation under Al stress. Imported malate and exported citrate through mitochondrial membrane were supposed to occur by GmDTC. The malate and citrate efflux across plasma membrane might have occurred by GmALMT1 and MATE family proteins (GmFRDL and GmAACT1), respectively.

the experiments of Liang et al. (2013). In the present study, malate efflux was not detected by HPLC from Al-induced root exudates in 14-day-old seedlings of Jiyu 62 and Jiyu 70 (data not shown). However, malate exudation could be detected in the hairy root experiment by the enzyme assay (**Figures 6C,D**), although it was approximately one-tenth that of citrate efflux.

Over-expressing *GmME1* in soybean hairy roots enhanced its own expression (**Figure 7A**) and resulted in a significant increase in malate and citrate concentrations under either +Al or −Al treatment (**Figures 6A,B**). Al-induced malate efflux was found to increase in the *GmME1*-OE hairy roots, although the transcription level of *GmALMT1* encoding malate transporter remained constant (**Figure 7D**). Thus, GmME1 was verified to be a malic enzyme similar to SgME1, responsible for malate synthesis and efflux under Al stress (Sun et al., 2014).

Citrate efflux was approximately 10-fold higher than malate efflux in the hairy roots of transgenic and wild-type plants (**Figures 6C,D**). With unchanged transcription levels of *GmFRDL* and *GmAACT1* putatively encoding citrate transporter (**Figures 7B,C**), more Al-induced citrate secretion was found from *GmME1*-OE root exudates than that of WT (**Figure 6D**), which might have resulted from their more internal citrate concentration (**Figure 6B**). GmME1, a malic enzyme, increased the citrate synthesis and citrate efflux, which supports our previous hypothesis that malate contributes to balance citrate synthesis and efflux in soybean. Discussion of how GmME1 affects the citrate pool and then efflux follows.

Mitochondrial TCA cycle-related enzymes, especially citrate synthase, have been proposed to prompt the Al-induced citrate efflux from soybean roots (Xu et al., 2010). Anaplerotic enzyme induction has been revealed to counteract the depletion of TCA intermediates. Root isoforms of PEPC and NAD malic enzyme are known to have various anaplerotic functions involved in carbon skeleton supply during N assimilation, maintenance of cytoplasmic pH or osmolarity regulation (Nisi and Zocchi, 2000; Held, 2005). Both PEPC and mitochondrial NAD-ME were proposed to be involved in anaplerotic functions in common bean under Al stress by fueling the TCA cycle (Rangel et al., 2010). This means that the anaplerotic reaction is necessary for some plant species under Al stress. One report on hypertrophied hearts suggested that cytosolic malic enzyme catalyzes pyruvate carboxylation to supply more malate to the mitochondrial TCA cycle, leading to more citrate synthesis (Pound et al., 2009). "Anaplerotic" influx depends on the direct shuttle of malate between the cytosol and mitochondria (Pound et al., 2009). In the present study, *GmME1*-OE hairy roots contained more malate, which prompted more synthesis and secretion of citrate (**Figures 6B,C**). This process is depicted in **Figure 9**. Cytosol-localized GmME1 might be involved in an alternate anaplerotic pathway to supply the TCA under Al stress by promoting more malate synthesis (**Figure 9**). Mitochondrial carrier proteins function to export or import metabolite to maintain the pools of TCA cycle intermediates

(Haferkamp and Schmitz-Esser, 2012; Etienne et al., 2013). Dicarboxylate/tricarboxylate carrier (DTC) was suggested to transport dicarboxylates, such as oxaloacetate and malate, and tricarboxylates, including citrate, isocitrate, *cis*-aconitate, and trans-aconitate across mitochondrial membrane by a counter-exchange mechanism (Deng et al., 2009). CjDTC was suggested to involve in organic acid excretion in *Citrus junos* because of its higher expression under Al stress (Deng et al., 2009). Consistently, the expression of *DTC* was increased in soybean root apices under Al stress (You et al., 2011). Citrate carrier inhibitor treatment decreased Al-induced citrate efflux from soybean, indicating its important role in the process of citrate release (Xu et al., 2010). In this paper, the import of malate and export of citrate in mitochondria might depend on mitochondrial carrier proteins such as DTC protein (**Figure 9**). The malate and citrate efflux across the plasma membrane was supposed to depend on GmALMT1 and members of the MATE family (GmAACT and GmFRDL) (**Figure 9**).

Consistent with the increased efflux and concentration of both malate and citrate, the *GmME1*-OE soybean hairy roots have light hematoxylin staining (**Figure 8A**) and lower Al contents (**Figure 8B**) in root apices, demonstrating better Al exclusion capacity and higher Al resistance.

CONCLUSION

GmME1 was revealed to encode a cytosolic malic enzyme, which increased malate and citrate synthesis and Al-induced malate and citrate efflux. Moreover, new evidence was added that GmME1 can function in anaplerotic pathways to supply the TCA cycle to prompt more citrate synthesis then efflux under Al stress (**Figure 9**).

AUTHOR CONTRIBUTIONS

YZ performed most of the experiments. ZY the supervisor of YZ, helped to design the experiments and performed organic acid measurement by HPLC. YX performed the subcellular localization experiments. BL and WS helped in plant culture and hairy root induction experiments. HS and ZS helped in qRT-PCR experiments. JY designed the entire experiment, performed organic acid examination by enzymatic assay, and wrote the manuscript. The final manuscript has been read and approved by all authors.

FUNDING

This research was financially supported by the National Natural Science Foundation of China (No. 31372124) for JY and Jilin Natural Science Foundation of China (No. 20130101084JC) for JY. This research was also funded by the National Undergraduates Innovating Experimentation Project (No. 2016A82362) for BL and WS.

ACKNOWLEDGMENTS

We would like to thank Hongyan Sheng at Washington State University for language revision and proofreading.

REFERENCES

Anoop, V. M., Basu, U., McCammon, M. T., McAlister-Henn, L., and Taylor, G. J. (2003). Modulation of citrate metabolism alters aluminum tolerance in yeast and transgenic canola overexpressing a mitochondrial citrate synthase. *Plant Physiol.* 132, 2205–2217. doi: 10.1104/pp.103.023903

Barone, P., Rosellini, D., LaFayette, P., Bouton, J., Veronesi, F., and Parrott, W. (2008). Bacterial citrate synthase expression and soil aluminum tolerance in transgenic alfalfa. *Plant Cell Rep.* 27, 893–901. doi: 10.1007/s00299-008-0517-x

Chen, L., Tsugama, D., Takano, T., and Liu, S. (2015). Rice (*Oryza sativa* L.) OsNADP-ME4 gene responds to adversity stresses. *Cell Biol. Biophys.* 4, 1–7.

Collins, N. C., Shirley, N. J., Saeed, M., Pallotta, M., and Gustafson, J. P. (2008). An ALMT1 gene cluster controlling aluminum tolerance at the Alt4 locus of rye (*Secale cereale* L.). *Genetics* 179, 669–682. doi: 10.1534/genetics.107.083451

Delhaize, E., and Ryan, P. R. (1995). Aluminum toxicity and tolerance in plants. *Plant Physiol.* 107, 315–321. doi: 10.1104/pp.107.2.315

Delhaize, E., Ryan, P. R., and Randall, P. J. (1993). Aluminum tolerance in wheat (*Triticum aestivum* L.) (II. Aluminum-stimulated excretion of malic acid from root apices). *Plant Physiol.* 103, 695–702. doi: 10.1104/pp.103.3.695

Deng, W., Luo, K., Li, Z., Yang, Y., Hu, N., and Wu, Y. (2009). Overexpression of *Citrus junos* mitochondrial citrate synthase gene in *Nicotiana benthamiana* confers aluminum tolerance. *Planta* 230, 355–365. doi: 10.1007/s00425-009-0945-z

Etienne, A., Genard, M., Lobit, P., Mbeguie-A-Mbeguie, D., and Bugaud, C. (2013). What controls fleshy fruit acidity? A review of malate and citrate accumulation in fruit cells. *J. Exp. Bot.* 64, 1451–1469. doi: 10.1093/jxb/ert035

Fernie, A. R., and Martinoia, E. (2009). Malate. Jack of all trades or master of a few? *Phytochemistry* 70, 828–832. doi: 10.1016/j.phytochem.2009.04.023

Haferkamp, I., and Schmitz-Esser, S. (2012). The plant mitochondrial carrier family: fuctional and evolutionary aspects. *Front. Plant Sci.* 3:2. doi: 10.3389/fpls.2012.00002

Han, Y., Zhang, W., Zhang, S., Wang, W., and Ming, F. (2009). One novel mitochondrial citrate synthase from *Oryza sativa* L. can enhance aluminum tolerance in transgenic tobacco. *Mol. Biotechnol.* 42, 299–305. doi: 10.1007/s12033-009-9162-z

Held, H. W. (2005). *Plant Biochemistry*. Burlington, VT: Elsevier Academic Press.

Horst, W. J., Asher, C. J., Cakmak, L., Szulkiewicz, P., and Wissemeier, A. H. (1992). Short-term response of soybean roots to aluminium. *J. Plant Physiol.* 140, 174–178. doi: 10.1016/S0176-1617(11)80930-2

Kochian, L. V., Hoekenga, O. A., and Pineros, M. A. (2004). How do crop plants tolerate acid soils? Mechanisms of aluminum tolerance and phosphorous efficiency. *Annu. Rev. Plant Biol.* 55, 459–493. doi: 10.1146/annurev.arplant.55.031903.141655

Kochian, L. V., Pineros, M. A., Liu, J. P., and Magalhaes, J. V. (2015). Plant adaptation to acid soils: the molecular basis for crop aluminum resistance. *Annu. Rev. Plant Biol.* 66, 571–598. doi: 10.1146/annurev-arplant-043014-114822

Koyama, H., Takita, E., Kawamura, A., Hara, T., and Shibata, D. (1999). Over expression of mitochondrial citrate synthase gene improves the growth of carrot cells in Al-phosphate medium. *Plant Cell Physiol.* 40, 482–488. doi: 10.1093/oxfordjournals.pcp.a029568

Laporte, M. M., Shen, B., and Tarczynski, M. C. (2002). Engineering for drought avoidance: expression of maize NADP-malic enzyme in tobacco results in altered stomatal function. *J. Exp. Bot.* 53, 699–705. doi: 10.1093/jexbot/53.369.699

Liang, C. Y., Piñeros, M. A., Tian, J., Yao, Z. F., Sun, L. L., Liu, J. P., et al. (2013). Low pH, aluminum, and phosphorus coordinately regulate malate exudation

through *GmALMT1* to improve soybean adaptation to acid soils. *Plant Physiol.* 161, 1347–1361. doi: 10.1104/pp.112.208934

Liu, J. P., Magalhaes, J. V., Shaff, J., and Kochian, L. V. (2009). Aluminum-activated citrate and malate transporters from the MATE and ALMT families function independently to confer Arabidopsis aluminum tolerance. *Plant J.* 57, 389–399. doi: 10.1111/j.1365-313X.2008.03696.x

Livak, K. J., and Schmittgen, T. D. (2001). Analysis of relative gene expression data using real-time quantitative PCR and the 2(-Delta Delta C(T)) Methods. *Methods* 25, 402–408. doi: 10.1006/meth.2001.1262

Lou, H. Q., Gong, Y. L., Fan, W., Xu, J. M., Liu, Y., Cao, M. J., et al. (2016a). A formate dehydrogenase confers tolerance to aluminum and low pH. *Plant Physiol.* 171, 294–305. doi: 10.1104/pp.16.01105

Lou, H. Q., Fan, W., Xu, J. M., Gong, Y. L., Jin, J. F., Chen, W. W., et al. (2016b). Anoxalyl-CoA synthetase is involved in oxalate degradation and aluminum tolerance. *Plant Physiol.* 172, 1679–1690.

Ma, J. F. (2000). Role of organic acids in detoxification of aluminum in higher plants. *Plant Cell Physiol.* 41, 383–390. doi: 10.1093/pcp/41.4.383

Ma, J. F., and Miyasaka, S. C. (1998). Oxalate exudation by taro in response to Al. *Plant Physiol.* 118, 861–865. doi: 10.1104/pp.118.3.861

Ma, J. F., Ryan, P. R., and Delhaize, E. (2001). Aluminium tolerance in plants and the complexing role of organic acids. *Trends Plant Sci.* 6, 273–278. doi: 10.1016/S1360-1385(01)01961-6

Ma, J. F., Zheng, S. J., and Matsumoto, H. (1997). Specific secretion of citric acid induced by Al stress in *Cassia tora* L. *Plant Cell Physiol.* 38, 1019–1025. doi: 10.1093/oxfordjournals.pcp.a029266

Magalhaes, J. V., Liu, J., Guimarães, C. T., Lana, U. G., Alves, V. M., Wang, Y. H., et al. (2007). A gene in the multidrug and toxic compound extrusion (MATE) family confers aluminum tolerance in sorghum. *Nat. Genet.* 39, 156–161. doi: 10.1038/ng2074

Maron, L. G., Guimarães, C. T., Kirst, M., Albert, P. S., Birchler, J. A., Bradbury, P. J., et al. (2013). Aluminum tolerance in maize is associated with higher MATE1 gene copy number. *Proc. Natl. Acad. Sci. U.S.A.* 110, 5241–5246. doi: 10.1073/pnas.1220766110

Martinoia, A. E., and Rentsch, D. (1994). Malate compartmentation: response to a complex metabolism. *Annu. Rev. Plant Physiol. Plant Mol. Biol.* 45, 447–467. doi: 10.1146/annurev.pp.45.060194.002311

Nisi, P. D., and Zocchi, G. (2000). Phosphoenolpyruvate carboxylase in cucumber (*Cucumis sativus* L.) roots under iron deficiency: activity and kinetic characterization. *J. Exp. Bot.* 51, 1903–1909. doi: 10.1093/jexbot/51.352.1903

Pound, K. M., Sorokina, N., Ballal, K., Berkich, D. A., Fasano, M., Lanoue, K. F., et al. (2009). Substrate-enzyme competition attenuates upregulated anaplerotic flux through malic enzyme in hypertrophied rat heat and restores triacylglyceride content. *Circ. Res.* 104, 805–812. doi: 10.1161/CIRCRESAHA.108.189951

Rangel, A. F., Rao, I. M., Braun, H. P., and Horst, W. J. (2010). Aluminum resistance in common bean (*Phaseolus vulgaris*) involves induction and maintenance of citrate exudation from root apices. *Physiol. Plant.* 138, 176–190. doi: 10.1111/j.1399-3054.2009.01303.x

Ryan, P. R., Delhaize, E., and Jones, D. L. (2001). Function and mechanism of organic anion exudation from plant roots. *Annu. Rev. Plant Physiol. Plant Mol. Biol.* 52, 527–560. doi: 10.1146/annurev.arplant.52.1.527

Ryan, P. R., Delhaize, E., and Randall, P. J. (1995). Malate efflux from root apices and tolerance to aluminum are highly correlated in wheat. *Funct. Plant Biol.* 22, 531–536.

Ryan, P. R., Tyerman, S. D., Sasaki, T., Furuichi, T., Yamamoto, Y., Zhang, W. H., et al. (2011). The identification of aluminium-resistance genes provides opportunities for enhancing crop production on acid soils. *J. Exp. Bot.* 62, 9–20. doi: 10.1093/jxb/erq272

Santelia, D., and Lawson, T. (2016). Rethinking guard cell metabolism. *Plant Physiol.* 172, 1371–1392. doi: 10.1104/pp.16.00767

Silva, I. R., Smyth, T. J., Israel, D. W., Raper, C. D., and Rufty, T. W. (2001). Magnesium ameliorates aluminum rhizotoxicity in soybean by increasing citric acid production and exudation by roots. *Plant Cell Physiol.* 42, 546–554. doi: 10.1093/pcp/pce067

Subramanian, S., Graham, M. Y., Yu, O., and Graham, T. L. (2005). RNA interference of soybean isoflavone synthase genes leads to silencing in tissues distal to the transformation site and to enhanced susceptibility to phytophthora sojae. *Plant Physiol.* 137, 1345–1353. doi: 10.1104/pp.104.057257

Sun, L., Liang, C., Chen, Z., Liu, P., Tian, J., Liu, G., et al. (2014). Superior aluminum (Al) tolerance of *Stylosanthes* is achieved mainly by malate synthesis through an Al-enhanced malic enzyme, SgME1. *New Phytol.* 202, 209–219. doi: 10.1111/nph.12629

Sweetman, C., Deluc, L. G., Cramer, G. R., Ford, C. M., and Soole, K. L. (2009). Regulation of malate metabolism in grape berry and other developing fruits. *Phytochemistry* 70, 1329–1344. doi: 10.1016/j.phytochem.2009.08.006

Tesfaye, M., Temple, S. J., Allan, D. L., Vance, C. P., and Samac, D. A. (2001). Overexpression of malate dehydrogenase in transgenic alfalfa enhances organic acid synthesis and confers tolerance to aluminum. *Plant Physiol.* 127, 1836–1844. doi: 10.1104/pp.010376

Wang, Q. F., Zhao, Y., Yi, Q., Li, K. Z., Yu, Y. X., and Chen, L. M. (2010). Overexpression of malate dehydroenase in transgenic tobacco leaves: enhanced malate synthesis and augmented Al resistance. *Acta Physiol. Plant.* 32, 1209–1220. doi: 10.1007/s11738-010-0522-x

Wheeler, M. C., Arias, C. L., Maurino, V. G., Andreo, C. S., and Drincovich, M. F. (2009). Identification of domains involved in the allosteric regulation of cytosolic *Arabidopsis thaliana* NADP-malic enzymes. *FEBS J.* 276, 5665–5677. doi: 10.1111/j.1742-4658.2009.07258.x

Wheeler, M. C., Arias, C. L., Tronconi, M. A., Maurino, V. G., Andreo, C. S., and Drincovich, M. F. (2008). *Arabidopsis thaliana* NADP-malic enzyme isoforms: high degree of identity but clearly distinct properties. *Plant Mol. Biol.* 67, 231–242. doi: 10.1007/s11103-008-9313-9

Xu, M. Y., You, J. F., Hou, N. N., Zhang, H. M., Chen, G., and Yang, Z. M. (2010). Mitochondrial enzymes and citrate transporter contribute to the aluminium-induced citrate secretion from soybean (*Glycine max*) roots. *Funct. Plant Biol.* 37, 285–295. doi: 10.1071/FP09223

Yang, Z. M., Nian, H., Sivaguru, M., Tanakamaru, S., and Matsumotob, H. (2001). Characterization of aluminium-induced citrate secretion in aluminium-tolerant soybean (*Glycine max*) plants. *Physiol. Plant.* 113, 64–71. doi: 10.1034/j.1399-3054.2001.1130109.x

Yang, Z. M., Sivaguru, M., Horst, W. J., and Matsumoto, H. (2000). Aluminium tolerance is achieved by exudation of citric acid from roots of soybean (*Glycine max*). *Physiol. Plant.* 110, 72–77. doi: 10.1034/j.1399-3054.2000.110110.x

You, J. F., Zhang, H., Liu, N., Gao, L. L., Kong, L. N., and Yang, Z. M. (2011). Transcriptomic responses to aluminum stress in soybean roots. *Genome* 54, 923–933. doi: 10.1139/g11-060

Zell, M. B., Fahnenstich, H., Maier, A., Saigo, M., Voznesenskaya, E. V., Edwards, G. E., et al. (2010). Analysis of Arabidopsis with highly reduced levels of malate and fumarate shed light on the role of these organic acids as storage carbon molecules. *Plant Physiol.* 152, 1251–1262. doi: 10.1104/pp.109.151795

Conflict of Interest Statement: The authors declare that the research was conducted in the absence of any commercial or financial relationships that could be construed as a potential conflict of interest.

Advantages of publishing in Frontiers

OPEN ACCESS
Articles are free to read for greatest visibility and readership

FAST PUBLICATION
Around 90 days from submission to decision

HIGH QUALITY PEER-REVIEW
Rigorous, collaborative, and constructive peer-review

TRANSPARENT PEER-REVIEW
Editors and reviewers acknowledged by name on published articles

Frontiers
Avenue du Tribunal-Fédéral 34
1005 Lausanne | Switzerland

Visit us: www.frontiersin.org
Contact us: info@frontiersin.org | +41 21 510 17 00

REPRODUCIBILITY OF RESEARCH
Support open data and methods to enhance research reproducibility

DIGITAL PUBLISHING
Articles designed for optimal readership across devices

FOLLOW US
@frontiersin

IMPACT METRICS
Advanced article metrics track visibility across digital media

EXTENSIVE PROMOTION
Marketing and promotion of impactful research

LOOP RESEARCH NETWORK
Our network increases your article's readership